This is to certify that the
dissertation entitled

TOWARDS RENEWABLE COMMODITY CHEMICALS:
BIOSYNTHESIS OF PHLOROGLUCINOL AND
CHEMOENZYMATIC SYNTHESIS OF CAPROLACTAM

presented by

Brad M Cox

has been accepted towards fulfillment
of the requirements for the

Doctoral degree in Chemistry

John W. Frost
Major Professor's Signature

4/28/08
Date

TOWARDS RENEWABLE COMMODITY CHEMICALS: BIOSYNTHESIS OF PHLOROGLUCINOL AND CHEMOENZYMATIC SYNTHESIS OF CAPROLACTAM

By

Brad M. Cox

A DISSERTATION

Submitted to
Michigan State University
in partial fulfillment of the requirements
for the degree of

DOCTOR OF PHILOSPOHY

Department of Chemistry

2008

ABSTRACT

TOWARDS RENEWABLE COMMODITY CHEMICALS: BIOSYNTHESIS OF PHLOROGLUCINOL AND CHEMOENZYMATIC SYNTHESIS OF CAPROLACTAM

By

Brad M. Cox

In rise of the uncertainty associated with the chemical industries reliance on non-renewable resources for virtually all commodity chemical manufacture, the research for sources with renewable feedstocks are of importance. The following research comprises of chemistry which progresses towards the deviation from a petroleum-based chemical economy, to one that thrives on starting materials from renewable sources through utilization of rapid and efficient syntheses dependent upon microbial biocatalysts. Efforts aimed to biocatalytically produce 1,3,5-trihydroxybenzene and an ε-caprolactam precursor from renewable resources at a level with commercial importance. To enhance the viability of commercial manufacture, following a successful biocatalytic production, efforts focused on delivering chemicals with the same level and purity to compete with non-renewable routes.

ε-Caprolactam, the monomer for nylon 6, was synthesized from L-β-lysine. As a renewable feedstock, D-glucose derived L-lysine had been shown to cyclize and deaminate to form ε-caprolactam in previous works. Alternatively, L-β-lysine was researched for applicability in an analogous synthesis of ε-caprolactam. Under anaerobic conditions, *Clostridium subterminale* SB4 degrades L-lysine as a carbon source with two initial metabolic, amino group isomerizations, to L-β-lysine and then 3,5-diaminohexanoate. Successful, selective inhibition of the second aminomutase enzyme was achieved through intense irradiation with light, providing an *in vivo* microbial synthesis of L-β-lysine. The

resulting biosynthetic L-β-lysine product, ultimately from renewable D-glucose, was cyclized to β-aminocaprolactam in near quantitative yields by reflux in high temperature alcohols. Hydrodenitrogenation of β-aminocaprolactam to ε-caprolactam was achieved only in trace amounts.

Phloroglucinol's vast synthetic utility is overshadowed by the problematic synthesis, which precludes its use in commodity chemical markets. Phloroglucinol *in vivo* biocatalysis, from D-glucose, had been shown previously by heterologous expression of phloroglucinol synthase (Type III polyketide synthase, phlD) from *Psuedomonas fluorescens* Pf-5 in *Escherichia coli*. Microbial synthesis of phloroglucinol in a controlled fermentation vessel was increased to concentrations approaching 5 g/L at 6% yield (mol phloroglucinol/mol D-glucose) in fed-batch mode with a 1 L working volume scale. Phloroglucinol toxicity is contributive to limited production, leading to an engineered continuous-extractive, two stage microbial synthesis that afforded concentrations up to 38 g/L at 12% yield (mol phloroglucinol/mol D-glucose). Besides continuous extraction to alleviate toxicity issues, transcriptome analysis was another avenue of research. Upregulated genes by transcriptome analysis, along side probable *E. coli* export machinery, were researched and manipulated in hopes of generating a phloroglucinol tolerant host, to no avail. Genetic advancement of the *Psuedomonas fluorescens* Pf-5 phlD gene through codon optimization increased the crude lysate specific activity, from malonyl CoA to phloroglucinol, two-fold to 0.045 μmol phloroglucinol/min/mg protein. Downstream purification of biocatalytically produced, phloroglucinol had recovery rates of 91% from production to bottled chemical, that was independently certified to be 99.6% pure.

ACKNOWLEDGMENTS

The research and preparation leading to this dissertation was contributed upon by many individuals throughout my career at Michigan State University. First and foremost my appreciation is given to Professor John W. Frost for his unwaivering support of the research, his criticism and breadth in knowledge of science, and the way he provokes excitement about experimentation. Another intergral scientist that has helped pave the way for success has been Dr. Karen M. Draths who offered invaluable suggestions and given treasured time and effort in my development as a scientist. I would like to share my thanks with Professors Babak Borhan, Milton R. Smith III, and Gregory L. Baker who have been my graduate committee advisors throughout my term and have shown interest and dedication to not only my dissertation, but what it represents. The members and colleagues within the science confines have been pivotable in learning and coexisting in a research environment. Thanks to Dr. Jihane Achkar, Diane Alessi, Craig Banotai, Dr. Vu Bui, Dr. Jiantao Guo, Dr. Chad Hansen, Dr. Wei Nui, Dr. Mapitso Molefe, Dr. Ningqing Ran, Dr. Heather Steuben, Dr. Dongming Xie, Dr. Jinsong Yang, Dr. William Yang and other past members whose research or experiences have laid the path for the opportunities I received and whose direct interactions expanded my knowledge. Dr. Man Kit Lau and Dr. Justas Jancauskas I would like to thank individually because without their constant support and friendship this experience would not have been as cherished as it was. Jennifer Froelich has been an irreplaceable asset in my career and life to which I owe a lifetime worth of gratitude. Last, but not at all least, are understatedly appreciated John, Dr. Cheryl and Bryan Cox along with my family and friends who have supported me with any means necessary.

TABLE OF CONTENTS

Chapter ONE 1
Introduction 1
Bioeconomy 1
Biocatalysis 23
Chemical manufacture 28
Hydroxy aromatics 32
CHAPTER ONE REFERENCE 43

Chapter TWO 50
L-lysine Derived ε-Caprolactam 50
Introduction 50
Results 61
Discussion 74
CHAPTER TWO REFERENCE 76

Chapter THREE 78
D-Glucose Derived Phloroglucinol 78
Introduction 78
Results 94
Discussion 133
CHAPTER THREE REFERENCE 137

Chapter FOUR 139
Downstream Processing and Chemistry of Phloroglucinol 139
Results 145
Discussion 160
CHAPTER FOUR REFERENCE 162

Chapter FIVE 163
Experimental 163
Reagents and solvents 163
Chromatography 164
Spectroscopic and analytical measurements 164
Bacterial strains, plasmids, primers and gene synthesis 166
Storage of microbial strains and plasmids 167
Culturing of *Clostridium subterminale* 167
Intact cell bioconversion of L-lysine 168
Purification of L-β-lysine 169
Deamination of L-β-lysine 169

Cyclization of L-lysine to α-Amino-caprolactam. 170
Chemical L-β-Lysine synthesis. 171
In vitro enzyme assays preparation 172
Plasmids 172
Comprehensive reference list of strains and plasmids 179
In house optimized phlD sequence 180
DNA2.0 gene designer optimized phlD sequence 181
Culture mediums 182
Fed-batch microbial synthesis 183
Process description of the biosynthesis of phloroglucinol 185
Phloroglucinol strain prior to microbial synthesis supplemental 186
Phloroglucinol Extraction for phloroglucinol biosynthesis 189
Overall Phloroglucinol Process Schematic 195
Multiple-stage Fed-batch Extractive Microbial synthesis 198
Analysis of microbial synthesis broth 199
Genetic manipulations 200
Wanner type gene inactivation technique 211
Transcriptome analysis 215
Phloroglucinol reduction methodology 251
CHAPTER FIVE REFERENCE 252

LIST OF TABLES

Table 1. *Clostridium subterminale* SB4 bioconversion of L-lysine to L-β-lysine. 63

Table 2. Procedural outline with time allotments for bioconversion to L-β-lysine.....66

Table 3. Procedural outline with time allotments for purification of L-β-lysine.....67

Table 4. Hydrodenitrogenation of acyclic L-β-lysine and β-aminocaprolactam.....71

Table 5. Upregulated genes found by transcriptome analysis in phloroglucinol producing strain.....105

Table 6. Corresponding up-regulation twofold and greater in phloroglucinol producing and phloroglucinol added transcriptome analyses.....106

Table 7. Corresponding up-regulation of transport or membrane protein encoding genes fourfold in phloroglucinol producing and phloroglucinol added transcriptome analyses.109

Table 8. Phosphate elution of phloroglucinol from anion exchange resin. 147

Table 9. Relative counterion selectivity for AG 1 anion exchange resin. 149

Table 10. Binding efficiency comparison of Dowex 1.....150

Table 11. Elution effects of temperature and ionic strength 151

Table 12. Cooperative ionic strength and free proton dependence elution.....154

Table 13. Recrystallization of Authentic phloroglucinol.....155

Table 14. Phloroglucinol producing transcriptome analysis: Upregulated at least 4x. ...219

Table 15. Phloroglucinol producing transcriptome analysis: Upregulated 2-4x. 220

Table 16. Phloroglucinol producing transcriptome analysis: Downregulated 2-4x. 221

Table 17. Phloroglucinol producing transcriptome analysis: Downregulated at least 4x. 222

Table 18. Membrane or transport transcriptome gene list: Upregulated at least 4x.....223

Table 19. Membrane or transport transcriptome gene list: Upregulated 2-4x.....224

Table 20. Membrane or transport transcriptome gene list: Downregulated at least 4x...225

Table 21. Membrane or transport transcriptome gene list: Downregulated 2-4x.....226

Table 22. Total transcriptome gene list: Downregulated at least 4x.....227

Table 23. Total transcriptome gene list: Downregulated 2-4x. 229

Table 24. Total transcriptome gene list: Upregulated 2-4x. 236

Table 25. Total transcriptome gene list: Upregulated at least 4x. 241

Table 26. Comparitive transcriptome membrane or transport gene list: Upregulated.....245

Table 27. Comparitive transcriptome cellular gene list: Upregulated 246

Table 28. Comparitive transcriptome total gene list: Downregulated 249

LIST OF FIGURES

Figure 1. Worldwide energy consumption sources....2
Figure 2. Global carbon emissions from fossil fuels....3
Figure 3. Miscanthus growth after 1 year....10
Figure 4. Reduction in cost for various technological advances....16
Figure 5. Current capabilities of the biofuel production process....18
Figure 6. Future capabilities of the biofuel production process....19
Figure 7. Major products of aromatic feedstocks....31
Figure 8. Shikimate pathway for aromatic amino acid synthesis....33
Figure 9. Hydroxy aromatics....34
Figure 10. Phenol and catechol current and microbial manufacture....35
Figure 11. Hydroquinone current and microbial manufacture....36
Figure 12. Pyrogallol current and microbial manufacture....38
Figure 13. Phloroglucinol and resorcinol current and microbial manufacture....39
Figure 14. Proposed polyhydroxyaromatic synthesis from a renewable source....41
Figure 15. Syntheses of ε-caprolactam from 1,3-butadiene....52
Figure 16. Current and biobased method of manufacture of ε-caprolactam....53
Figure 17. ε-Caprolactam from L-lysine....54
Figure 18. Potential mechanisms for hydrodenitrogenation of α-aminocaprolactam....55
Figure 19. Relative cyclizations of amino acid precursors....56
Figure 20. Degradation of L-lysine in *Clostridium subterminale*....57
Figure 21. L-lysine-2,3-aminomutase active site AdoMet generation mechanism....58
Figure 22. L-lysine-2,3-aminomutase reaction mechanism....59
Figure 23. Arndt-Eistert homologation of L-ornithine yielding L-β-lysine....61

Figure 24. Cyclodehydration of L-β-lysine. 69

Figure 25. L-β-lysine to pyrollidine adaptation from L-lysine to pipecolinic acid. 73

Figure 26. Current manufacture of TATB 78

Figure 27. Current manufacture of phloroglucinol 79

Figure 28. Synthesis of trimethoxybenzene from glucose 80

Figure 29. Potential polymer applications of phloroglucinol. 81

Figure 30. Phloroglucinol from TAL, TNT and glucose. 82

Figure 31. Derivatized phloroglucinol biomolecules with reported biological activity. 83

Figure 32. Biosyntheses of TAL, phloroglucinol and diacetylphloroglucinol. 84

Figure 33. Type I polyketide synthase depiction. 86

Figure 34. Catalytic triad and priming PhlD mechanism. 88

Figure 35. Polyketide ring closing mechanism 89

Figure 36. Comparative fed-batch phloroglucinol microbial synthesis of *E. coli*. 90

Figure 37. Schematic diagram of fed-batch, *in situ* resin based extractive microbial synthesis 91

Figure 38. Schematic diagram of two-stage, fed-batch, *in situ* extractive microbial synthesis 93

Figure 39. Phloroglucinol toxicity screening of W3110serA(DE3)/pJA3.131A 95

Figure 40. *E. coli* phloroglucinol production from microbial synthesis. 96

Figure 41. *E. coli* phloroglucinol fed-batch extractive microbial synthesis profile 96

Figure 42. *E. coli* phloroglucinol single stage fed-batch extractive microbial synthesis profile 97

Figure 43. *E. coli* phloroglucinol two stage fed-batch extractive microbial synthesis profile 97

Figure 44. *E. coli* phloroglucinol five stage fed-batch extractive microbial synthesis profile 98

Figure 45. Ideology behind use of transcriptome analysis 99

Figure 46. Affymetrix genechip microarray technology 100

Figure 47. Transcriptome analysis of *E. coli* after addition of phloroglucinol 101

Figure 48. Plasmids pJA3.131A and pBC1.146. 102

Figure 49. Transcriptome analysis of induced phloroglucinol producing *E. coli* 103

Figure 50. Corresponding up-regulation twofold and greater in phloroglucinol producing and phloroglucinol added transcriptome analyses. 106

Figure 51. Corresponding up-regulation of transport or membrane protein encoding genes fourfold in phloroglucinol producing and phloroglucinol added transcriptome analyses. 109

Figure 52. Sensitivity experiments of gene deletion, phloroglucinol producing strains . 111

Figure 53. Controlled insertion of the T7 *phl*D genetic region into pKD3 113

Figure 54. Wanner-type insertion of T7 phlD into the lacZ orf on the chromosome of *E. coli* W3110(DE3). 114

Figure 55. Construction of plasmid pBC2.179 en route to pBC2.187 117

Figure 56. Construction of plasmid pBC2.187 118

Figure 57. SDS-PAGE analysis of BL21serA(DE3)/pBC2.187 120

Figure 58. SDS-PAGE protein solubility analysis of BL21serA(DE3)/pBC2.187 121

Figure 59. Codon optimization for expression of *P. fluoroscens* Pf-5 phlD in *E. coli*. ... 123

Figure 60. Construction of plasmid pBC2.212 en route to pBC2.219 124

Figure 61. Construction of plasmid pBC2.219. 125

Figure 62. Specific activity comparison for induction time and temperature 126

Figure 63. Construction of plasmid pBC2.252 en route to pBC2.257 127

Figure 64. Construction of plasmid pBC2.257. 128

Figure 65. Construction of plasmid pBC2.271 en route to pBC2.274 130

Figure 66. Construction of plasmid pBC2.274. 131

Figure 67. Yeast extract supplementation effect on microbial synthesis 132

Figure 68. Crude lysate specific activity comparison of wild-type, in house optimized, and DNA2.0 optimized phlD with and without supplementation 133

Figure 69. Keto-enol chemistry of phloroglucinol. 140

Figure 70. pH dependent equilibration of tautomers. 141

Figure 71. Phloroglucinol reduction to resorcinol. 141

Figure 72. Catalytic deoxygenation reactions of polyhydroxyarimatics. 142

Figure 73. Schematic diagram of *in situ* resin based extraction. 144

Figure 74. Density effect on elution. 153

Figure 75. Downstream processing for phloroglucinol production. 156

Figure 76. Phloroglucinol process from biosynthesis to product isolation 157

Figure 77. Pretreatments and hydrogenations of phloroglucinol 159

Figure 78. Schematic diagram of a two-stage continuous extractive microbial synthesis. 198

Figure 79. Gene knock-out strategy 212

LIST OF ABBREVIATIONS

AFEX	Ammonia fiber expansion
Ap	ampicillin
Ap^R	ampicillin resistance gene
ATP	adenosine triphosphate
bp	base pair
BSTFA	*N*,*O*-bis(trimethylsilyl)trifluoroacetamide
CIAP	calf intestinal alkaline phosphatase
Cm	chloramphenicol
Cm^R	chloramphenicol resistance gene
D.O.	dissolved oxygen
DTT	dithiothreitol
Flp	flipase
FRT	flipase recognition target sequence
GC	gas chromatography
h	hour
HPLC	high performance liquid chromatography
IPTG	isopropyl β-D-thiogalactopyranoside
Km	kanamycin
Kan^R	kanamycin resistance gene
kb	kilobase
kg	kilogram

LB	Luria-Bertani medium
M	molar
mg	milligram
mL	milliliter
μL	microliter
mM	millimolar
μM	micromolar
min	minute
mRNA	messenger RNA
NMR	nuclear magnetic resonance
OD	optical density
OOMT	orcinol *o*-methyl transferase
ORF	open reading frame
PCR	polymerase chain reaction
pfu	plaque forming units
PG	phloroglucinol
PID	proportional-integral-derivative
POMT	phloroglucinol *o*-methyl transferase
ppm	parts per million
psi	pounds per square inch
RBS	ribosome binding site
rpm	revolutions per minute
rt	room temperature

SAM	*S*-adenosylmethionine
SDS	sodium dodecyl sulfate
SDS-PAGE	SDS polyacrylamide gel electrophoresis
tRNA	transfer RNA
TMS	trimethylsilyl
TSP	sodium 3-(trimethylsilyl)propionic-2,2,3,3-d_4
UV	ultraviolet
V_{max}	maximal velocity
yr	year

CHAPTER ONE

Introduction

Bioeconomy

Eyes have been widened and minds are realizing the detriment humans have caused to this Earth. In a closed system in which epitomizes the Earth, resources are limited and wastes are accumulated. Education, awareness and action will determine not only the lives of 6.7 billion, but the livelihood of one planet. Even though population and greenhouse gases are on the rise with average temperatures and sea levels following suit, there is some light in renewable trends and investment that will allow for a more sustainable future. In 2006 renewable sources accounted for 18% of the energy consumption worldwide and is broken down into the sectors outlined in (Figure 1).[1] More than $100 billion were devoted to renewable energy assets, manufacturing, research and development with growth in renewable technologies and industries of 20-60% yearly. 65 countries have goals for a sustainable future and are legislating towards these goals.[1]

Sources of carbon for manufacturing feedstocks and their uses in chemical production spawn emissions that contribute to global warming. The greenhouse gases role are commonly misunderstood because of the misnomering analogy of what happens realistically in greenhouses.

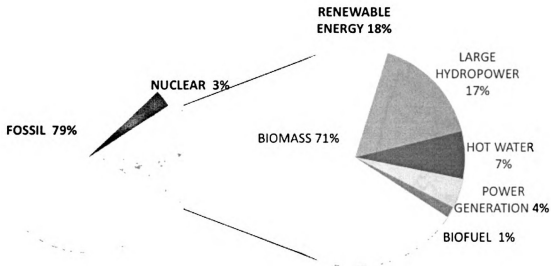

Figure 1. Worldwide energy consumption sources.

fossil fuels = petroleum and coal based: nuclear energy = splitting or fission of atoms: biomass traditionally = unprocessed agricultural waste, forestry product waste, collected fuel wood and animal dung that is burned: modern biomass = biomass co-generation, gasification, anaerobic digestion and liquid biofuels: hydropower uses gravity driven water flow to generate electricity: hot water = solar heated water from rooftop panels or geothermal avenues: power generation = electricity primarily used from wind turbines.

The higher energy rays emitted from the sun are absorbed by the surface, dampened and irradiated back where molecules that can absorb the energy, mostly in the form of infrared light, that keeps the energy in our atmosphere. Fortunately nitrogen and oxygen do not readily absorb infrared light whereas water vapor, methane, carbon dioxide, ozone and nitrous oxide do, contributing to global warming. Humans are directly involved in the spike of atmospheric CO_2 through burning of fossil fuels and deforestation. The carbon emission forms are outlined in (Figure 2).

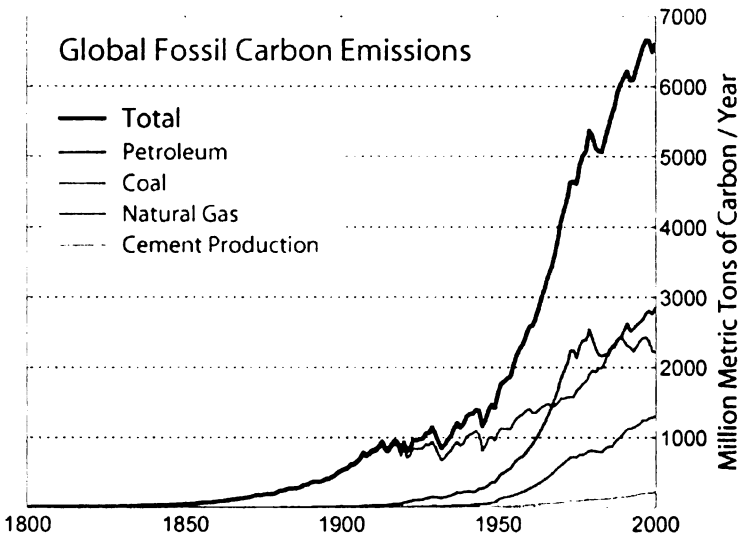

Figure 2. Global carbon emissions from fossil fuels.[2]

Commonly illustrated CO_2 emissions graphs indicative from the times of the pre-industrial era depict drastic trends in CO_2 production as in (Figure 2), and sometimes conveniently or not, leave out graphs that perceive a shift in CO_2 emissions that seem to peak every 100,000 years.[3]

Nature has had to attend with volcanic eruptions that have sent many greenhouse gases into the atmosphere, but until the last 150 years have unnatural sources been partially to blame. If as a society we can become closer to a carbon neutral lifestyle the Earth may reduce atmospheric greenhouse gases like it has for the last few hundred thousand years.[3]

Nevertheless, West Antarctica and the Antarctic Peninsula lost approximately 200 billion metric tons of ice to the sea in 2006 alone.[4] That is enough drinking water for the UK for 50 years or enough to raise the entire ocean 0.5 mm. The temperature of the Earth's surface, at current rate, will rise 3.2 °F every century supported by the fact that the top ten warmest years have occurred since 1990.[5] The answer to decrease global warming trends in the immediate future is to stop producing as much greenhouse gases and try to sequester what is already out there.

A lesson on efficiency can be taken from Brazil's bio-fuel market that uses streamlined processes that utilize every aspect of production wastes, offering an insight to how near perfect a process can be. Bioethanol, a product in the US currently produced by fermenting the sugars found in corn, drastically wastes product considering only about 30% of the kernel's mass is used of the entire plant, besides some of the stover dried for animal feed, where Brazil grows sugarcane and wastes almost none.[6] Trucks, fueled by biodiesel from neighboring plants, bring in sugarcane that is stripped of any leaves and washed. The residual and treated process water from the plant are collected and used for irrigation. Five steam-powered crushers will then shred the cane to access the syrup. The syrup is concentrated, crystallized and centrifugated leaving behind pure white granular sugar. The Santa Elisa plant in Brazil produces 475,000 metric tons of sugar per year, which leaves in 1-metric-ton sacks.

To make ethanol, a crude stream of the cane syrup from the crushers is diluted to a 20% sugar solution and pumped into large fermentation vats directly without the use of enzymes. Over 8 hours, yeasts ferment the sugar to a 6 to 10% ethanolic, aqueous solution. The yeasts are then removed and either recycled to ferment more sugar or dried

and sold as animal feed. The ethanol is distilled and dehydrated in stages to greater than 99% purity, denatured, loaded into biodiesel driven tanker trucks and delivered to fuel distributors.

The fibrous, grass-like fluff left over from the sugarcane crusher is sent along on conveyers to furnaces where it is burned to produce steam (which may have a particulate inhalation health risk[7]). The steam, in turn, powers the crushers and other equipment at the facility and turns a set of generators to make electricity. While bioethanol plants in the US typically only consume electricity, the Santa Elisa plant in Brazil generates 60 MW of electricity. About 19 MW is used to power the plant while the remainder is sold to power local towns. The residual ash from the furnaces is spent on sugarcane fields supplying the sole fertilizer. Although burning and fermentation exhausts CO_2, given that all machinery run on the biomass derived fuels and the plant runs on and diverts electricity, the entire process must have no net CO_2 production because the sugars fermented are in essence sequestered CO_2. Plant matter is composed of more than 1/3 cellulose, which is the largest organic matter on the planet and some plants (i.e. cotton) contain over 90% cellulose. Cellulose is a biopolymer made from the monomer D-glucose, which is constructed during photosynthesis in plants. The overall reaction of CO_2 sequestration in the Calvin cycle is $6CO_2 + 12H_2O + \text{light} \rightarrow \text{D-glucose} + 6O_2 + 6H_2O$. If the Brazilian plant is completely run on the products of their crop, all the CO_2 that is released during ethanol production with inclusion of CO_2 production from the burning of the ethanol fuel

in vehicles, the net CO_2 production is at worst a fraction of what was sustainably captured in the short time-frame allowed for the growth of the plant.

The shift from fossil fuels to renewables is not a one-man show. A diversity of sources will need development to steer society away from petroleum, curb greenhouse gas production and not derail into a struggle for survival on a desolate planet. Building 1.5 million wind turbines could satisfy 40% of the Earth's energy needs, 250,000 acres of US land in the southwest could be used for solar panels harnessing as little as 2.5% of the Btu's that are received in that area to satisfy our electricity needs and biomass could drastically cut our need for fuels.[8] With the boom in renewable energies, caution must be constant as recently green marketing processes offer carbon off-sets that can be somewhat deceptive.[9]

When government gets involved in renewable energy bills, linking energies and climate change with mandated reductions in emissions or fuel usage etc. the US is at much debate.[10] With expectations for drastic change in limited time the US inevitably looks at high costs for change through many avenues. High costs to corporate America can lead to even more jobs leaving the US for countries whose regulation are not as strict. For example, energy legislature enacted towards the end of 2007 requires the production of 36 billion gallons of fuel ethanol by the US in 2022 with 15 billion from corn and 21 billion from cellulosic feedstock. The US burns about 140 billion gallons of gasoline a year and about 7 billion gallons of ethanol are produced from corn with no commercial processes in cellulosic ethanol.[11] This initial deadline, though needed, may have the ethical issue of diverting a food source towards fuels. The cost of corn has almost tripled in the last five

years to just less than $6/bushel due to ethanol fermentation and the prices of some foods related to this animal feedstock have already shown reflection. The immediate threat is realized, but may be curbed by the decrease of shipping costs that are eminent from the use of ethanol, that can drop the price of a gallon of bioethanol to a projected $1.50/gallon. In many of the following arguments it is important to note that it is not fair to equate one gallon of ethanol to one gallon of gasoline though in today's engines, because on average ethanol only possesses that energy output equivalent of 60-70% that gasoline does. This offset in price of corn to ethanol, instead of as a source for food and the evolution of engines tuned for ethanol burning will only be determined in the future.

Ethanol is not only envisioned from fermentation from sugars, but also syngas. Syngas is a hydrogen and carbon monoxide mixture currently produced from steam reforming natural gas or the gasification of coal. Researchers are now looking towards pyrolysis of biomass to make syngas.[12] Coskata, a start up biofuels company funded partially by Khosla ventures, announced at the Detroit Auto Show that their ethanol production from syngas, with a delivery cost of $1.00 per gallon, would be cheaper compared to the $2.00 per gallon selling price at wholesale.[13] Coskata claims a production method that uses syngas for a fermentation feed that could be derived from burning tires and municiple or agricultural wastes.

At the forefront of biofuels debates and discussions are our own Michigan State University's Bruce E. Dale alongside David Pimentel from Cornell respectively as the pro and con.[14] Dale points out that two ideas are crucial in any talk concerning petroleum replacement, deviation from dependence on resources from mostly third world countries and climate security. He continues to show decreases of greenhouse gases and energy

inputs to produce 1 MJ of ethanol even now from corn, let alone cellulosic sources, compared to production of 1 MJ gasoline. The processes for capture of D-glucose are rapidly improving which would even further detract people from use of gasoline. Pimentel exhaustively talks about the point that with all the available resources that only a fraction of US consumption is possible when we would be at maximum ethanol production from corn and that food prices will increase while other resources such as fertilizers and irrigation water will be problematic. Pimentel argues that the energy input to make ethanol is 40% more than what it supplies when you factor in farm labor, machinery, genetically engineered seed, irrigation and processing equipment. There is also debate on how much by-product 10-60% can be used for cattle feed. Pimentel then states about the increase in the prices of meats, eggs and milk from food diversion and the extra CO_2 produced during fermentation. Dale fires back refuting Pimentels flawed approach which relies on energy equalities of coal, gasoline and ethanol and that another overlooked view of resources would be the cessation of military assets guarding our oil pipelines and reserves. Dale mentions that Pimentel's views on how labor intensive cellulosic ethanol production is shared only by few and that leftover biomass could be used to steam power electricity production cutting costs further, while significant increases in switch-grass yields per acre are probable for land usage. In a last point by Dale, he mentions how wealth could be brought to rural communities because cellulosic material would be bulky enough to entice factories to be set-up close to the growth source.

Fact is, renewable energy sources are becoming more attractive, evident from increases in renewables research funds[15], the decline of crude oil in viscosity, (which limits the quantity of unreformed lighter fractions) and higher levels of sulfur that need to

be removed. The desulfurization process may have some new insights that help with the discovery that large aromatics may be blocking catalyst active sites in which chemists could design better catalysts.[16] The heavier fractions will take in even more energy to produce than what the finished product will give (gasoline production even now is slightly energy negative).

Perennial grasses are one of the frontrunners for cellulosic energy sources (Figure 3). A recent study indicates that more than enough cellulosic ethanol could be produced on a per-acre basis to offset the energy needed to grow and convert the grass to fuels.[17] Advantages for grasses include that they are fast-growing, hearty, tall, pest resistant and can grow on marginal land or cooler climates with extremely limited fertilizers. Over a period of five years Vogel from the University of Nebraska has harvested 10 farm sites in fields up to 23 acres in size keeping track of all costs associated.[18] On average 320 gallons of fuel ethanol would have been produced per acre. Vogel states an energy gain of 540% energy compared to the fossil energy required to produce ethanol. The current switchgrass crop yields were achieved in the same years, in the same states, as corn devoted to biofuels. With further increases in switchgrass genetics and growth conditions they will drastically overtake current corn practices in usable plant mass. Critics are only concerned with some of the calculations used, based upon theory and not actual data in the conversion of cellulosic material to glucose.

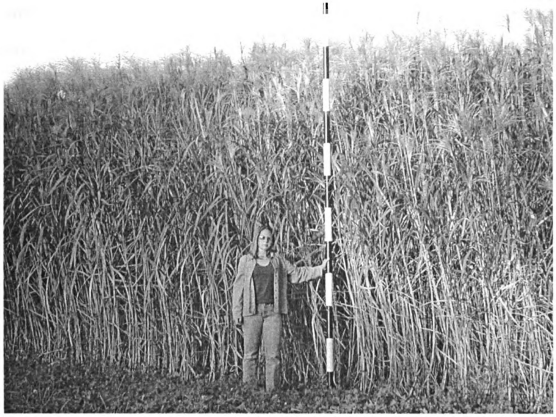

Figure 3. Miscanthus growth after 1 year.[19]

Another sought after source to cellulosic ethanol are softwood trees and by-product waste from forestation. These feedstocks can be used similarly to the plans for switchgrass with the enzymatic breakdown to sugars to be used in fermentation. Trees do have the added advantage of cellulose density that would aid in transportation and presumably in total acreage devoted to biofuels. The downfall to use of varying feedstocks can be the ideology that optimal enzymes can mostly be efficient on one type of feedstock. Converting biomass into syngas could be beneficial because one production plant could take in limitless types of feedstock wastes of not only trees, but vegetation and other wastes as well. Range Fuels, another Khosla Ventures investment, is breaking ground on a cellulosic ethanol production plant in Soperton, Georgia.[20] Range Fuels is

invested in thermochemical breakdown of biomass that uses gasification wherein heat and oxygen or steam is used to break down biomass to syngas. Use of established Fischer-Tropsch type chemistries would then be conducted for fuel production. ConocoPhillips, mostly recognized as working on the biochemical conversion to sugars, recently has dumped some money into thermochemical processing and are on the verge of commercializing thermal processes to convert soybean oil or animal fats into bio-diesel and propane. Thermochemical processes are not a complete answer though, because it was estimated that all of forestry in Georgia could supply 2 billion gallons of ethanol per year, a far cry from the 140 billion gallons of gasoline consumed every year. It is facile to think that both fermentative and thermochemical processes could be synergistic.

Other renewable sources of energy exist that have followers. The current US consumption of hydrogen gas is about 50 million metric tons, mostly used for the production of ammonia fertilizers and chemical refining.[21] Most hydrogen is produced by steam reforming methane or lighter hydrocarbons, with smaller fractions made from coal and even less from electrolysis. Hydrogen can be produced biologically by algal and cyanobacterial photolysis of water, fermentation of acidogenic bacteria and thermophilic organisms.[22] At current technology hydrogen can be produced at about four times the cost of gasoline[23] and when compressed to 10,000 psi hydrogen occupies 8 x the equivalent volume of a gallon of gasoline (it is disregarded that the energy given from one gallon of gas would not equal one gallon of compressed hydrogen at 10,000 psi).[24] Liquification is too energy intensive to maintain at -253 °C. Owing primarily to liquifaction difficulties and storage, most hydrogen is produced on site for consumption with options[25], feasibility

and delivery discussed elsewhere.[26] Solid supports for hydrogen storage seem to be a plausible answer to shipping and compression issues if cost and safety can be shown.[27] Research for the hydrogen economy is strong owing to the benefit of use in every sector where energy is required, that it can be produced from multiple sources, that it could be stored almost indefinitely (ethanol etc. absorb water) and has the sole by-product of water upon burning for energy.

George Olah is one of the leaders in a methanol economy.[28] Methanol has chemistries to syngas, formaldehyde, acetic acid, olefins and dimethyl ether (possibly a cleaner burning diesel). Two of the largest chemical building blocks in propylene and ethylene can be derived from methanol. Coal-gasification is currently being investigated for large-scale production of methanol in the US, China and India which house more than half of the world's recoverable coal.[29] Biobased methanol was used as a fuel in Germany during World War II found by the thermochemical breakdown of wood (to harvest wood alcohol).[22] A biomass to biomethanol process using bacteria with sugar beet pulp as substrate was researched as well.[30] Dry sugar beet pulp contains about 60% (w/w) pectin of which contains methyl esters. Overexpressing pectin methylesterase from *Erwinia chrysanthemi* in *E. coli* produced methanol. Methanol can be used similarly to ethanol and has been used in Indy Racing League cars, which just recently moved to ethanol for promotion (and that the fuel is given at no cost).[31] Methanol has the added benefit to be used in fuel cells generating hydrogen, a concept tested in a cross-country drive by Daimler Chrysler's NECAR 5. A promising thought related to the methanol economy is

the recycling of CO_2 or oxidation of methane, especially what is burned off of oil wells or chemical flue gases, into methanol for use in fuels.

Often wrongly described as a "new fuel", biobutanol has been around since 1916.[22] Butanol is looked to have value as diesel and kerosene replacements, a silage preserver, biocides and a C4 chemical building block. Butanol has potential to be a fuel with advantages over ethanol in energy and blending with gasoline owing to ethanols enhanced ability to increase partitioning when wet. It was demonstrated in 2006 that butanol can be used in 100% to power unmodified 4-cycle ignition engines, blended at 30% in diesel engines and 20% (with kerosene) in a jet turbine engine.[32,33] *Clostridium acetobutylicum* was the first identified butanol producing strain, which was a no value by-product, along side ethanol, in the intended manufacture of acetone in World War I. Acetone was used in the production of cordite, a cartridge and shell propellant.[22] A modern biobutanol, fermentation facility is being built by BP and DuPont that will likely heterologously express the clostridial genes responsible for butanol production in a more tolerant host organism.[34] Initially the renewable feedstock will be the previously mentioned sugar beets.[33] The economic aspects of butanol and other options for microbial hosts are discussed elsewhere.[35]

Bioethanol process

The bioethanol process will ultimately be the driving force for other microbial syntheses as technology for D-glucose capture from biomass is greatly improved. In the

long run, biofuels research should further decrease the already low price of D-glucose. The largest production cost reductions of ethanol in the immediate future will rely on technological advances in the realm of converting biomass into fermentable sugars.[36] According to the cited literature corn ethanol, in terms of equivalent energy output, is already produced cheaper than petroleum feedstock gasoline and cellulosic ethanol could more than halve the corn ethanol price with added benefits of land used for growth, fertilizers and other benefits discussed previously. Feasible land usage for biomass cultivation is reasonable and fermentation by ethanologenic yeast strains, *Zymomonas mobilis, Klebsiella oxytoca,* and *E. coli* are mainstream.

Biomass processing in microbial organisms involves four key steps: the production of saccharolytic enzymes (cellulases and hemicelluases), hydrolysis of pretreated biomass to sugars, fermentation of hexose sugars and the fermentation of pentose sugars. Some envision, and would make a stone-clad case for a sustainable and highly lucrative process, a single microbe that is capable of all four steps termed consolidated bioprocessing.[37]

Cellulase, an enzyme concoction required for the hydrolysis of cellulose, is a target of the US Department of Energy. The cost estimate for cellulase is about 30 to 50 cents per gallon of the ethanol cost.[38] Currently most cellulases are produced by *Trichoderma* and *Aspergillus* species.[39] Cellulases are already used in the cotton industry as a softening agent and in denim finishing; in detergents for color care; cleaning; mashing in the food industry; and in the pulp and paper industries for de-inking, drainage improvement and fiber modification.[40] The widely accepted mechanism involves the synergistic degradation of cellulose by endogluconase, exogluconase or cellobiohydrolase and β-glucosidase. Endogluconases hydrolyze accessible intramolecular β-1,4-glucosidic

bonds to free chain ends, exoglucanases cleave cellulose chains at the end to produce cellobiose and β-glucosidases break down cellobiose to glucose. It is dangerous to compare activity correlation due to heterogeneity of biomass, even from the same source with the same pretreatment, the complex dynamic interaction between the three separable enzymes required and the insoluble biomass. Two basic results are being followed for improvement through rational design and directed evolution with additional comments on assay conditions in reference 40.

A percentage of influence of biological improvements on the ethanol process is presented in (Figure 4). It is important to note that ease of percentage gain is not correlated to ease of success. It is most likely easier to get two-fold improvement in cellulase activity and gain the 13% reduction in cost than to have a consolidated bioprocess that would likely take much more effort to achieve with the 41% reduction in process cost.

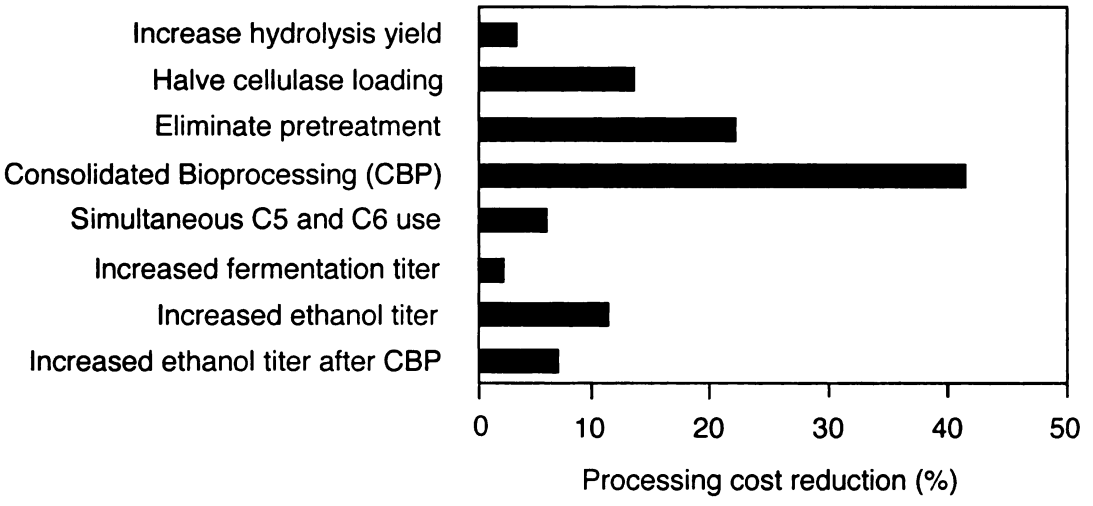

Figure 4. Reduction in cost for various technological advances.[36]

(Reproduced) Values represent the average for the indicated advance relative to two-base configurations (Figure 5 and Figure 6) scenario 1 at 2,205 dry tons feedstock/day; scenario 2 at 5,000 dry tons feedstock/day. Error bars denote the range of processing costs reductions for each scenario. (for a more detailed description see ref. 36)

Bruce E. Dale is one of the leaders in many bioeconomy references, the associate director of the Office of Biobased Technologies at Michigan State University and the editor-in-chief of Biofuels, Bioproducts and Biorefineries, a new Wiley journal. Dale in many works attempts to work hand-in-hand, thermochemical breakdown of biomass and enzymatic hydrolysis of cellulose to fermentable sugars. Corn stover, switchgrass (*Panicum vergatum)* and giant chinese silver grass (*Miscanthus gigateus*) were investigated in the thermochemical breakdown and subsequent enzymatic saccharization.[41,42,43]

100 million dry tonnes of corn stover is achieved yearly.[44] Various current pretreatments to clarify cellulose depletes nutrients and before introduction to microbial organisms, must then be supplemented with rich laboratory media for saccharification.

The leftover dried grains and solubles are shipped off as animal feed. If the cellulose is more accessible than in unprocessed biomass, supplementation would not be necessary because the dried grains and solubles in the hydrosylate have more than enough nutrients for the cellulase enzymes. Ammonia fiber expansion is one of the leading technologies for blowing apart biomass.[45,46] Leaving the nutrient rich dried grains in the unclarified, masticated biomass allows enzymatic access to the cellulose without addition of nutrients. After treatment with cellulase, fermentation with an a evolved, ethanologenic *E. coli* strain (which may not be the optimal choice for ethanol production) did ferment ethanol near the theoretical limit of 0.51 g ethanol/g consumed sugar from cellulosic hydrosylates at 36-51 g/L glucose at a rate of 1.2 g/L/h from corn stover.[43]

The ammonia fiber expansion occurred in a 300 mL Parr apparatus with optimized conditions for switchgrass being 100 °C, an ammonia loading of 1 kg ammonia : 1 kg biomass with an 80% moisture content for 5 min. Rapid release of pressure explodes the biomass apart. Glucose and xylose conversion was 93% and 70% compared to untreated conversions of 16% and 3% with a total ethanol production after treatment with cellulase of 0.2 g ethanol/1 g dry biomass. From the same lab a slightly modified approach allows some of the protein to be extracted for animal feed.[47]

The ammonia fiber expansion occurred in a 300 mL Parr apparatus with optimized conditions for *Miscanthus* being 160 °C, an ammonia loading of 2 kg ammonia : 1 kg biomass with an 233% moisture content for 5 min. Glucose and xylose conversion was 96% and 81%. The total ethanol production was not reported and there were some additional additives compared with switchgrass.

A process outlook schematic would look something along the lines of (Figure 5). Scenario 1 is based on current technology and could be implemented within a year. Scenario 2 uses incorporation of advanced, non-biological technologies into the scope of Scenario 1.

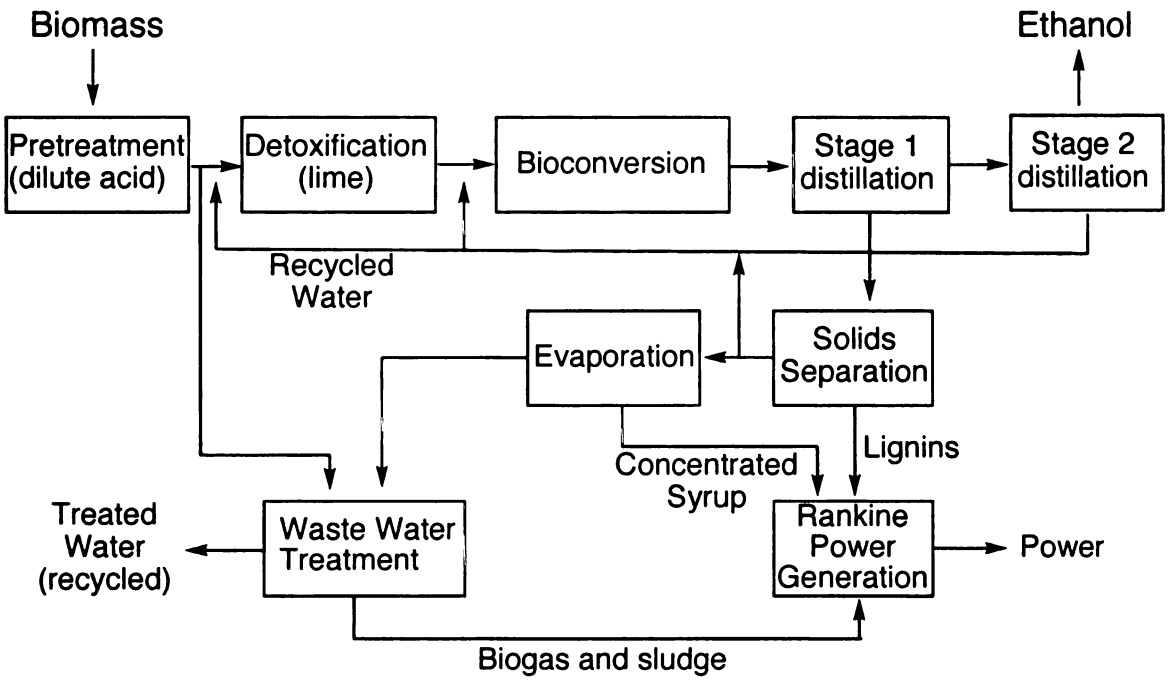

Figure 5. Current capabilities of the biofuel production process[36]

(Reproduced) Schematic diagram of scenario 1: feedstock biomass is pretreated with dilute sulfuric acid; pretreated material is mixed with lime to adjust pH and remove inhibitory compounds for downstream biconversion; ethanol is purified by two-column distillation and molecular sieve adsorption; residual solids are removed from the distillation bottoms liquid and fed to a power plant boiler; distillation bottoms liquid is concentrated by evaporation with the resulting syrup also being fed to the boiler; remaining wastewater is treated on-site by anaerobic digestion and recycled to the process.

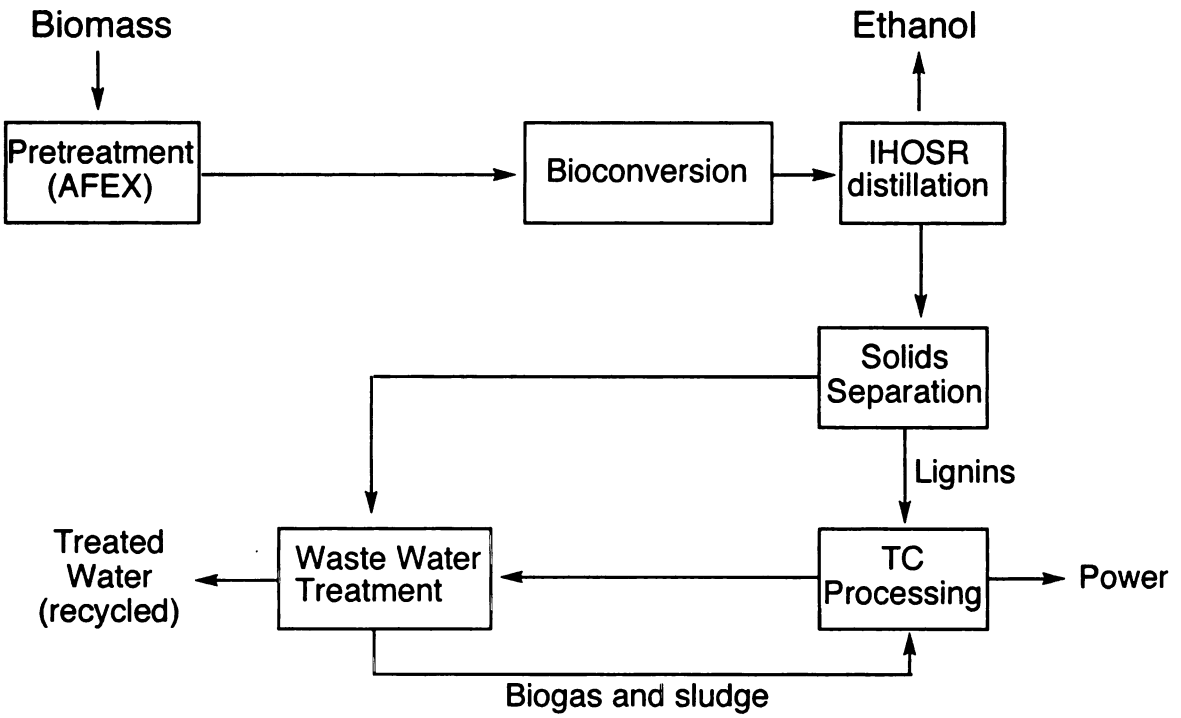

Figure 6. Future capabilities of the biofuel production process.[36]

(Reproduced) Schematic diagram of scenario 2: feedstock biomass is pretreated with ammonia fiber expansion and delivered directly to bioconversion with no detoxification; ethanol is purified using a single-stage intermediate via heat pump and optimal sidestream return (IHOSR) and molecular sieves adsorption; residual solids are removed from the distillation bottoms liquid and fed into a thermochemical processing operation; distillation bottoms liquid is treated on-site by anaerobic digestion and recycled to the process.

CO_2 Sequestration

CO_2 sequestration is a daunting task in which initial responses looked towards pumping it beneath the ground. Burning of coal for electricity is responsible for one third of 26 billion metric tons, globally, of anthropogenic CO_2 that is released into our atmosphere yearly.[48] Experts look at 550 ppm of CO_2 in our atmosphere to be the threshold of no return. Currently hovering around 380 ppm, up 100 ppm from the

preindustrial era, experts expect that emissions need to decline before 2020 or 2030. Deviation from coal burning should be helped by production of wind turbines and solar cells, all of which in the meantime will take much coal-derived electricity to make. Pumping CO_2 underground is a trick that has already been used by oil companies to harvest residual oil in depleting oil reserves and North America already has some 3000 miles of CO_2 pipeline in existence. Initial studies indicate the 9.5 trillion metric tons could be sequestered in depleted wells and offer more compressed CO_2 for oil companies to use for financial gain in enhanced oil recovery. The authors unfortunately continue to make the remark that instead of dealing with the problem now that sequestration could warrant the continued use of coal burning. According to calculations made, the US has capacity for only about 3 years worth of global CO_2 production in unminable coal seams and depleted oil and natural gas reserves. The largest area, and therefore potential for CO_2 sequestration, is in deep saline aquifers in sandstone. The US could house about 150 years worth of global CO_2 production and seems the only option that is worth a breath of exhausted CO_2 to even talk about.

The Intergovernmental Panel on Climate Change report explains how CO_2 storage would be achieved in a saline aquifer.[48] Supercritical CO_2 would be injected through concrete-lined wells, past multiple geologic strata and below drinking water aquifers. There, deep in a sandstone saline aquifer, CO_2 is relatively buoyant compared with sandstone and formation brine. It would rise to the capstone, an impermeable rock

layer at the top of the reservoir. The CO_2 would dissolve into the aquifer's fluids, and over hundreds to thousands of years, the CO_2-laden water would become dense, sinking into the formation and precipitating to a solid carbonate mineral.

The largest scale sequestration projects are injecting CO_2 at two natural gas facilities: Statoil's Sleipner facility in the North Sea off the coast of Norway and BP's In Salah gas field in Algeria. At both sites, CO_2 is being stripped from natural gas and injected into saline aquifers at a rate of about 1 million tons per year. BP and Statoil are collecting some data on the behavior of the CO_2 in the aquifers, but the commercial operations are not designed for research. Starting in 2008, DOE researchers in partnership with universities and industry will inject some 1 million tons of CO_2 annually into saline aquifers at as many as a half-dozen sites. They hope to determine how quickly CO_2 dissolves in brine, where it circulates within the aquifer, and how much an aquifer can hold. They also hope to determine monitoring needs and whether large plumes of supercritical CO_2 can trigger earthquakes.

Ammonium bicarbonate has been used to scrub CO_2 from flue gas streams in a Wisconsin utility.[49] Flue gas containing less than 1% CO_2 is cooled and ammonium carbonate/bicarbonate equilibriums form allowing bicarbonates to crystallize out. The crystals are heated to regenerate the ammonium carbonate to recycle back into the flue gas stream and the CO_2 is compressed at more than 90% pure. This CO_2 capture,

however, the investors say is energy intensive enough that at mainstream this technology would use 25% of the plant's energy consumption. Unless this is energy from turbines or solar panels, is this not producing more CO_2 despite the fact that they still have compressed tanks of CO_2 to deal with? The investors also comment that if plants employed this technology it would likely double the price of electricity in the US.

If CO_2 was sequestered and made into a stable species chemically, that would be a solid at conditions in the aquifers that scientists plan on injecting gaseous CO_2, then focus should be diverted towards this goal. This landfill idea would satisfy CO_2 sequestration with a faint possibility of added costs, but bearing the assurance that in the event of a geological mishap would not release all of the CO_2 that's sequestration caused production of more CO_2 (in the energy required to pump it below the surface). Nature already made a way to chemically sequester CO_2 in plants. Burying plants underground should not be ruled out if degradation could be avoided. The temperatures of these aquifers are not optimal for most bacterial growth, and humidity is low which diverts thoughts of giant compost heaps. Planting trees instead of rapid deforestation and helping overpopulation here and abroad is where efforts need to be focused, but this does not garnish much attention presumably for the reason that it will not increase anyone's bottom line!

Biocatalysis

Catalysts either lower the activation barrier or raise the energies of the reactants to allow the realization of product with a minimum input of energy without a net loss or gain. Biocatalysis relies upon catalysts predominantly in the form of proteins, referred to as enzymes, for organic manipulations of substrates into compounds of greater value or importance. Whether catalysts used *in vitro* utilizing some level of clarified enzyme or *in vivo* enzymatic use in intact microbial organisms, biocatalysis can be a powerful alternative or complementary to classical organic synthesis.

Enzymes can seemingly without limits transform relatively un-reactive species with the right combination of energetic gains excluding major temperature fluctuations. Organisms are designed to optimally thrive in a limited temperature range and although temperature can drastically alter the outcome of the free energy, and thus the likelihood of whether a process will happen or not, it can only have minimal variance *in vivo*.

Some of the ideas that allow enzymes to convert un-reactive species cross the gamut, including orbital steering, orientation, solvation, transition state complimentarity, acid/base/nucleophilic catalysis, electronic stabilization, intrinsic binding energies, strain, hydrophobicity, proximity and entropy among others.[50,51,52] With all of the added advantages that nature employs to lower the energy required to make a transformation possible, substrates still must contain that minimized amount of energy to commence reaction. Entropy is widely accepted as a major factor in enzyme catalysis first discovered by Linus Pauling.[53] In 1865 Clausius introduced the concept of entropy based on the claim that a cold body could not transfer warmth to a warm body. In the coming decades

Thomson, Gibbs, and Boltzmann also weighed in. Boltzmann helped define the second law of thermodynamics substantiated in the kinetic theory of gases with his H theorem coming from the mean logarithm of the particle distribution function. The Boltzmann H function is proportional to the entropy of a perfect gas. Boltzmann demonstrated that the entropy is related to the logarithm of thermodynamic probability. When exponentially compounded by electrostatic forces of molecules these simple logarithms become somewhat useless. It is well established that molecules occupy many vibrational, translational and rotational energies that give vastly different total energies that lead to energy patterns to exhibit a Boltzmann distribution. If the majority of this distribution of molecules has enough energy to react they need to be in proximity of the other reactant. When enzymes bind substrate the binding energy released compensates for the entropic loss associated and almost no entropy is lost during reaction, because the effective concentrations of reactants are extremely high.

The awe and diversity of enzymatic reaction are only trumped by the idea that their composition is solely based upon a limited amino acid makeup. Intermediates of reactants and products formed during enzymatic catalysis are orientations of molecules in definable states of higher energies that can be lowered by providing static or electronic stabilization or even bonding motifs. By increasing the ratio of the transition state to the ground state the enzyme effectively exhibits catalysis. Enzymes can also rule out much of the chance of reactants proximity. By lining up two molecules in proper orientation they are more likely to react in structurally engineered pockets elicited by a simplistic set of 20 naturally occurring building blocks. Nature also utilizes one of the most intriguing, universally reactive and abundant chemicals that conveniently acts in multiple modes of catalysis.

Water can act as an acid or a base, both of which are effective in catalysis, with the added ability of enhancing solubility of charged intermediates due to its polar nature. All of the simplicity that nature ingeniously utilizes combines it in a collage of complexity that are intrinsically difficult to probe. Enzymatic assays are often taken in dilute, homogeneous solutions where substrate binding constants are measured, selectivities are determined and inhibition properties are found. Within a cell the opposite scenario is true. Cells are densely packed with protein and exhibit massively diverse transcriptomes often shuffling substrates to other domains in intimate, heterogeneous protein-protein interactions. Notwithstanding is the fact that even though enzymes are tailored to accommodate preferentially a limited subset of potential substrates, often many substrates will compete for binding and have strong influences on overall states of enzymatic processes. Substrates may also have multiple proteins to which they can bind. If a weaker binding substrate is much higher in concentration it may readily compete for active site occupation. The overall balance of everything mentioned thus far is constantly changing at different rates with or without relation and gives rise to the reason that a thorough understanding of exact energy definitions are rather elusive, if not unattainable.

The potential energy surface diagrams of static proteins often depict ingeniously engineered pockets and binding motifs to accommodate rather specific substrates in some cases. The intimate relationship of an enzyme and substrate is usually one in which all of the combined binding motifs of ground states, transition states and products need be summed to allow the enormous task of surpassing an energy barrier eliciting reaction. Even with an enzyme's intrinsic use of a multiple-headed energy lowering plan, with the

battle of catalysis being an uphill fight in which energy is never in excess, one minor deviation in gained energy can cause enzyme deficiency.

Well understood enzymatic reactions composed of such limited makeup of primarily L-amino acids and sequences delivering secondary, tertiary and quaternary structures offer many advantages over classical synthesis in the form of selectivities. With three-dimensional binding pockets diastereomers can oftentimes be differentiated, while regioselection can be attained as well.[54] Reaction by-products can be rather limited in cases leading to enhanced efficiency of reaction recovery by selective organic transformation to a specific functional group when classical conditions may not selectively transform one group leaving another susceptible group unreacted. Enantioselectivity can be understatedly important especially in pharma where one purifed enantiomer is the active molecule in nine of the top ten drugs.[55] Asymmetric catalysis can be achieved in many cases and have influenced mimicry by classic syntheses[56] alongside kinetic resolution.[57] While making enantiopure chemicals is powerful in a few instances, racemizing chemicals achievable by some enzymes, can have benefits in certain areas.[58]

The enzymes utilized in *in vitro* biocatalysis can be crude, partially purified or what is to be considered homogeneity by a defined purification level. Solubility in media and finding purification, that in the end must retain activity are oftentimes energy and cost intensive which can be the downfall to industrial use.[59] Recombinant methods, such as introduction of plasmid bearing genes, can drastically increase levels of protein over genomic expression that aids in the ratio of protein sought after versus the level of crude background protein. Proteins themselves oftentimes require expensive and usually labile

cofactors, endogenously supplied from a host organism in nature, which must be externally added for a proper protein environment or catalytic state that can preclude their widespread use for many chemical productions. Whole-cell biocatalysis can express multiple protein encoding genes without the addition of expensive co-factors. The downfalls of microorganism chemical production can be the time and resource involvement in research and development compared to classical synthesis. Thorough understanding of many experimental observations can lead one down tedious paths of investigation. Magnitudes more variables exist when working with viable organisms when it comes to finding out why something was perceived. Is it because the molecule is not stabile in cellular environments, is the molecule toxic, is a precursor limiting, is transport a problem, is gene expression or protein translation inhibitory, is the gene expressed at the correct level, is the cell limited by co-factors or minerals, are the cells induced at the correct phase in their life cycle, are the cells production at the correct temperature, is the right host organism being utilized, are metabolic paths competing for substrate and are there precedent tools for host manipulation are just of the few of the questions asked in every biocatalytic production. Research using biological systems can pay off in big ways because of what the results can reap in process costs reduction. The benefits of using live machinery for chemical production are the mostly innocuous and oftentimes biodegradable waste streams, utilization of aqueous low-salt solutions for solvent with reactions at ambient temperatures and pressures. The viability of whole-cell biocatalysis hinges upon the metabolic effects of small molecule production, the chemical tolerance of the host organism and the transport machinery to extrude the molecule without osmotic stress. Biocatalysis often utilizes sugar or metabolic sugar derivatives as

building blocks that garner immediate attention in light of the current hike in non-renewable building block feedstock.

Chemical manufacture

About 13% of crude oil, that just topped the feared $100/bbl mark recently, is used for non-fuel chemical manufacture.[60] With most of the biomass attention looking towards replacement of transportation fuels[61] it is also important to cover this other 13% that has potential to be a more rapidly transformed area with a modest impact. As a starting point for potentials to chemicals, building blocks or intermediates, in 2004 the staffs at the Pacific Northwest National Lab (PNNL) and the National Renewable Energy Laboratory (NREL) put together a list of the top value added chemicals that could be produced from biomass through utilization of sugars or syngas derived from pyrolysis.[62]

Current commodity chemicals produced from microbial synthesis include glutamic acid, citric acid, and lysine all consumed at quantities close to or above 1 billion kg/year.[63] At 16,000 ton per year production indigo is used to dye denim. Chemically, phenylglycine is reacted in KOH-NaOH with $NaNH_2$ at 900 °C making indoxyl, which spontaneously oxidizes to indigo.[64] With heterologously expressed naphthalene dioxygenase from *Psuedomonas putida* in *E. coli*, Genencor developed the route from D-glucose. Siphoning off of indole in the tryptophan biosynthetic pathway was achieved by naphthalene dioxygenase for conversion to indoxyl, which just as in the chemical manufacture, oxidizes to indigo. 1,3-propanediol, the building block of

polypropyleneterephthalate (PPT) out of Genencor and DuPont is produced from biomass.[65] In the final construct, four genes required for 1,3-propanediol microbial synthesis were heterologously expressed in *E. coli* to currently produce product in titers of 129 g/L at 34% yield (g 1,3-propanediol / g D-glucose). Other polymers could be formed by methyl lactate, lactide or polylactic acid which can be chemically derived from microbially synthesized lactic acid.[66] Polylactic acid is a potential replacement for polyethyleneterephthalate (PET) that also has the benefit of being biodegradable. Maleic anhydride, used in solvents and polymers, could be replaced with succinic acid derived from renewables.[67] Adipic acid in Nylon 6,6 could be chemically derived from cis-cis muconic acid in technology developed in the Frost lab.[68]

One of the most important raw materials for chemical manufacture comes to the US in the form of petroleum based aromatics that lead to the production of many of America's commodity chemicals including plastics, fibers, rubbers and biologically active drugs.[69] Benzene, toluene and xylenes are the lightest aromatics and were originally produced with the pyrolysis of coal. During WWII, with the onset of gasoline production, the aromatics were siphoned off reformate streams. Aromatics are a large component of gasoline having high "octane ratings" and although there are specific sequestrations of aromatics from crude oil, they are largely produced as a gasoline additive. Reforming of the naphtha layer (bp of 70-190 °C) of crude oil, hydrocarbons of primarily C_6-C_{12} are vaporized, with temperatures and pressure ranges from 450-550 kPa and 470-530 °C, and passed through a 1% platinum catalyst on a high surface area acidic support such as alumina. A typical reformate contains a 20:50:30 mixture of benzene:toluene:xylene.

Toluene, which makes up the majority is dealkylated to form larger amounts of benzene.[70] The uses of major aromatic feedstocks are outlined in (Figure 7). In 2005, the U.S. produced 1,828 x 10^6 gal of toluene.[71] Of this total, 76% was used in the production of benzene and xylenes. In 2006, world capacity of benzene reached 48 x 10^6 ton. Production of ethylbenzene, cumene, and cyclohexane accounted for 85% of the benzene produced.[72] In 2004, 9,745 x 10^6 pounds of *p*-xylene were produced in the United States. Of this, 77% was used to produce dimethyl terephthalate.[73] Benzene is a known carcinogen and exposure has been evident to lead to both acute leukemia and non-Hodgkins lymphoma.[74] A mandate by the Environmental Protection Agency has outlined the limitations for future benzene emissions.[75]

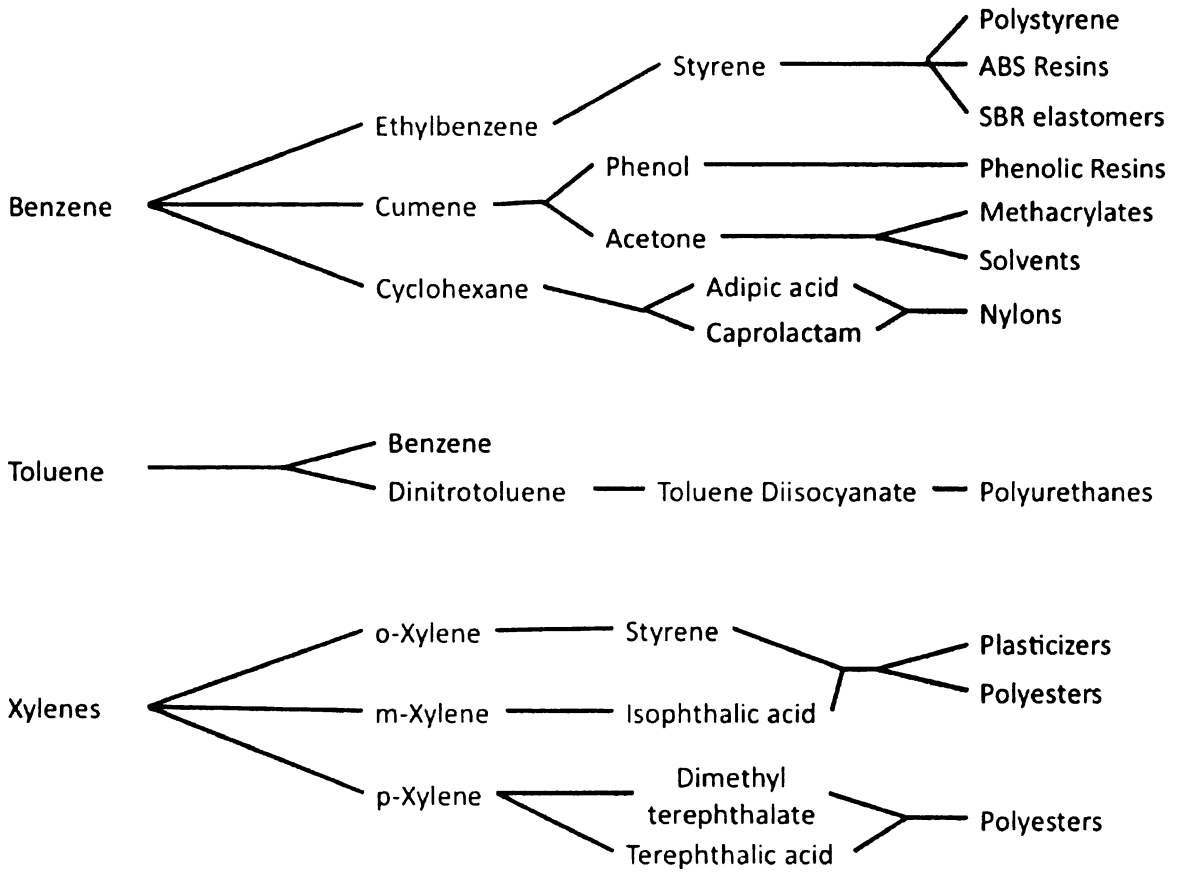

Figure 7. Major products of aromatic feedstocks.

An alternative to aromatic feedstocks could take advantage of the largest biopolymer on Earth. Cellulose gives a densely packaged substrate in D-glucose that is currently made from the depolymerization of starch[76] and hydrolysis of hemicellulose offers D-xylose[77] and L-arabinose.[78] Another important feedstock, especially in light of the fact that D-glucose prices will probably increase in the immediate future owing to the siphoning of ethanol to biofuels, is glycerol whose prices are decreasing rapidly. Glycerol is a direct by-product in the manufacture of another biofuel, biodiesel. Biodiesel is a sustainable and renewable alternative to conventional petrodiesel that upon combustion comparatively releases less CO_2. Different plant oils and animal fats are transesterified to

use short chain alkyl esters in unmodified diesel engines as a blend or even straight. The transesterification by-product is glycerol that is dubbed a limited value by-product. Glycerol may play an immediate role in production of epichlorohydrin, propylene glycol and polyurethanes.[63] Glycerol could however, be a sole-carbon source for many microbial organisms. All the mentioned substrates have been used in microbial synthesis, some of which in the Frost lab, en route to a multitude of valuable chemicals normally derived from petroleum.

Hydroxy aromatics

Many of the less densely hydroxylated benzenes are currently known to be derived from microbial synthesis either from a direct biocatalysis, catabolism of a precursor or chemical manipulation of biosynthesized substrate. Outlined in (Figure 9) the boxed aromatics offer syntheses from renewables from the Frost lab. Manipulation of the shikimate pathway (Figure 8), used for aromatic biosynthesis in *E. coli*, yields access to catechol[79], hydroquinone[80] and pyrogallol.[81]

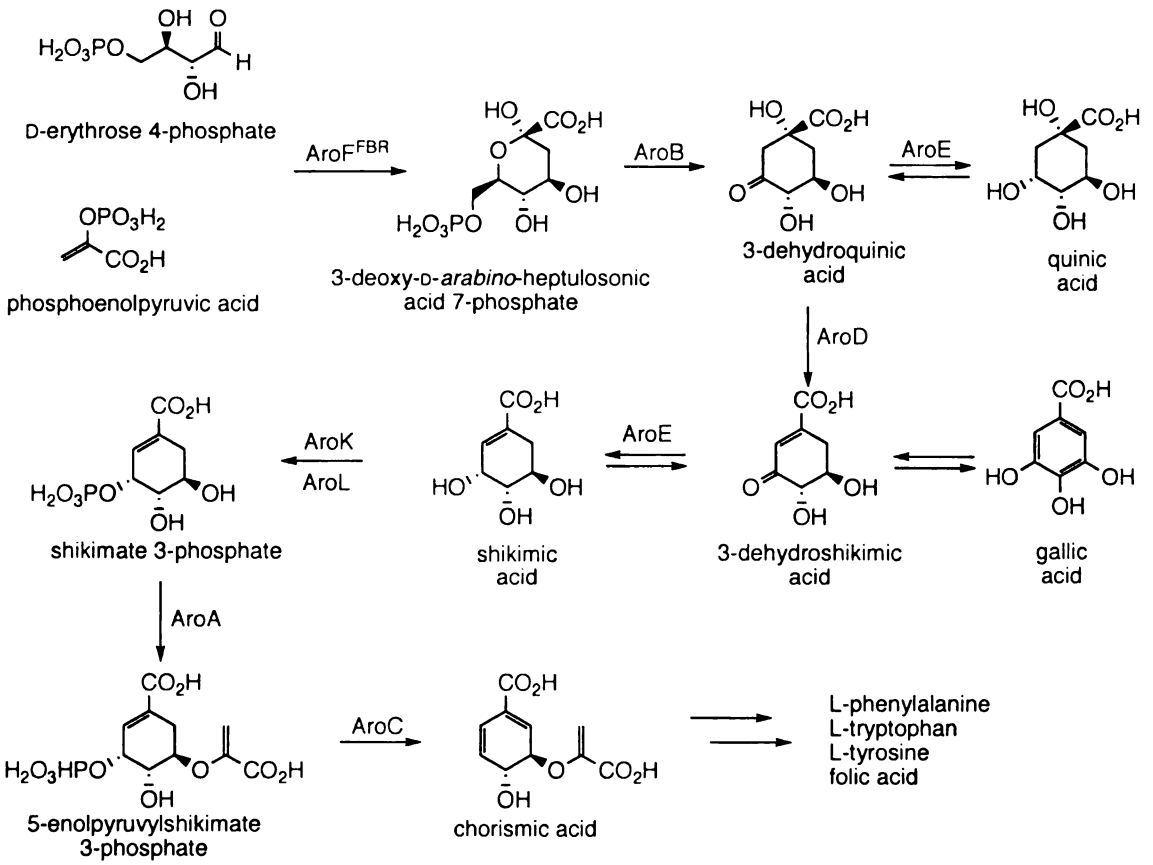

Figure 8. Shikimate pathway for aromatic amino acid synthesis

Microbial routes to catechol and pyrogallol are plagued with toxicity of the product towards the organism. Routes can be employed to circumvent sensitivity by indirect biocatalysis of a precursor to an aromatic such as in the syntheses of hydroquinone and phenol.[82] A quick look at all the hydroxy aromatics follows.

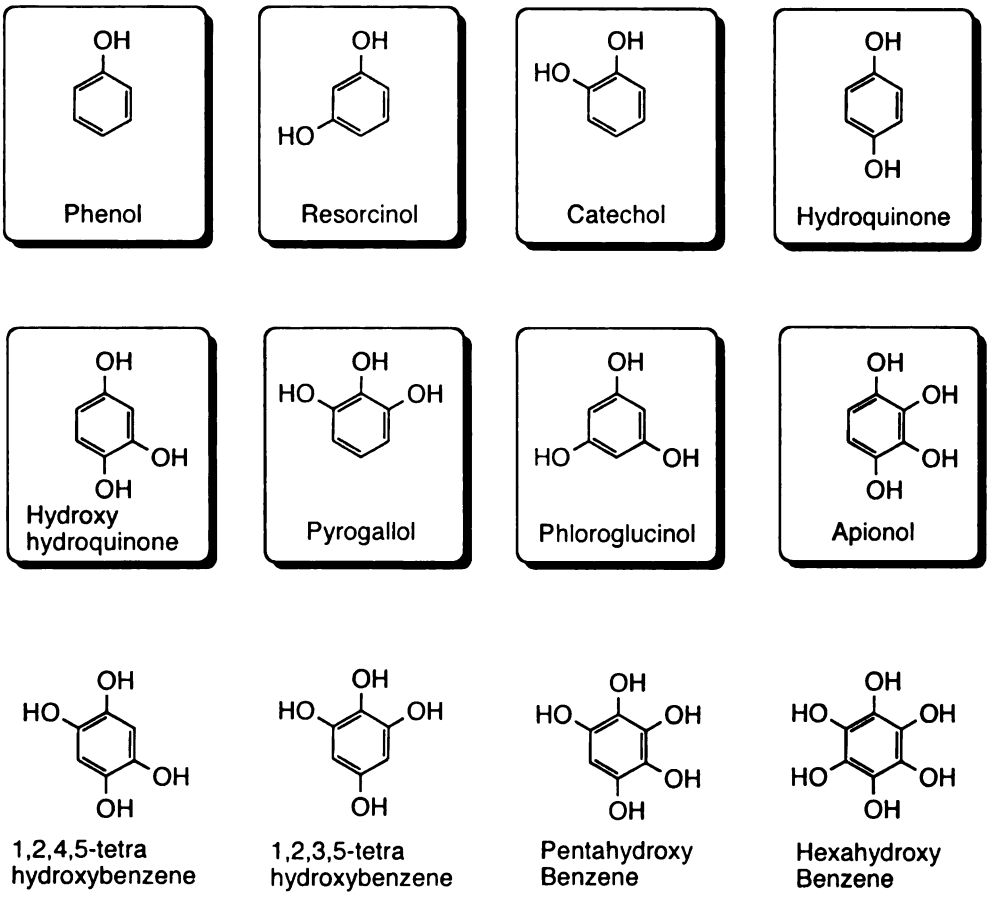

Figure 9. Hydroxy aromatics.

Boxed molecules have current or precursor renewable, biocatalytic syntheses.

Virtually all 7 million metric tons per year of phenol is chemically manufactured from benzene.[83] The uses primarily are for manufacture of bisphenol A, phenolic resins, ε-caprolactam, aniline and alkylated phenols. Friedel-Crafts alkylation of benzene with propylene yields cumene, which upon oxidation and cleavage, produces phenol and acetone (Figure 10). Phenol undergoes *o*-, *p*-hydroxylation with peroxide to afford hydroquinone and catechol that are differentially distilled. More direct routes to hydroquinone exist, without the separation from catechol. Phenol can instead be produced

from renewables after reaction of shikimic acid (biocatalytically produced in over 100 g/L concentrations) in near-critical water to an isolated yield of 51% (Figure 10).[82]

With an annual production of over 22,000 metric tons, catechol finds use as a starting material in the manufacture of pharmaceuticals (L-DOPA, adrenaline), flavors (vanillin, eugenol, isoeugenol), agrochemicals (carbofuran, propoxur), polymerization inhibitors and antioxidants (4-*tert*-butylcatechol, veratrol).[84] Hydroxylation of phenol is the current production method of catechol with hydroquinone as a recovered by-product. Catechol can be microbially synthesized, directly from glucose, albeit in limited quantities of 2 g/L due to product sensitivity to the organism.[79]

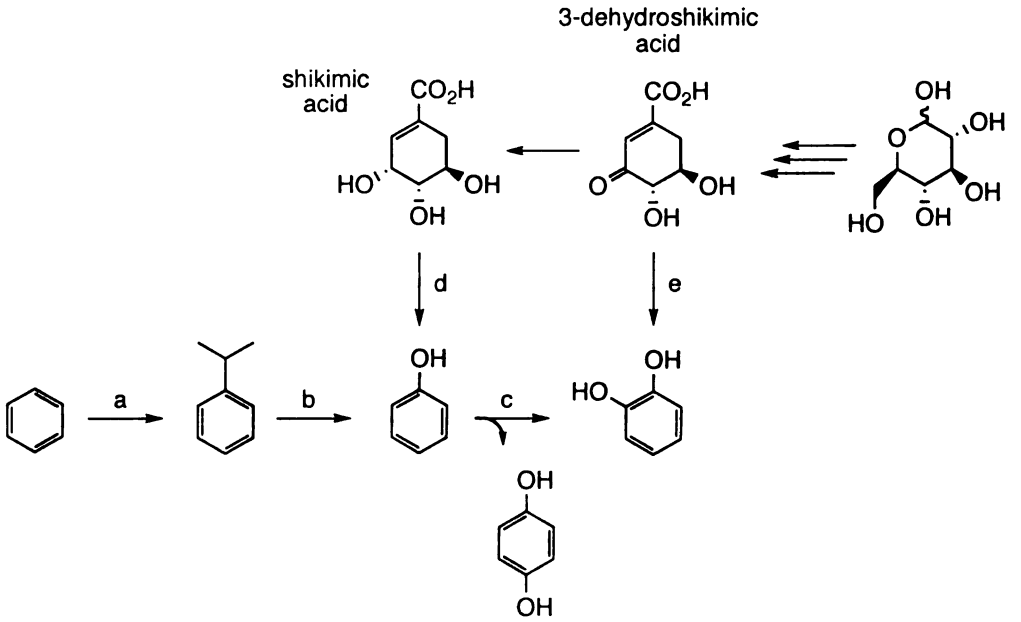

Figure 10. Phenol and catechol current and microbial manufacture

(a) Propylene, $AlCl_3$. (b) i) O_2, 100 °C, ii) Δ, H_2SO_4. (c) 70% H_2O_2 EDTA, Fe^{2+} or Co^{2+}, 80 °C. (d) H_2O, 350 °C. (e) *E. coli* AB2834/pKD136/pKD9.069A, 37 °C.

Hydroquinone is produced globally at approximately 45,000 metric tons per year and utilized in antioxidants and polymerization inhibitors.[85] Similarly to phenol production, benzene is alkylated with propylene and reacted in a Hock oxidation to hydroquinone or produced as a by-product shown in catechol manufacture. Alternatively, nitrobenzene can be reduced to aniline, treated with stoichiometric amounts of manganese oxide in the presence of acid to benzoquinone, that upon the addition of iron aromatizes to hydroquinone. Quinic acid can be synthesized microbially from D-glucose at concentrations approaching 70 g/L and can be converted to hydroquinone with stoichiometric amounts of bleach to 87% isolated yield after extraction with *t*-butylmethylether followed by sublimation.[80] In the same study, catalytic Ag_3PO_4 at 2 mol% was used with $K_2S_2O_8$ as a co-oxidant offering isolated yields of 74%. The toxicity of hydroquinone toward ethanologenic *E. coli* cultured on xylose under fermentative conditions has been analyzed from the perspective of hydroquinone's inhibition of sugar catabolism and damage to the plasma membrane.[86]

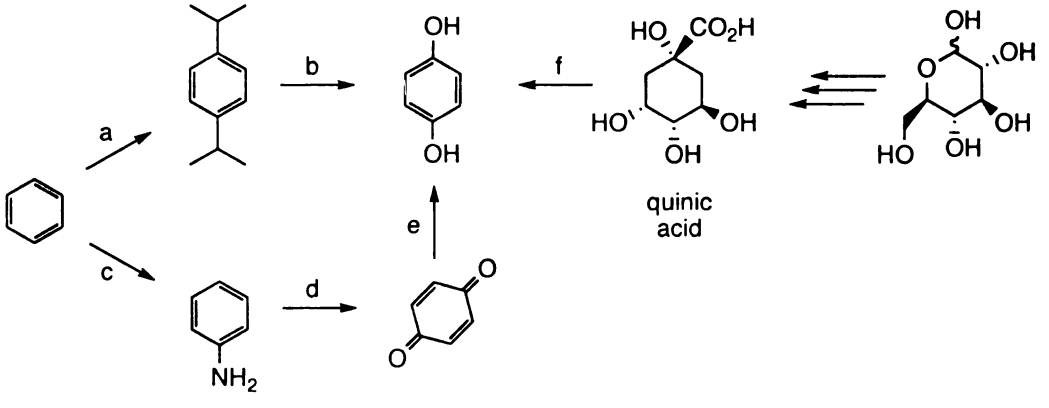

Figure 11. Hydroquinone current and microbial manufacture

(a) propylene, HZSM-12. (b) i) O_2, NaOH, ii) Δ, H_2SO_4. (c) i) HNO_3, H_2SO_4 ii) Cu/SiO_2, H_2. (d) MnO_2, H_2SO_4. (e) Fe^0. (f) HOCl or $Ag_3PO_4/K_2S_2O_8$.

Gallic acid first and foremost is used as a veterinary urinary astrigent and antihemorrhageant, but also has applications as a plant growth regulator, besides being the precursor to pyrogallol.[87] Pyrogallol is a pharmaceutical (Trimethoprim, gallaminetriethiodide) and pesticide (Bendiocarb) precursor providing the hydroxylated benzene ring. Pyrogallol happens to be the oldest and one of the most versatile photographic developing agents. Gallic acid availability is directly related to the natural sources of insect carapices (gall nuts) and the seed pods of a Peruvian tree (*Coulteria tinctoria* tara powder) which are neither a controlled cultivation. Some syntheses have been brought to industrial applications from benzene. Conversion to tetrachlorocyclohexanone from cyclohexanone with subsequent base catalyzed hydrolysis affords gallic acid. Either source of gallic acid is treated in a copper lined autoclave at high pressures and decarboxylated to pyrogallol (Figure 12). *E. coli* KL7/pSK6.161 can convert D-glucose to gallic acid in over 20 g/L titer in 12% yield. *E. coli* RB791serA::aroB/pSK6.234 can convert gallic acid to pyrogallol in near quantitative yields either through 3-dehydroshikimic acid or protocatechuic acid.[81]

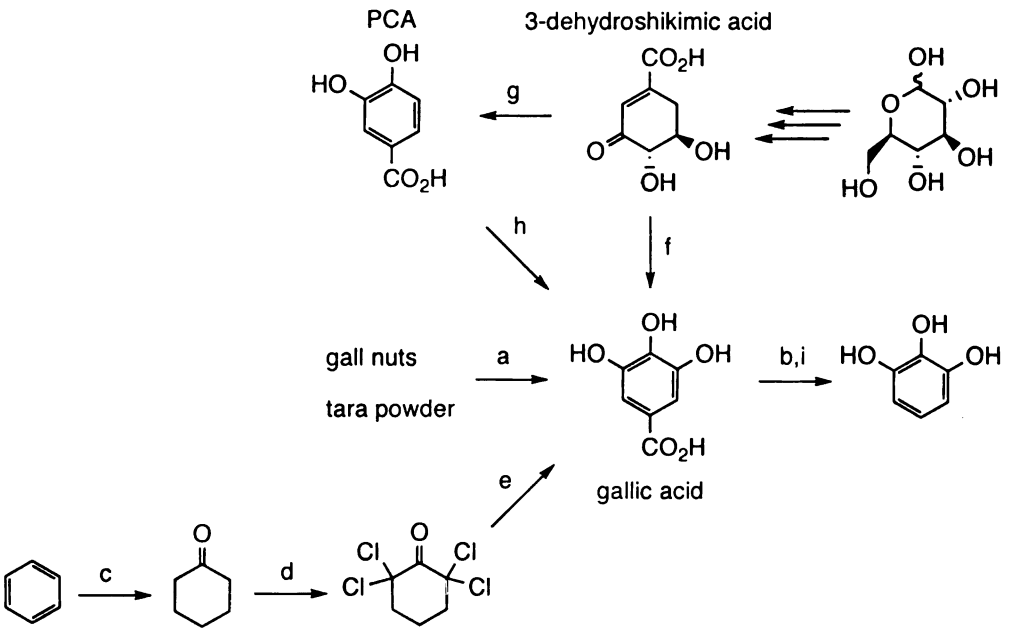

Figure 12. Pyrogallol current and microbial manufacture

(a) Natural product isolation. (b) Cu^0, 12 atm, 175 °C. (c) i) H_2/Pt ii) O_2/Co, iii) Cu/Zn. (d) Cl_2. (e) NaOAc. (f) 3-dehydroshikimic acid dehydrogenase. (g) 3-dehydroshikimic acid dehydratase (AroZ). (h) *p*-hydroxybenzoate hydroxylase (PobA). (i) PCA decarboxylase (AroY).

Phloroglucinols use in industry and production is discussed in depth in Chapter three. Resorcinol has a worldwide production of 45,000 metric tons per year[88] and finds most of it use in tires and wood adhesives as a tackifier.[85] Resorcinol also has application in UV protective coatings, throat lozenges and molecules with biological activity. Both industrial productions of resorcinol use benzene as starting material (Figure 13). In one synthesis, conversion of diisopropyl benzene, by propylene addition to benzene, takes an analogous path as the cumene/phenol synthesis. In other efforts oleum/sodium sulfite is used to sulfonate benzene, followed by alkali fusion, that generates large sulfate salt streams. Resorcinol can be derived in 82% isolated yield from phloroglucinol using a

base-catalyzed hydrogenation with Rhodium on alumina after Kugel-Rohr distillation.[89] Phloroglucinol is microbially synthesized from D-glucose in varying titers with use of external extractive techniques (discussed in Chapter three).[90]

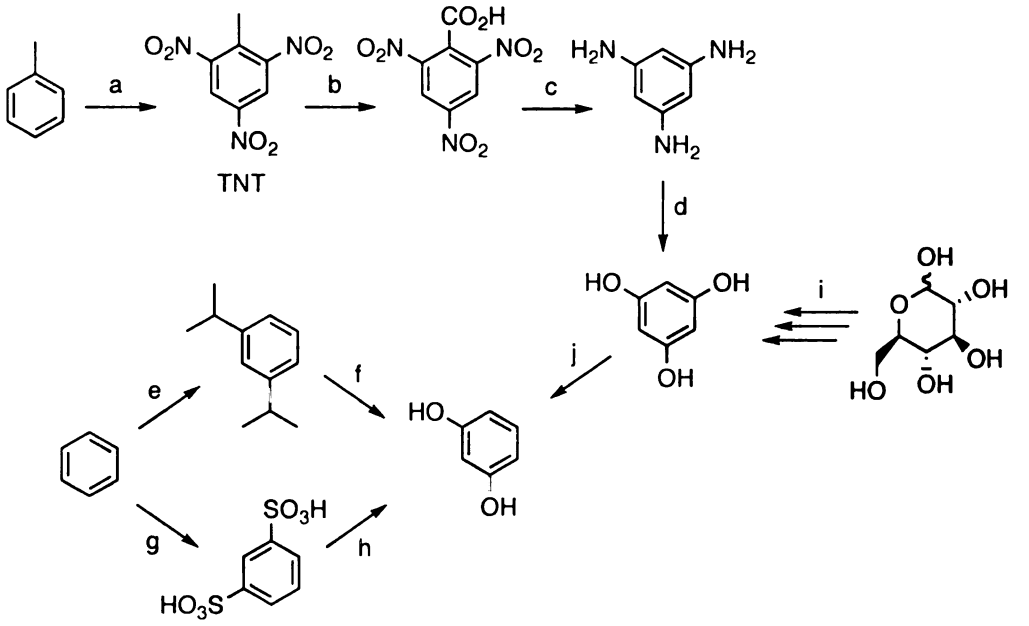

Figure 13. Phloroglucinol and resorcinol current and microbial manufacture

(a) HNO_3, H_2SO_4. (b) $Na_2Cr_2O_7$, H_2SO_4. (c) Fe^0, HCl. (d) H_2SO_4, 108 °C. (e) propylene, HZSM-12. (f) O_2, NaOH, 90-100 °C. (g) SO_3, Na_2SO_4, 150 °C. (h) NaOH, 350 °C. (i) W3110serA(DE3)/pBC2.274. (j) i) Rh/Al_2O_3, H_2, NaOH; ii) H_2SO_4, reflux.

Other hydroaromatics are not in mainstream industrial applications and their difficulty in production precludes use as commodity chemicals. Some proposed syntheses have been shown at bench-scale (Figure 14). Hydroxyhydroquinone is not produced industrially, but is found in several insecticides.[87] D-glucose derived 2-deoxy-scyllo-inososе[91] can be converted to hydroxyhydroquinone with reflux in 0.5 M phosphoric acid.[89] Functionalized apionol molecules include antioxidant coenzyme Q_{10}, which

inhibits oxidative stress to low-density lipoproteins[92], fumagatin and aurontiogliocladin, which have antibiotic activity.[93] Apionol comes from D-glucose via an acid catalyzed aromatization of selectively oxidized *myo*-inositol. 1,2,3,5-tetrahydroxybenzene is the first product in the proposed phloroglucinol degradative pathway in *Rhodococcus* sp BPG-8 and with identification and inhibition of subsequent enzyme(s) this hydroxy-aromatic could be achieved.[94] 1,2,3,5-tetrahydroxybenzene can be made by acid hydrolysis of 2,4,6-triaminophenol. 1,2,4,5-tetrahydroxybenzene is produced by the reduction of 2,5-dihydroxyl-1,4-benzoquinone and would most likely have to be derived from a higher order hydroxybenzene or unsaturated polyol with a reactive end functionality for ring closure. Tetrahydroxybenzoquinone is reduced with stannous chloride under acidic conditions to yield hexahydroxybenzene. D-glucose derived, cellular inositols are the most densely chiral molecules known and, although unlikely, there is a possibility of dehydrogenating to aromatize to hexahydroxybenzene which maybe selectively deoxygenated to pentahydroxybenzene has been synthesized previously by boiling 2,4,6-triaminoresorcinoldiethylether in water followed by ether cleavage.[87]

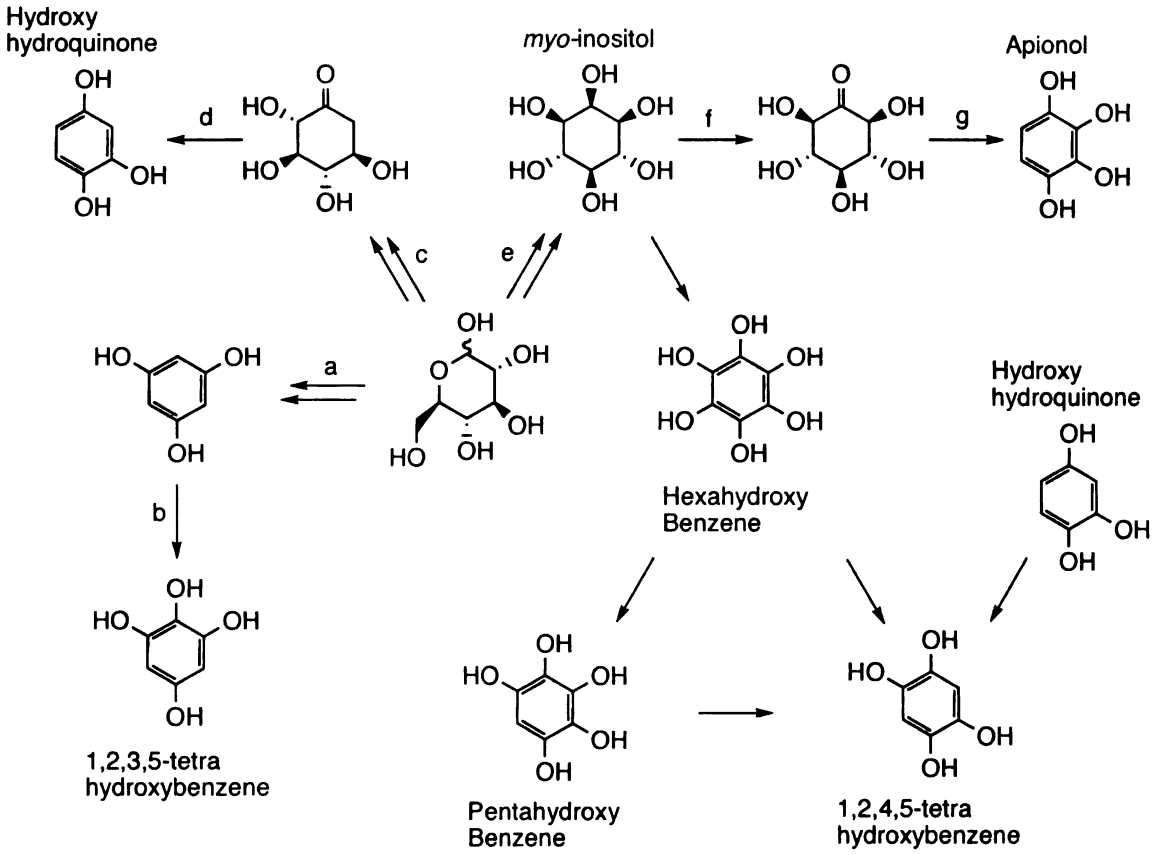

Figure 14. Proposed polyhydroxyaromatic synthesis from a renewable source.
(a) W3110serA(DE3)/pBC2.274. (b) Recombinant *Rhodococcus* sp BPG-8. (c) i) hexokinase, ii) 2-deoxy-scyllo-inosose synthase 38%. (d) 0.5 M H_3PO_4 reflux, 39%. (e) *E. coli* JWF1/pAD1.88A, 11%[95]. (f) *G. oxydans*, 95%[95]. (g) H_2O, H_2SO_4, reflux, 66%[95].

In rise of the uncertainty associated with the chemical industries reliance on non-renewable resources for virtually all commodity chemical manufacture the research for sources with renewable feedstocks are of importance. The following research comprises of chemistry that progresses towards the deviation from a petroleum-based chemical economy to one that thrives on starting materials from renewable sources through utilization of rapid and efficient syntheses dependent upon microbial biocatalysts. Efforts aimed to biocatalytically produce 1,3,5-trihydroxybenzene and an ε-caprolactam precursor

from renewable resources at a level with commercial importance. To enhance the viability of commercial manufacture following a successful biocatalytic production, focused on delivering molecules with the same purity and level to compete with non-renewable routes.

CHAPTER ONE REFERENCE

[1] El-Ashry, M. "Renewables 2007 Global Status Report". **2007**. www.ren21.net

[2] "Greenhouse gas", http://en.wikipedia.org, (accessed March 5, 2008).

[3] "Past climate change", www.epa.gov/climatechange, (accessed March 5, 2008).

[4] Schulz, W.G.; Chambers, A.J. *Chem. Eng. News*. **2008**. *January 21*, 9.

[5] "Recent climate change", www.epa.gov/climatechange, (accessed March 5, 2008).

[6] Ritter S.K. *Chem. Eng. News*. **2007**. *June 25*, 15.

[7] dos Santos, C.Y.M.; Azevedo, D.D.; Neto, F.R.D. *Atmos. Environ*. **2002**, *36*, 3009.

[8] Hileman, B. *Chem. Eng. News*. **2008**. *February 18*, 35.

[9] Hogue, C. *Chem. Eng. News*. **2008**. *February 4*, 24.

[10] Hess, G. *Chem. Eng. News*. **2008**. *March 10*, 42.

[11] Erickson, B. *Chem. Eng. News*. **2008**. *January 7*, 10.

[12] (a) Asadullah, M.; Ito, S.I.; Kunimori, K.; Yamada, M.; Tomishige, K. *Environ. Sci. Technol*. **2002**, *36*, 4476. (b) Tomishige, K.; Asadullah, M.; Kunimori, K. *Catalysis Today*. **2004**, *89*, 389. (c) Rohde, M.; Unruh, D.; Piap, P.; Lee, K.W.; Shaub, G. *Studies in Surface Science and Catalysis*. **2004**, *153*, 97. Among many conference abstracts of papers.

[13] Mccoy, M. *Chem. Eng. News*. **2008**. *January 21*, 11.

[14] *Chem. Eng. News*. **2008**. *December 17*, 12.

[15] Voith, M. *Chem. Eng. News*. **2008**. *February 11*, 34.

[16] Jacoby, M. *Chem. Eng. News*. **2008**. *February 27*, 7.

[17] Schmer, M.R.; Vogel, K.P.; Mitchell, R.B.; Perrin, R.K. *Proc. Nat. Acad. Sci.* **2008**, *105*, 464.

[18] Ritter, S. *Chem. Eng. News.* **2008**. *January 21*, 45.

[19] "Miscanthus", www.bical.net.

[20] Tullo, A. *Chem. Eng. News.* **2007**. *November 26*, 28.

[21] Crabtree, G.; Dresselhaus, M.; Buchanan, M. *Physics Today*. **2004**, *57*, 39.

[22] Antoni, D.; Zverlov, V.V.; Schwarz, W.H. *Appl. Microbiol. Biotechnol.* **2007**, *77*, 23.

[23] US Department of Energy. Todays Hydrogen Production Industry. **2006**. http://www.fossil.energy.gov/programs/fuels/hydrogen/currenttechnology.html. (Accessed March 7, 2008).

[24] Lattin, W.C.; Utgikar, V.P. *International Journal of Hydrogen Energy*. **2007**, *32*, 3230.

[25] Mueller-Langer, F.; Tzimas, E.; Kaltschmitt, M.; Peteves, S. *International Journal of Hydrogen Energy*. **2007**, *32*, 3797.

[26] McDowall, W.; Eames, M. *International Journal of Hydrogen Energy*. **2007**, *32*, 4611.

[27] Jacoby, M. *Chem. Eng. News.* **2008**. *January 28*, 67.

[28] Olah, G.A.; Goeppert, A.; Prakash, G.K.S. *Beyond Oil and Gas: The Methanol Economy*. 1st ed.; Wiley-VCH: 2006.

[29] Tullo, A. *Chem. Eng. News.* **2008**. *March 17*, 15.

[30] Wang, Q. *Masters Thesis*. University of Maryland, 2006. https://drum.umd.edu/dspace/bitstream/1903/3833/1/umi-umd-3678.pdf

[31] Kemsley, J. *Chem. Eng. News.* **2007**. *December 3*, 55.

[32] (a) Schwarz, W.H.; Gapes, J.R. *BioWorld Europe*. **2006**, *01-2006*, 16. (b) Schwarz, W.H.; Gapes, J.R.; Zverlov, V.V.; Antoni, D.; Erhard, W.; Slattery, M. Demonstration at the TU Muenchen. June 2006.

[33] Durre, P. *Biotechnol. J.* **2007**, *2*, 1525.

[34] Biobutanol. http://www2.dupont.com/Biofuels/en_US/index.html. Accessed March 16, 2008.

[35] Ezeji, T.C.; Qureshi, N.; Blaschek, H.P. *Curr. Opin. Biotechnol.* **2007**, *18*, 220.

[36] Lynd, L.R.; Laser, M.S.; Bransby, D.; Dale, B.E.; Davison, B.; Hamilton, R.; Himmel, M.; Keller, M.; McMillian, J.D.; Sheehan, J.; Wyman, C.E. *Nat. Biotechnol.* **2008**, *26*, 169.

[37] (a)Lynd, L.R.; Weimer, P.J.; van Zyl, W.H.; Pretorius, I.S. *Microbial. Mol. Biol. Rev.* **2002**, *66*, 506. (b) Lynd, L.R.; van Zyl, W.H.; McBride, J.E.; Laser, M. *Curr. Opin. Biotechnol.* **2005**, *16*, 577.

[38] www1.eere.energy.gov/biomass/cellulase_enzyme.html. (Accessed March 9, 2008).

[39] (a) Cherry, J.R.; Fidantsef, A.L. *Curr. Opin. Biotechnol.* **2003**, *14*, 438. (b) Esterbauer, H.; Steiner, W.; Labudova, I.; Hermann, A.; Hayn, M. *Bioresour. Technol.* **1991**, *36*, 51. (c) Kirk, O.; Borchert, T.V.; Fugslang, C.C. *Curr. Opin. Biotechnol.* **2002**, *13*, 345.

[40] Percival-Zhang, Y.H.; Himmel, M.E.; Mielenz, J.R. *Biotechnol. Adv.* **2006**, *24*, 452.

[41] Alizadeh, H.; Teymouri, F.; Gilbert, T.I.; Dale, B. *Appl. Biochem. Biotechnol.* **2005**, *121*, 1133.

[42] Murnen, H.K.; Balan, V.; Chundawat, S.P.S.; Bals, B.; da Costa Sousa, L.; Dale, B.E. *Biotechnol. Prog.* **2007**, *23*, 846.

[43] Lau, M.W.; Dale, B.E.; Balan, V. *Biotechnol. Bioengin.* **2007**, *99*, 529.

[44] Kadam, K.L.; McMillan, J.D. *Bioresour. Technol.* **2003**, *88*, 17.

[45] Lynd, L.R. *Annu. Rev. Energy Environ.* **1996**, *21*, 403.

[46] Holtzapple, M.T.; Jun, J.; Ashok, G.; Patibanadala, S.L.; Dale, B.E. *Appl. Biochem. Bioethanol.* **1991**, *28/29*, 59.

[47] Bals, B.; Teachworth, L.; Dale, B.; Balan, V. *Appl. Biochem. Biotechnol.* **2007**, *143*, 187.

[48] Hileman, B.; Johnson, J. *Chem. Eng. News.* **2007**. *September 24*, 74.

[49] Johnson, J. *Chem. Eng. News.* **2008**. *March 3*, 7.

[50] Menger, F.M. *Pure Appl. Chem.* **2005**, *77*, 1873.

[51] Villa, J.; Strajbl, M.; Glennon T.M.; Sham Y.Y.; Chu, Z.T.; Warshel, A. *Proc. Nat. Acad. Sci.* **2000**, *97*, 11899.

[52] Udgaonkar, J.B. *Resonance.* **2001**. *Sept.* 61.

[53] Pauling, L. *Nature.* **1948**. *16*, 707.

[54] Muller, M.; Wolberg, M.; Schubert, T.; Hummel, W. *Adv. Biochem. Engin. Biotechnol.* **2005**, *92*, 261.

[55] Rouhi A.M. *Chem. Eng. News.* **2004**, *82*, 47.

[56] Ikunaka, M. *Organic Process Research and Development.* **2007**, *11*, 495.

[57] Martin-Matute, B.; Backvall, J.E. *Curr., Opin. Chem. Biol.* **2007**, *11*, 226.

[58] Scnell, B.; Faber, K.; Kroutil, W. *Adv. Synth. Catal.* **2003**, *345*, 653.

[59] Jenkins, R. O. In *Biotechnological Innovations in Chemical Synthesis*; van Dam-Mieras, M. C. E., de Jeu, W. H., de Vries, J., Currell, B. R., James, J. W., Leach, C. K., Patmare, R. A., Eds.; Butterworth Heinemann: Oxford 1997: pp. 9-34.

[60] www.eia.doe.gov (Mar 4, 2008).

[61] Lewis, N.S. *Science*. **2007**, *315*, 798.

[62] Werpy, T.; Peterson, P. "Top Value Added Chemicals From Biomass: Volume 1". www1.eere.energy.gov/biomass/pdfs/35523.pdf

[63] Dodds, D.R.; Gross, R.A. *Science*. **2007**, *318*, 1250.

[64] (a) Ferreira, E. S. B.; Hulme, A. N.; McNab, H.; Quye, A. *Chem. Soc. Rev.* **2004**, *33*, 329. (b) Bommarius, A. S.; Riebel, B. R. *Biocatalysis*; Wiley-VCH: Weinheim, 2004.

[65] Emptage, M; Haynie, S.; Laffend, L.; Pucci, J.; Whited, G. European Patent Application 1586647A1, Published October 19, 2005.

[66] Carlson, T.L.; Peters, E.M. US Patent Application US2006/094093 A1. Published May 4, 2006.

[67] Donnelly, M.; Millard, C.S.; Stols, L. US Patent Application 5770435. Published 1998.

[68] Niu, W.; Draths, K.M.; Frost, J.W. *Biotechnol. Prog.* **2002**, *18*, 201.

[69] Weissermel, K.; Arpe, H.J. *Industrial Organic Chemistry, 3rd ed.*; VCH: New York, **1997**: p. 310.

[70] Sweeney, W.A.; Bryan, P.F. "BTX Processing", *Kirk-Othmer Encyclopedia of Chemical Technology*. **2007**.

[71] "Toluene, Chemical Profile" *Chem. Market Rep.* **2006**, *30*, (April 3-9).

[72] Davis, S. "Benzene", *Chemical Economics Handbook*. **2007**, SRI Consulting, Menlo Park, Calif. (Jan).

[73] "Paraxylene, Chemical Profile" *Chem. Market Rep.* **2004**, *31*, (Aug 9-16).

[74] (a) O' Connor, S. R.; Farmer, P. B.; Lauder, I. *J. Pathol.* **1999**, *189*, 448. (b) Farris, G. M.; Everitt, J. I.; Irons, R.; Popp, J. A. *Fundam. Appl. Toxicol.* **1993**, *20*, 503. (c) Huff, J. E.; Haseman, J. K.; DeMarini, D. M. *Environ. Health Perspect.* **1989**, *82*, 125.

[75] (a) Noah, T. *Wall Street J.* **1994**, B2 (March 2); (b) *Washington Post* **1994**, A3 (March 2); (c) Ember, L. *Chem. Eng. News* **1994**, *72*, 4 (March 7).

[76] *Corn: Chemistry and Technology*; Watson, S. A.; Ramstad, P. E., Eds.; American Association of Cereal Chemists: St. Paul, MN, 1987.

[77] Swiss Pat. 514,675 (Dec. 15, 1971), H. J. Schultze and R. Mondry (to Inventa AG fuer Forschung and Patentverwer-tung).

[78] Belozerova L.A. Tr. *Leningrad. Lesotekh. Akad.* **1966**, *105*, 89.

[79] Draths, K.M.; Frost, J.W. *J. Amer. Chem. Soc.* **1995**, *117*, 2395.

[80] Ran, N.; Knop, D. R.; Draths, K. M.; Frost, J.W. *J. Am. Chem. Soc.* **2001**, *123*, 10927.

[81] Kambourakis, S.; Draths, K. M.; Frost, J. W. *J. Am. Chem. Soc.* **2000**, *122*, 9042.

[82] Gibson, J. M.; Thomas, P. S.; Thomas, J. D.; Barker, J. L.; Chandran, S. S.; Harrup, M. K.; Frost, J. W. *Angew. Chem., Int. Ed.* **2001**, *40*, 1945.

[83] Wallace, J. *Kirk-Othmer Encyclopedia of Chemical Technology;* Wiley: New York, 2001. "Phenol", updated online May 13, 2005.

[84] (a) Franck, H.-G.; Stadelhofer, J. W. *Industrial Aromatic Chemistry*; Springer-Verlag: New York, 1988; pp. 183-190. (b) Varagnat, J. In *Kirk-Othmer Encyclopedia of Chemical Technology*, 3rd ed.; Grayson, M. Ed.; Wiley: New York, 1981; Vol. 13, pp. 39-69. (c) Szmant, H. H. *Organic Building Blocks of the Chemical Industry*; Wiley: New York, 1989; pp. 512-519.

[85] Krumenacker, L.; Constantini, M.; Pontal, P.; Sentnac, J. *Kirk-Othmer Encyclopedia of Chemical Technology;* Wiley: New York, 2001.

[86] Zaldivar, J.; Martinez, A.; Ingram, L.O. *Biotechnol. Bioeng.* **2000**, *68*, 524.

[87] Leston, G. "Polyhydroxybenzenes". *Kirk-Othmer Encyclopedia of Chemical Technology;* Wiley: New York, 2001.

[88] INDSPEC chemical producer. http://www.indspec-chem.com/ABOUT/AboutUs.asp. Accessed March 8, 2008.

[89] Hansen, C.A.; Frost, J.W. *J. Amer. Chem. Soc.* **2002**, *124*, 5926.

[90] This thesis and results from Dr. Dongmig Xie.

[91] Kakinuma, K.; Nango, E.; Kudo, F.; Matsushima, Y.; Eguchi, T. *Tetrahedron Lett.* **2000**, *41*, 1935.

[92] (a) Ingold, K. U.; Bowry, V. W.; Stocker, R.; Walling, C. *Proc. Natl. Acad. Sci. U.S.A.* **1993**, *90*, 45. (b) Stocker, R.; Bowry, V. W.; Frei, B. *Proc. Natl. Acad. Sci. U.S.A.* **1991**, *88*, 1646. (c) Steinberg, D. *Circulation* **1991**, *84*, 1420.

[93] (a) Vischer, E. B. *J. Chem. Soc.* **1953**, 815. (b) Baker, W.; McOmie, J. F. W.; Miles, D. *J. Chem. Soc.* **1953**, 820. (c) Baker, W.; Raistrick, H. *J. Chem. Soc.* **1941**, 670.

[94] Armstrong, S.M.; Patel, T.R. *J. Basic Microbiol.* **1994**, *2*, 123.

[95] Hansen, C.A.; Dean, A.B.; Draths, K.M.; Frost, J.W. *J. Amer. Chem. Soc.* **1999**, *121*, 3799.

CHAPTER TWO

L-lysine Derived ε-Caprolactam

Introduction

Nylon 6 and Nylon 6,6 account for 98% of the total Nylon manufacture worldwide.[1] Nylon 6 fibers are composed of the monomer unit ε-caprolactam. Forecasts have projected an annual growth of almost 3% reaching 4.5 million metric tons per year by 2010.[2] As with any commodity chemical manufacture the processes are highly cost and resource dependent. Petroleum, defined as a non-renewable resource, is the origin for starting materials used in the production of ε-caprolactam. Current routes to ε-caprolactam include the use of benzene, toluene or butadiene as starting materials (Figure 15 and Figure 16) and although demand, competition and environmental impact have contributed heavily to process improvements[3] there is still the fundamental flaw that the sources are not renewable.

Benzene, the starting material for ε-caprolactam manufacture, and other alkylated benzenes make up to 20% of the lighter fractions of crude oil and are also made as a gasoline additive as discussed in Chapter one. Various routes to phenol from benzene exist and hydrogenation with another petrochemical H_2 to cyclohexanone is fairly fundamental (Figure 16). Most of the improvements exist in the massive waste accumulations of the subsequent steps. Stoichiometric hydroxylamine sulfate is used to convert cyclohexanone to the oxime, generating massive amounts of ammonium sulfate in the process which can only be slightly discounted because some of the salts can be used as

fertilizers. DSM has helped this situation by using a nitrous oxide reduction and a phosphate oxime process.[4] Sumimoto completely eliminates the salt stream through use of an NH_3 and H_2O_2 ammoxidation using a titanosilicate catalyst.[5] Alternatively, cyclohexane is converted into cyclohexanone oxime in the presence of nitrous oxide and HCl. Both cyclohexanone and hydroxylamine are eliminated in this process.[6] The Beckmann rearrangment often uses oleum as the electrophile and converts the oxime to the lactam.[7] Another waste stream production step is neutralization of the oleum. Thomas has devised use of bifunctional, heterogeneous, nanoporous catalysts containing isolated acidic and redox sites to seamlessly convert cyclohexanone to ε-caprolactam using air and ammonia at 80 °C.[8] Some of the processes mentioned have only been proven on laboratory scale and are not practiced on an industrial scale. In the end up to 4.3 tons of ammonium sulfate alone is produced per ton of ε-caprolactam.[9]

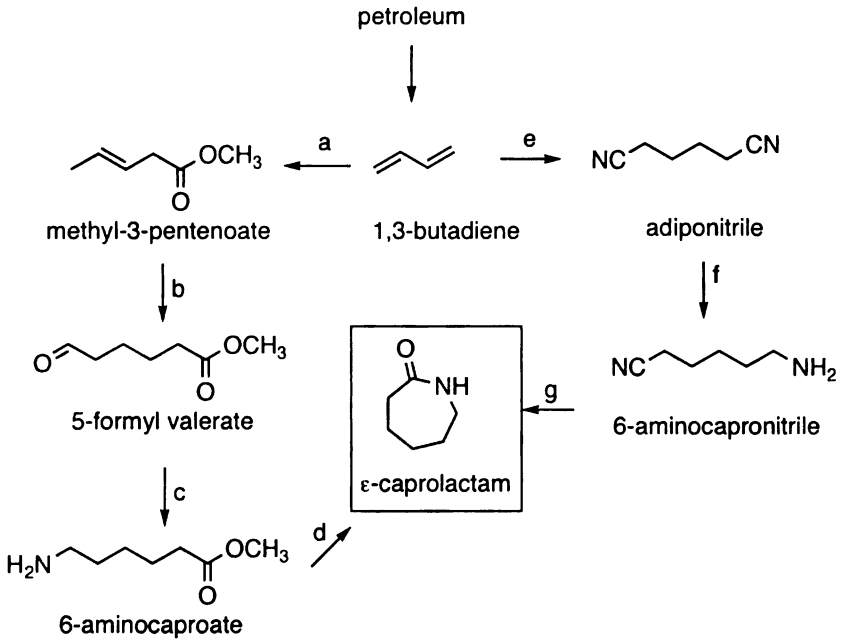

Figure 15. Syntheses of ε-caprolactam from 1,3-butadiene. (a) CO, MeOH, Ni-zeolites. (b) CO, H_2, Co, Rh. (c) NH_3/H_2, Ru. (d) 250 °C. (e) HCN. (f) Ni/Co, H_2. (g) TiO_2, H_2O.

In addition to being carcinogenic, the price and availability of benzene has shown recent instability and this demands experimentation that looks elsewhere for starting materials. More efficient and environmentally sound production methods have been investigated. In efforts to derive a renewable route to ε-caprolactam, L-lysine, a source readily produced from glucose, was investigated through research conducted by Dr. Mapitso Molefe[10] and Dr. Jinsong Yang[11] in the Frost lab (Figure 16). L-lysine has all the functional groups necessary to supply the ε-caprolactam backbone.

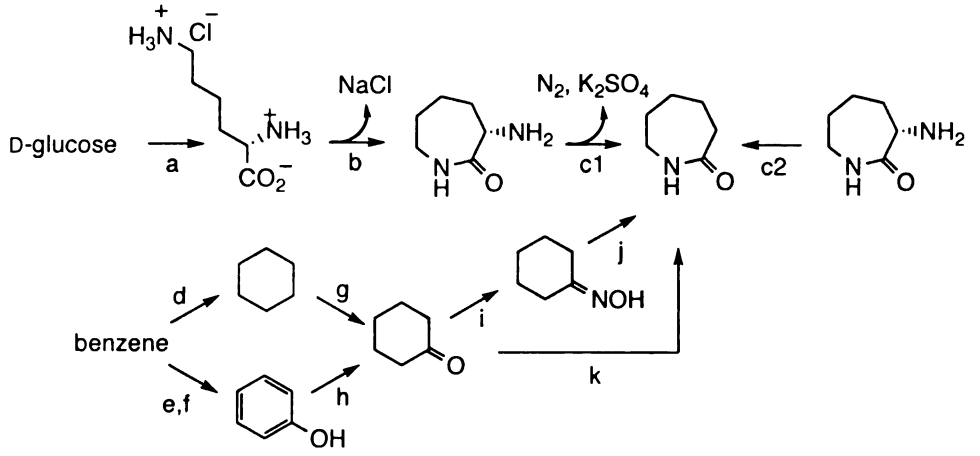

Figure 16. Current and biobased method of manufacture of ε-caprolactam.

(a) *Corynebacterium glutanicum*.[14] (b) refluxing hexanol. (c_1) NH_2OSO_3H, KOH. (c_2) Pt-S/C ,250 °C, 150 psi H_2S/H_2. (d) H_2/Pt. (e) propylene, HZSM-12. (f) i) O_2 ii) H_2SO_4. (g) i) O_2/Co, ii) Cu/Zn. (h) H_2/Pd. (i) i)$(NH_2OH)_2H_2SO_4$ ii) NH_3. (j) i) H_2SO_4 SO_3, ii) NH_3. (k)TS-1.

L-Lysine as starting material also benefits from being the second most abundant amino acid produced[12] because of its importance in agriculture. Farmers, in essence, are in the business of protein turnover. When a marketable protein, in the form of poultry, swine or bovine type, needs to build mass through protein, feed is administered containing supplemented limiting amino acids. It is more cost effective to supplement the limiting amino acids from a purified stock than to use twice as much bulk feed resulting in the same amount of overall useful protein mass accumulation. The same idea drives why L-lysine has become a major revenue stream for producers because of the utilization in food additives, feed supplements, therapeutic agents and precursors for the syntheses of peptides or agrochemicals.[13] Introduced in 1957, the current manufacture of L-lysine is from microbial fermentation of *Corynebacterium glutamicum* and has since been improved to afford a titer of 170 g/L from D-glucose.[14]

Drs. Yang and Molefe looked at three different potential routes to ε-caprolactam using glucose derived L-lysine (Figure 17). Direct deamination to 6-aminocaproic acid was not fruitful giving many undesired products with lack of separable distinction of amino groups. A one-step direct deaminition and lactamization did not elicit desired product selectivity and was unfit for industrial processes. The most promising results came from first cyclizing the lactam to mask the terminal amine as an amide, and deaminating the α-amino group. Cyclizations were quantitative in high boiling alcohols and ethanol in a sealed Parr hydrogenation apparatus at 200 °C.

Catalytic deamination over Pt on SiO_2 and Mo-Ni-S on Al_2O_3 catalysts were attempted to deaminate α-aminocaprolactam. Partial deamination was observed when α-aminocaprolactam was subjected to reduction with sodium metal in 2-propanol (20%).[10] Hydroxylamine-*O*-sulfonic acid was used to stoichiometrically deaminate α-aminocaprolactam in 75% overall yield. Catalytic deamination with various transition metals with or without sulfidation led to a maximum 60% yield of product by NMR.[11]

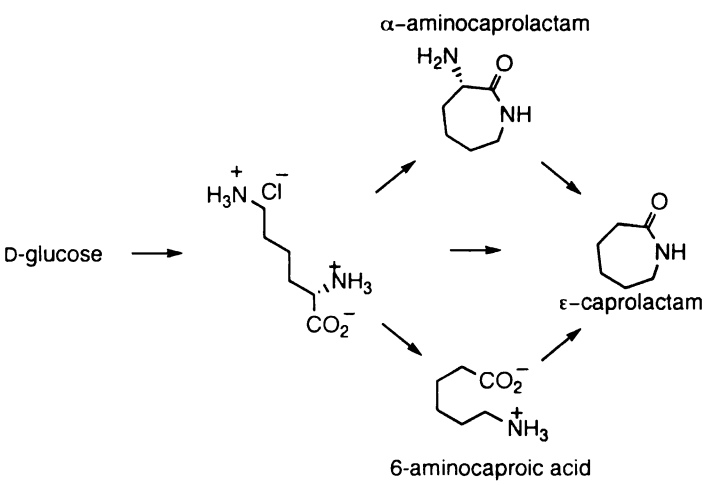

Figure 17. ε-Caprolactam from L-lysine.

With intimate knowledge in the research of the utilization of L-lysine as a precursor to ε-caprolactam another source was looked upon in L-β-lysine. L-lysine cyclized yields α-aminocaprolactam that upon hydrodenitrogenation gives our desired ε-caprolactam. The three proposed mechanisms for deamination include two S_N2 type mechanisms based on what looks like a hydride or thiol nucleophile or an E_2 elimination[15] (Figure 18).

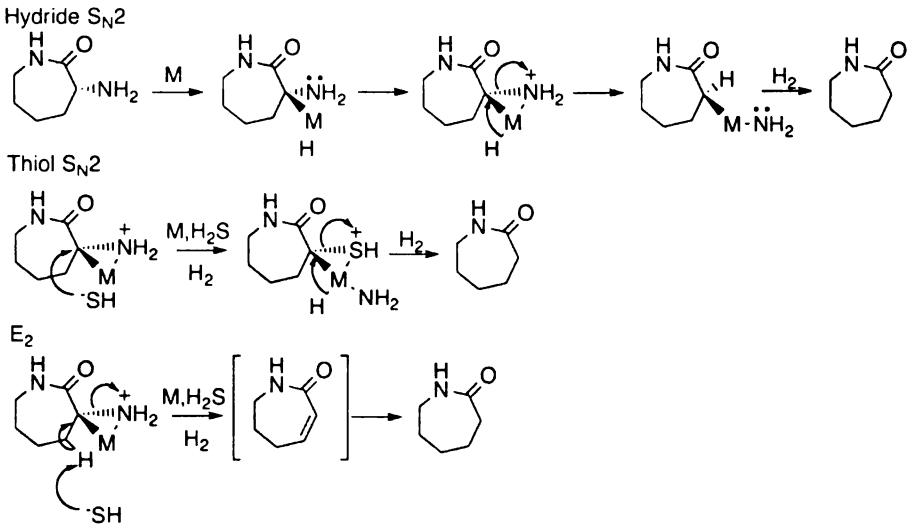

Figure 18. Potential mechanisms for hydrodenitrogenation of α-aminocaprolactam.

If the mechanism indeed goes through an E_2 mechanism the denitrogenation may be better facilitated if the amino group was on the carbon in the β-position. The corresponding cyclized product would have a more labile proton which may enhance the possibility of increasing the yield of the hydrodenitrogenation reaction (Figure 19). This hypothesis could be easily satisfied by a migration of the amino group prior to cyclization.

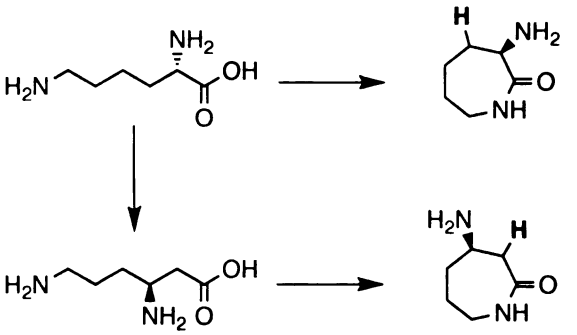

Figure 19. Relative cyclizations of amino acid precursors.

Efforts proceeded towards the chemical, *in vitro* and *in vivo* microbial synthesis of L-β-lysine. Under anaerobic conditions some *Clostridium* species utilize L-lysine as a sole carbon source in which the first biodegradation step is an aminomutase reaction that migrates the amino group to the β-position catalyzed by L-lysine-2,3-aminomutase (Figure 20). If L-β-lysine-5,6-aminomutase can be selectively inhibited and accumulation of L-β-lysine is achieved, a suitable substrate for β-aminocaprolactam is just a cyclization away. Dr. Molefe found that approximately 100 mg of protein from crude lysate was required to convert 100 mg L-lysine to 77 mg of L-β-lysine under optimal conditions. This much protein was obtained from 12 L of cultures incubated for 5 h.

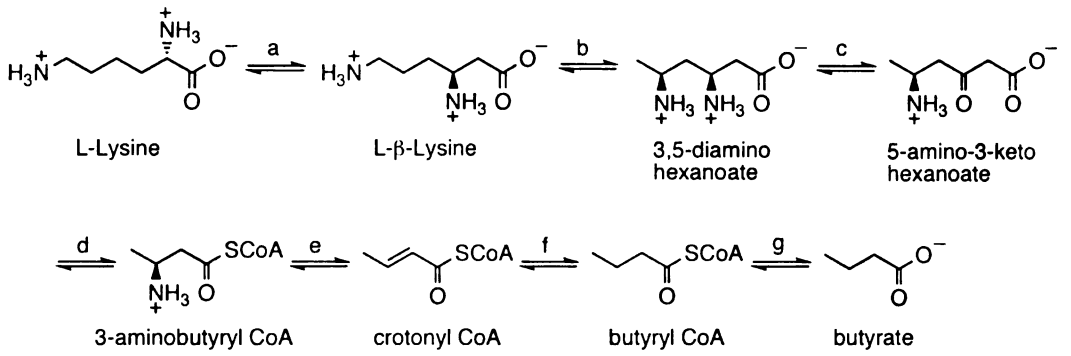

Figure 20. Degradation of L-lysine in *Clostridium subterminale*.

(a) L-lysine-2,3-aminomutase. (b) L-β-lysine-5,6-aminomutase. (c) oxidative deamination. (d) 3-keto-5-aminohexanoate cleavage enzyme. (e) 3-aminobutyrl CoA deaminase. (f) reductase. (g) hydrolysis.

In addition, additives are necessary for the bioconversion in crude cell lysates. α-Ketoglutarate and pyridoxal phosphate are required to make the imine with L-lysine whereas *S*-adenosylmethionine is required to generate the 5'-deoxyadenosyl radical necessary to initiate the 1,2-migration reaction of the amino group (Figure 22). L-lysine-2,3-aminomutase is a 285 kDa protein, with K_m= 2.8 x 10^{-8} M and 6.6 mM for *S*-adenosylmethionine and L-lysine respectively. The enzyme catalyzes a reversible reaction that has an equilibrium constant in favor of L-β-lysine over L-lysine of 6.7 at 37 °C and shows no incorporation of solvent hydrogen atoms to substrates.[16]

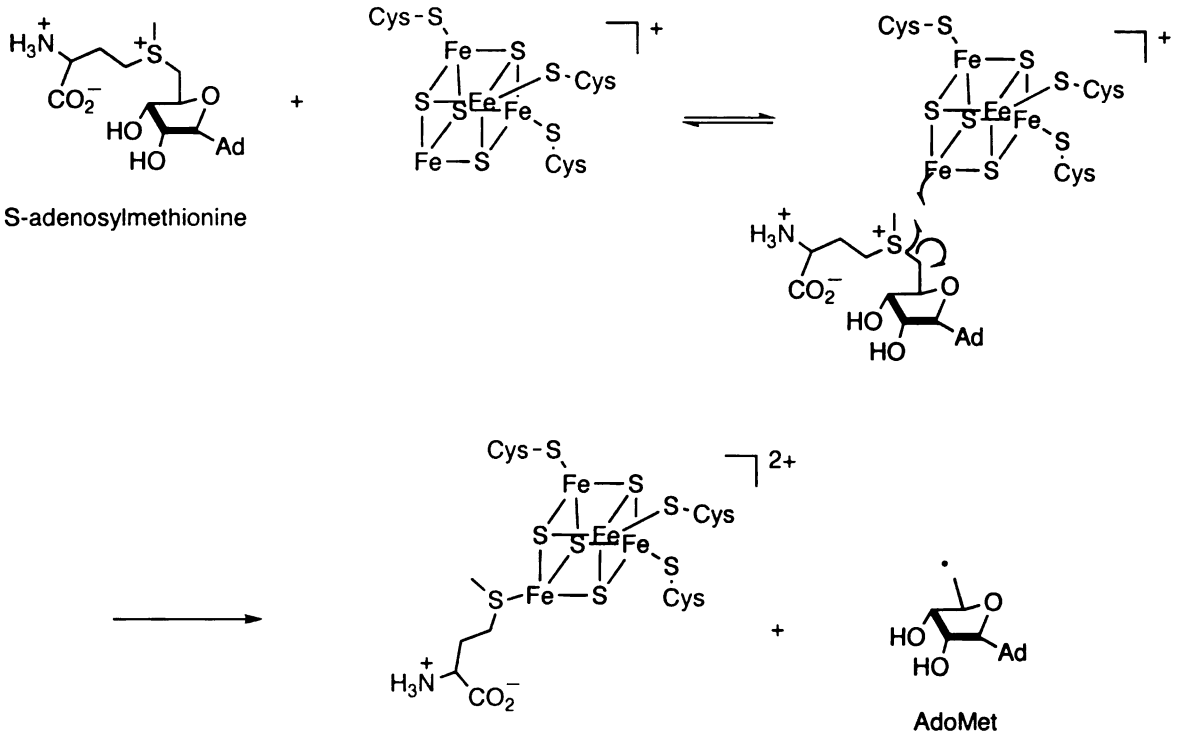

Figure 21. L-lysine-2,3-aminomutase active site AdoMet generation mechanism.

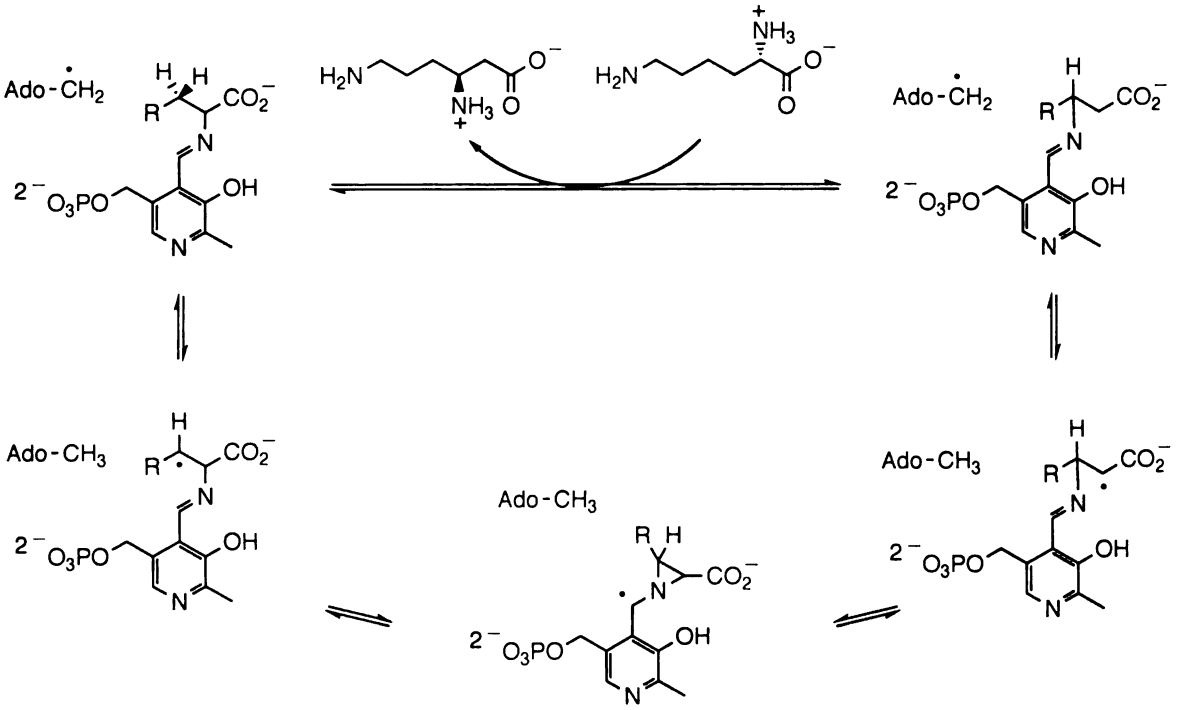

Figure 22. L-lysine-2,3-aminomutase reaction mechanism.

Glutathione or mercaptoethanol is required to reduce the iron-sulfur cluster. This implies that scaling up the isomerization in crude cell lysate would also require scaling-up of these expensive additives in pyridoxal phosphate, *S*-adenosylmethionine and a reducing agent regardless of the amount of time and effort required to harvest active lysate.[10]

The aminomutases in the biodegradation pathway can be differentiated. L-lysine-2,3-aminomutase is an *S*-adenosylmethionine dependent iron-sulfur [4Fe4S] cluster active site enzyme whereas L-β-lysine-5,6-aminomutase has a adenosylcobalamine active site reaction. The only difference in reaction is in the source of the adenosylmethionine (AdoMet) radical. Both are also pyridoxal phosphate dependent (Figure 21).

In L-β-lysine-5,6-aminomutase it has been documented that intense light (550 nm)[17] can presumably inactivate the active site irreversibly[18] by scission of the weak Co-C (25-40 kcal/mol) bond of the adenosylcobalamine *in vitro*.

Results

Bioconversion of L-lysine to L-β-lysine

Since L-β-lysine is not commercially available authentic material was synthesized concurrently according to work in the Seebach lab[19] and achieved as in literature description (Figure 23).

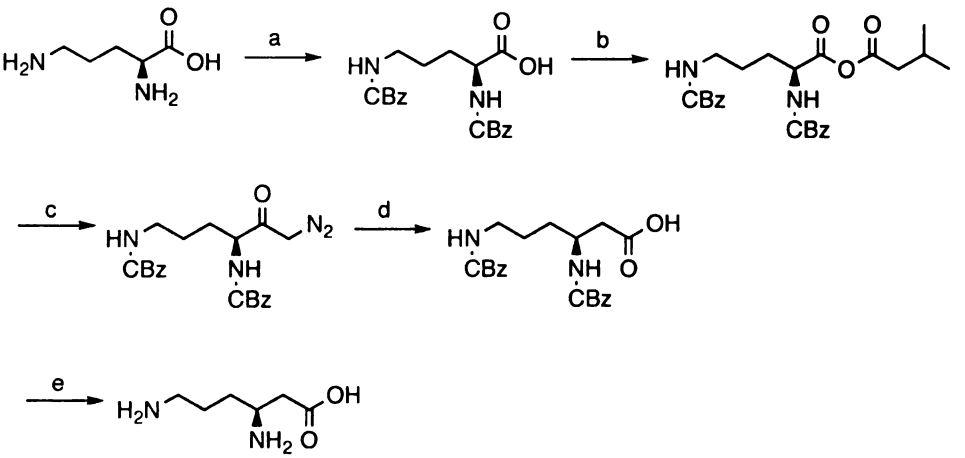

Figure 23. Arndt-Eistert homologation of L-ornithine yielding L-β-lysine.

(a) NaOH, CBzCl, CH_2Cl_2, 0 °C. (b) i-BuOCOCl, N-methyl-morpholine, THF, -5 °C. (c) CH_2N_2, Ether. (d) $PhCO_2Ag$, N-methyl-morpholine, THF, H_2O, 0 °C. (e) Pd/C, HCO_2H, MeOH.

Clostridium subterminale SB4 from ATCC (29748) is grown on L-lysine and yeast extract rich agar plates. *C. subterminale* is an anaerobic bacterium isolated from sludge in a L-lysine rich medium. L-lysine-2,3-aminomutase is itself an enzyme that needs to be stored in an anaerobic environment. All manipulations were carried out in an anaerobic Coy chamber (with an atmosphere consisting of 5:15:80 mixture of

hydrogen:CO_2:nitrogen) in sealed Hungate tubes, Pyrex bottles or bags. After incubation a single colony inoculates 5 mL of semisolid (soft agar) L-lysine and yeast extract medium. The 5 mL culture tube is placed on a 37 °C bench-top shaker until $OD_{600} \sim 2$. 400 mL of a 4 L L-lysine and yeast extract rich medium is inoculated with the 5 mL growth medium and incubated at 37 °C and 200 rpm. Once the OD_{600} reaches 2-2.5 the 400 mL growth medium inoculates the remaining 4 L medium. Once the aforementioned optical density is achieved, about 24 h, the cells are centrifugated at 7000 *g* for 15 min and the cells are collected yielding about 1.5-2.5 g of an off-white pellet of cells per liter. The cells are directly placed in the –20 °C freezer unless noted. Prior to use, the cells are thawed in ice and then resuspended in a L-lysine rich medium, with sodium dithionite or dithiothreitol and $FeSO_4$ (3 mM) and allowed to shake at 37 °C, 200 rpm and irradiated with a common, tungsten based, flood lamp to inhibit 5,6-aminomutase.[18] Without irradiation or with partial irradiation, isomerizations resulted in trace amounts of L-β-lysine, if detected, and all carbon flow led to acetate and butyrate as evidenced by NMR and resulting pH that was detrimental to the cultures. The resulting medium is acidified and the supernatant is decanted after centrifugation. The supernatant is then passed through an Amicon Ultrafiltration apparatus (10 kDa filter) to remove any remaining cell debris and protein. All the following experiments were at least averages of duplicate experiments (Table 1).

Entry	Suspension Volume (mL)	L-lysine Concentration (mM)	Buffer (80mM)	Days Frozen	% Conversion
1	250	50	Tris	0	14
2	250	50	Tris	1	56
3	250 [a]	50	Tris	1	53 (56)[b]
4	250	50	Phosphate	1	54
5	250	50	Phosphate(10mM)	1	11
6	250	100	Phosphate	1	18
7	500	50	Phosphate	1	28
8	250	25	Phosphate	1	100
9	250	50	Phosphate	1	73
10	250	100	Phosphate	1	55
11	500	50	Phosphate	13	100
12	250	100	Phosphate	13	100

Table 1. ***Clostridium subterminale*** **SB4 bioconversion of L-lysine to L-β-lysine.**

(a) Entry 3 is an additional experiment using a resuspension of cells used in entry 2 for a second isomerization fermentation. (b) % conversion of prior run with identical cell resuspension.

Initial bioconversions using fresh cell pellets did not yield good results. It was serendipitous that cells frozen for a particular experiment resulted in a higher conversion rate (Table 1 entries 1 vs 2). Turnover seems apparent when comparable results were obtained from two sequential bioconversions. After bioconversion cells were centrifugated and resuspended in a fresh L-lysine rich medium yielding the same result (Table 1 entries 2 vs 3). Using phosphate as a buffer is more cost efficient and widely accepted industrially leading to a switch in buffers that did not affect the conversion (Table 1 entries 2 vs 4) while lowering the concentration, ie buffering capacity, had a negative effect (Table 1 entries 4 vs 5). To verify the limits of the bioconversion, substrate concentrations and volumes were doubled (Table 1 entries 6 vs 7) with little promise for further throughput. As seen in (Table 1 entries 4 vs 9) variability in

conversion capabilities did exist and further experimentation used colonies grown from the same glycerol stock. Lowering of the L-lysine starting concentration did lead to complete isomerization of L-lysine to L-β-lysine (Table 1entries 8 vs 9 and 10). Stemming from the observation that freezing the cells led to better conversion of substrate, cells were kept in the freezer for 2 weeks and surprisingly the isomerization amounts went two-fold higher either in terms of concentration or volume (Table 1 entries 10 vs 12 and 9 vs 11). Past experience shows that running crude lysate enzyme activities are usually two-fold less when cells are frozen prior to the assay than when run fresh. Experimental reasoning was not sought to determine what affect the frozen cell pellet had on the bioconversion. Possibly low temperature affects L-β-lysine-5,6-aminomutase moreso than other proteins or more likely the thawing process may be detrimental to the active site. Lysing of cells and, in essence, posing an *in vitro* synthesis of L-β-lysine as a whole is unlikely because much larger quantities of L-lysine were isomerized than in traditional *in vitro* experiments and resuspensions showed that the subsequent syntheses were reproducible.

Purification of L-β-lysine

In incomplete conversion experiments L-β-lysine was differentially eluted from L-lysine based upon slight basicity differences. The L-lysine carboxyl group pKa is about 2.2 while L-β-lysine is closer to 3. When the buffered eluent is at a pH of 2.75 with a mixture of L-lysine and L-β-lysine there are differently charged substrates allowing a means of separation of two similar compounds. The isolation of L-β-lysine is carried out on strong cation exchange resin Dowex-50Wx4 (H^+) 200-400 mesh.[16] Supernatant of the

C. subterminale bioconversions is brought to pH 2 with HCl and run into 500 mL of resin. The samples are thoroughly washed and L-β-lysine and L-lysine are then differentially eluted with a 0.2 M sodium formate, 0.35 M sodium chloride system at pH 2.75. The pooled L-β-lysine fractions, determined by ^{1}HNMR, are diluted two-fold and run into a separate 75 mL of cation exchange resin and desalted by washing with water. Dilution may or may not be necessary, the reasoning for this step is to ensure that there is ample contact time so the amino acids can bind to the resin. The amino acid retained on the resin is then eluted with 1 N ammonium hydroxide. The resulting solution is concentrated *in vacuo* to yield L-β-lysine. An ethyl acetate extraction may be necessary to remove an unidentified organic impurity after elution from the column. Acetic acid accumulates due to hydrolysis of ethyl acetate and is removed by acidifying with HCl and concentrating the product to dryness.

In complete conversions where all L-lysine is consumed the purification of L-β-lysine follows the preceding paragraph with the exception of the first Dowex column.

Abbreviated process for bioconversion of L-lysine to L-β-lysine

A look into (Table 2 and Table 3) gives insight to the compiled steps and time allotments in order to isomerizes L-lysine to L-β-lysine and purify the product.

Step	Procedure for Bioconversion	Time (h)
1	*Clostridium subterminale* from ATCC is grown anaerobically on yeast extract, L-lysine, buffered agar plates and incubated.	24
2	Individual colonies are grown anaerobically in 5 mL yeast extract, L-lysine, buffered, semisolid media and incubated.	24
3	The 5 mL growth culture inoculates 400 mL yeast extract, L-lysine, buffered media and is incubated.	12
4	The 400 mL growth culture inoculates 4 L yeast extract, L-lysine, buffered media and is incubated.	12
5	*C. sub* cells are harvested by centrifugation.	2
6	*C. sub* cells are quick-frozen and stored at –20 °C.	12
7	*C. sub* cells are thawed in ice.	3
8	*C. sub* cells are resuspended in L-lysine, buffered media and incubated under irradiative conditions.	24
	Alotted time for complete bioconversion	**113**

Table 2. Procedural outline with time allotments for bioconversion to L-β-lysine.

Step	Procedure for Purification	Time (h)
1	Centrifugation to remove cell debris	0.5
2	Acidify to precipitate protein and centrifugation	0.5
3	Ultrafiltration to remove any residual protein	4
4	Bring sample to pH 2.0 and load onto 500 mL of Dowex 50Wx4	0.5
5	Wash column	8
6	Differentially elute β-lysine with 0.2M formic acid, .35M sodium chloride solution	8
7	Dilute like fractions (2x) (pH 2) and load onto 75 mL of Dowex 50Wx4	6
8	Wash column	2
9	Elute product with 5 bed volumes of 1M ammonium hydroxide	1
10	Concentrate sample to dryness	1
11	Continuous extraction with ethyl acetate	4
12	Acidify aqueous layer with hydrochloric acid (pH 1) and concentrate	0.5
	Alotted time for complete purification	**36**

Table 3. Procedural outline with time allotments for purification of L-β-lysine.

Attempts towards a convergent route to β-amino acids

β-Amino acids have interest pharmacologically and to a lesser extent industrially. Drug targets that use β-amino acids have a distinct advantage over their common counterpart. Proteases do not generally destroy β-amino acids leading to the possibility of longer half-lives in the body. β-amino acid drug targets at peptide levels and higher also have been shown to fold secondary structures in a predictable fashion.[20] Production by

traditional chemical synthesis is a possibility with expensive reagents in multiple steps that in the end produce racemized enatiomers that require purification. If a whole cell biocatalysis is possible and L-lysine-2,3-aminomutase has promiscuity, this could be a plausible alternative synthesis of β-amino acids. Isomerizations using L-lysine-2,3-aminomutase have patented promiscuity and isomerizes an array of amino acids *in vitro*.[21]

Just as conducted for the L-lysine to L-β-lysine bioconversion, the *in vivo* experiments were conducted on ten buffered amino acids solutions: ornithine, glutamine, cysteine, threonine, arginine, methionine, glutamic acid, aspartic acid, asparagine and serine. Basis for conversion was visualized by the resonance of newly formed methylene during isomerization by ^{1}HNMR. At first glance a feeling of gratitude was achieved when finding the diagnostic methylene resonance for the isomerization of aspartic acid. After a quick deliberation it was realized that this experiment was not definitive in this case because the isomerization yields the starting material! The amino isomerization to the beta position was not observed in any case. Interestingly some metabolites from different amino acids were identical and cysteine was toxic to the cells evidenced by a precipitation of the cells. Further promiscuity experimentation was not conducted.

Cyclodehydration towards lactams

Lactamization differentiates the amino groups for deamination. Conditions for this cyclodehydration forming 7-membered lactams were investigated previously.[11] Essentially quantitative cyclodehydration was observed in 2-4 h when refluxed with high boiling point alcohols such as 1,2 propanediol, hexanol, among others and also worked

well with ethanol in a Parr apparatus that could be pressurized sufficiently to ramp the temperatures to 200 °C (Figure 24).

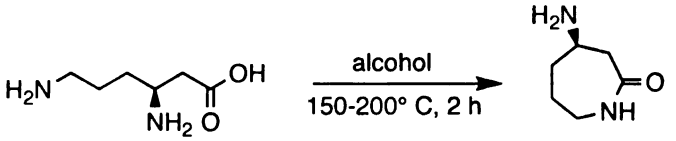

Figure 24. Cyclodehydration of L-β-lysine.

Interestingly, the highest yield (98%) and shortest time (2 h) for the conversion of L-lysine to α-amino-ε-caprolactam were observed in refluxing 1,2-propanediol. 1,2-propanediol is obtained from the hydrogenation of lactic acid, which is obtained from fermentation on large scale for food and polymer applications. As observed before, the reaction yield in the cyclization of L-lysine decreased when the reaction temperature is above a certain temperature. In fact, all L-lysine was consumed after refluxing in glycerol (290 °C) for less than 10 min and no desired product was observed.

Different size lactams play an important role even outside of Nylons and can be beneficial in natural product syntheses, pharmaceuticals among other potential uses. The cyclodehydration methodology was further subject to the formation of 8-membered ring lactams. 7-aminoheptanoic acid was purchased and D,L-homolysine was synthesized according to literature precedent.[22] Lactamization was detected in refluxing hexanol, propanediol and ethanol at 200 °C, however the yields all failed to rise above 10%. Eight membered rings are implicitly difficult in formation. The torsional strain and conformations of eclipsing hydrogens in the product help explain the limitations. L-lysine and L-β-lysine were lactamized under these conditions in > 95% yield.

Hydrodenitrogenation of β-aminocaprolactam

With successful quantitative, multi-gram scale, *in vivo* isomerization of L-lysine to and purification of L-β-lysine, the substrate was probed as a hopeful precursor to ε-caprolactam. After purification, cyclization of L-β-lysine yields β-amino-ε-caprolactam in yields above 95%. The hydrodenitrogenation conditions of both the cyclic and acyclic forms of the molecule were to be investigated based upon previous work by Dr. Yang.[11] Hydrodenitrogenation of α-amino-ε-caprolactam was researched in the group and optimized conditions on this substrate were instituted on β-amino-ε-caprolactam in hopes for a more dominant production yield with milder conditions (Table 4). Time-points within reaction completion were analyzed by NMR.

Substrate	Catalyst (1 mol %)	Temp (°C)	Time (h)	Atmosphere (gas, psi)	Solvent	Result (compound, yield)
L-β-lysine	Pt/C	300	6	H_2, 50	H_2O	pyrrolidine, 60
L-β-lysine	Pt/C	250	6	H_2, 50	H_2O	pyrrolidine, 61
L-β-lysine•HCl	Pt/C	300	6	H_2, 50	H_2O	pyrrolidine, 59
L-β-lysine•HCl	Pt/C	300	6	D_2, 50	H_2O	D incorporation
L-β-lysine•HCl	Pt/C	300	6	H_2, 50	D_2O	No D incorporation
β-amino-ε-caprolactam	Pd/C	300	8	H_2, 50	THF	decomposition
β-amino-ε-caprolactam	Pd/C	200	8	H_2, 50	THF	decomposition
β-amino-ε-caprolactam	Pd/C	100	8	H_2, 50	THF	decomposition
β-amino-ε-caprolactam	Pt-S/C	300	8	H_2:H_2S, 50	THF	decomposition
β-amino-ε-caprolactam	Pt-S/C	200	8	H_2:H_2S, 50	THF	decomposition
β-amino-ε-caprolactam	Pt-S/C	100	8	H_2:H_2S, 50	THF	ε-caprolactam, trace

Table 4. Hydrodenitrogenation of acyclic L-β-lysine and β-aminocaprolactam

The reaction conditions applied to β-aminocaprolactam lead to unwanted results of mostly decomposition products when conditions reached levels that starting material was converted. ε-Caprolactam was produced in < 1% yield based on ^{1}HNMR in the case of (Table 4 last entry). Interestingly, pyrrolidine was the final product of the aqueous hydrodenitrogenation reactions of L-β-lysine with little impurity present directly from the

Parr apparatus. Authentic pyrrolidine was characterized against the hydrodenitrogenation product by ^{1}H and $^{13}CNMR$.

Pyrrolidine is used as a building block within several industries. Pharmaceuticals use pyrrolidine in the manufature of Buflomedil (vasodilator, spasmolyticum), Bepridil (Calcium antagonist), Simvastatin (Cholesterol-lowering drug) and Cefepime (Cephalosporin antibiotic). Agrochemicals include pesticides and agents for crop protection. Material uses of pyrrolidine include: polyurethane catalysts, plasticizers, photographic chemicals, curing agents in epoxy resins, dyes, water treatment related polymers, catalysts for aldol-condensations, emulsifiers, corrosion inhibitors and rubber auxiliaries.[23]

This ring closure type of rearrangement was observed in the hydrodenitrogenation reactions of α-aminocaprolactam.[11] Using L-lysine as substrate the mechanism proposed by Pal[24] to pipecolinic acid went through an oxidation of the amine group forming an imine, followed by hydrolysis of the imine to yield an α-keto acid or an aldehyde with the by-product release of ammonia, allowing for an intramolecular condensation of the remaining amino group with the carbonyl forming two cyclic Schiff base intermediates which are just a reduction away from pipecolinic acid. An example of this reaction mechanism is given with L-β-lysine as substrate (Figure 25).

Deuteration in both the alpha and possibly the beta positions (purification of pyrollidine is necessary because of overlapping resonances in the $^{2}DNMR$ spectrum) to the nitrogen in the pyrrolidine ring was demonstrated using D_2 as the hydrogenation gas. Incorporation of deuterium was not evident using deuterated solvent.

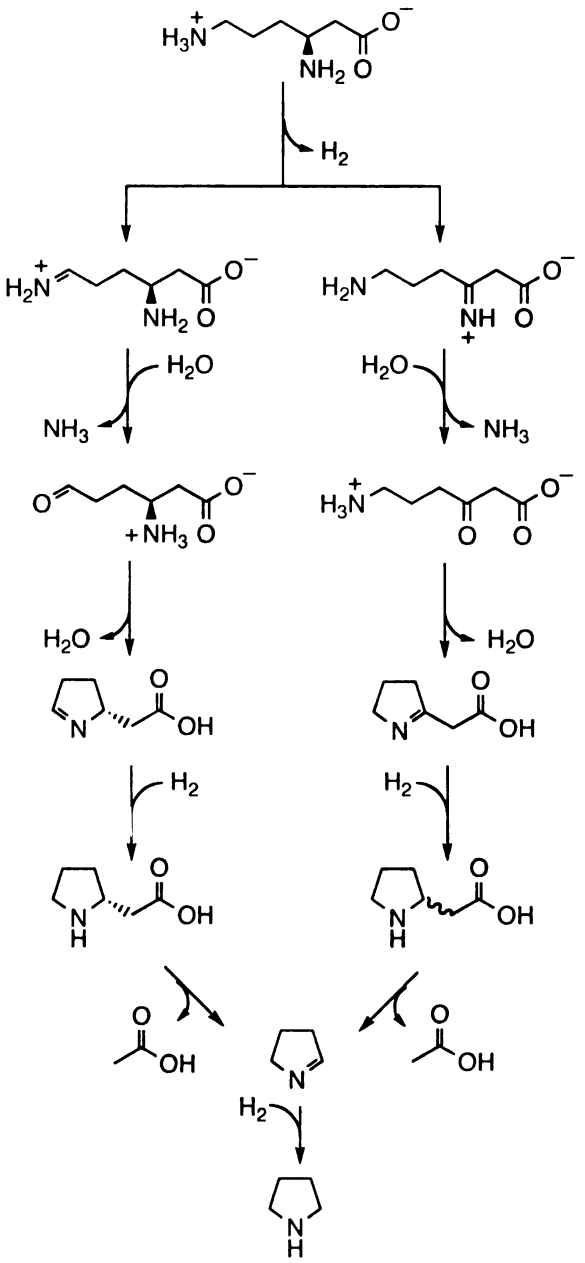

Figure 25. L-β-lysine to pyrollidine adaptation from L-lysine to pipecolinic acid.

Discussion

Chemoenzymatic synthesis of ε-caprolactam from glucose was marginally achieved albeit only in a demonstrative way. Whole cell biocatalysis of industrially, glucose derived L-lysine to L-β-lysine was demonstrated with use of anaerobic fermentation of *Clostridum subterminale* SB4 recruiting natural enzyme, expressed at genomic levels, lysine-2,3-aminomutase and selectively inhibiting lysine-5,6-aminomutase in the biodegradation pathway of L-lysine to acetate and butyrate. Inhibition was successful with light irradiation from a tungsten-based flood-lamp presumably assisting in the suicide inactivation of the weak Co-C bond in the adenosylcobalamin active site yielding gram-scale, *in vivo* and complete isomerization conditions of L-lysine to L-β-lysine.

Subsequent cyclization methodology developed in the Frost lab was applied to L-β-lysine, homolysine and 7-aminocaproic acid further demonstrating lactam forming cyclodehydration reactions with use of high boiling point alcohols or of pressurized low boiling point alcohols. The formation of 7-membered lactams was successful in near quantitative yields, while the formation of 8-membered lactams resulted in less than 10% conversion, which was not surprising with the inherent problems associated with ring structures of that size.

Hydrodenitrogenation of β-aminocaprolactam led to unwanted decomposition products where only trace amounts of ε-caprolactam was detected by NMR. Decomposition of substrate even at much milder conditions than the deaminations of α-aminocaprolactam is unfortunate stemming from the fact that the selective C-N bond

cleavages are not trivial with comparably or less energetic bonds elsewhere in the molecule.

Hydrodenitrogenation conditions for acyclic L-β-lysine in aqueous conditions were interesting in the serendipitous reactions yielding another petroleum-derived chemical in pyrollidine. Optimization and further mechanistic studies towards the generation of pyrollidine was not pursued being tangential to the project of focus.

In order for ε-caprolactam produced chemoenzymatically to compete with petroleum derived manufacture at around $2.50/kg would require high yielding, cost effective routes. It is becoming more attractive as societies awareness of renewable resources surfaces and petroleum prices go up as predicted. Yet a facility, assuming the improbable hydrodenitrogenation reaction gave a moderate to high yield of ε-caprolactam from L-β-lysine and had more cost effective purifications associated with it, would have to supply both aerobic and anaerobic fermentation knowledge and specialized equipment. The number of unit operations, compounded by the low yielding reactions make this route to a commodity chemical unrealistic.

CHAPTER TWO REFERENCE

[1] *Chemical Week* **2003**, *165* (29), *26*.

[2] Dahlhoff, G.; Niederer, J.P. M.; Hoelderich, W. F. *Cat. Rev.* **2001**, *43*, 381.

[3] a) Hoffman, J. *Chemical Market Report*, **2000**, *258 (9)*, 3. b) O'Driscoll, C. *Eur. Chem. News* **2005**, *82*, 2152. c) Ichihashi, H.; Sato, H. *Appl.Catal. A: General* **2001**, *221*, 359. d) Thomas, J. M.; Raja, R. *Proc. Nat. Acad. Sci.* **2005**, *102*, 13732.

[4] (a) Dahlhoff, G.; Niederer, J. P. M.; Hoelderich, W. F. *Catal. Rev.* **2001**, *43*, 381; (b)Morgan, M. *European Chem. News* **2005**, *81*, 2128.

[5] Eul, W.; Moeller, A.; Steiner, N. *Kirk-Othmer Encyclopedia of Chemical Technology;* Wiley: New York, http://www.mrw.interscience.wiley.com/kirk/articles/hydrhess.a01/sect11-fs.html

[6] Funken, K. H.; Muller, F. J.; Ortner, J.; Riffelmann, K. J.; Sattler, C. *Energy*, **1999**, *24*, 681.

[7] (a) Beckmann, E. *Ber.* **1886**, *19*, 988; (b) L. De Luca, G. Giacomelli, A. Porcheddu, *J. Org. Chem.*, **2002**, *67*, 6272-6274; (c) S. Chandrasekhar, K. Gopalaiah, *Tetrahedron Lett.*, **2003**, *44*, 755-756.

[8] Thomas, J. M.; Raja, R. *Proc. Nat. Acad. Sci.* **2005**, *102*, 13732.

[9] Fisher, W. B.; Crescentini, L. *Kirk-Othmer Encyclopedia of Chemical Technology;* Wiley: New York, 2004.

[10] Molefe, M. *PhD Dissertation,* Michigan State University, 2005.

[11] Yang, J. *PhD Dissertation,* Michigan State University, 2007.

[12] Comara Greiner, E. O.; Gubler, R.; Yokose, K. *CEH Marketing Research Report: Amino Acids*; SRI Consulting: Menlo Park, CA, 2003.

[13] a) Tryfona, T.; Bustard, M. T. *Process Biochem.* **2005**, *40*, 499.

b) Weuster-Botz, D.; Kelle, R.; Frantzen, M.; Wandrey, C. *Biotechnol. Prog.* **1997**, *13*, 387.

[14] Kinoshita, S.; Udaka, S.; Shomono, M. *J. Gen. Microbiol.* **1957**, *3*, 193.

[15] Hadjiloizou G.C.; Butt J.B.; Dranoff J.S., *Ind. Eng. Chem. Res.* **1992**, *31*, 2503.

[16] Chirpich, T.P.; Zappia, V.; Costilow, R.N.; Barker, H.A. *J. Biol. Chem.* **1970**, *245*, 1778.

[17] Andrunion, T.; Zgierski, M. Z. *J. Am. Chem. Soc.* **2001**, *123*, 2679.

[18] Tang, K.H.; Chang, C.H.; Frey, P.A. *Biochemistry.* **2001**, *40*, 5190.

[19] Abele, S.; Guichard, G.; Seebach, D. *Helv. Chim. Acta.* **1998**, *81*, 2141.

[20] Liljeblad, A.; Kanerva, L.T. *Tetrahedron.* **2006**, *62*, 5831.

[21] Frey, P.A.; Ruzicka F.J. U.S. Patent Application 20030113882. September

[22] Payne, L.S.; Boger, J. *J. Syn. Commun.* **1985**, *15*, 1277.

[23] DSM.com, "Exclusive Synthesis/Intermediates" http://www.dsm.com/en_US/html/dfc/products_actis_pyrrolidine.htm (accessed February, 08)

[24] Pal, B.; Ikeda, S.; Kominami, H.; Kera, Y.; Ohtani, B. *J. Catal.* **2003**, *217*,152.

CHAPTER THREE

D-Glucose Derived Phloroglucinol

Introduction

Phloroglucinol is currently most utilized in diazodyes, polymer crosslinking, pharmaceutical agent building blocks[1], and as a precursor to stable energetics, particularly 1,3,5-triamino-2,4,6-trinitrobenzene (TATB) (Figure 26).[23]

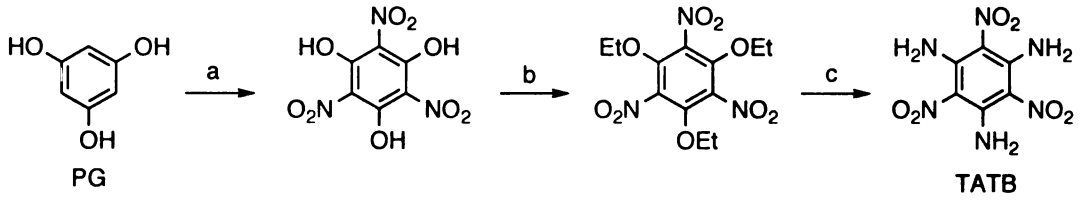

Figure 26. Current manufacture of TATB

(a) i) $NaNO_2$,NaOH, ii) dilute HNO_3, iii) 70% HNO_3. (b) $(C_2H_5O_3)_3CH$. (c)NH_3, C_2H_5OH.

The synthetic utility of phloroglucinol is vastly overshadowed by the pitfalls of its current manufacture (Figure 27). Petroleum-derived trinitrotoluene (TNT) is the precursor to phloroglucinol and ultimately TATB synthesis.[14] TATB has a higher detonation velocity relative to TNT and comparable to RDX and HDX, two of the highest explosive materials used in the military, with greater thermal stability. TATB is used in formulations of PBXN-7 a fuse booster associated in the FMU-139 series bomb fuses that are part of the MK80 general purpose bombs. The MK80 series account for a majority of bombs used in aerial assaults.

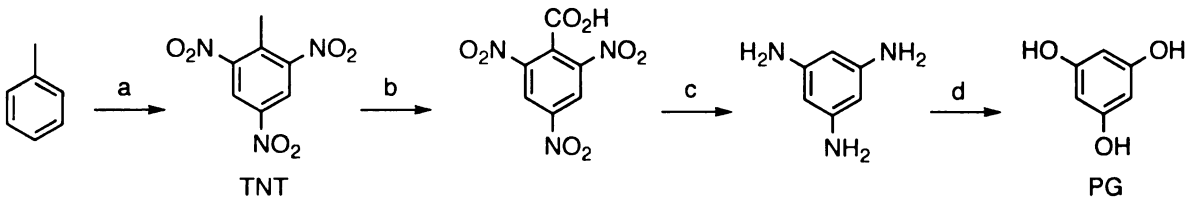

Figure 27. Current manufacture of phloroglucinol

(a) HNO_3, H_2SO_4. (b) $Na_2Cr_2O_7$, H_2SO_4. (c) Fe^0, HCl. (d)H_2SO_4, 108 °C.

Aside from the fact that TNT has obvious explosion risks, it is flawed by necessary separation from incomplete nitration by-products that have had treatment with sodium sulfite. These treated by-products are the culprits of large "red water" environmentally detrimental waste streams. Large quantities of metal salts, one being carcinogenic hexavalent chromium, are produced in the chemical reactions from TNT to phloroglucinol as well. The aforementioned downfalls of phloroglucinol manufacture have precluded the production in the states and Europe.

Phloroglucinol could have applications in the cosmetic industry through manufacture of trimethoxybenzene that is one of the three compounds in the essence of rose. Use of a phloroglucinol *o*-methyltransferase and orcinol *o*-methyltransferases a biocatalytic approach can be envisioned for *in vivo* methylation of phloroglucinol. There is also possibility of a chemoezymatic synthesis of trimethoxy benzene taking biocatalytically derived phloroglucinol and finding conditions for chemical methylation (Figure 28).

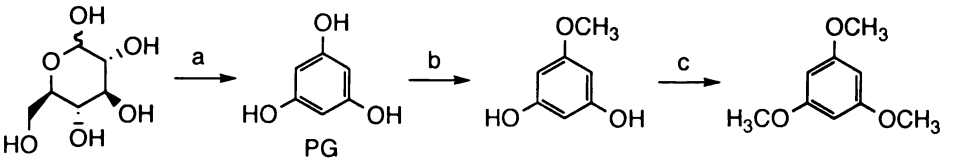

Figure 28. Synthesis of trimethoxybenzene from glucose.

(a) W3110serA(DE3)/pBC2.274 (b) phloroglucinol *o*-methyltransferase (c) orcinol *o*-methyltransferases.

Phloroglucinol may have a profound impact in the near future with introduction into the phenol-formaldehyde resins. So-called novolak and resole-type resins account for almost a $4 billion per year industry. Phenolic resins uses are found in a wide array of adhesives, coatings, glues and paints. In 2000, 4 million tons of phenolic resins were consumed worldwide with roughly half produced in the US.[5] About 50% of the US consumption is in the adhesives used in plywoods that add structural integrity and weather resistance. Another large consumer product containing phenolic resins include the binding material that keeps the glass strings of insulation together. The reason that phloroglucinol may be important stems oddly enough from the ties of formaldehyde making the list as a known carcinogen in 2004 by the World Health Organization. Out-gas of formaldehyde, the root cause of "sick building syndrome", from these common construction materials has made developers look elsewhere for a nontoxic aldehyde. To balance out the lower reactivity of possible replacement aldehydes the co-monomer must be more reactive to yield similar polymers. Phloroglucinol and resorcinol have magnitudes higher polymerization reactivity compared to phenol that could also benefit the use of a variety of renewable source aldehydes. Resorcinol (1,3-dihydroxybenzene), which can be derived from phloroglucinol as discussed later, and phloroglucinol have that potential with added benefits of tunability with derivatization of the hydroxy groups

and/or aromatic ring (Figure 29). Derivitization and tunability lead to more control over what characteristics the final polymer yields. Resorcinol and phloroglucinol, being polyols could react with diacids and form aromatic bearing polyesters (Figure 29).

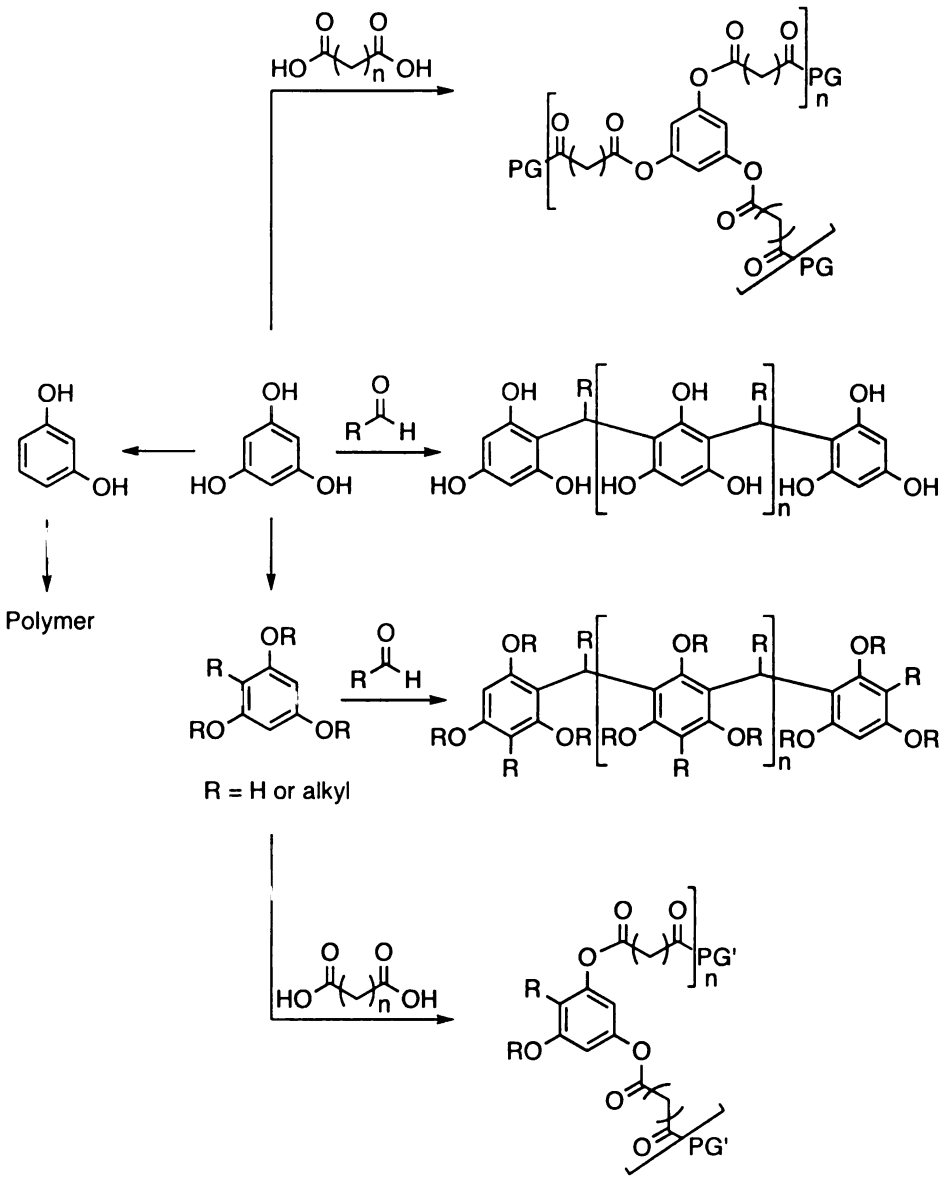

Figure 29. Potential polymer applications of phloroglucinol.
(PG = unmodified phloroglucinol, PG'=modified phloroglucinol).

If within a single microbe catalyzed reaction from nontoxic glucose phloroglucinol can be produced, then all of the aforementioned faults are avoided. The first microbial biocatalysts giving a bio-based approach to phloroglucinol synthesis converted glucose to triacetic acid lactone by design of a fatty acid biosynthetic pathway, using *Brevibacterium ammoniagenes* fatty acid synthase B.[6] Triacetic acid lactone can be chemically manipulated to phloroglucinol (Figure 30). The highest titer (1.8 g/L) and yield (6%, mol/mol) of triacetic acid lactone was synthesized from glucose by *S. cerevisiae* INV*Sc1*.[6]

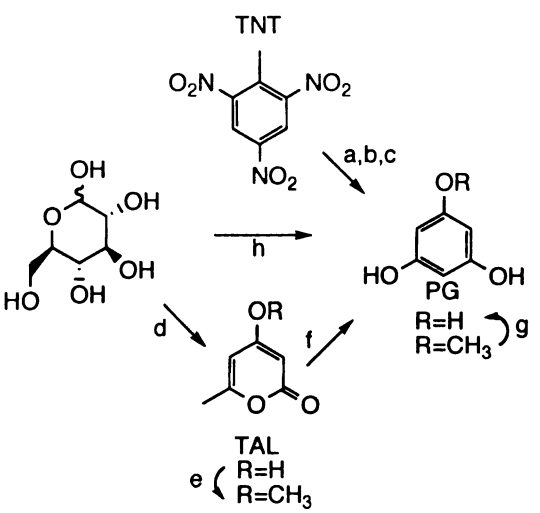

Figure 30. Phloroglucinol from TAL, TNT and glucose.[6]

(a) $Na_2Cr_2O_7$, H_2SO_4. (b) Fe, HCl. (c) H_2SO_4, 108 °C. (d) ref. 6 (e) Dowex 50 H^+, MeOH. (f) Na, MeOH, 185 °C. (g) 12 N HCl. (h) *phlD*-expressing microbe.

Phloroglucinol exists in some derivitization in countless biomolecules, with 700 cited by Bharate[7], a more succinct set of examples are given in (Figure 31). The biological activities of phloroglucinol containing molecules are widespread leading to possibilities for massive amounts of pharmaceuticals and agro chemicals. 2,4-

diacetylphloroglucinol is a fungicide while thouvenol A has cytotoxic affects towards ovarian cancer cells (Figure 31). Macrocarpals A,B inhibit HIV reverse transcriptase and lysiside A reversed phenylephrine-induced vasoconstriction in rats. Chinensins have inhibitory effects upon vesicular stomatitis virus and herpes simplex virus I and II. Oligomeric phloroglucinol make up phlorotannin molecules that are abundant in nature.

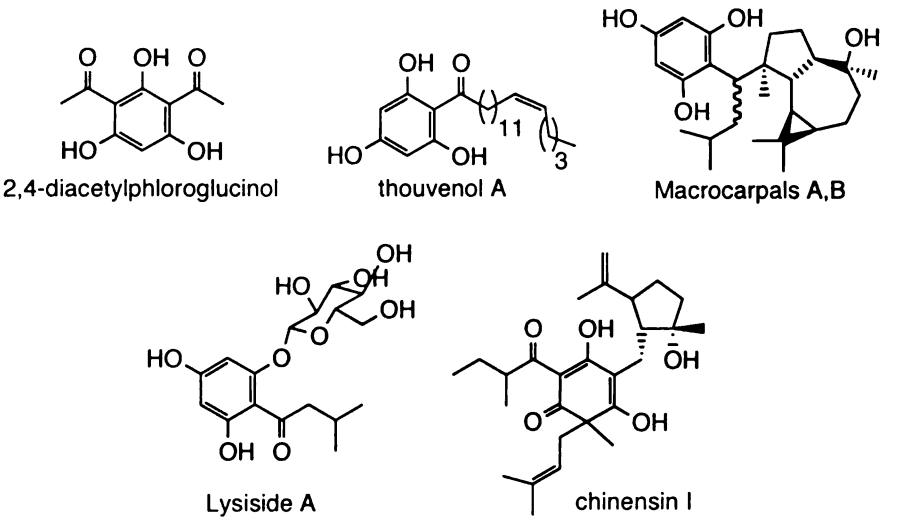

Figure 31. Derivatized phloroglucinol biomolecules with reported biological activity.

It was not until 2005 that a single gene responsible for the synthesis of unaltered phloroglucinol was discovered.[8] The biosynthetic gene cluster *phlACBDE* in *Pseudomonas fluorescens* Pf-5 produces diacetylphloroglucinol.[9] *Pseudomonas fluorescens* Pf-5 was isolated in the plant rhizosphere of disease resistant plants and was found to be directly involved in the prevention of black root rot in tobacco and take-all disease in wheat.[10] The appropriate heterologously, plasmid expressed, individual genes led to the accumulation of phloroglucinol by PhlD alone.[8] Acetylphloroglucinols are

synthesized first by cyclization of three malonyl CoA precursors by PhlD and is presumably acylated sequentially by PhlACB (Figure 32). A protein PhlE is involved in product export with a divergently transcribed *phlF*-encoded regulator.[11] The differentiation of triacetic acid lactone and phloroglucinol may be in the orientation of decarboxylation (Figure 32).

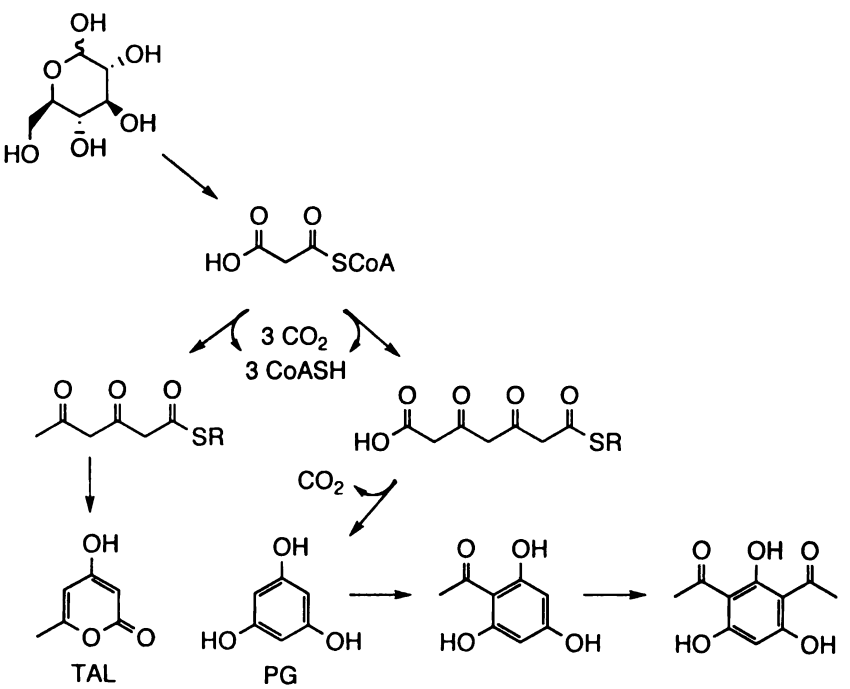

Figure 32. Biosyntheses of TAL, phloroglucinol and diacetylphloroglucinol.

The class of proteins that catalyze synthesis and closure to these aromatic molecules are polyketide synthases (PKS). Three distinct types of PKS exist to date. PKS's all exhibit a β-keto-synthase (KS) unit that, in a head-to-tail fashion, incorporate sequentially the addition of acetate units linking together a polyketide of various lengths. Unlike their most commonly accepted ancestor, fatty acid synthases, PKS do not share, to the same extent, the systems causing reduction or dehydrations to occur, therefore leaving

in tact the more reactive, polarized ketones. Configuration and proximity of these reactive groups yield multitudes of substituted mono- and polycyclic products. With a varied number of incorporated acetate units, derived from decarboxylations of malonyl CoA, and the added number of ring closure conditions, the types of polyketide products elicited range the entire spectrum of size, biological activity, and uses all from one simple acetate building block. Some of the forefront uses for polyketide natural products include treatments for physiological disorders, antibiotics, fungicides and pesticides, among others.

Type I PKS are large, modular in order and consist of sequential domains that catalyze desired reactions (Figure 33). Type II PKS rely on separable proteins, oftentimes with distant positioning on the chromosome, that must come together independently and form complexes that behave similarly to the Type I PKS subset mentioned earlier. Type III, the smallest and simplest PKS, only utilize a KS domain with an active site cysteine as the catalytic unit. Type III PKS usually exist as homodimers around 50 kDa in size and consisted of primarily plant genes of the Chalcone synthase (CHS) and Stilbene synthase (STS) likeness until about a decade ago when bacterial type III PKS were identified, mostly due to bioinformatics searches of sequence similarity spawning from the informationally rich genomic era.[12]

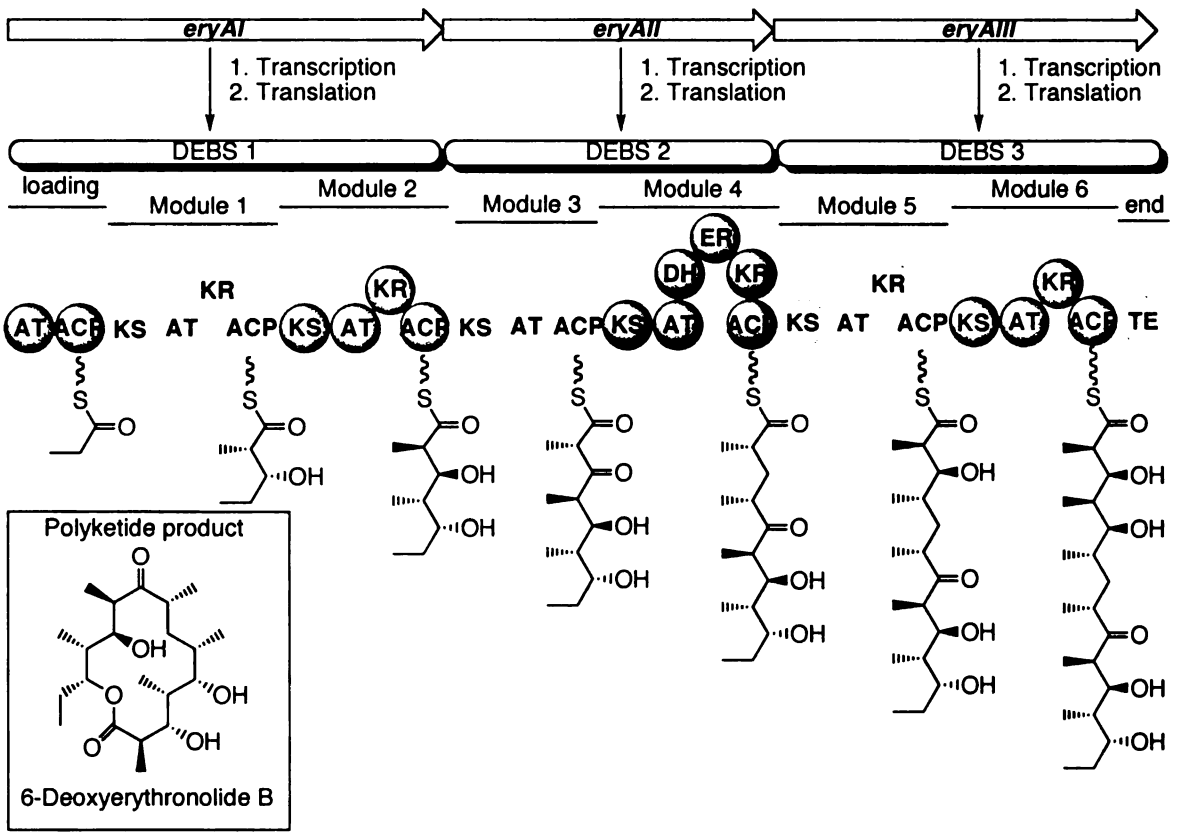

Figure 33. Type I polyketide synthase depiction.[13]

AT=Acyltransferase; ACP=Acyl carrier protein; KS=Ketosynthase; KR=Ketoreductase; ER=Enoyl reductase; DH=Dehydratase; TE=Thioesterase.

PhlD was assigned as a 38 kDa protein that exists as a homodimer in solution. PhlD utilizes malonyl CoA as the primary substrate albeit with the possibility of incorporation of one varied CoA substrate. The broad substrate specificity is demonstrated accepting C4-C12 aliphatic acyl-CoAs along with phenylacetyl-CoAs to form C6-polyoxoalkylated α-pyrones mediated by a tunnel exiting the active site.[14] Zha also reports the kinetics and stability of PhlD showing the k_{cat} = 24+/-4 min^{-1}, K_m = 13+/-1 μM, k_{cat}/K_m= 1883 $mM^{-1}min^{-1}$, all similar to the results found in the Frost lab along with the feedback insensitivity data, which are substantially higher than other Chalcone

synthases. PhlD is a relatively unstable protein losing 50% activity in 128, 74 and 7.2 min at 25, 30 and 37 °C, respectively.[14]

Chalcone synthases and other Type III PKS have a highly conserved cysteine residue within the active site.[12] As a model the PhlD was aligned with a more characterized protein in 1,3,6,8-Tetrahydroxynapthalene Synthase (THNS) isolated from *Streptomyces coelicolor*, a known type III PKS. When the catalytic cysteines were overlaid the known cys-his-asn catalytic triad of THNS was conserved in the input PhlD sequence along with the "gatekeeper" phenylalanines that either aid in decarboxylation and/or detouring water that may hydrolyze the thioesters formed during the reaction.

Using known comparison to the mechanisms of the chalcone family a mechanism for PhlD can be proposed (Figure 34). The active site cysteine, ionically supported by the charged histidine residue, is primed with an acyl CoA through a thioester linkage and releases the CoA thiol.

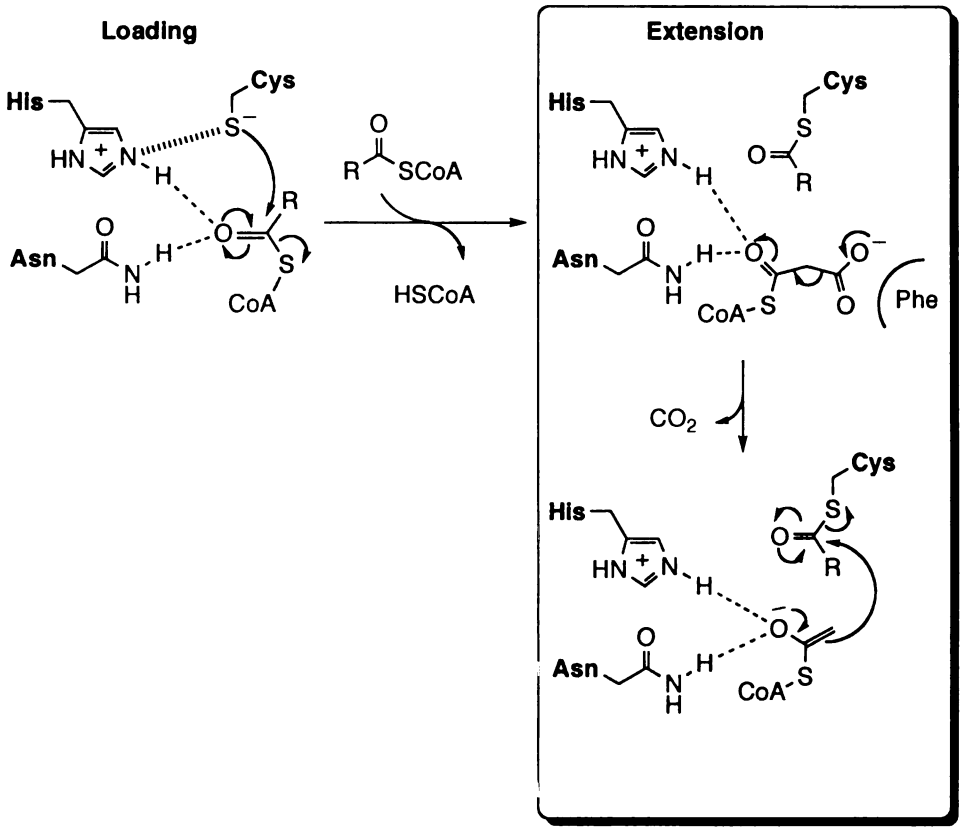

Figure 34. Catalytic triad and priming PhlD mechanism.

The subsequent decarboxylation of another acyl-CoA undergoes a Claisen condensation with the acylated cysteine residue and chemically breaks the thioester, releasing the active cysteine for further extension of the polyketide. PhlD has only been seen to utilize up to three malonyl-CoA, or one additive acyl-CoA and two malonyl-CoA starter units, so it is postulated that in a final self-condensation of a decarboxylated polyketide phloroglucinol is produced (Figure 35).

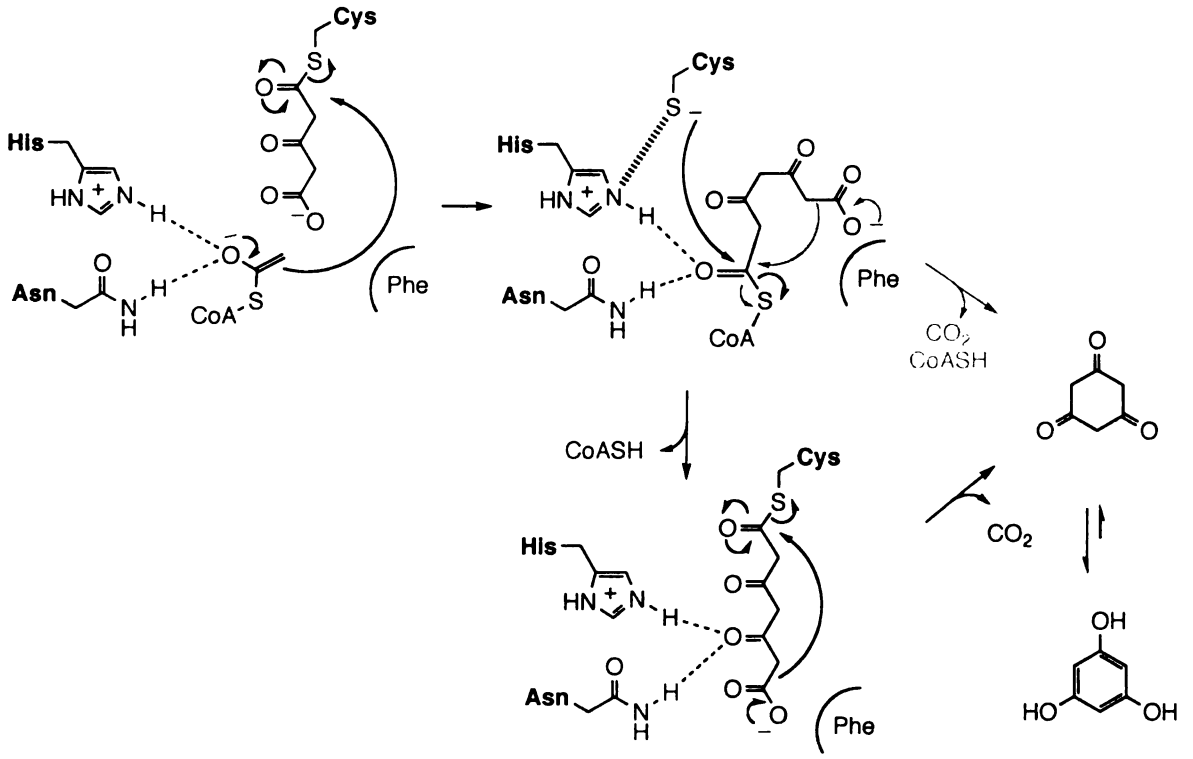

Figure 35. Polyketide ring closing mechanism.

Drs. Jihane Achkar, Dongming Xie, and Mo Xain in the Frost lab collaborated on the initial screenings of host and promoters for heterologous expression. The *E. coli* K-12 strains JWF1(DE3), KL3(DE3), and W3110serA(DE3) and *E. coli* B strain BL21serA(DE3) were chosen to investigate the effect of host strains on phloroglucinol production. The phloroglucinol productions, in M9 minimal salts culture medium with glucose as the sole-carbon source, for *E. coli* BL21serA(DE3) or BL21serA expressing *phlD* under P_{T7}, P_{T5}, and P_{tac} promoters were also compared. All the experiments were performed under glucose-limited fed-batch fermentor conditions and the temperature was controlled at 36 °C. The *E. coli* BL21serA(DE3) expressing *phlD* under P_{T7} promoter synthesized 3.5 g/L phloroglucinol while BL21serA expressing *phlD* under P_{T5} or P_{tac}

promoter synthesized 2.3 g/L. Among all the strains investigated the *E. coli* BL21serA(DE3)/pJA3.131A (Figure 48) synthesized the highest titer and yield of phloroglucinol, but the concentrations reached the maximum at 18 h, which is only 6 h after the first IPTG induction (Figure 36). W3110serA(DE3)/pJA3.131A was the highest titer and yield producing *E. coli* K-12 strain and synthesized the second highest titer of phloroglucinol, which appeared at 24 h, *i.e.* 12 h after the first IPTG induction. Both BL21serA(DE3)/ pJA3.131A and W3110serA(DE3)/pJA3.131A were chosen for further investigation.

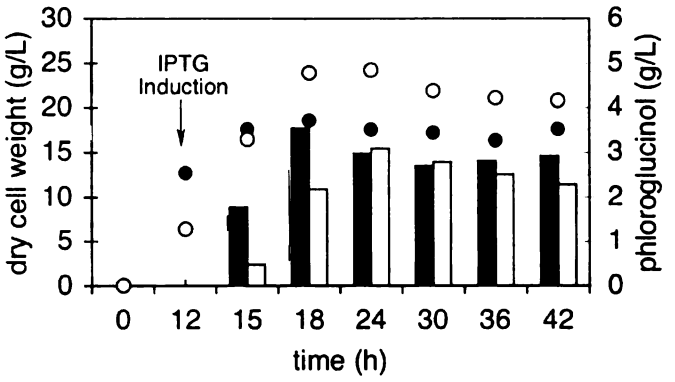

Figure 36. Comparative fed-batch phloroglucinol microbial synthesis of *E. coli*.
Phloroglucinol synthesized by W3110serA(DE3)/pJA3.131A (open circles, dry cell weight; open bars, phloroglucinol) and BL21serA(DE3)/pJA3.131A (black circles, dry cell weight; black bars, phloroglucinol) under glucose-limited culture conditions.

Optimized fed-batch microbial syntheses of W3110serA(DE3)/pJA3.131A and BL21serA(DE3)/ pJA3.131A, which are K-12 and B-type *E. coli* strains respectively, with plasmid harboring the phlD gene isolated from *P. fluorescens* Pf-5 behind a T7 promoter and a serA nutritional marker for plasmid maintenance was used for the process optimization.

It was soon realized that there was a ceiling on phloroglucinol production of about 4-5 g/L, and that cells began to show stress when titers achieved 2 g/L indicated by observance of culture characteristics and glutamic acid later identifed.[15] The sensitivity to phloroglucinol was verified on liquid and solid medium with added authentic phloroglucinol and determined with IPTG induced production strains. Based on the previous experience in the microbial synthesis of catechol[16] the *in situ*, resin-based extractive microbial synthesis was employed to eliminate sensitivity to phloroglucinol by binding the produced phloroglucinol on resin (Figure 37).

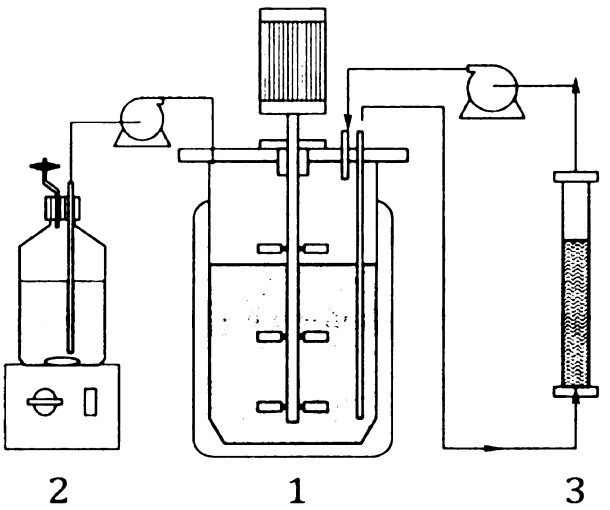

Figure 37. Schematic diagram of fed-batch, *in situ* resin based extractive microbial synthesis. (1) 1L working volume fermentation vessel; (2) PID controlled glucose addition; (3) Externally looped, peristaltic pump driven, fluidized resin bed extractive unit.

Using the *in situ*, multi-column (columns were typically changed every 8-12 h following induction while flowing at 8-12 mL/min), resin-based extraction, the phloroglucinol concentrations in the culture medium were maintained below 1.5 g/L. Compared with the fed-batch microbial synthesis without using resin-based extraction, the

extractive microbial synthesis improved the titers of phloroglucinol threefold and the yield by twofold to 15 g/L and 11% mol phloroglucinol/mol glucose, respectively. To establish whether or not phloroglucinol production could be a continuous process along side the addition of young cells that can have more robust cellular function that have not been subject to a sensitizer, a 2-stage, fed-batch continuous extractive microbial synthesis was investigated (Figure 38). In many microbial synthesis processes, particularly for secondary metabolite production, cell growth and product formation steps should be separately operated owing to the fact that optimal conditions for each step are different. Therefore, a two-stage continuous culture system may be more efficient than the single-stage mode by controlling cell growth and product formation in different stages.[17,18,19] For example temperature optimization at 36 °C for *E. coli* growth was found not to be the optimal temperature for phloroglucinol production at 33 °C. This may be because of phlD genes host *Pseudomonas* has an optimal growth temperature of 30 °C, or that expression of toxic protein have been shown to occur optimally at lower temperatures than ideal for a given host.

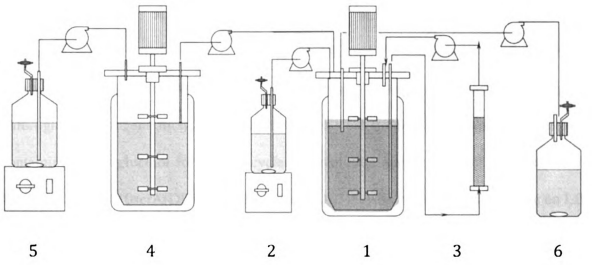

Figure 38. Schematic diagram of two-stage, fed-batch, *in situ* extractive microbial synthesis.

(1) 1L working volume production microbial synthesis vessel. (2) PID controlled glucose addition. (3) Externally looped, peristaltic pump driven, fluidized resin bed extractive unit. (4) 1L working volume seed microbial synthesis vessel. (5) PID controlled diluted glucose addition. (6) overflow collection.

Phloroglucinol production was doubled to 35 g/L (without inclusion of the volume associated with the uninduced vessel), while the yield remained around 10% due to the glucose consumption of the extra, uninduced, seed vessel. During the time of the two-stage phloroglucinol production experiment evolution of the *E. coli* production strain was attempted.

The sensitivity of the producing strains to phloroglucinol in the medium was targeted for further improvement of *in vivo* phloroglucinol synthesis. Although the sensitivity was alleviated by maintaining the phloroglucinol at low concentration using *in situ* resin-based extraction, a phloroglucinol resistant producer would lower costs if an external loop was discarded. The strategy used was to get cells from the microbial synthesis of W3110serA(DE3) and BL21serA(DE3) when phloroglucinol concentrations

in the medium were above 3 g/L, streak out the strain onto LB plates containing phloroglucinol (LB with 1-5 g/L phloroglucinol), and then incubate at 37 °C for a selection of a colony that could grow on plates containing consistently higher phloroglucinol concentrations. The single colonies were streaked out again onto LB plates containing phloroglucinol for further cycles of evolution and excision of plasmid DNA. Two strains, W3110serA(DE3)* and BL21serA(DE3)*, which could stably survive on LB plates containing phloroglucinol were evolved from their parent strains, W3110serA(DE3) and BL21serA(DE3).

Results

Sensitivity Screening

Growth curves of W3110serA(DE3)/pJA3.131A were established along side sensitivity assays to phloroglucinol. Toxicity assays were developed in both liquid and solid medium. Minimal salts plates were poured with glucose and authentic phloroglucinol was added. W3110serA(DE3)/pJA3.131A was grown on 0, 0.01, 0.05, 0.1, 0.2, and 0.4 g/L phloroglucinol on M9 minimal salts medium containing glucose plates and allowed to grow at 37 °C for 24 h with signs of inhibition at 0.2 g/L and no growth on plates containing 0.4 g/L phloroglucinol. In liquid M9 minimal salts medium containing glucose, a 125 mL culture was aliquoted into tubes with appropriate amount of phloroglucinol and blank medium added to consistently dilute the cultures and absorbance at 600 nm was recorded with up to 10 g/L phloroglucinol concentration added. The sensitivity is lower in liquid medium as only 5 g/L phloroglucinol (Figure 39) started to

have a profound negative impact on growth while lower concentrations of phloroglucinol increase growth rate.

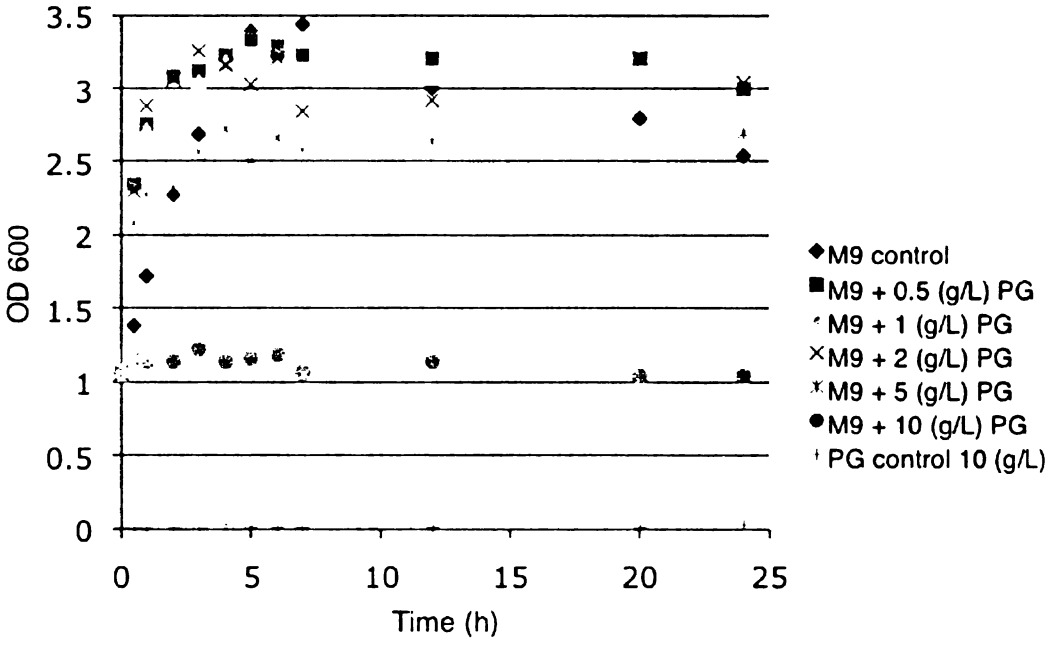

Figure 39. Phloroglucinol toxicity screening of W3110serA(DE3)/pJA3.131A

Phloroglucinol Microbial Synthesis

Microbial synthesis of W3110serA(DE3)/pJA3.131A, W3110serA(DE3)*/ pJA3.131A, BL21serA(DE3)/pJA3.131A and BL21serA(DE3)*/pJA3.131A commenced in fed-batch, single stage fed-batch extractive, two stage fed-batch extractive and five-stage fed batch modes with phloroglucinol titers and yields depicted in (Figure 40), with a representative profile in (Figure 41), (Figure 42), (Figure 43) and (Figure 44) and quantified by gas chromatography according to response factor and isolated yields (as

discussed later). As a proof of concept towards reproducibility of the process, close to 300 g of phloroglucinol was isolated using the two-stage extractive microbial synthesis of BL21serA(DE3)*/pJA3.131A.

Entry	Strain	Fed-Batch Titer(g/L) : Yield(%mol/mol)	Fed-Batch Extr. Titer(g/L) : Yield(%mol/mol)	2-Stg Contn Extr. Titer(g/L) : Yield(%mol/mol)
1	BL21serA(DE3)/pJA3.131A	3.8 : 3	16.8 : 12	35.0 : 6
2	BL21serA(DE3)*/pJA3.131A	4.3 : 5	17.2 : 12	37.6 : 6
3	W3110serA(DE3)/pJA3.131A	3.6 : 3	15.0 : 11	N/A
4	W3110serA(DE3)*/pJA3.131A	4.0 : 5	17.0 : 12	36.6 : 6

Figure 40. *E. coli* phloroglucinol production from microbial synthesis.

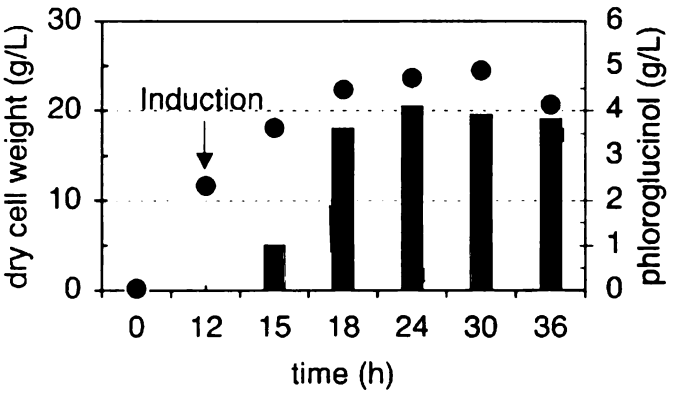

Figure 41. *E. coli* phloroglucinol fed-batch extractive microbial synthesis profile.
(black circles=dry cell weight, black bars=phloroglucinol in culture medium)

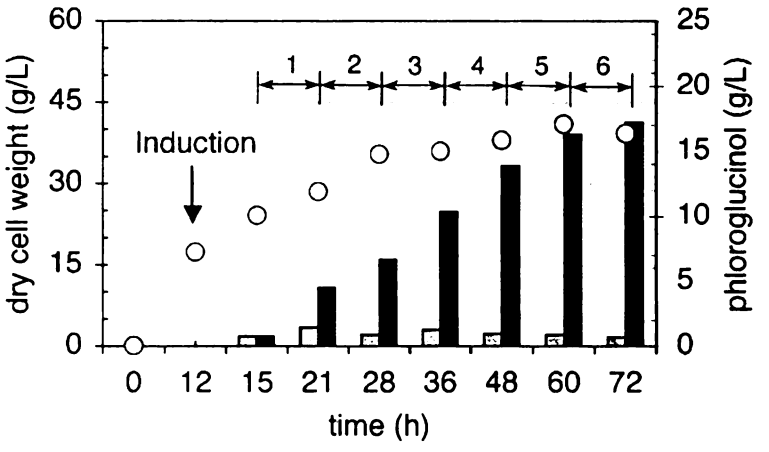

Figure 42. *E. coli* phloroglucinol single stage fed-batch extractive microbial synthesis profile. (white circles=dry cell weight, grey bars=phloroglucinol in culture medium, black bars=phloroglucinol total, number and arrows indicate a change in extractive column and duration of time used respectively)

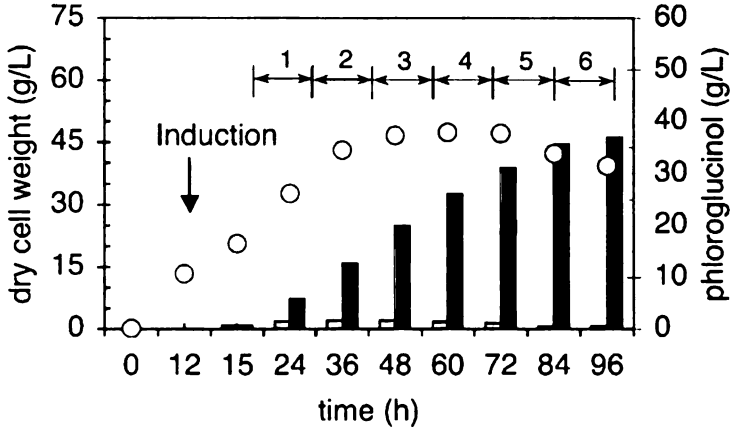

Figure 43. *E. coli* phloroglucinol two stage fed-batch extractive microbial synthesis profile. (white circles=dry cell weight, grey bars=phloroglucinol in culture medium, black bars=phloroglucinol total, number and arrows indicate a change in extractive column and duration of time used respectively)

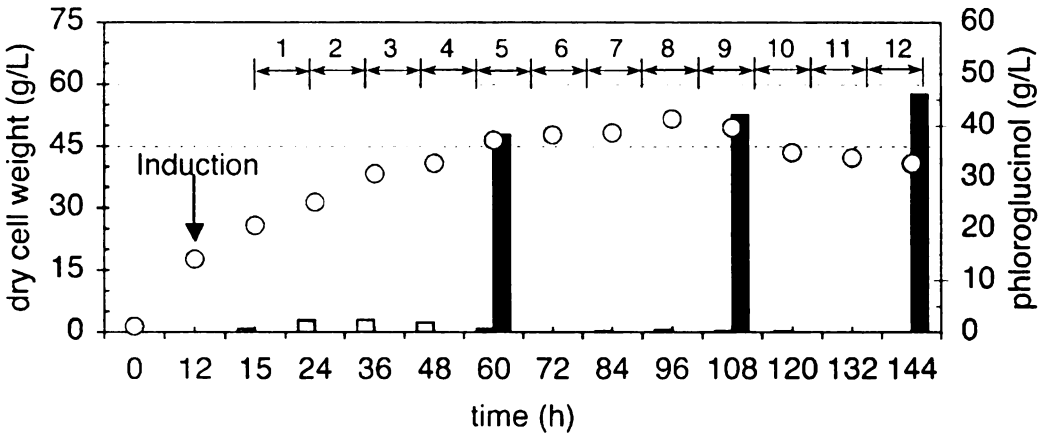

Figure 44. ***E. coli*** **phloroglucinol five stage fed-batch extractive microbial synthesis profile.** (white circles=dry cell weight, grey bars=phloroglucinol in culture medium, black bars=phloroglucinol total, number and arrows indicate a change in extractive column and duration of time used respectively)

Transcriptome analysis of W3110serA(DE3)/pJA3.131A

An approach to combat proposed phloroglucinol sensitivity to *E. coli* strains is to determine what and if phloroglucinol targets to cause cell-death and bioengineer a new microbial biocatalyst that is phloroglucinol resistant. Microbial organisms will oftentimes induce expression of defense and export proteins when subjected to toxic chemicals. The panic mode of the cell may induce efflux or transport systems along with membrane channel protein expression (Figure 45). Transcriptome analysis can be a powerful tool to indirectly analyze protein regulation.

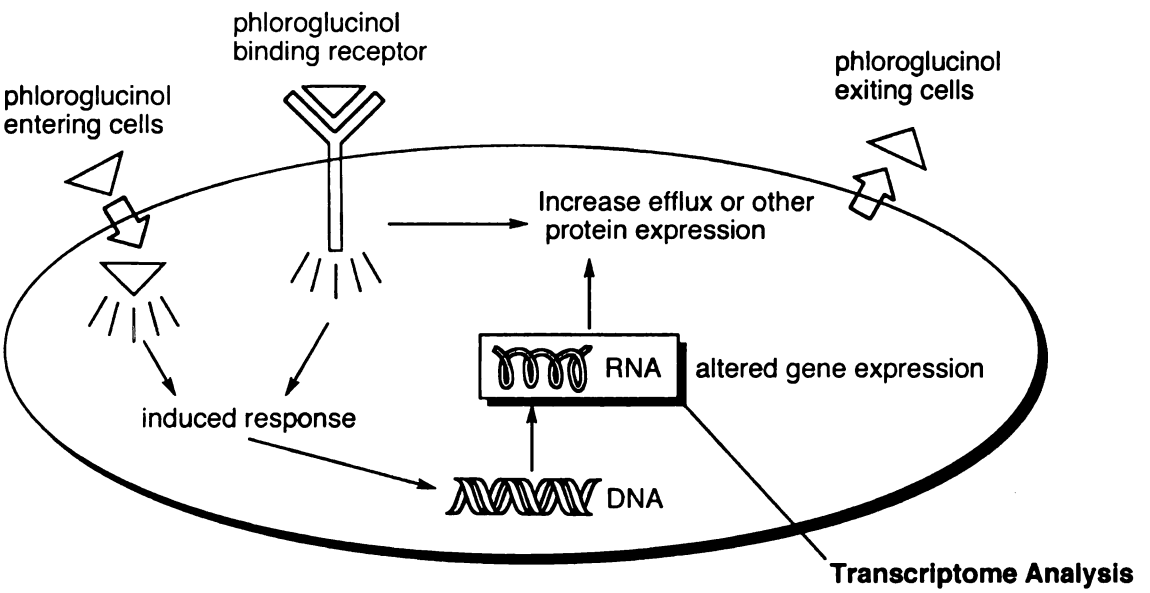

Figure 45. Ideology behind use of transcriptome analysis

Affymetrix genechip microarray technology was utilized in the transcriptome analysis. These genechips monitor RNA expression levels through fluorescence measurements. Distinctive fragmented sequences of gene compliments are embedded as "probes" to seek out subjected sequences. Sample cDNA with a fluorescent tag is placed

on the genechip. Complimentary strands will bind, the genechip will then be stained and washed, and fluorescence will be monitored (Figure 46). Once analyzed, gene expression levels are obtained and the information must be sorted with the utmost scrutiny. It is important to note that regulation values do not necessarily correlate with increased expression of proteins and even if that were true, upregulation of protein levels vary with increased function of that protein, all disregarding the possibility of post-translational modification deficiencies towards an unrelated over-expressed gene.

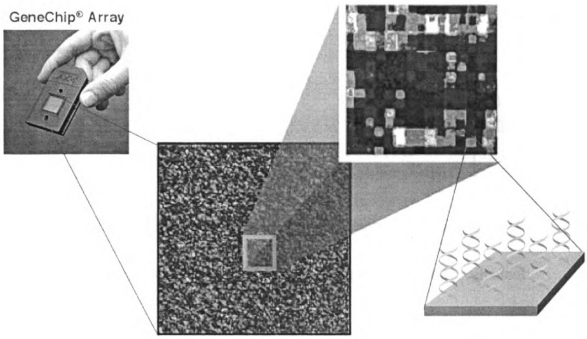

Figure 46. Affymetrix genechip microarray technology

E. coli 2.0 genechip array contains 10,000 probes for all 20,366 genes in four *E. coli* strains: K-12, two 0157 strains, and CFT073.

Since it is not known how and if phloroglucinol is directly toxic to cells, two different experiments were conducted. Dr. Ningqing Ran of the Frost lab was a coworker

on this project who looked at an approach subjecting outside additions of authentic phloroglucinol (2 g/L) to healthy, non-phloroglucinol producing cells and analyzed gene expressions 1 h after subjection (Figure 47).

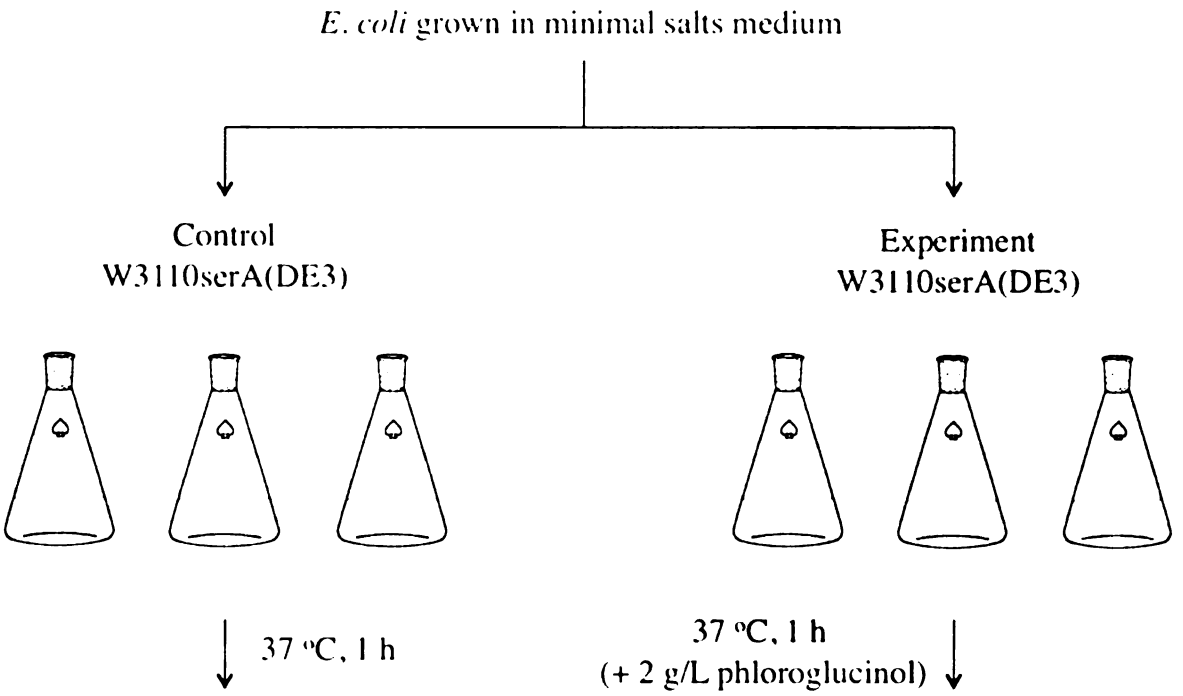

Figure 47. Transcriptome analysis of *E. coli* after addition of phloroglucinol

In other efforts, RNA levels are analyzed looking at phloroglucinol producing strains. Knowing what genes are over-expressed may lead to delineating a phloroglucinol export system, and it is possible that if phloroglucinol is toxic to the inside of the cell over-expressing this export system may result in a more phloroglucinol resistant host strain. Transcriptome analysis was conducted to determine up-regulated genes of a phloroglucinol producing *E. coli* strain W3110 serA(DE3)/pJA3.131A. In order to

substantially limit the number of up-regulated genes that are possibly unimportant in phloroglucinol export, a non-phloroglucinol producing *E. coli* strain W3110 serA(DE3)/pBC1.146 was constructed. pBC1.164 is a plasmid identical to pJA3.131A except that the region of the plasmid encoding the phlD gene is missing (Figure 48).

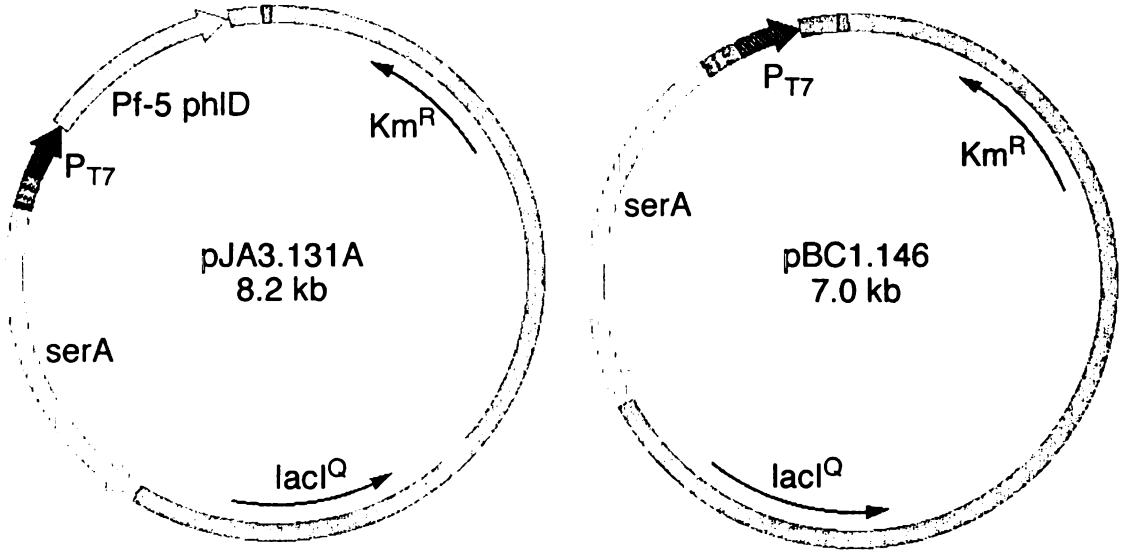

Figure 48. Plasmids pJA3.131A and pBC1.146.

Comparison of the control and the phloroglucinol producing strain eliminates up-regulation associated with other cellular functions and the burden of carrying a plasmid of comparble size.

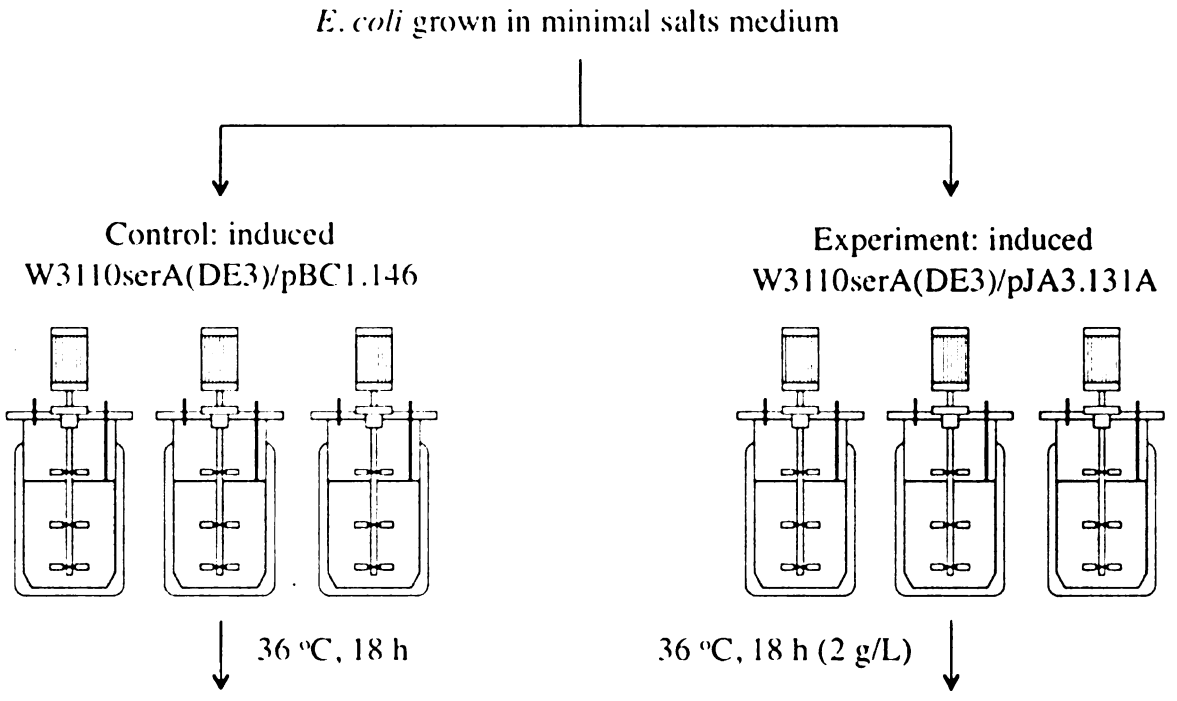

Figure 49. Transcriptome analysis of induced phloroglucinol producing *E. coli*

Once target protein inducing genes are found to be upregulated by transcriptome analysis two strategies can help determine possible phloroglucinol efflux mechanisms. One tactic employs chromosomal deletions of the critical nucleotide bases that encode the protein. This deletion methodology is often called a "gene knock-out". Once the knock-out is successful the new host will undergo a series of toxicity screenings in both suspension and solid medium. If the strain is hypersensitive to phloroglucinol then the deleted gene will be over-expressed and the new host will then be subject to a microbial synthesis process and phloroglucinol production will be monitored by established gas chromatography methods. Should the host with over-expression of the gene, in which the deletion caused hypersensitivity, increase phloroglucinol accumulation then the targeted

gene may be involved in phloroglucinol export. However showing a knocked-out gene is hypersensitive does not explicitly give data that supports it is involved in phloroglucinol export. The knock-out could be affecting another crucial export or encode for other downstream expressions that are important in cell viability. If over-expression of the knocked-out gene that lead to no phloroglucinol production leads to a more resistant host and produces elevated levels of phloroglucinol there is reason to believe that the protein that gene encodes for may have a role in phloroglucinol transport. The other strategy is the reverse approach where you over-express the up-regulated genes and look for a resistant host. There are chances for inherent problems to arise using this reverse approach such as verification of actively expressed protein.

The following charts indicate some of the resulting cross referencing of experiments that were found to have interesting gene expressions in comparison with the aforementioned control, along with the extent of regulation indicated by fold cutoffs determined post experiment where applicable. For complete transcriptome analyses and graphical comparisons see experimental. Since up-regulated genes is the obvious starting point, the genes found to be upregulated compared to the control of the phloroglucinol producing experiment are listed in (Table 5).

Genes Upregulated (4x)				
acpD	bio**AD**	moaBC	wecB	yegN
acrD	**cchB**	mopAB	xerC	yfaE
apaH	celF	nagABC	yabN	yfbN
argA**BCDFG**HI	clpB	nrdABCD**EFGHI**	**yacH**	yfiA
aroH	**cspI**	nth	yaeC	ygbE
artJMPQ	cysACD**HIJ**MNW	plsB	yagDL	ygcK
asnC	dnaJK	ppx	ybbN	ygiAC
b0830, b0832,b0833	elaD	pykF	**ybcK**	**yhdV**
b1436	eno	rfaC	ybeFZ	yibG
b1498, **b1499, b1500, b1501, b1502, b1503, b1504**	evgS	rfaL	ybg**DH**	**yigB**
b1551	fimE	rffGH	ybhRS	yjcV
b1632	glnD	**rygAB**	ybiJM	**yjfN**
b2074	gltB	selB	**ycbB**	yjhB**C**
b2085	hisP	sgcQ	ycel	yjiD
b2385	Hpr	**sodA**	ycfS	**yjjM**
b2460	htp**GX**	**spy**	**yciW**	ykgH
b2758	**ibpAB**	sseB	ycjFX	ymfDE
b3400, b3401	manXYZ	trpA	**ydeH**	yqel**J**
b3913,b3914	mcrC	udhA	ydgQ	**yqhD**
betA	metJK	uvrC	**yeaD**	yqjBI
bglA	micF	uxuB	yebE	yrfHI

Table 5. Upregulated genes found by transcriptome analysis in phloroglucinol producing strain. (a) genes are at least upregulated fourfold while the bolded genes are at least eightfold upregulated.

Narrowing down the roughly 4,400 genes of *E. coli* by transcriptome analysis was a starting point for elucidation of a possible phloroglucinol export system. The corresponding genes were carefully analyzed across phloroglucinol produced and phloroglucinol added analyses (Figure 50 and Table 6) with emphasis towards overlapping known export and membrane proteins (Figure 51 and Table 7). Further experimentation was orchestrated by coupling the transcriptome results with both the 37 known *E. coli* transport proteins and intuition of probable targets theorized prior to transcriptome analysis from established literature.

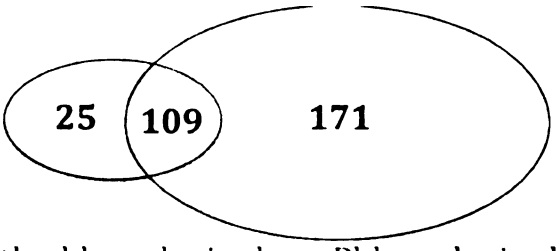

Figure 50. Corresponding up-regulation twofold and greater in phloroglucinol producing and phloroglucinol added transcriptome analyses.

Genes Up-regulated in both transcriptome analyses W3110	
	Definition
acpD	acyl carrier protein phosphodiesterase
acrD	possible efflux pump
apaH	diadenosine tetraphosphatase
argA	N-acetylglutamate synthase; amino acid acetyltransferase
argB	acetylglutamate kinase
argC	N-acetyl-gamma-glutamylphosphate reductase
argD	acetylornithine delta-aminotransferase
argF	ornithine carbamoyltransferase 2
argG	argininosuccinate synthetase
aroH	3-deoxy-D-arabinoheptulosonate-7-phosphate synthase (DAHP synthetase
artJ	arginine 3rd transport system periplasmic binding protein
b0261	yagD
b0309	
b0476	putative lipase
b0833	
b0834	hypothetical protein
b0851	modulator of drug activity A
b1057	putative cytochrome
b1451	putative outer membrane receptor for iron transport
b1498	putative sulfatase
b1499	putative ARAC-type regulatory protein
b1500	
b1501	putative oxidoreductase, major subunit
b1502	putative adhesin; similar to FimH protein
b1504	putative fimbrial-like protein

Table 6. Corresponding up-regulation twofold and greater in phloroglucinol producing and phloroglucinol added transcriptome analyses.

Table 6. cont

b1679	hypothetical protein
b1683	hypothetical protein
b1684	hypothetical protein
b1730	hypothetical protein
b2074	putative membrane protein
b2085	
b2385	putative peptidase
b2680	hypothetical protein
b3050	putative oxidoreductase
b3051	putative membrane protein
b3840	Mg-dependent DNase
b3913	
b3914	
baeS	sensor protein (for BaeR)
bcr	bicyclomycin resistance protein; transmembrane protein
bioA	8-diaminopelargonic acid synthetase
bioD	dethiobiotin synthetase
celF	phospho-beta-glucosidase; cryptic
elaD	putative sulfatase / phosphatase
fimZ	fimbrial Z protein; probable signal transducer
fpr	ferredoxin-NADP reductase
garD	(D)-galactarate dehydrogenase
gidB	glucose-inhibited division; chromosome replication?
hscA	DnaK-homologue chaperone Hsc66
manX	PTS enzyme IIAB
manY	PTS enzyme IIC mannose-specific
manZ	PTS enzyme IID mannose-specific
metJ	repressor of all met genes but metF
metK	methionine adenosyltransferase 1 (AdoMet synthetase); methyl and propylamine donor
micF	regulatory antisense RNA affecting ompF expression
nagA	N-acetylglucosamine-6-phosphate deacetylase
nagB	glucosamine-6-phosphate deaminase
nrdE	ribonucleoside-diphosphate reductase 2
nrdF	ribonucleoside-diphosphate reductase 2
nrdH	glutaredoxin-like protein; hydrogen donor
nrdI	
pfkB	6-phosphofructokinase II; suppressor of pfkA
rffH	glucose-1-phosphate thymidylyltransferase
rhsB	rhsB protein in rhs element
rygA	
rygB	
spy	
sseB	enhanced serine sensitivity
sufS	selenocysteine lyase, PLP-dependent
tdcD	putative kinase
trkA	transport of potassium
uxuB	D-mannonate oxidoreductase
wecB	UDP-N-acetyl glucosamine -2-epimerase; synthesis of enterobacterial common antigen (ECA)
wecD	

Table 6. cont

yacH	putative membrane protein
yagL	DNA-binding protein
ybcK	
ybgD	putative fimbrial-like protein
ybhB	hypothetical protein
ybiJ	
ycbB	putative amidase
ydeH	
yebE	
yecP	putative enzyme
YegN	multidrug transporter
yfbN	
yfiA	putative yhbH sigma 54 modulator
ygcB	hypothetical protein
ygiB	hypothetical protein
ygiC	putative synthetase/amidase
yhaK	hypothetical protein
yhbW	putative enzyme
yhdV	
yibG	
yibJ	
yieF	
yigB	putative phosphatase
yigF	
yigG	
yiiX	
yjfN	
yjgL	
yjiD	
yjjM	
ykgH	
ymfD	
ymfE	
yqhD	putative oxidoreductase
yqjI	

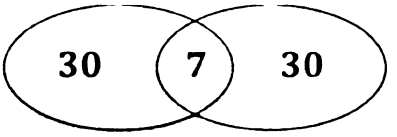

Figure 51. Corresponding up-regulation of transport or membrane protein encoding genes fourfold in phloroglucinol producing and phloroglucinol added transcriptome analyses.

Genes Up-regulated in both transcriptome Analysis W3110	
Known genes encoding transport or membrane proteins	Description
acrD	RND multidrug efflux pump (typical substrate: aminoglycosides)
b1451	putative outer membrane receptor for iron transport
b3051	putative membrane protein
bcr	bicyclomycin resistance protein; transmembrane protein
trkA	transport of potassium
yacH	putative membrane protein
YegN	(mdtB) RND multidrug transporter

Table 7. Corresponding up-regulation of transport or membrane protein encoding genes fourfold in phloroglucinol producing and phloroglucinol added transcriptome analyses.

Two known multi-drug export proteins with high transcriptional levels and regulation were identified in AcrD and YegN (MtdB). These two genes are prime targets for a phloroglucinol export system. Some of the unknown proteins were not over-looked. Many other known drug and toxic molecule transporters were also found to be up-regulated in differing amounts by the two transcriptional analysis strategies. Down-regulation of RNA expression is another target of interest. Import proteins may be shut down to stop phloroglucinol from entering the cell.

ERGO BLAST bioinformatics searches gave rise to two *E. coli* proteins that had greater than 50% homology with PhlE, the known diacetylphloroglucinol export protein in *P. fluorescens*. YjjL and YjhB were hits in W3110 strains with yjhB upregulated in both transcriptome analyses and YjjM, the putative regulator of YjjL, was overexpressed during the phloroglucinol producing analysis.

Several resources were utilized to target potential gene disruptions. acrD, acrAB, yegMN, bcr, trkA and yacH were targeted from the transcriptome analysis, yjhB was targeted from homology with phlE and yieO, yicM, yhcD, ytfL, and yqiK were looked at because of literature precedent of the gene encoding for proteins with multi component transport.

All knock-outs were conducted using the Wanner[20] methodology with the exception of yegMN which failed three times and was not completed. Confirmation of each knock-out was verified by PCR amplification of genomic DNA outside of the target sequence and observing a lower band shift indicating a loss of the gene on the chromosome. Of the knock-out mutants not one showed significant deviation from the control in the sensitivity assays in solid or liquid medium (Figure 52).

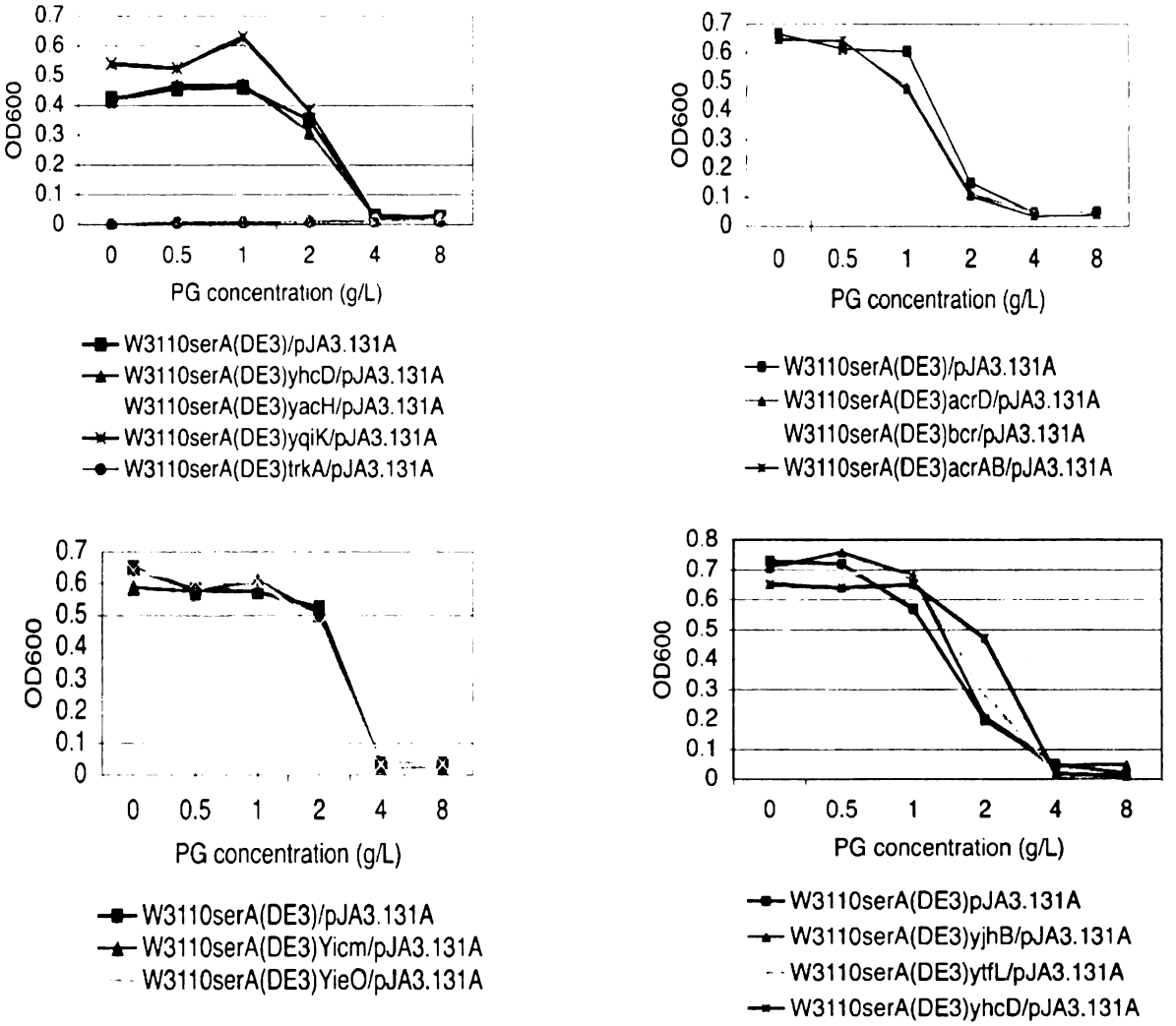

Figure 52. Sensitivity experiments of gene deletion, phloroglucinol producing strains

Genomic insertion of T7 phlD

Up to this point microbial synthesis of *E. coli* uses expression of the phlD gene from a plasmid. After a period of productivity the host construct yields a drastic decline in rate of production. Many reasons for decline can exist, but plasmid loss has been shown to be concurrent late into the microbial synthesis with the drop in productivity. Placing the phlD gene onto the chromosome of *E. coli* may aid in delineating the cause of the experimentally observed loss of phloroglucinol production if it is in fact due to loss of the phlD encoding plasmid, or may provide additional information that could be pivotal towards generating a biocatalyst that is more resistant to phloroglucinol .

The insertion of phlD utilizes slightly modified methodology outlined by Wanner. The following genomic insertion strategy up to this point has not been reported in the literature. Instead of pKD3 being used as the template plasmid for amplification of the FRT flanked DNA fragment to be recombined into a genetic region of choice, a plasmid was constructed by first inserting phlD into pKD3. This modification allows for a gene replacement to be conducted instead of deletion of genetic material as intended. The central idea is to insert phlD into lacZ with the outlined procedures in (Figure 53).

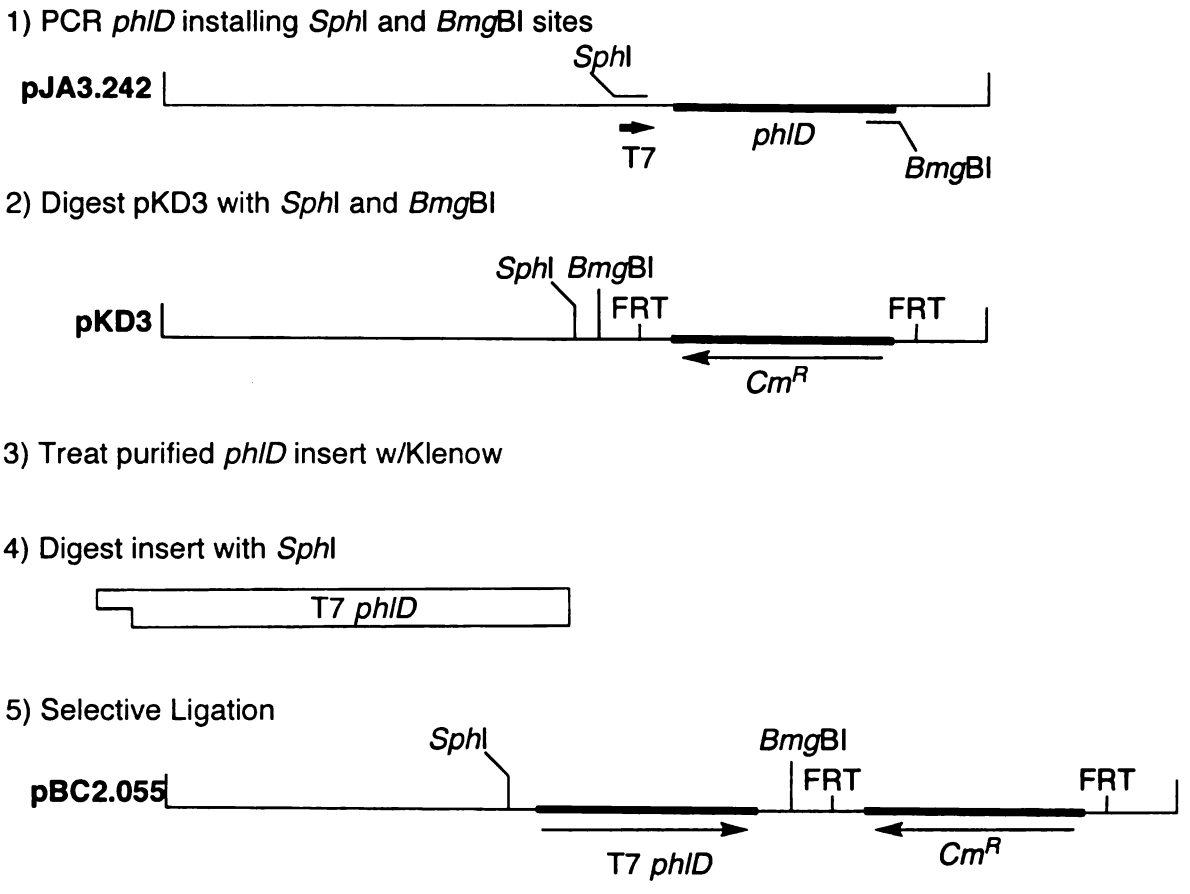

Figure 53. Controlled insertion of the T7 *phlD* genetic region into pKD3.

With a newly formed, verified plasmid in hand the Wanner methodology can be followed to insert phlD onto the chromosome of *E. coli*. The insertion is outlined in (Figure 54).

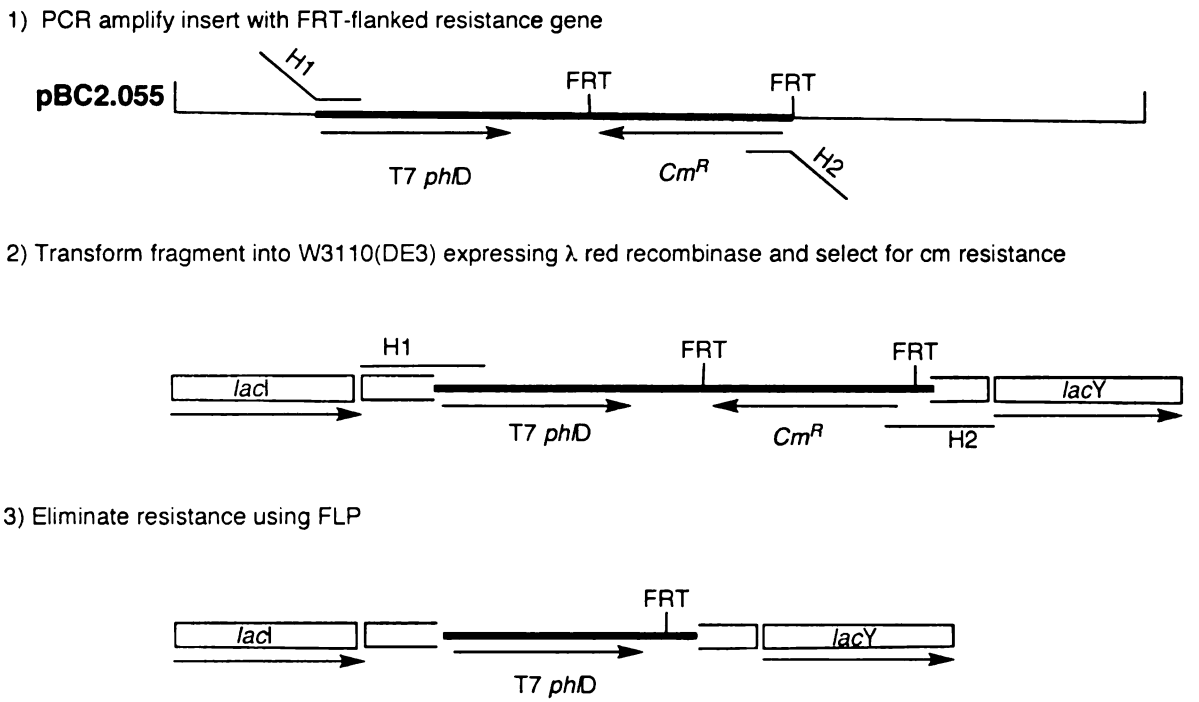

Figure 54. Wanner-type insertion of T7 phlD into the lacZ orf on the chromosome of *E. coli* W3110(DE3).

A blue-white selection on LB plates containing chloramphenicol was used as a first wave screening of mutants. When a functional β-galactosidase, a protein transcribed from the lacZ orf, is cultured with selective solid medium containing 5-bromo-4-chloro-3-indolyl-beta-D-galactopyranoside (x-gal) hydrolysis of the sugar from the indolyl functionality results in a dimerized chromophore. Those mutants who did not give evidence for a functional lacZ orf were cultured for extraction of DNA. PCR primers were chosen outside the lacZ orf, and the resulting bands did indicate a loss from the native 3.3 kb (200 bp addition of molecular weight with chosen primers over the 3.1 kb unit weight of lacZ) to a successful insertion of the T7 phlD FRT-Cm^R-FRT DNA fragment corresponding to a 2.4 kb band. Experimental results have indicated that abilities of *E. coli* to produce target molecules are lessened when the unnecessary Cm

resistance gene is kept in the chromosome. Two FRT (Flipase Recognition Target) sites flank the genetic region encoding the resistance protein.

In order to abolish resistance pCP20 is the necessary plasmid to encode the flipase to "flip-out" genetic regions between FRT sites. Electrocompetent W3110(DE3) lacZ::T7phlD FRT Cm^R FRT was transformed with pCP20 and the procedure followed the Wanner protocol. A total of 16 colonies were picked and plated on LB, LB containing chloramphenicol, and LB containing ampicillin. Correct mutants shall exhibit growth only on LB plates.

The colonies that passed the selective plate screenings were cultured and DNA was extracted. The DNA solution was the template for PCR amplification with the primers used to establish the size of the lacZ orf. The majority (75%) of the original 16 colonies were correct as indicated from a loss from 2.4 kb (lacZ::T7phlD FRT Cm^R FRT) to 1.4 kb (lacZ::T7phlD FRT). In summary, evidence of the W3110(DE3) lacZ::T7phlD FRT successful cloning includes PCR amplification of the lacZ orf indicating stepwise insertion of T7phlD FRT Cm^R FRT and then loss of the cat resistance gene as indicated by a decrease in band sizes. Besides PCR, selective plates and x-gal treated plates verified disruption of lacZ and drug resistance where appropriate.

Unfortunately, despite many efforts, the T7 phlD mutant did not grow in minimal salts medium on multiple attempts. Efforts for growth included culturing in LB medium and centrifugating, washing, and resuspending in M9 minimal salts medium with glucose. Centrifugation after 24 h would not pellet indicating cell lysis. It has been found that expression prior to stationary phase is detrimental to the cell. In the case that the genomic copy of lacI did not produce enough protein to regulate expression of the T7 RNA

polymerase, pJF118EH was transformed into the mutant and grown on LB containing ampicillin. pJF118EH has a copy of lacI. Colonies were picked and streaked on M9 minimal salts medium with glucose supplemented with ampicillin leading to a result of no growth after rather extended periods of time.

Enhancing phlD genetic expression

Specific activities of Pf-5 phlD, behind a T7 promoter expressed from the pET-based expression vector pJA3.131A, has repeatedly been shown to peak at .02 U/mg/min and lose activity sharply past a 6-12 h post-induction time period. Surpassing this barrier was looked at in the following ways. pJA3.131A has been utilized heavily in phloroglucinol biosyntheses to date, and contains excess DNA before the front terminus of the expression gene. The excess DNA could have a beneficial effect if the PhlD protein is toxic by hindering proper expression. Since it has not been ruled out though that proper gene expression could be increased with an optimally positioned promoter and ribosomal binding site, this task is important. Using pET-27b+ (Novagen cat no. 69863-3), also a pET-based plasmid, with phlD and serA genes from laboratory sources, pJA3.131A was reformed with minimal differences and optimal phlD gene positioning as pBC2.187 (Figure 55 and Figure 56).

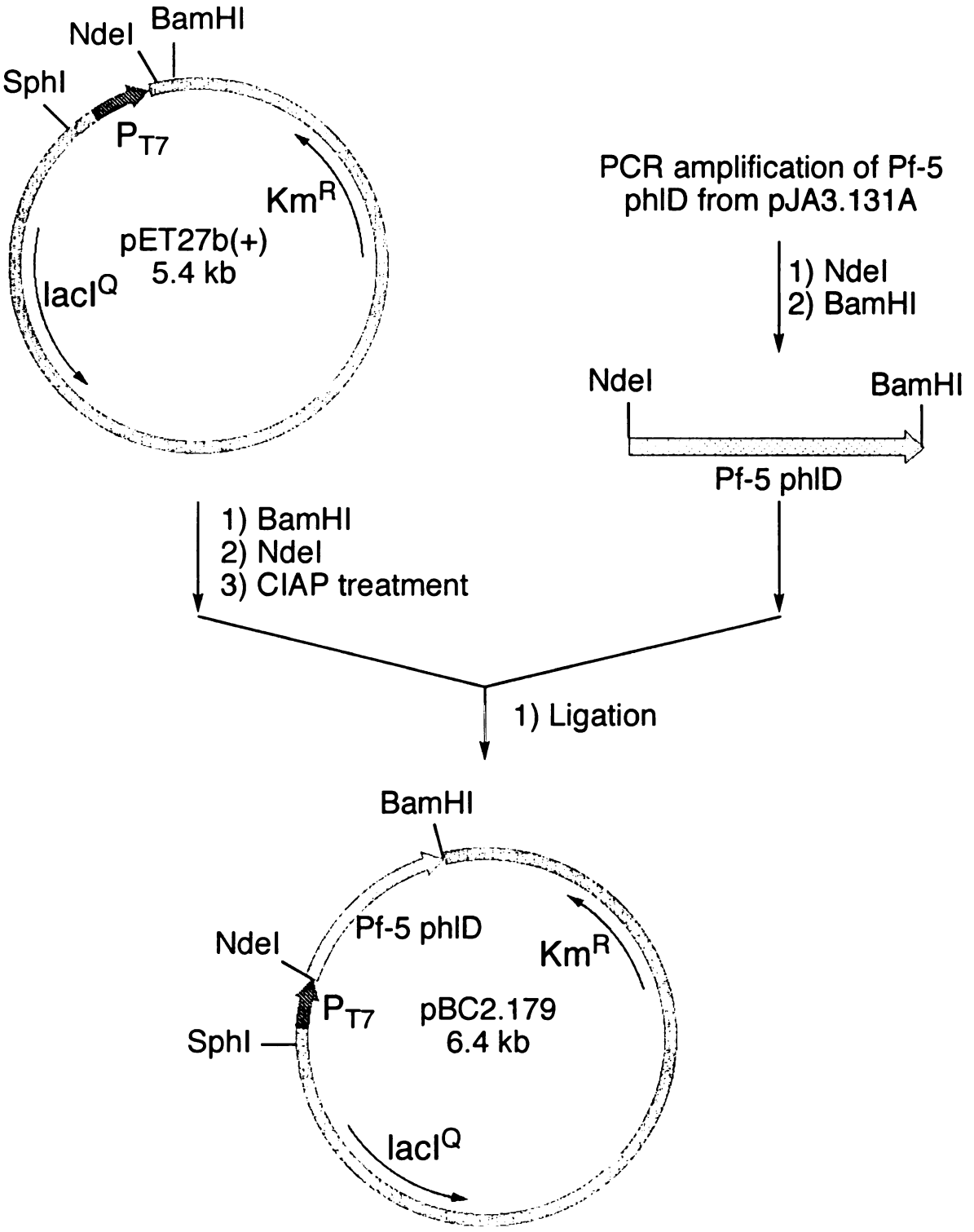

Figure 55. Construction of plasmid pBC2.179 en route to pBC2.187

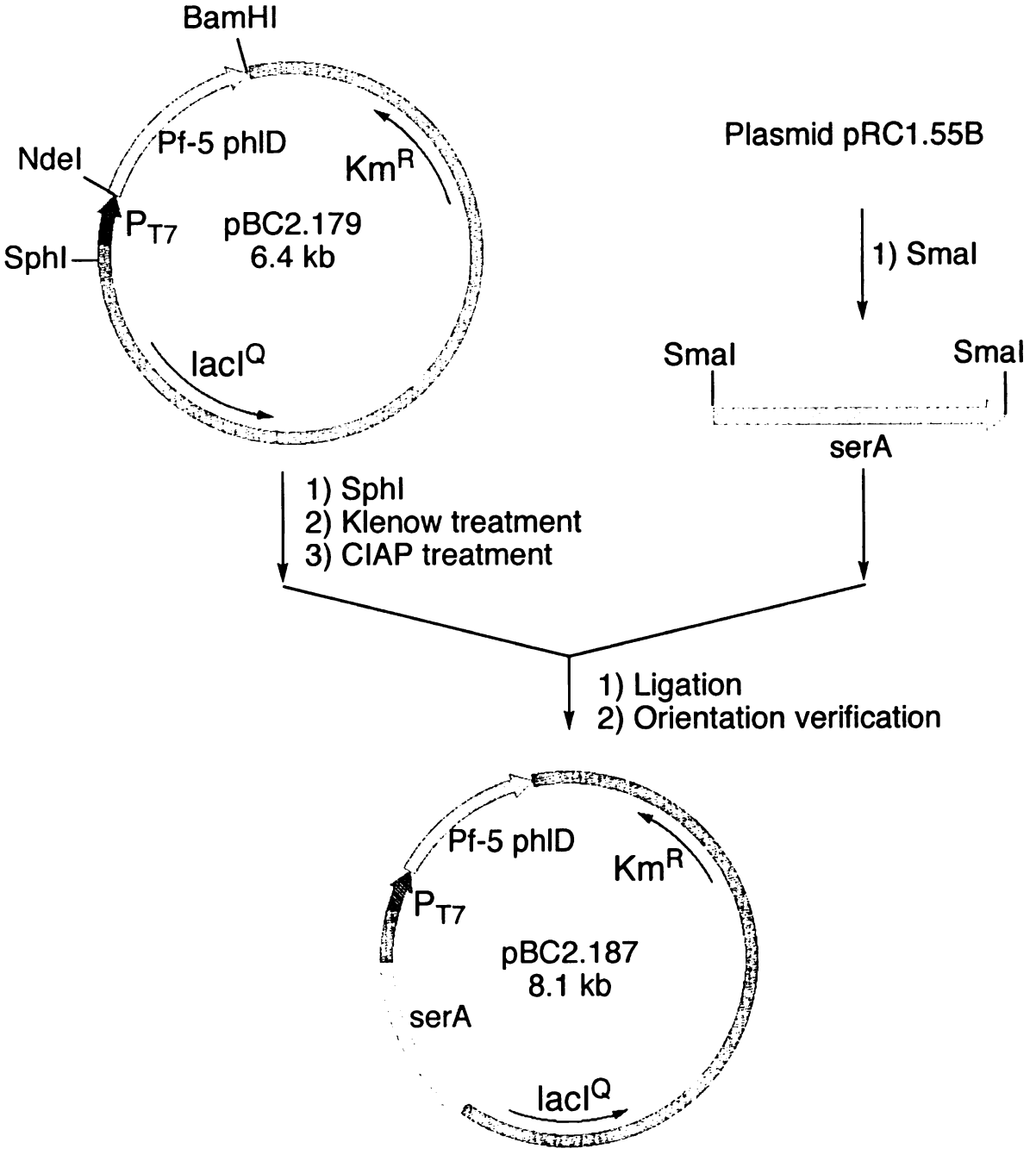

Figure 56. Construction of plasmid pBC2.187

Enzymology and phloroglucinol titers and yields comparing biosyntheses of BL21serA(DE3) transformed with pJA3.131A or pBC2.187 were not statistically different leading to the idea that optimal positioning did not alter the gene expression to an appreciable amount to change any biocatalytic production numbers. A representative SDS-PAGE gel analysis is depicted in (Figure 57 and Figure 58). In (Figure 57) time is equal to the hours after induction and See-Blue Plus 2 are molecular weight markers with bands indicated along the y-axis. Lanes 2-6 are samples taken from unmodified culture, while lanes 8-13 are culture supernatant diluted with water 5:1, water:culture supernatant. Protein depictions are based upon N-terminal protein sequencing conducted by the Michigan State University Mass Spectrometry Facility.

(Figure 58) is an SDS-PAGE analysis of soluble vs. insoluble protein (see experimental for details). The time is equal to the hours after induction and See-Blue Plus 2 are molecular weight markers with bands indicated along the y-axis. SN is equivalent to the lysate supernatant, and thus soluble protein, whereas the lysate pellet indicates what protein was not soluble in the culture supernatant and resuspended in a detergent solution. PhlD is found predominately in the insoluble fraction leading to evidence of support that most of the protein translation is used for the formation of non-phloroglucinol producing inclusion bodies. It is important to note that PhlD is the lower band of the doublet that looks as if it were one band.

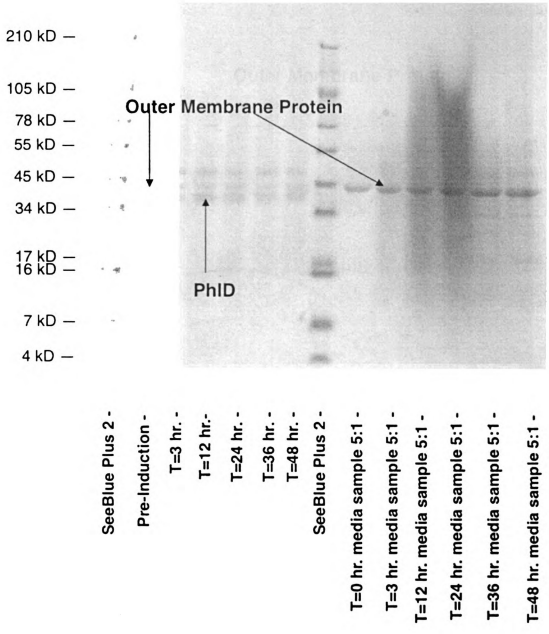

Figure 57. SDS-PAGE analysis of BL21serA(DE3)/pBC2.187

All lanes are normalized to $OD_{600} = 1$.

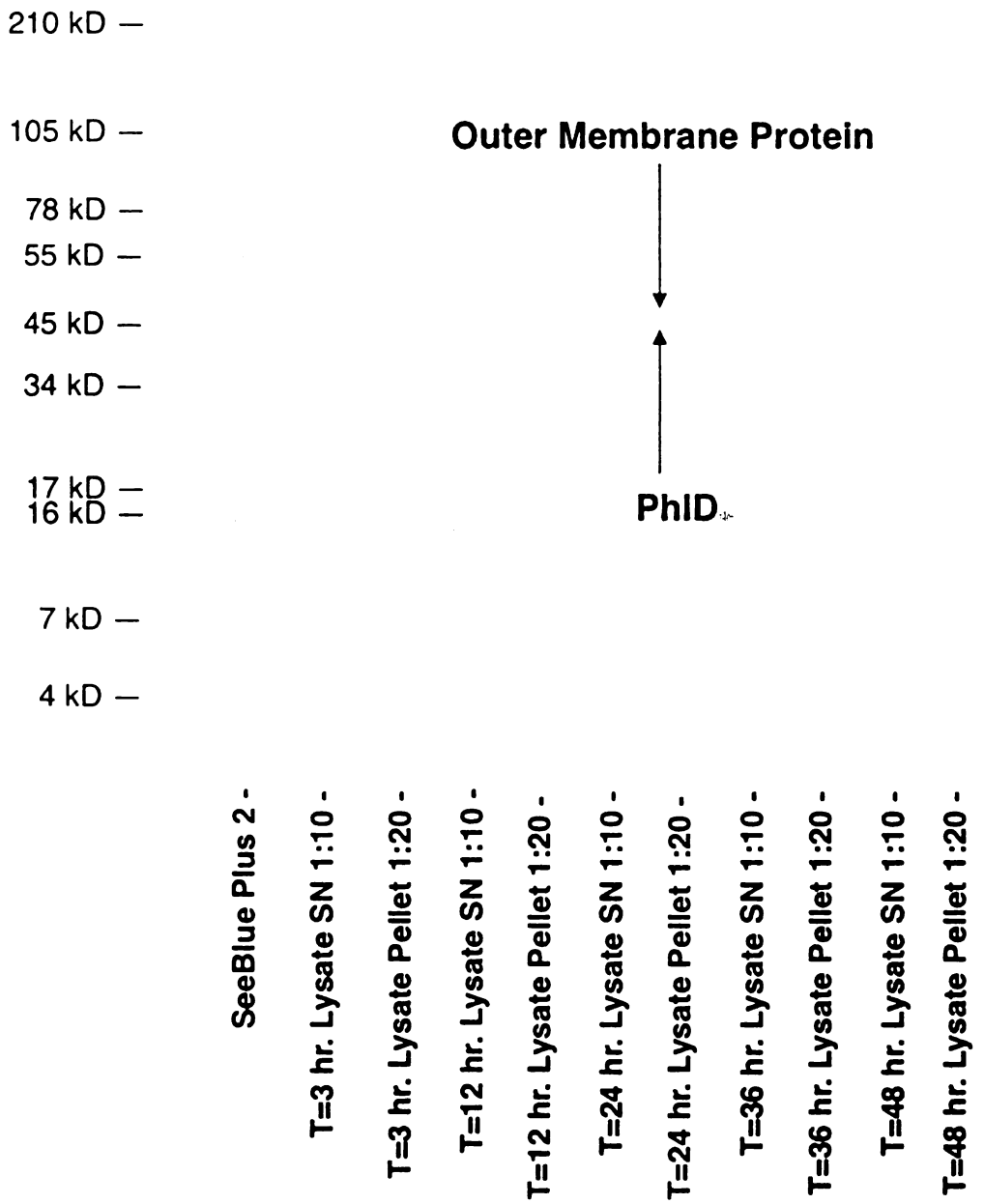

Figure 58. SDS-PAGE protein solubility analysis of BL21serA(DE3)/pBC2.187

All lanes are normalized to $OD_{600} = 1$.

Codon usage is the single most important variable when expressing genes in hosts other than the source of the gene. Codon usage is directly based upon the t-RNA pool percentages in a particular organism and disrupting t-RNA concentrations can lead to poor expression. Codon optimization was done manually and changes in codons were made accordingly with attention to keeping regions from overlapping codons and highly localized GC content (Figure 59).

The final hand sorted, gene construct was given to DNA2.0 for synthesis. Once received the optimized gene was cloned into the same pET27-b+ vector along with serA (Figure 60 and Figure 61) and biosynthesis commenced with W3110serA(DE3) and BL21serA(DE3)* after establishing a growth curve. With the new construct microbial synthesis were conducted at 33 and 36 °C and induced at late log phase (OD_{600} = 30), early stationary phase (OD_{600} = 50) and well into stationary phase (OD_{600} = 80). The maximum titer and yield were observed as 4.1 g/L and 3% with the biosynthesis conducted at 36 °C and stationary induction while the greatest specific activity of 0.038 and 0.042 U/mg/min was found to be at early stationary induction at 33 or 36 °C (Figure 62). Similar data was found with BL21serA(DE3)*/pBC2.219.

Optimization of Codon Usage for Expression of the *Pseudomonas fluorescens* Pf-5 *phlD* Gene in *Escherichia coli* B

		I	II	III	IV	V
A	GCG	0.36	11	0.28	14	3
	GCC	0.28	24	0.62	11	-13
	GCA	0.21	4	0.10	8	4
	GCU	0.15	0	0.00	6	6
C	UGC	0.58	5	0.83	3	-2
	UGU	0.42	1	0.17	3	2
D	GAU	0.66	5	0.23	15	10
	GAC	0.34	17	0.77	7	-10
E	GAA	0.62	8	0.47	11	3
	GAG	0.38	9	0.53	6	-3
F	UUU	0.61	2	0.11	12	10
	UUC	0.39	17	0.89	7	-10
G	GGC	0.41	11	0.65	7	-4
	GGU	0.30	4	0.24	5	1
	GGG	0.19	2	0.12	3	1
	GGA	0.10	0	0.00	2	2
H	CAU	0.56	1	0.06	9	8
	CAC	0.44	15	0.94	7	-8
I	AUU	0.48	2	0.10	10	8
	AUC	0.44	18	0.90	9	-9
	AUA	0.08	0	0.00	1	1
K	AAA	0.77	0	0.00	10	10
	AAG	0.23	13	1.00	3	-10
L	CUG	0.45	24	0.71	15	-9
	UUG	0.15	2	0.06	5	3
	UUA	0.14	0	0.00	5	5
	CUC	0.12	6	0.18	4	-2
	CUU	0.11	2	0.06	4	2
	CUA	0.03	0	0.00	1	1
M	AUG	1.00	13	1.00	13	0
N	AAU	0.57	2	0.13	9	7
	AAC	0.43	14	0.88	7	-7
P	CCG	0.61	7	0.64	7	0
	CCA	0.18	3	0.27	2	-1
	CCU	0.14	0	0.00	2	2
	CCC	0.07	1	0.09	0	-1
Q	CAG	0.65	11	0.79	9	-2
	CAA	0.35	3	0.21	5	2
R	CGC	0.40	12	0.67	7	-5
	CGU	0.35	1	0.06	6	5
	CGG	0.11	5	0.28	2	-3
	CGA	0.05	0	0.00	1	1
	AGA	0.05	0	0.00	1	1
	AGG	0.04	0	0.00	1	1
S	AGC	0.25	7	0.28	6	-1
	UCG	0.20	8	0.32	5	-3
	AGU	0.16	0	0.00	4	4
	UCU	0.15	1	0.04	4	3
	UCC	0.14	9	0.36	4	-5
	UCA	0.10	0	0.00	2	2
T	ACC	0.47	15	0.88	8	-7
	ACG	0.27	0	0.00	5	5
	ACU	0.14	1	0.06	2	1
	ACA	0.12	1	0.06	2	1
V	GUG	0.43	15	0.60	11	-4
	GUU	0.25	0	0.00	6	6
	GUC	0.18	7	0.28	5	-2
	GUA	0.14	3	0.12	3	0
W	UGG	1.00	1	1.00	1	0
Y	UAU	0.69	0	0.00	4	4
	UAC	0.31	6	1.00	2	-4
stop	UAA	0.64	0	0.00	1	1
	UGA	0.27	1	1.00	0	-1
	UAG	0.09	0	0.00	0	0

Figure 59. Codon optimization for expression of *P. fluoroscens* Pf-5 phlD in *E. coli*.

(I) = *E. coli* B codon frequency. (II) = Native phlD codon usage. (III) Native phlD codon frequency. (IV) Optimized phlD codon frequency. (V) Relative change in codon usage.

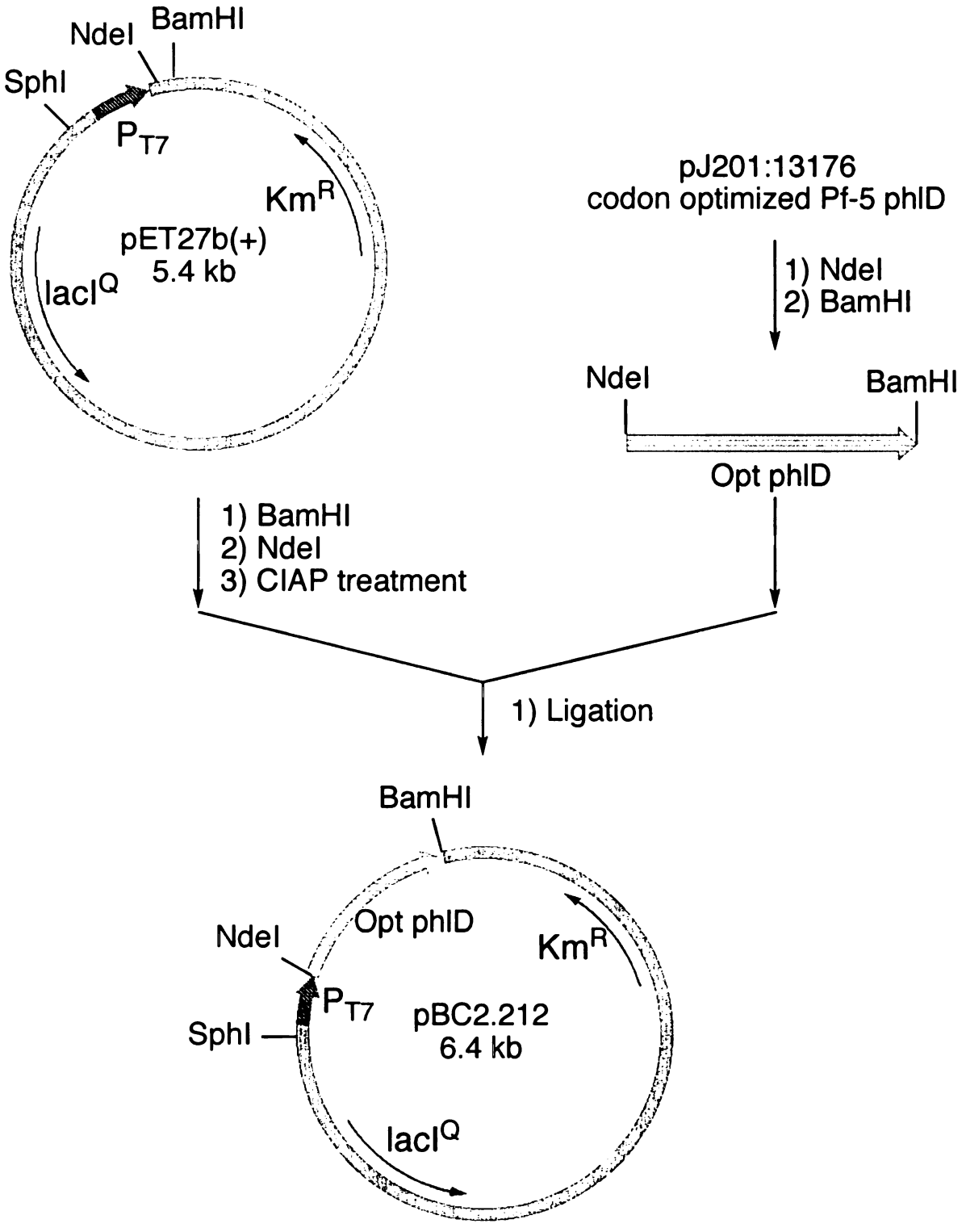

Figure 60. Construction of plasmid pBC2.212 en route to pBC2.219.

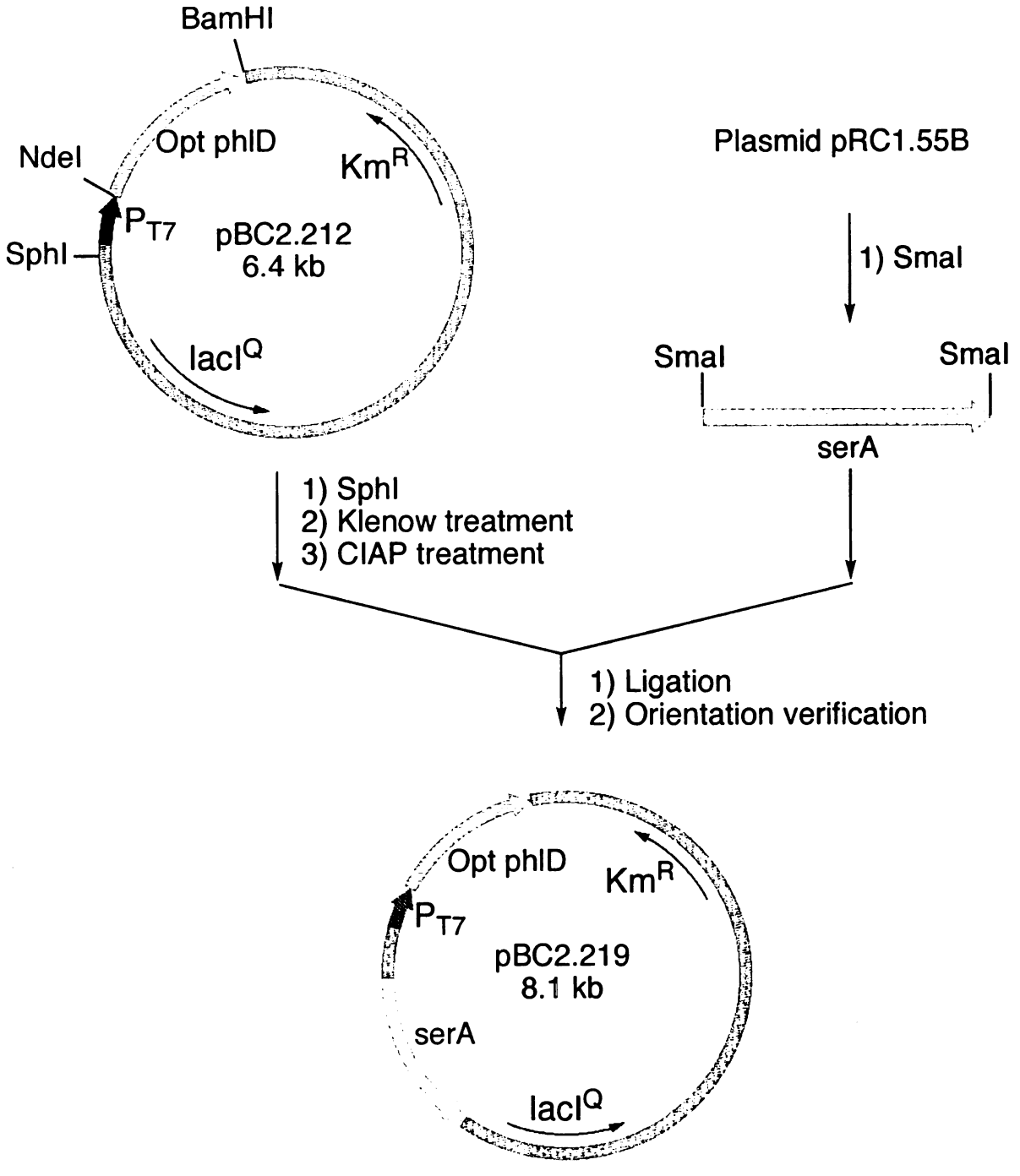

Figure 61. Construction of plasmid pBC2.219.

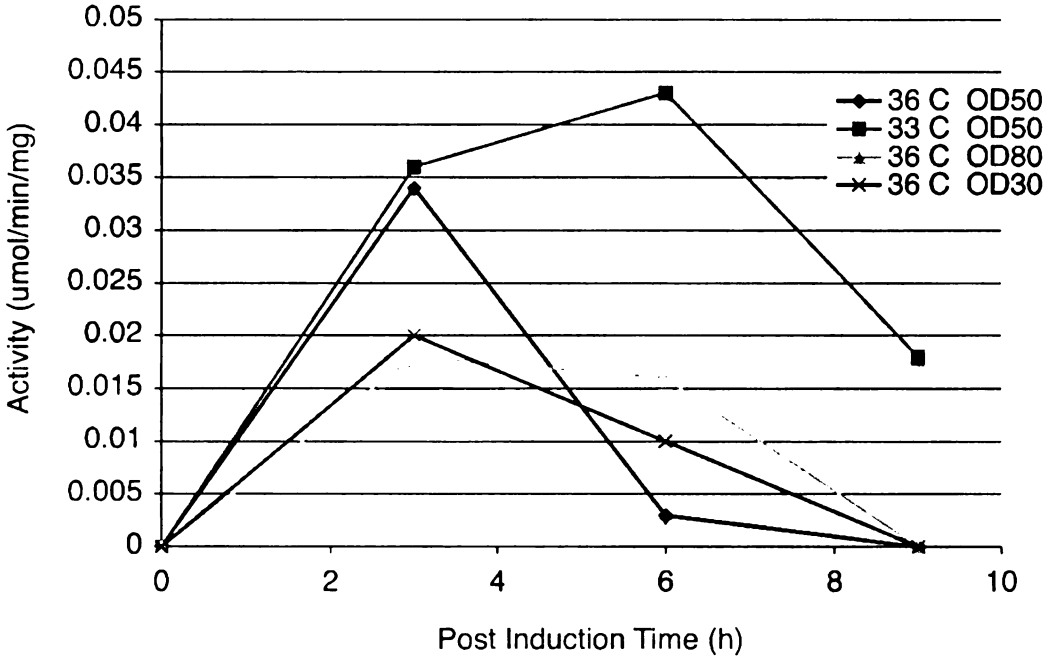

Figure 62. Specific activity comparison for induction time and temperature.

In different efforts in increasing active protein expression the in-house, visually optimized phlD was cloned into pJF118EH which is a lower copy plasmid of about 30 copies per cell compared to the pET-based plasmid which can have up to 300 copies per cell. Besides the burden inherent with plasmid bearing cells, lower amounts of transcribed DNA can possibly lead to better RNA that can be properly translated yielding more active protein instead of the host packaging them all to inclusion bodies. The same idea is apparent in the use of a less strong promoter, replacing T7 with Tac (Figure 63 and Figure 64).

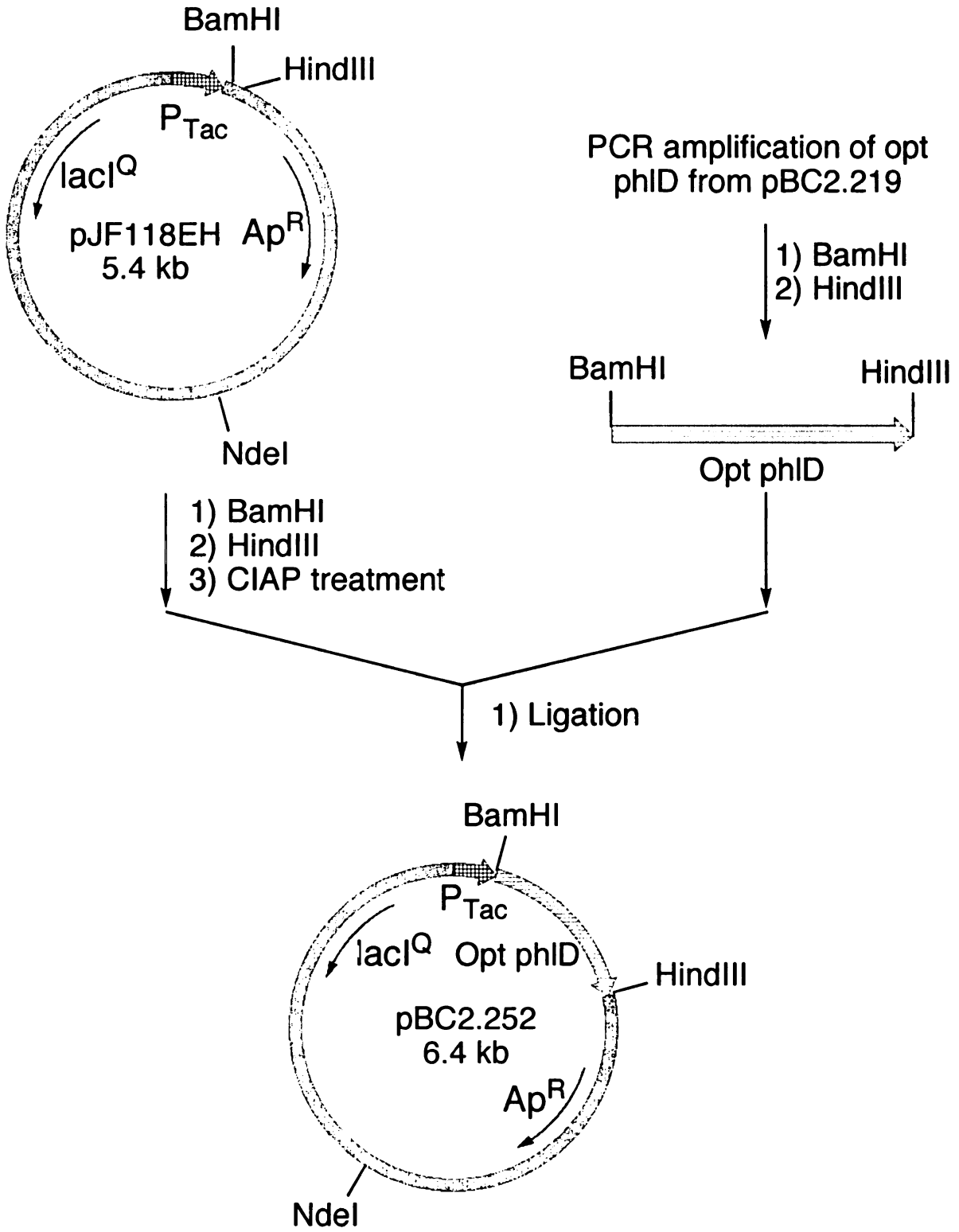

Figure 63. Construction of plasmid pBC2.252 en route to pBC2.257.

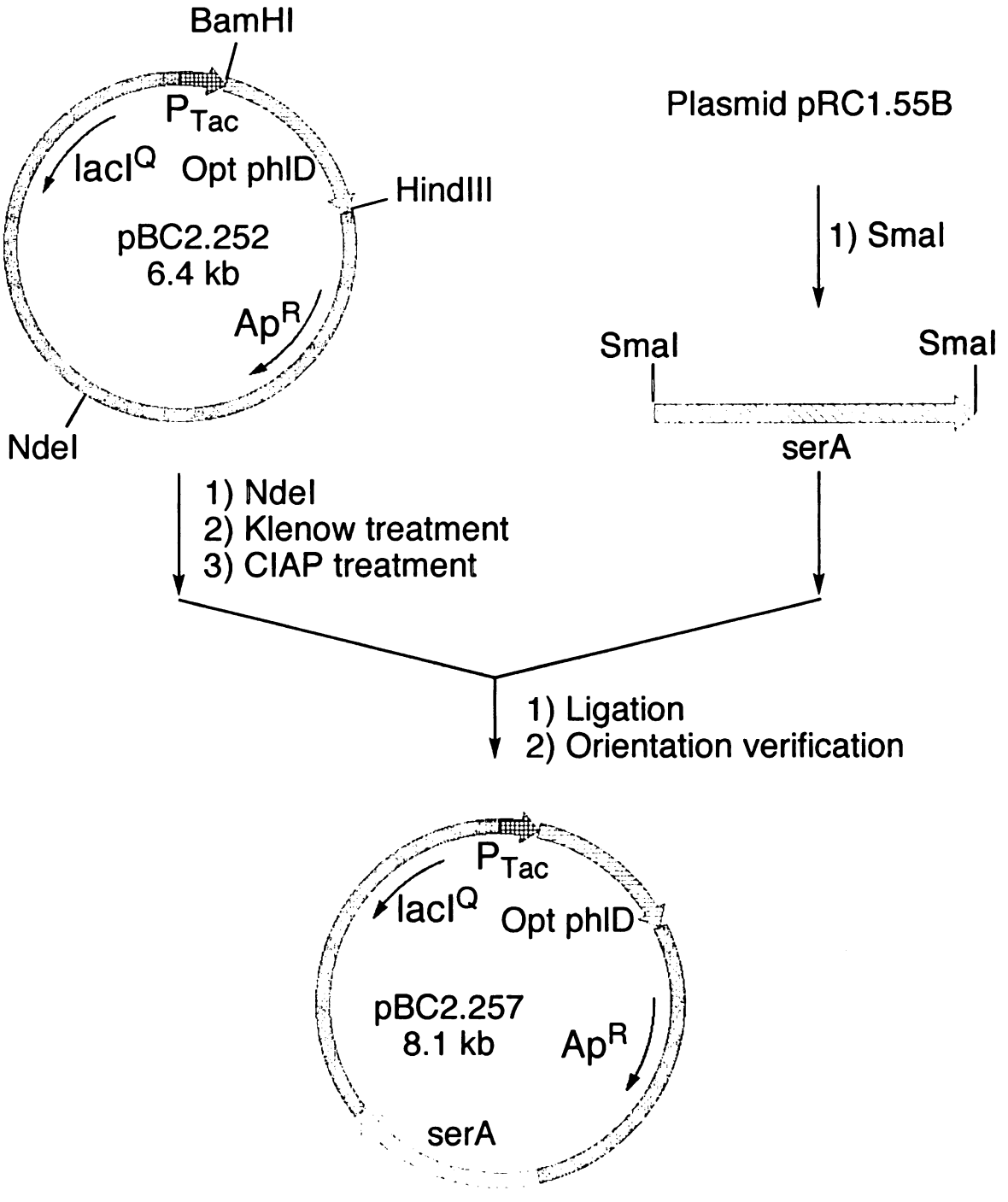

Figure 64. Construction of plasmid pBC2.257.

The Tac promoter in the medium copy plasmid expression system produced 0.5 g/L phloroglucinol and specific activites were not acquired.

Several programs and software exist for codon optimization. DNA2.0, a California based company, provides gene synthesis services with codon optimization software from any amino acid sequence.[21,22] The added benefits of using Gene Designer, the free software available from DNA2.0, is that not only can codon usage be optimized for an amino acid sequence in a multitude of given hosts, but there are also many features that can add purification tags, restriction enzymes inclusions or exclusions, alignments of promoters and ribosomal binding sites, among others. These services and tools can expedite many researchers ability to obtain genetic materials to answer their scientific questions for less cost and time than an individual would take to construct. The Pf-5 phlD gene was submitted for sequencing and once received was cloned into pET27-b+ just as described for all of the pBC phlD containing plasmids (Figure 65 and Figure 66). Once constructed the plasmid was subject to microbial synthesis using W3110serA(DE3) as the host. With induction at early stationary (OD_{600} = 50) the consistent titer of 3.7 g/L was achieved, although the yield was over 6% which is almost double that of historical yields (Figure 40) and the crude lysate specific activity again doubled the benchmark wild-type phlD.

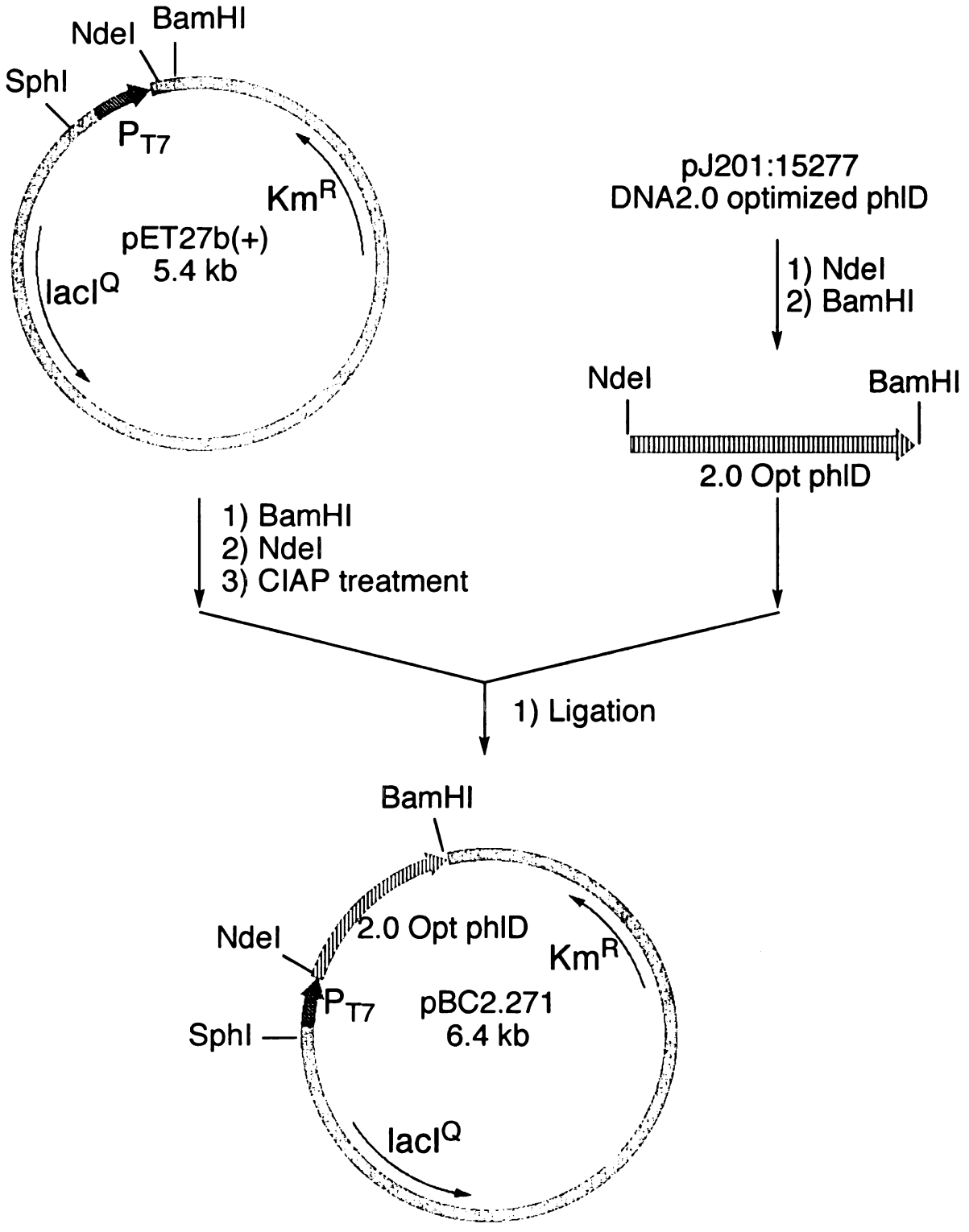

Figure 65. Construction of plasmid pBC2.271 en route to pBC2.274.

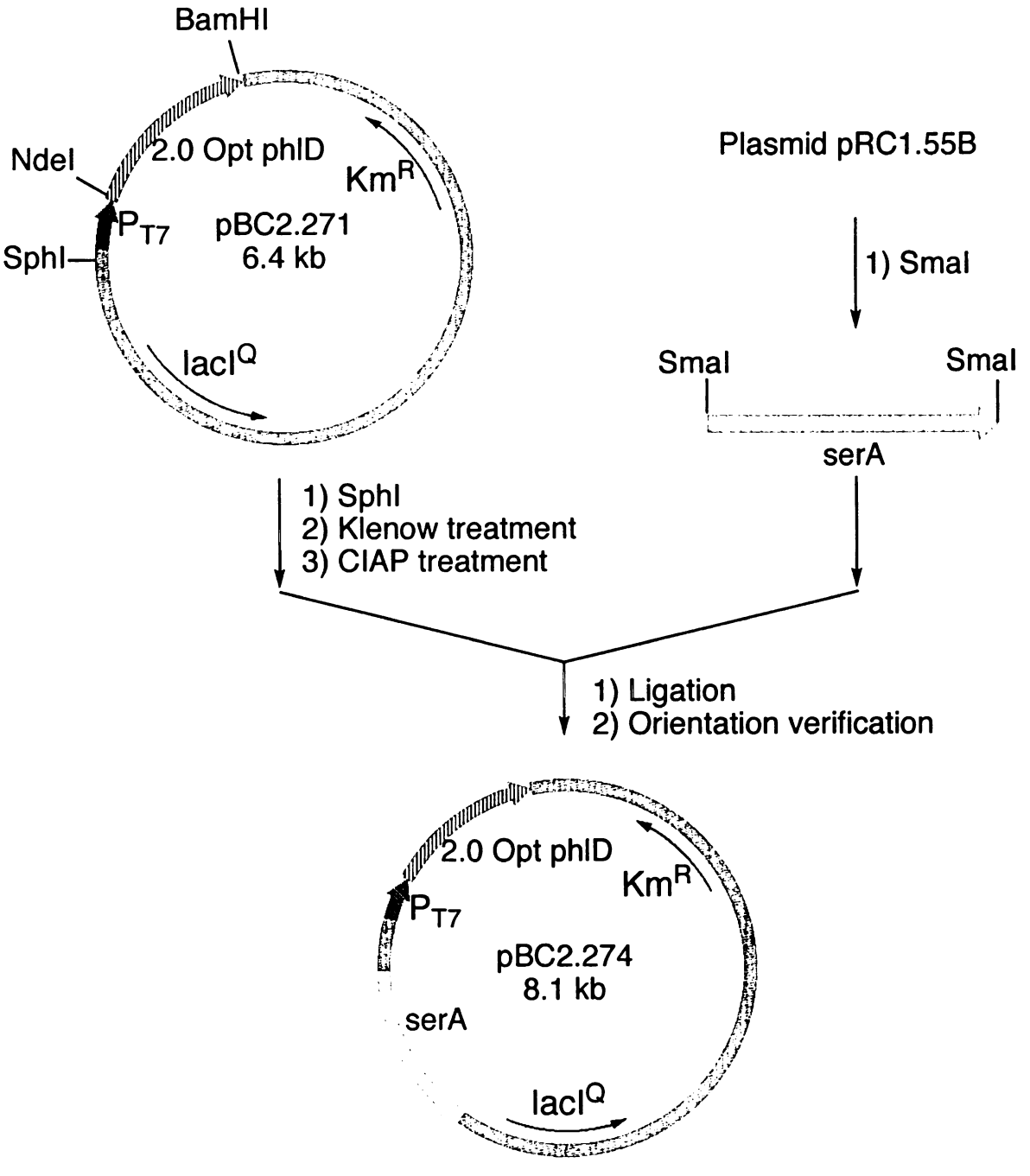

Figure 66. Construction of plasmid pBC2.274.

To ensure that phloroglucinol production was not limited by lack of a mineral or nutrient source, a biosynthesis was conducted similarly to the minimal salts medum usually employed with the addition of a sterilized and concentrated stock of yeast extract solution added just prior to induction. A similar method was applied in the biosynthesis of shikimic acid that helped improve fermentative results.[23] With comparison to the experiment of the same construct using W3110serA(DE3) as the host without supplementation of 15 g/L yeast extract, the titer (Figure 67), yield from glucose and specific activity of crude lysate was similar with the only difference showing a slightly slower drop in activity over time (Figure 68).

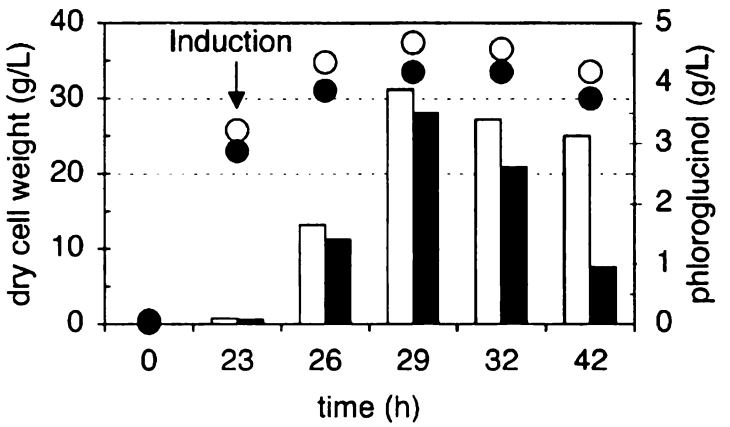

Figure 67. Yeast extract supplementation effect on microbial synthesis.

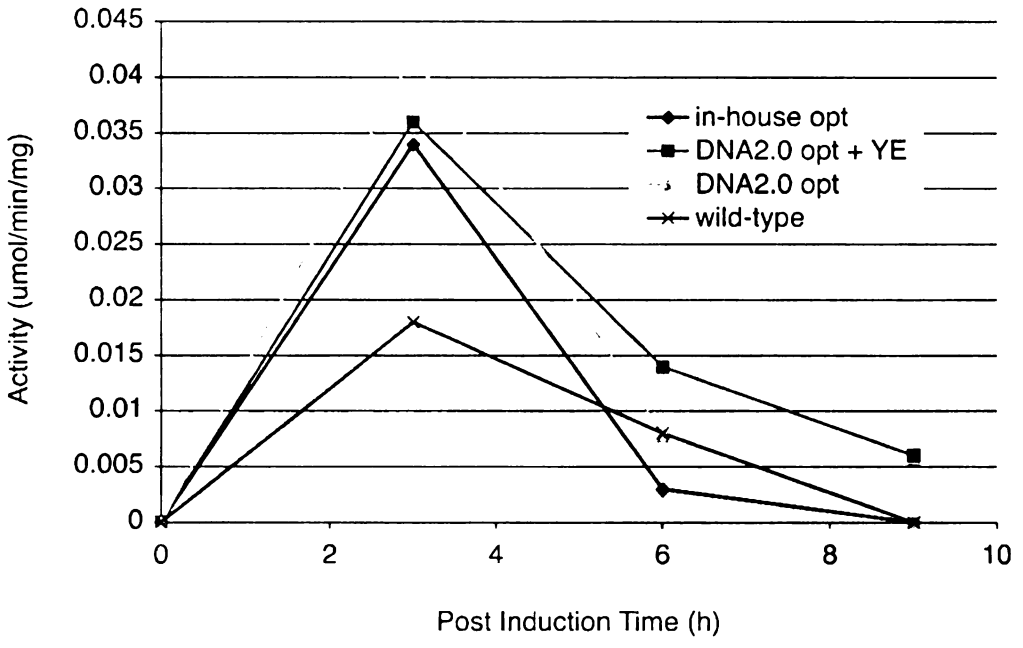

Figure 68. Crude lysate specific activity comparison of wild-type, in house optimized, and DNA2.0 optimized phlD with and without supplementation.

Discussion

In combined efforts, the parameters for the whole-cell biocatalysis of phloroglucinol from renewable glucose by microbial synthesis using two sources of *E. coli* as host organisms in minimal salts medium were established. phlD from *P. fluorescens* Pf-5 was heterologously expressed behind a T7 promoter in a pET based plasmid encoding a type III polyketide synthase responsible for condensation of three malonyl CoA subunits to afford phloroglucinol. Successful production was achieved in sequentially increasing titers from 4 g/L in a fed-batch microbial synthesis to a single

stage fed-batch extractive microbial synthesis that produced 17 g/L and doubled the yield to about 10%. Introduction of younger cells lacking sensitivity from phloroglucinol exposure via a second stage fermenter vessel resulted in a doubling of titer to 37 g/L albeit maintaining the same yield due to the non-production stage glucose feeding. An exhaustive five stage, staggered introduction spawning from the same idea as the two-stage microbial synthesis setup, with the added benefit of learning if this process could have a continuous production vessel, did not bear fruit only producing a slightly higher titer than the two-stage with a drop in yield consistent with the extra number of preparatory cell feed vessels. As an aside, an increase in titer of about 10% was found when the initial minerals of the batch feed were supplemented throughout the microbial synthesis by slow addition from solvation in the glucose addition stock (see experimental). Close to 300 g of phloroglucinol was collected from two-stage microbial synthesis of BL21serA(DE3)*/pJA3.131A for production of resorcinol (Chapter four).

Transcriptome analysis, although informative, may be looked at in the future as a secondary line of evidence for a hypothesis of what regulatory paths changed or need to be changed for a perceived finding. Focusing on all the conjectured leads was impractical and this information will be used to decipher a finding rather than lead to experimental paths.

The isolated *P. fluoroscens* Pf-5 phlD was codon optimized by relative amount of charged t-RNA concentration pools towards *E. coli*. A two-fold improvement in crude lysate specific activity was observed whether use of visual codon optimization or algorithims used by Gene Designer software from DNA2.0. Crude lysate specific activity is in essence a measure of the concentration of expressed and active phlD relative to

endogenous protein that has been normalized. Mineral deficiency could be at most a minor cause in the observed ceiling of less than 5 g/L of phloroglucinol to be produced evident through a miniscule increase of titer when 15 g/L of yeast extract was added to the minimal salts medium just prior to induction.

Three main obstacles in limited phloroglucinol accumulation are PhlD activity, substrate availability (malonyl CoA) and/or phloroglucinol or protein toxicity. These targets are what can be improved upon yielding a biocatalyst that provides high enough titers and yields to move to the forefront of a commodity chemical production.

What was not noted thus far was the perceived drop in titer and viability of especially the evolved "*" strain. Upon the introduction of the extractive biosyntheses it was not four months when the maximum titers were not achieved by Dr. Xie. In the two-stage extractive microbial synthesis a small difference of 2-3 g/L was looked upon as just statistical deviation. A total of six months when reproduction of Dr. Xie's results were attempted another drop of about 10% was achieved. Once the 300 g of phloroglucinol was collected, the microbial synthesis ceased for optimization of the downstream processing with limited immediumte concern over the small decreases in titers.

It was not until almost one year from the highest titers of phloroglucinol recorded that in the extractive microbial synthesis the titer was cut almost to 33% of the original numbers obtained. The obvious issues were immediately addressed: phloroglucinol was monitored carefully for proper extraction without detrimental accumulation, the resin was conditioned properly with subsequent ordering of different batches and different sources, bottled air tanks were used as an air source instead of house air, extensive cleaning, filtration changes, and temperature characterization of the autoclave used for sterilization,

water changes from completely different purification sources, complete swapping out for new additive salts and minerals, retransforming of cells streaked out from untouched glycerol freezes, recalibration of the DCU control units for the fermenters, elution conditions for collection of phloroglucinol off the resin. With no other explanations it seemed the microbe had somehow changed. With careful examination of growth characteristics and profiles some ideas were gained. The growth curve has slowly changed over time. It was repeatedly shown that the evolved "*" strains indeed amassed about 20% more cell mass and reached peak densities hours quicker. Cryptic mutations may be a culprit of explaining why these microorganisms changed.[24] After establishing and testing optimal induction times it seems the majority of the perceived low titers was due to an early induction because of the difference in cell mass production. The fed-batch titers and yields returned to normal. A similar situation was perceived in the literature citing that cells screened for resistance to phlorizin, a glycosylated and acylated phloroglucinol, lost resistance and became sensitive over time if not pressured by the toxicant, even in the glycerol freeze. It is probable that the titers for the extractive biosynthesis would be at least marginally returned, but efforts were focused elsewhere.

CHAPTER THREE REFERENCE

[1] Leston, G. In Kirk-Othmer Encyclopedia of Chemical Technology; Kroschwitz, J. I.; Howe-Grant, M., Eds.; Wiley: New York, **1996**; Vol. 19, p. 778.

[2] Agarwal, J.P. *Prog. Energy Combust. Sci.* **1998**, *24*, 1-30.

[3] Mitchell, A. Amination of Electrophilic Aromatic Compounds by Various Nucleophilic Substitution. International Patent Application WO 96/35659, **1996**.

[4] McKillop, A.; Howarth, B. D.; Kobylecki, R. J. *Syn. Commun.* **1974**, *4*, 35.

[5] Kopf, P.W. Kirk-Othmer Encyclopedia of Chemical Technology; "Phenolic Resins", John Wiley & Sons Inc: New York, **2001**.

[6] Zha, W.; Shao, Z.; Frost, J.W.; Zhao, H. *J. Am. Chem. Soc.* **2004**, *126*, 4534.

[7] Singh, I.P.; Bharate, S.B. *Nat. Prod. Rep.* **2006**, *23*, 558.

[8] Achkar J.; Xian M.; Zhao H.; Frost J.W. **2005**, *127*, 5332.

[9] Novak-Thompson, B.; Gould, S. J.; Kraus, J.; Loper, J. E. *Can. J. Microbiol.* **1994**, *40*, 1064.

[10] Weller, D.M.; Landa, B.B.; Mavrodi, O.V.; Schroeder, K.L.; De La Fuente, L.; Blouin Bankhead, S.; Allende Molar, R.; Bonsall, R.F.; Mavrodi, D.V.; Thomashow, L. *Plant Biol.* **2006**, *9*, 4.

[11] Bangera, M.G.; Thomashow, L.S. *J. Bacteriol.* **1999**, *181*, 3155.

[12] Austin, M.B.; Noel, J.P. *Nat. Prod. Rev.* **2003**, *20*, 79.

[13] Adapted from Staunton, J.; Weissman, K.J. *Nat. Prod. Rep.* **2001**, *4*, 380.

[14] Zha, W.; Rubin-Pitel, S.B.; Zhao, H. *J. Biol. Chem.* **2006**, *281*, 32036.

[15] McLaggan, D.; Naprstek, J.; Buurman, E.T.; Epstein, W. *J. Biol. Chem.* **1994**, *269*, 1911.

[16] Li W.; Xie D.; Frost J.W. *J Am Chem Soc*, **2005**, *127*, 2874.

[17] Park, S.; Ryu, D.D.Y.; Kim, J.Y. *Biotechnol. Bioeng.* **1990**, *36*, 493.

[18] Fu, J.; Wilson, D.B.; Shuler, M.L. *Biotechnol. Bioeng.* **1993**, *41*, 937.

[19] Bruno-Barcena, J.M.; Ragout, A.L.; Cordoba, P.R.; Sineriz, F. *Appl. Microbiol. Biotechnol.* **1999**, *51*, 316.

[20] Datsenko, K.A.; Wanner B.L. *Proc. Natl. Acad. Sci. U.S.A.* **2000**, *97*, 6640-6645.

[21] Villalobos, A.; Ness, J.E.; Gustafsson, C.; Minshull, J.; Govindarajan, S. *BMC Bioinformatics*. **2006**, *7*, 285.

[22] Gustafsson, C.; Minshull, J.; Govindarajan, S. *TRENDS in Biotechnology*. **2004**, *22*, 346.

[23] Chandran, S.S.; Yi, J.; Draths, K.M.; von Daeniken, R.; Weber, W.; Frost, J.W. *Biotechnol. Prog*. **2003**, *19*, 808.

[24] (a) Parker, L.L.; Betts, P.W.; Hall, B.G. *J. Bacteriol.* **1988**, *170*, 218. (b) Hall, B.G. *Genetica*. **1999**, *107*, 181.

CHAPTER FOUR

Downstream Processing and Chemistry of Phloroglucinol

Current efforts aim to produce 1,3,5-trihydroxybenzene, known as phloroglucinol, biocatalytically from D-glucose at a level with commercial importance. To enhance the viability of commercial manufacture following a successful biocatalytic production the downstream purification must be crisp and concise delivering phloroglucinol with the same purity and level to compete with non-renewable routes. Chemical methods or treatment to other target compounds will aid in developing markets and interest in phloroglucinol.

Varied physical properties spawned by unique chemical properties add to the intrigue of phloroglucinol. The solubility in water at room temperature is about 10 g/L, but if the temperature is increased to 37 °C the solubility raises to more than 30 g/L. An appreciable keto-enol tautomerism sets this molecule apart from many others.[1] With hydroxylamine the trioxime is produced through what seems like an addition to a ketone, and excess methyl iodide or halogen in base leads to hexamethylated or hexahalogenated tricyclohexanone products (Figure 69).[2] When in the presence of diazomethane or acetyl chloride the enolic products are formed in the trimethyl ether or acetylated versions.

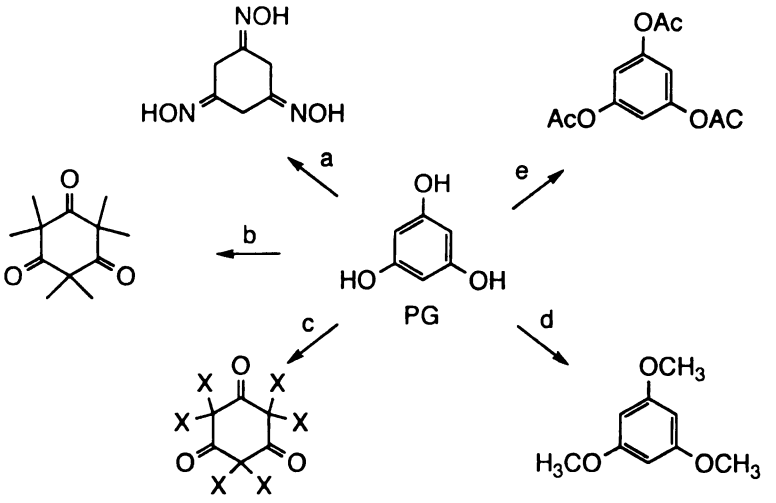

Figure 69. Keto-enol chemistry of phloroglucinol.
(a) hydroxylamine; (b) CH_3I, KOH; (c) Cl_2 or Br_2; (d) CH_2N_2; (e) AcCl

Phloroglucinol in the solid state or solution at neutral pH has failed to yield any evidence by Raman, ultraviolet and infrared spectroscopies of the keto tautomer. The commonality of the keto reactions are the use of base. The ^{1}HNMR of phloroglucinol at neutral pH shows a single peak in the aromatic region in D_2O.[3] The aromatic peak shifts upfield into the alkene region with an addition of a second peak indicative of a methylene in 2 mole equivalence of base. ^{13}CNMR and UV spectroscopy give further support of the complex equilibrium that exists when phloroglucinol is dissolved in an aqueous solution of base.[4] With data gathered across the representative literature the pH dependent isomerization is as depicted in (Figure 70).

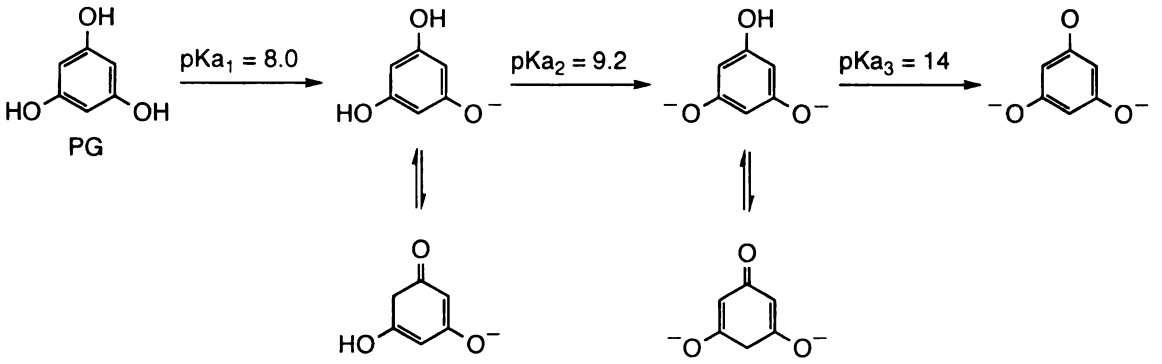

Figure 70. pH dependent equilibration of tautomers.

Fray reported the stoichiometric sodium borohydride reduction of phloroglucinol to resorcinol in 90% yield presumably going through a dihydrophloroglucinol salt intermediate (Figure 71).[5] Base was necessary for the reaction to take place, at neutral pH either phloroglucinol was recovered or 1,3,5-cyclohexanetriol was produced.[6] An adapted synthesis of dihydrokavain by Smissman[7] was used to make the dihydrophloroglucinol salt that upon reflux in dilute acid afforded resorcinol.[8]

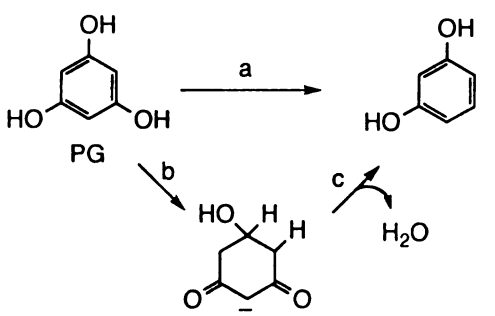

Figure 71. Phloroglucinol reduction to resorcinol.
(a) $NaBH_4$. (b) 50 psi H_2, 5% Rh/Al_2O_3, 1N NaOH. (c) 0.5 M H_2SO_4, Δ.

A 1 M solution of phloroglucinol in 1 N NaOH was shaken under 50 psi H_2 in the presence of a 1.2 mol% loading of 5% Rh/Al_2O_3. After filtering off the catalyst through a plug of Celite, the aqueous solution was acidified to pH 6.0 with 10% HCl followed by concentration to a yellow oil. Heating the oil at reflux in a solution of 0.5 M H_2SO_4 afforded resorcinol in 82% yield after Kugelrohr distillation. A series of catalysts were applied to phloroglucinol, 1,2,3,4-tetrahydroxybenzene and hydroxyhydroquinone to yield successful deoxygenation reactions (Figure 72).[8] Evidence led to mechanistic insight that hydrogenation occurred through the dianionic species at the neutral oxygen evident from resorcinol production using *o*-methylated phloroglucinol, with loss of methanol, among other supports.[6]

Polyhydroxy benzene	Catalyst	Product	Yield
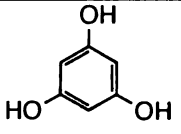 Phloroglucinol	Rh/Al_2O_3 Rh/C Pt/C Pd/C	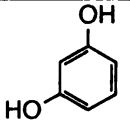 Resorcinol	82 74 60 32
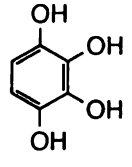 Apionol	Rh/Al_2O_3 Rh/C Pt/C Pd/C	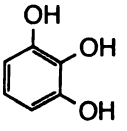 Pyrogallol	44 43 42 41
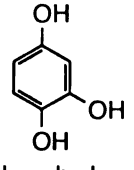 Hydroxyhydro quinone	Rh/Al_2O_3 Rh/C Pt/C Pd/C	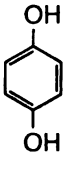 Hydroquinone	53 47 46 18

Figure 72. Catalytic deoxygenation reactions of polyhydroxyarimatics.[8]

To this point phloroglucinol has been produced from glucose in titers and yields that warrant efforts towards efficient downstream processing techniques for recapture of purified product. Phloroglucinol had been trapped on AG 1x8 or Dowex 1x8 strong anion exchange resin thusfar. AG 1 resins have styrene, divinyl benzene polymer gel matrices with quaternary amines as the cationic species that can bind anionic analytes. Dowex 1 is a lesser grade of a strikingly similar product to AG 1 at a more reasonable price. For practical purposes once washed, clarified and generated the resins behave as equivalents. Anion exchange resins come in vast arrays of sizes and effective cross-linkings. The mesh size given is proportionate to the size mesh that particles are allowed to pass. Usually mesh sizes are reported as ranges. For example 200-400 mesh resin bead sizes are small enough to pass through 200 mesh and are large enough not to pass through 400 mesh. The smaller the mesh size range the larger the particle size. The number after the x, as in Dowex 1x8, is the effective percentages of cross-linkings that bind adjacent linear strands together. As one could imagine theses numbers have a drastic effect on the flow characteristics through the resin. The larger the beads (and lower the mesh size), the less the flow is perturbed. On the other hand, the less the cross-linking percentage, the less the flow is perturbed. The optimization though, is not solely dependent upon flow. The ability to capture an analyte is increased when particle sizes are smaller and cross-linking is maximized. A balance was sought between efficient capture of phloroglucinol and the ability to flow the unfiltered, viscous and live cell culture through the resin. Flow needs to be high enough such that the cells can be funneled back into the fermenter, because outside the precisely controlled fermenter environment the cells are surviving in a strongly organic medium likely devoid of air, nutrients and pH control (Figure 73).

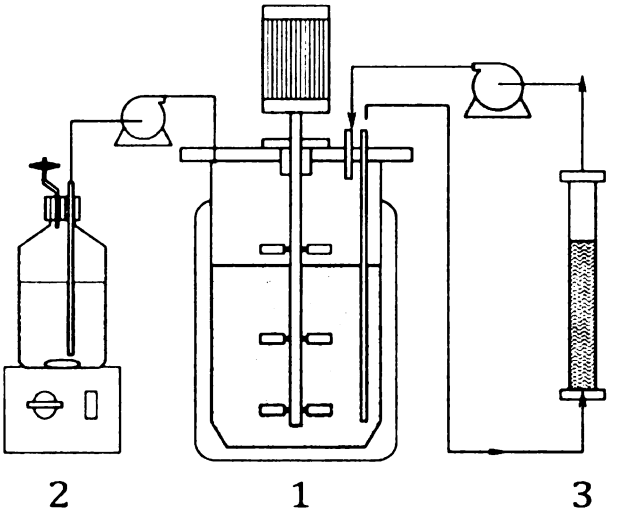

Figure 73. Schematic diagram of *in situ* resin based extraction.

(1) 1L working volume fermentation vessel. (2) PID controlled glucose addition. (3) Externally looped, peristaltic pump driven, fluidized resin bed extractive unit.

Dr. Dongmig Xie optimized the resin usage for AG 1x8, 50-100 mesh. To recover the phloroglucinol bound on the AG 1x8 resin, the column was initially washed in a fluidized-bed mode with 10 bed volumes of distilled, deionized water to remove the residual cells and recover part of phloroglucinol on the resin. Then, the column was rinsed with 15 bed volumes of acidic aqueous ethanol (acetic acid, 10% (v/v); ethanol, 75% (v/v); H_2O, 15% (v/v)) in a gravity-flow mode to recover the remaining phloroglucinol on the resin. The resin after phloroglucinol recovery was regenerated by a rinse with 15 bed volumes of KH_2PO_4 (0.5 M). To purify the recovered phloroglucinol, the cells in the resulting water solution were removed by centrifugation and the cell-free water solution was concentrated to about 1/10 of the original volume. The resulting acidic ethanol solution was concentrated to dryness and combined with the concentrated water

solution. The resulting aqueous solution was extracted three times with equal volumes of ethyl acetate. The organic phases were combined, concentrated to dryness and redissolved in H_2O. Phloroglucinol was recrystallized from H_2O at about 50% recovery, affording pale yellow crystals.

Results

Resin optimization for phloroglucinol capture

The binding phenomena of phloroglucinol to Dowex 1x8 resin has been optimized for mesh size, counter-ion, eluent, elution rate and temperature for a delicate balance between binding capacity, elution efficiency and practicality. As eluded to before, conditions are desired in which phloroglucinol is extracted efficiently to detour its toxicity effects while allowing efficient recapture post microbial synthesis, all keeping in constant cognition that the producing cells be allowed to flow and spend minimal time in the extraction column.

Efforts were first applied towards simplifying the elution conditions of phloroglucinol from Dowex 1x8 anion exchange resin. The current protocol has inherent problems and can be optimized. Monobasic phosphates are used to regenerate the resin initially and elution with a solution of phosphates has the important advantage of minimizing concentration of time, materials, and money associated with resin preparation. Eluting and regenerating in the same step will constitute a major benefit of this protocol phasing out excess washes, equilibrations, and unnecessary resource use. After extraction of phloroglucinol, consistently shown to be the only major product with organic solvent

solubility, the eluent should be recycled at least marginally. Monobasic phosphates have the added advantage of an acidic proton to neutralize any loosely bound anions contrary of reliance on simply replacing the counter-ion on the resin, assuming the pKa of the protonated conjugate base is greater than the phosphate species.

The eluent screening experiment used a large batch generation of the phosphate form Dowex 1x8. A uniformly massed resin amount was slurried in minimal salts medium to 25 mL of resin into fritted bio-rad, econo columns. In order to saturate the resin, which has a capacity rating of 1.4 milliequivalence/mL of slurried resin, 5 g of phloroglucinol was dissolved in 500 mL of minimal salts medium, adjusted to pH 7 and passed at a experimentally practiced elution flow rate of 8-12 mL/min in a fixed-bed mode. Typically eight experiments were done at a time leading to the infamous column Christmas tree in the lab that was festive towards the holidays. Binding of phloroglucinol was determined by subtracting the amount quantified from the flowthrough by gas chromatography. Phloroglucinol eluted was quantified in terms of how many bed volumes (25 mL fractions) were necessary to elute off the indicated percentage of the phloroglucinol that bound to the resin (1 BV, 2 BV and 5 BV) as depicted (Table 8). Preliminary results of using phosphates in different forms have benefits over current elution routes.

entry	PG bound (%)	eluent	temperature (°C)	elution rate (mL/min +/-1)	PG eluted (%) 1 BV	2 BV	5 BV
1	40	1M NaH_2PO_4	23	10	18	25	50
2	36	0.5M NaH_2PO_4	23	10	20	28	53
3	37	0.1M NaH_2PO_4	23	10	20	30	67
4	45	1M H_3PO_4	23	10	21	32	52
5	33	1M NaH_2PO_4	23	4	22	32	73
6	32	1M H_3PO_4/1M NaH_2PO_4	23	10	37	52	100
7	34	1M NaH_2PO_4	95	10	42	67	103

resins are approx 3 yrs old with frequent use.

Table 8. Phosphate elution of phloroglucinol from anion exchange resin.

Initial responses showed a slight indication that lower ionic strength can have a positive effect on elution (Table 8 entries 1-3). Lowering of the concentration of reagents can have drastic effects on work-up costs. Use of the fully protonated phosphoric acid compared with the monobasic salt had virtually no effect indicating that excess protons are not necessary (Table 8 entries 1 vs 4). The combined efforts of essentially a 2 M acidic phophate seems contradictory to the observations just discussed (Table 8 entry 6). The fact that this experiment did have the lowest phloroglucinol binding capacity observed may lead to the need for reproduction. Temperature looks as if it will elute of phloroglucinol more rapidly at 95 °C than at rt (Table 8 entries 1 vs 7). The cost reflection of boiling an eluent compared to storage and use of more bed volumes would have to be considered.

The phloroglucinol binding efficiency was considered to be a point of interest, because increased binding could lower the amount of resin used for extraction. The resin used in the scout experiment (Table 8) was approximately 3 years old with frequent use and this was a concern if extraction ability was lost. Another thought was that if the affinity of phosphate was low compared to other counter-ions (Table 9) then how would phloroglucinol bind if a more tightly bound counter-ion needed displacement. Phosphate is the prime candidate to use keeping in mind that the biosynthesis schematic diverts column flow through to be recycled back into the fermenter (Figure 73). Bumping off a counter-ion will subject the cells to enrichment of that corresponding product back into the fermenter vessel. This limits the choice of the resin form drastically. Many of the counter-ions will have a negative effect if dumped back into the fermenter. Phosphates are the major salt in the microbial synthesis medium and so this choice was obvious. Sulfate, another batched additive required as a sulfur source for amino acid production, could give us some insight into how a more tightly bound ion (Table 9) affects phloroglucinol binding.

If the binding is not much lower than the case in the phosphate form resin then phloroglucinol may be eluted more efficiently, cutting costs related to salts. Not only is sulfuric acid relatively a cheaper feedstock for industrial consumption, it also does not have eutrophication properties when compared to phosphates (Table 10).

Counterion (-)	Relative Selectivity
OH	1
benzene sulfonate	500
salicylate	450
citrate	220
I	175
phenate	110
HSO_4	85
ClO_3	74
NO_3	65
Br	50
CN	28
HSO_3	27
BrO_3	37
NO_2	24
Cl	22
HCO_3	6.0
IO_3	5.5
HPO_4	5.0
formate	4.6
acetate	3.2
Propionate	2.6
F	1.6

Table 9. Relative counterion selectivity for AG 1 anion exchange resin.

entry	PG bound (ave %)	condition	crosslinking (%)	mesh size	resin form
1	37	used	8	50-100	phosphate
2	44	new	8	50-100	phosphate
3	14	new	2	50-100	phosphate
4	98	new	8	200-400	phosphate
5	60	new	8	50-100	sulfate
6	28	new	2	50-100	sulfate

Table 10. Binding efficiency comparison of Dowex 1.

As expected, many variables play a role in the phloroglucinol binding efficiency. Used vs new resin (Table 10 entries 1 vs 2) indicate that even though resin has been thoroughly used in excess of 30, 60+ h biosyntheses that the longevity of the resin in our biocatalysis conditions are stable for frequent use over time as only a slight fall-off in binding capacity was observed. The mesh size difference from larger beads to smaller ones (Table 10 entries 2 vs 4) is noticeable, but despite the binding advantage there is also an elution disadvantage observing only half the amount of phloroglucinol was eluted comparatively. Also noticed, in regard to practicality, the flow rates were slow. On these criteria the mesh size was optimized for 50-100. It is harder to predict biomass flow through varied cross-linking effects, but binding is drastically affected (Table 10 entries 2 vs 3 and 5 vs 6) so the optimized resin cross-linking was chosen as 8%. Sulfates also have a much tighter binding coefficient to the resin's quaternary amine ionic binding group. Therefore, phosphates in the vessel would be less likely to deplete first off because of overall affinity, but also the fact that if phosphates are indeed bound the expelled sulfate will soon pass through the resin bed again and preferentially displace the phosphate. With

the added benefits, the sulfate form of the resin and the surprisingly increased phloroglucinol binding (Table 10 entries 2 vs 5) will be looked at in more detail.

Temperature was an important boundary detected earlier (Table 8) and a closer look was warranted. An increase of elution rate is observed with increases in the temperature (Table 11 entries 1-4) with a maximum effect observed between 37 and 60 °C. Higher temperatures increase the solubility of phloroglucinol in aqueous medium, while a slower elution rate also increases extraction efficiency (Table 8 entries 1 vs 5). Again it was observed that when a decrease in the concentration of phosphate was used the number of bed volumes was less for product elution (Table 11 entries 2 vs 6).

entry	PG bound (%)	eluent	temperature (°C)	elution rate (mL/min +/-2)	PG eluted (%)		
					1 BV	2 BV	5 BV
1	40	1 M NaH_2PO_4	23	10	18	25	50
2	45	1 M NaH_2PO_4	37	10	24	36	65
3	46	1 M NaH_2PO_4	60	10	21	49	81
4	44	1 M NaH_2PO_4	95	10	21	41	80
5	40	1 M NaH_2PO_4	23	4	22	32	73
6	39	0.1 M NaH_2PO_4	37	10	25	43	74

Table 11. Elution effects of temperature and ionic strength

Thought of how the resin was binding phloroglucinol is likely more of a mixture of anionic binding and an adsorption phenomena than just anionic binding which would account for all of the perceived differences in theory vs experimental results. If phloroglucinol was interacting with the polystyrene, divinylbenzene backbone, then the smaller sulfate anion would increase the ratio of organic phase (i.e. the backbone) to ionic

phase (quaternary amine with counter-ion and aqueous mobile phase) to increase the binding capacity in favor of the larger phosphate ions per amount of resin. This idea would also help explain how lowering of the ionic strength (i.e. lowering the concentration of phosphates in elution Table 8) increases phloroglucinol elution. Another support would be the unmentioned observance of the decrease of the effective density of the resin when higher salt concentrations were introduced. Disregarding the chance of bead swelling, which would ultimately lead to the same argument, a pictoral representation will help explain in another way (Figure 74). The bead to bead distance in a low ionic strength mobile phase is much lower than in a mobile phase of higher ionic strength. Phloroglucinol would be more efficiently eluted with closer bead to bead distances considering the enhanced adsorption to the beads compared to solubility in the aqueous mobile phase. Yet more evidence supporting the adsorption of phloroglucinol to the resin is the fact that the controlled pH in the fermentation vessel is 7.0 +/- 0.05 and that at this pH (and that if there is deviation of pH in the uncontrolled extraction column loop, normal metabolism makes organic acids and would lower the pH, keeping phloroglucinol fully protonated) phloroglucinol should be fully protonated thus passing through the resin bed unperturbed. It should not be ruled out that a percentage of the phloroglucinol is attached ionically, because addition of acid that would start to show the effects of the decreased density does aid in phloroglucinol elution against the control use of water slowly eluting phloroglucinol.

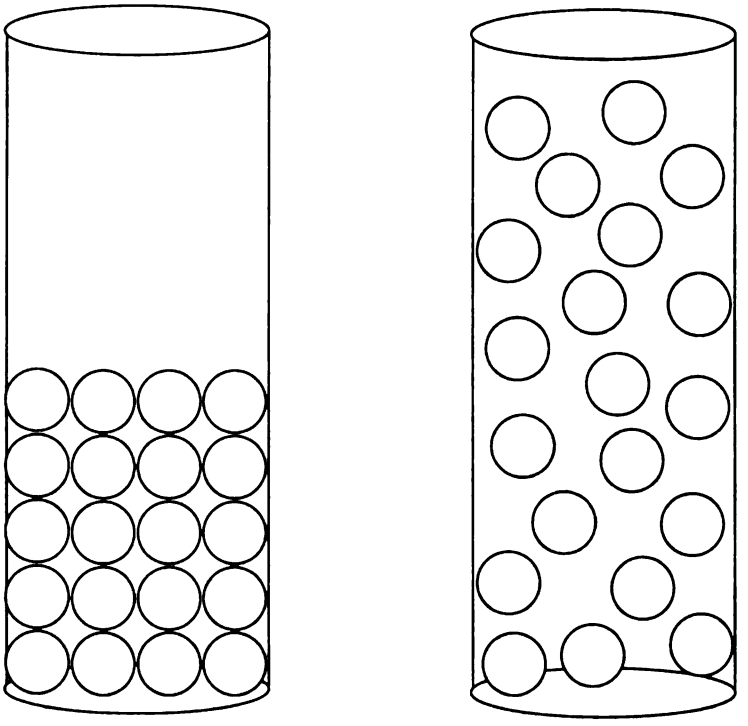

Figure 74. Density effect on elution.

In a last supportive effort different concentrations of sulfuric acid and monobasic phosphates were used to elute phloroglucinol from their respectively formed resins (Table 12). The idea of increases in ionic strength were apparent in the effective density by visualization of the rise in the resin bed volume. The trend is obvious with indication of the lower concentrations of phosphates that elute off phloroglucinol more efficiently (Table 12 entries 5 vs 6 vs 7). The concentration of sulfuric acid is not as noticeable at small concentrations (Table 12 entries 2 vs 3 vs 4) presumably due to the relative size and charge densities of a proton vs a sodium ion and a phosphate vs a sulfate ion. An acid source is also important with comparison to a water elution (Table 12 entry 1).

entry	PG bound (%)	resin form	eluent	temp (°C)	PG eluted (%) 1 BV	2 BV	5 BV
1	67	sulfate	H_2O	37	14	26	48
2	59	sulfate	0.05 M H_2SO_4	37	28	50	68
3	52	sulfate	0.5 M H_2SO_4	37	34	66	103
4	65	sulfate	2 M H_2SO_4	37	29	45	74
5	50	phosphate	5 M NaH_2PO_4	95	7	14	22
6	44	phosphate	1 M NaH_2PO_4	95	21	41	80
7	40	phosphate	0.1 M NaH_2PO_4	95	42	62	102

Table 12. Cooperative ionic strength and free proton dependence elution.

Phloroglucinol Recovery Optimization

Recrystallization studies commenced on authentic phloroglucinol trying various eluents from the resin survey as to have a stream-lined downstream processing with as few process steps as possible. Phloroglucinol does recrystallize nicely in aqueous solvents and ethyl acetate and hexanes (Table 13). It should be noted that the phloroglucinol recrystallizes as the dihydrate as white crystals noticed within 1 h and complete within 12 h.

solvent	treatment	recrystallization recovery(%)
0.1 M NaH_2PO_4	2% by weight, gentle heating to dissolve, place in 4 °C	96
0.5 M NaH_2PO_4	2% by weight, gentle heating to dissolve, place in 4 °C	90
1 M NaH_2PO_4	2% by weight, gentle heating to dissolve, place in 4 °C	93
2 M NaH_2PO_4	2% by weight, gentle heating to dissolve, place in 4 °C	92
0.5 M H_2SO_4	2% by weight, gentle heating to dissolve, place in 4 °C	84
2 M H_2SO_4	2% by weight, gentle heating to dissolve, place in 4 °C	80
conc H_2SO_4	2% by weight, gentle heating to dissolve, place in 4 °C	0
EtOAc	12% by weight, gentle heating to dissolve, place in 4 °C	0
EtOAc/hexanes	9% by weight, add hexanes until cloudiness appears and dissipates slowly, place in 4 °C	87

Table 13. Recrystallization of Authentic phloroglucinol.
(Recrystallizes as the dihydrate form of phloroglucinol)

When recrystallization procedures were applied to eluted phloroglucinol from a microbial synthesis, an orange color of the elution mixture co-crystallizes in the phloroglucinol that is clean by GC, ^{1}H and $^{13}CNMR$, but as stated has a bright orange hue. Initial intuition led to the possible formation of oligomers, but contrary to thought, upon extraction with ethyl acetate, phloroglucinol was selectively extracted leaving most of the rather intense coloration behind in the aqueous layer. Decolorization with activated charcoal (2 x 5% phloroglucinol by weight) offered a colorless solution of phloroglucinol in ethyl acetate. At this point half of the phloroglucinol was recrystallized in hexanes as mentioned above (Table 13) while the other half was added to 5 V of hexanes and allowed to precipitate. Both experiments yielded phloroglucinol that is clean by GC, ^{1}H and $^{13}CNMR$ as a colorless powder.

As mentioned above, phloroglucinol at this stage is in the dihydrate form. The water is released upon heating at 110 °C or *in vacuo*. The following downstream processing procedures are highlighted in (Figure 75) along with the yield remaining after each subsequent step.

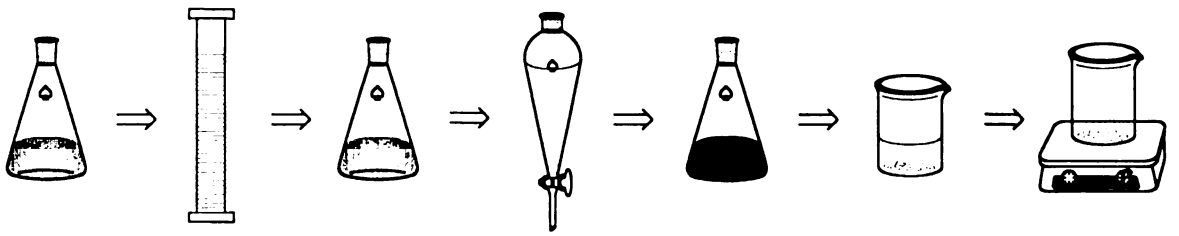

Figure 75. Downstream processing for phloroglucinol production.

* percentages are a running tally of phloroglucinol remaining.

(5) Removal of cellular debris; 3-5 BV water at 4 °C, batch-mode. (6) Elution of phloroglucinol; 5 BV of 0.1M NaH_2PO_4 at 60 °C. (7) Extraction; 3 x V with ethyl acetate. (8) Decolorization and filtration; 2 x 5% charcoal to phloroglucinol by weight. (9) Precipitation and filtration; hexanes 22 °C. (10) Remove hydration; 110°C.

From microbial synthesis to purified product in hand 91% recovery was obtained. Optimization of the decolorization technique, and a column prefiltration to limit the amount of cells and debris entering the column (work with hollow fibers and separation cassettes were troubled by lack of flow-rate because of the high density culture) could result in recoveries upwards of 95%. Combining the downstream processing procedural operations an outline of the entire procedure would follow in (Figure 76).

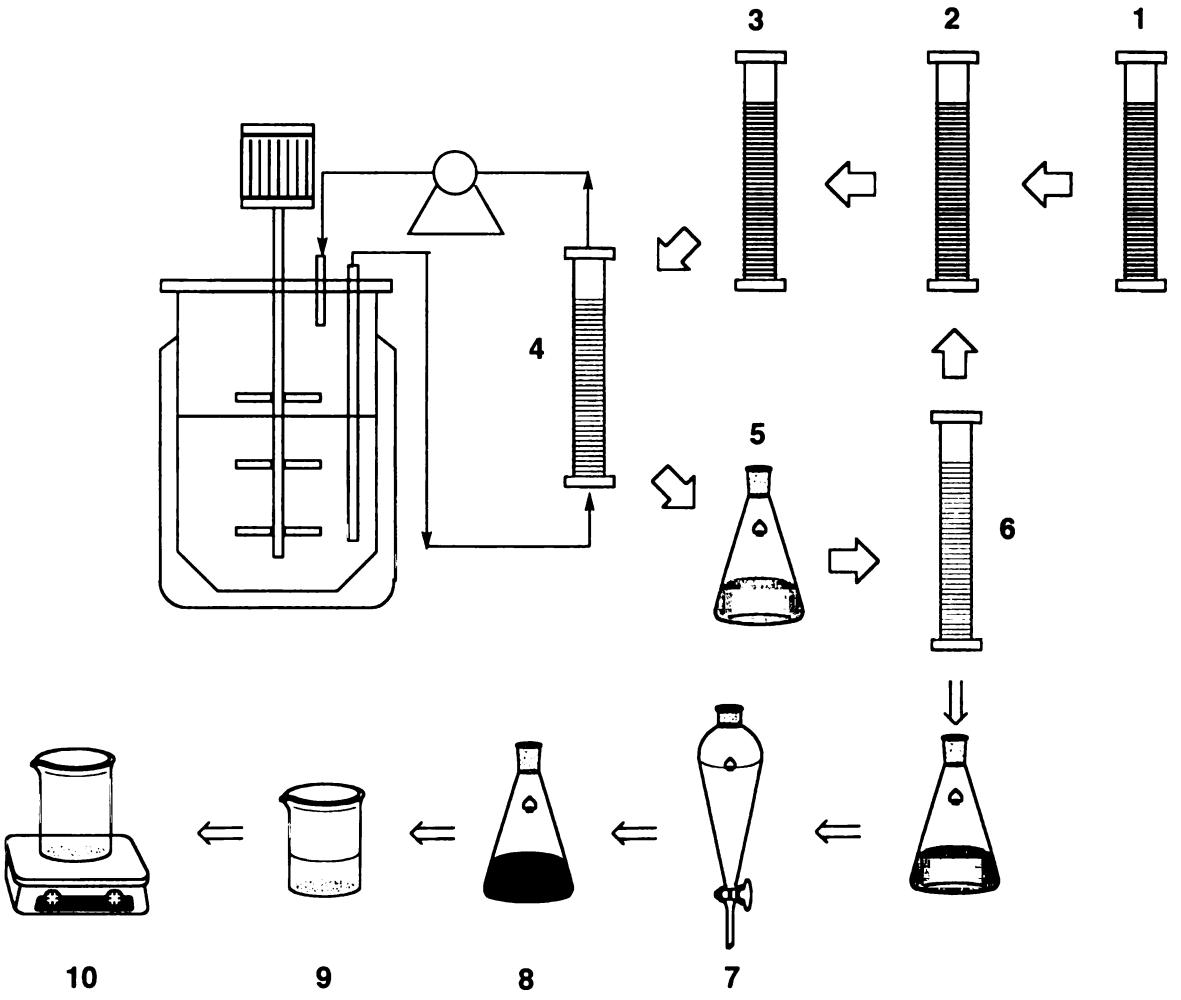

Figure 76. Phloroglucinol process from biosynthesis to product isolation.

(1) Generate phosphate resin form; 15 BV of 1M NaH_2PO_4. (2) Sterilize resin bed; 1 BV of 70% EtOH. (3) Sterile wash; 3 BV of autoclaved water. (4) Extraction; phloroglucinol bound to resin. (5) Removal of cellular debris; 3-5 BV water at 4 °C, batch-mode. (6) Elution of phloroglucinol; 5 BV of 0.1M NaH_2PO_4 at 60 °C. (7) Extraction; 3 x V with ethyl acetate. (8) Decolorization and filtration; 2 x 5% charcoal to phloroglucinol by weight. (9) Precipitation and filtration; hexanes 22 °C. (10) Remove hydration; 110°C.

Resorcinol from hydrogenation of biobased phloroglucinol

Hydrogenation of authentic phloroglucinol was reproduced from the work of Dr. Hansen.[8] Early hydrogenation results indicated there was some sort of catalyst poison contaminating the biobased phloroglucinol without indication by NMR and GC (Figure 77). This poison is yet to be identified. Purification was best achieved with treatment of activated charcoal.

Sublimation gave a 54% recovery rate with decomposition of starting material consistent with the literature. Charcoal treatment as indicated gave a recovery of 92% upon two treatments and 85% with five treatments. After the hydrogenation and prior to aromatization, the reaction goes through the salt of dihydrophloroglucinol.

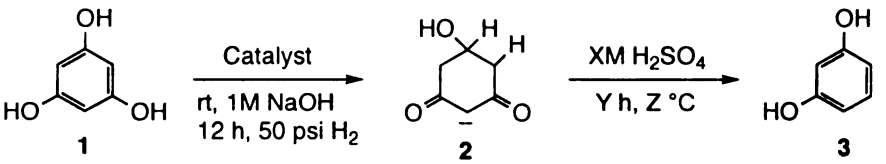

Hydrogenation Results					
Phloroglucinol	Scale (g)	Purification, loss (%)	Catalyst (mol%)	Products (%) 1	3
Authentic	5		1.2 Rh/Al_2O_3		83
	5		1.2 Rh/C		78
	5		1.2 Pt/C		63
	20		1.2 Rh/Al_2O_3		84
Biobased	5		1.2 Rh/Al_2O_3	94	
	5		1.2 Rh/C	90	
	5		1.2 Pt/C		62
	5	A (46)*	1.2 Pt/C		62
	20		1.2 Pt/C	92	5
	20	B (8)*	1.2 Pt/C	82	15
	20	C (15)*	1.2 Pt/C		63
	20		5.0 Pt/C		64
	20	B (8)*	1.2 Rh/Al_2O_3	91	
	20	C (15)*	1.2 Rh/Al_2O_3		81
	20		5.0 Rh/Al_2O_3		79
	20	B (8)*	1.2 Rh/C	86	10

*A = sublimation

B = 2 x Treatment

C = 5 x Treatment

Treatment: 5% by weight Darco KB 100 mesh wet powder activated charcoal was added to a corresponding 20 g/L PG solution in water.

Rearomatization				
Concentration PG (g/L)	X	Y	Z	Conversion of **2** to **3** (%)
20	0.5	8	110	100
20	0.5	1	110	100
20	0.5	24	23	43
10	0.5	1	110	100
10	0.08	1	110	100
1.5 [1]	n/a	8	23	30 [2]
0.15 [1]	n/a	8	23	87 [2]

1 = g Dowex-50Wx4 (H^+) / g PG in 5mL ddH_2O

2 = Conversion **2** to **1**

Figure 77. Pretreatments and hydrogenations of phloroglucinol.

Discussion

Conditions for Dowex 1 strong anion exchange resin were optimized for practical cycling of culture through the fluidized resin bed, phloroglucinol capture and elution. A low mesh size was utilized for ease of flow of a high-density microbial synthesis culture through a Bio-rad econo column in a fluidized bed mode. Cross-linking of the beads was maximized for phloroglucinol capture at 8%. The phosphate form of the resin was optimal, because of the need of phosphates in the fermenter as a nutrient and the lability to optimize anionic phloroglucinol capture. The sulfate form should be thoroughly tested by experimentation because of the similar need for nutrition along side the cost benefits over phosphate and the lack of eutrophication properties. In order to have a streamlined elution and regeneration, monobasic phophates were used supplying a form of acid and phosphate counter-ion. Acids are used to first protonate any anionically bound molecule and allow it to wash away, but then the conjugate base can take the place of the released neutral molecule. The number of protons or other ions changes the effective density of the resin, as seen by a rise in bed volume with increasing salt concentrations, and phloroglucinol cannot be efficiently pushed through the resin beds presumably because of gaps between the highly "solublizing" stationary phase. With the resin compacted the phloroglucinol does not have to escape the binding affinity to the backbone of the resin and can be effectively pushed by slight interaction with mobile phase until it comes off the column. These ideas also give a peace of mind in phloroglucinol extraction because if water elutes phloroglucinol then one might ask why phloroglucinol will not elute in 36 °C microbial synthesis culture? During extractive microbial synthesis the resin is operated in a fluidized bed mode, drastically decreasing the "effective density" of the resin. Extraction

was successful in ethyl acetate, followed by discoloration with charcoal and precipitation with hexanes to afford the dihydrate version of phloroglucinol, that when heated to 110 °C, dehydrated to yield phloroglucinol in 91% recovery from column to phloroglucinol in a bottle that has been independently characterized to be a white solid with 99.6% purity.

Resorcinol was produced from hydrogenation of phloroglucinol with Rh/Al_2O_3 in basic solution with comparable yields to the literature going through the dihydrophlorogluinol salt that upon reflux in acid gives resorcinol. When Dowex cation exchange resin was used as a potential acid source the dihydrophloroglucinol salt was retransformed into phloroglucinol. After distillation in a Kugel-Rohr apparatus resorcinol was produced in over 100 g quantity from biobased phloroglucinol as a result of heterologous expression of phlD in W3110serA(DE3) giving white crystals independently certified to be 99.9% pure with only contaminates observed was phloroglucinol in 0.01% which is on target with industrially used resorcinol.

CHAPTER FOUR REFERENCE

[1] Lohrie, M.; Knoche, W. *J. Am. Chem. Soc.* **1993**, *115*, 919.

[2] Baeyer, A. *Ber. Dtsch. Chem. Ges.* **1886**, *19*, 159. For a review on various reactions with phloroglucinol: Ershov, V.V.; Nikiforov, G.A. *Russ. Chem. Rev.* **1966**, *35*, 817.

[3] Highet, R.; Batterham, T. *J. Org. Chem.* **1964**, *29*, 475.

[4] Wang, D.; Hildenbrand, K.; Leitich, J.; Schuchmann, H.P.; Sonntag, C. v. *Zeits. Fur Natur. B.* **1993**, *48*, 478.

[5] Fray, G.I. *Tetrahedron.* **1958**, *3*, 316.

[6] Hansen, C. *PhD Dissertation,* Michigan State University, 2002.

[7] Smissman, E. E.; Voldeng, A. N.; McCarthy, J. F. *J. Pharm. Sci.* **1966**, *55*, 1101.

[8] Hansen, C.A.; Frost, J.W. *J. Amer. Chem. Soc.* **2002**, *124*, 5926.

CHAPTER FIVE

Experimental

All reactions sensitive to air and moisture were carried out in oven and/or flame dried glassware under positive argon or nitrogen pressure. Air or moisture sensitive reagents and solvents were transferred to reaction flasks fitted with rubber septa via syringes or cannula. Solvents were removed using either a Büchi rotary evaporator at water aspirator pressure or under high vacuum. Hydrodenitrogenations were performed in the Parr 4575 stainless steel high temperature-high pressure reactor equipped with the Parr 4842 temperature controller, which controlled the temperature and stirring rate. Hydrogenations were performed on a Parr hydrogenation apparatus under 50 psi of hydrogen at rt unless otherwise specified.

Reagents and solvents

THF and diethyl ether were distilled under nitrogen from sodium benzophenone ketyl. DMF, DMSO, hexanes and acetone were dried over activated Linde 4 Å molecular sieves under nitrogen. Water was glass distilled and deionized. All reagents and solvents were used as available from commercial sources or purified according to published procedures. If applicable organic solutions of products were dried over anhydrous $MgSO_4$. Charcoal (Darco® G-60 ~ 100 mesh) was used for discoloration of solutions. Sodium salt of 3-(trimethylsilyl)-propionic*2,2,3,3-d*$_4$ acid (TSP) was purchased from

Lancaster Synthesis Inc. Diazomethane was generated from Diazald® following a literature procedure.

Chromatography

AG 1x8 Cl^- was converted to the hydroxide form by washing with twenty column volumes of 1N NaOH. The column was then washed with distilled deionized water until all the chloride was displaced as determined by silver nitrate test.

Dowex 50Wx8 100-200 (H^+) and Dowex 1x8 200-400 (Cl^-) were purchased from Sigma- Aldrich. Previously used Dowex 50 (H^+) was cleaned by treatment with bromine. An aqueous suspension of resin was adjusted to pH 14 by addition of solid KOH. Bromine was added to the solution until the suspension turned a golden yellow color. Additional bromine was added (1-2 mL) to obtain a saturated solution. The mixture stood at room temperature overnight, and the Dowex 50 resin was collected by filtration and washed exhaustively with water followed by 6 N HCl. Dowex 50 (H^+) was stored at 4 °C. AG 1x8 (acetate form and chloride form) and hydroxyapatite Bio-Gel HTP gel were purchased from Bio-Rad.

Spectroscopic and analytical measurements

^1H NMR and ^{13}C NMR spectra were recorded on a Varian VX-300 FT-NMR spectrometer or a Varian VXR-500 FT-NMR spectrometer. Chemical shifts for ^1H NMR spectra are reported in parts per million (ppm) relative to internal tetramethylsilane

(Me_4Si, δ = 0.0 ppm) with $CDCl_3$ as the solvent and to internal sodium 3-(trimethylsilyl) propionate-*2,2,3,3-d*$_4$ (TSP, δ = 0.0 ppm) when D_2O was the solvent. ^{13}C NMR spectra were recorded at 75 MHz on a Varian VX-300 FT-NMR spectrometer or at 125 MHz on a Varian VXR-500 FT-NMR spectrometer. Chemical shifts for ^{13}C NMR spectra were reported in parts per million (ppm) relative to $CDCl_3$ (δ = 77.0 ppm) or CD_3OD (δ = 49.0 ppm) in D_2O. 1 mL of the bioconversion mixture was taken every h and the protein was precipitated with 10% HCl and spun down in a microfuge. The supernatant was concentrated to dryness, the residue redissolved in 1 mL D_2O, concentrated again to dryness and the residue redissolved in 1 mL D_2O containing 10 mM TSP. The molar concentration during the bioconversion of L-lysine to β-L-lysine was determined as mentioned above. The concentration of β-L-lysine and L-lysine were determined by the ratios of the integrated ^1H NMR resonances at δ 2.8 and δ 2.0, respectively, with the integrated resonance corresponding to TSP at δ 0.00.

Gas chromatography was used to determine the product yields obtained during the bioconversions. Chromatograms were obtained using an Agilent 6890N equipped with an HP-5 column (30 m x 0.25 mm x 0.25 μm) after samples were derivatized with bis(trimethylsilyl) trifluoroacetamide (BSTFA). Analysis was optimized by using a temperature program in the range from 120 °C to 210 °C at 15 °C/min. GC derivatization was initiated by dissolving the extracted or dried material in pyridine (1 mL) followed by the addition of dodecane (0.001 mL) and bis(trimethylsilyl)fluoroacetamide BSTFA (1 mL) per sample. A stock of the derivatization components is generally prepared and used

promptly within 3 h. Derivatization reactions are stirred at room temperature in darkness for a minimum of 2 h. No change in yield was observed when reaction times were increased up to 12 h. Yield was determined using response factors obtained when authentic phloroglucinol (Fluka, catalog number 79330) was extracted or dried and derivitized using the same protocol. Halving the derivitization mixture showed no deviance from the calibration curve. Samples were injected (2-5 μL) using an Agilent 7683 series injector. Yields were determined with response factors obtained from authentic samples that were quantified relative to dodecane internal standard.

Bacterial strains, plasmids, primers and gene synthesis

Clostridium subterminale SB4, *Escherichia coli* W3110 and *Pseudomonas fluorescens* Pf-5 were obtained from ATCC. *Escherichia coli* BL21 was obtained from Novagen. *Escherichia coli* DH5α was purchased from Invitrogen. Primers were synthesized by the Research Technology Support Facility at Michigan State University. Plasmid sequencing was completed at the Research Technology Support Facility at Michigan State University. Genes submitted for synthesis were constructed by DNA2.0 (Menlo Park, CA).

Storage of microbial strains and plasmids

All bacterial strains were stored at -78 °C in glycerol. Plasmids were transformed into DH5α for long-term storage. Glycerol samples were prepared by adding 0.75 mL of an overnight culture to a sterile vial containing 0.25 mL of 80% (v/v) glycerol. The solution was mixed, flash frozen in liquid N_2 and then stored at -78 °C.

Culturing of *Clostridium subterminale*

Clostridium subterminale SB4 was obtained from the American Type Culture Collection (ATCC 29748). Cells were grown in a medium (1 L) containing yeast extract (6 g), L-lysine·HCl (6 g), 1 M phosphate buffer (45 mL), and 1 M K_2CO_3 (7.5 mL) at pH 7.5 (*Clostridium* medium). After the medium was autoclaved in a Pyrex bottle, it was purged with N_2 while it was allowed to cool to rt. All subsequent manipulations were performed in a Coy anaerobic chamber. Sodium dithionite (30 mg) was added to the medium inside a Coy anaerobic chamber. Cultures were initiated by inoculating a single colony into 5 mL of semisolid (0.2% agar) *Clostridium* medium. The test tubes were sealed tightly with septa and the inoculants were cultured at 37 °C with agitation at 250 rpm for 12 h outside of the Coy chamber. The 5 mL semisolid aliquot was subsequently transferred (inside a Coy chamber) to a 100 mL containing clostridium medium. The cells were grown at 37 °C with agitation at 150 rpm for 12 h and subsequently transferred to 1

L of growth medium, which was cultured for 12-18 h at 37 °C to OD_{600} ~2-3.2. Following centrifugation at 9,000*g* for 10 min, approximately 2-4 g of wet cells were obtained. Precaution was taken not to expose cells to air by conducting all transfers inside the Coy chamber.

Intact cell bioconversion of L-lysine

All manipulations are carried out in a Coy anaerobic chamber unless otherwise noted. *Clostridium subterminale* SB4 cells harvested after 18 h (OD_{600} ~ 2) from a 4 L medium, either thawed from -80 °C freezer or freshly cultured, were resuspended in a reaction mixture, previously purged with N_2, containing 150 mM L-lysine, 80 mM Tris-HCl (pH 7.5), 5 mM potassium phosphate (pH 7.5), and $FeSO_4$ (3 mM). The reaction mixture contained ~20 g of cells/250 mL Pyrex bottle, which was sealed with a screw-cap. The reaction mixture was incubated outside of the Coy chamber, in a 37 °C shaker (150 rpm) with a tungsten lamp (75 watt, 120 V) directly shone at the Pyrex bottles for 24 h. Outside of the coy chamber the reaction mixture was centrifuged at 9000*g* to remove intact cells and the resulting supernatant was concentrated to 20 mL, which was then acidified to pH 2.5 with HCl. A mL of the product mixture was concentrated to dryness and the residue was redissolved in D_2O (1 mL) and concentrated three times. L-β-Lysine was quantified by integration of its 2.8 ppm peak relative to TSP internal standard.

Purification of L-β-lysine

The main reaction mixture was acidified to pH 2.5, centrifuged to remove protein, and then loaded on the Dowex 50 (H^+) column (3 x 40 cm) previously washed with 10 mM HCl. The L-lysine and L-β-lysine were differentially eluted with 0.2 M sodium formate buffer, pH 2.75, containing 0.35 M NaCl. Fractions of 10 mL were collected after ~200 mL of eluent was discarded. L-Lysine eluted first in the fractions 22-56 and L-β-lysine in fractions 78-115. The L-β-lysine fraction were pooled and concentrated to 50 mL and loaded on a fresh Dowex 50-column and washed with water. The amino acid was retained on the column and then was eluted with 1 N ammonium hydroxide, which came out as a single 40-mL fraction. The L-β-lysine solution was evaporated under reduced pressure to remove excess ammonia and the resulting yellow solid was redissolved in ethanol and concentrated several times to a to afford a yellow solid in 43% isolated yield based on starting L-lysine. L-β-Lysine obtained was very hygroscopic and was used in the next step.

Deamination of L-β-lysine

A solution of L-β-lysine (0.4 g, 2.8 mmol) was dissolved in ethanol (80 mL) in a glass reaction vessel. 5 mol % of Ru/Al_2O_3 (0.28 g, 0.14 mmol) was suspended in the reaction solution. The glass reaction vessel was inserted into the 500 mL Parr 4575 stainless steel high temperature-high pressure reactor and the vessel sealed. The

temperature and the stirring rate were controlled by a Parr 4842 temperature controller. Hydrogen was bubbled through the reaction mixture for 10-15 min to remove air while stirring at 100 rpm. The vessel was heated to 200 °C and stirred for 2 h. After 2 h, the reaction vessel was pressurized to 1,000 psi H_2 pressure. The reaction was stirred at 400 rpm for another 2 h. After removal of the catalyst by filtration, the reaction mixture was concentrated to dryness under vacuum to afford a brown residue. Quantification was conducted by integration of the caprolactam peak centered at 2.5 ppm relative to TSP as an internal standard.

Cyclization of L-lysine to α-Amino-caprolactam.[1]

A stirrer mixture of L-lysine·HCl (55 g, 0.3 mol) and NaOH (12 g, 0.3 mol) in 1,2,-propanediol (1.2 L) was heated to reflux for 2 h in the presence of Dean-Stark trap. The solution was then cooled and concentrated under vacuum to afford to α-aminocaprolactam along with byproduct NaCl, which was removed by filtration.

In an alternative method, α-aminocaprolactam was obtained from heating a mixture of L-lysine in EtOH to 200 °C for 2 h inside a 4575 Parr reaction vessel. After removal of ethanol, α-aminocaprolactam was obtained as the only product as confirmed by ^{1}HNMR.

Chemical L-β-Lysine synthesis.[2]

A solution of L-ornithine·HCl (30.0 g, 0.178 mol) in 5 M NaOH (450 mL) was stirred with icebath cooling while benzyl chloroformate (63.5 mL, 0.440 mol) was added dropwise over 15 min. The resulting mixture was stirred for an additional 6 h in an icebath before it was diluted with H_2O (400 mL) and acidified to pH 5 with concentrated HCl. The solution was extracted 5x with ethyl acetate (200 mL) and the combined extracts were washed with brine, dried over Na_2SO_4, and concentrated *in vacuo* to afford a white wax, which was suspended in boiling petroleum ether and filtered to afford N,N'-dibenzyloxycarbonyl L-ornithine (52 g, 80%). To a solution of N,N'-dibenzyloxy-carbonyl L-ornithine (9.15 g, 0.0250 mol) in ethyl acetate (250 mL) was added N-methylmorpholine (3.0 mL, 0.0275 mol). The solution was stirred at –10 °C while ethylchloroformate (4.75 mL, 0.050 mol) was introduced dropwise over 20 min. The resulting milky mixture was stirred for an addition 3 h at –10 °C before it was filtered through Celite. The resulting filtrate was combined with a 0.8 M diazomethane in diethyl ether (400 mL) and stirred at 0 °C for 6 h. Excess diazomethane was destroyed by addition of acetic acid before the reaction mixture was concentrated under reduced pressure to afford a diazoketone as a yellow solid (6.25 g, 85%).

The diazoketone (6.25 g, 0.0214 mol) was dissolved in methanol (100 mL) and the reaction flask was wrapped with aluminium foil. All subsequent reactions were performed in the dark room. A solution of silver benzoate (1.25 g, 6.55 mmol) in triethylamine (20 mL) was introduced dropwise into the diazoketone solution held at 0 °C. The reaction

mixture was stirred for 1 h before an additional solution of silver benzoate was introduced. The resulting muddy mixture was concentrated to dryness and the resulting residue was redissolved in ethyl acetate (20 mL) and subsequently washed with $NaHCO_3$ (10 mL), brine (2 x 10 mL) and 5% HCl (10 mL). After the organic layer was dried and concentrated under reduced pressure, L-β-lysine ester was obtained as an orange solid (4.11 g, 65%).

In vitro enzyme assays preparation

After collected and resuspended in the proper resuspension buffer, the cells were disrupted by two passages through a French pressure cell (SLM Aminco) at 16,000 psi. Cellular debris was removed from the lysate by centrifugation (48,000*g*, 20 min, 4 °C). Protein was quantified using the Bradford dye-binding procedure.[3] A standard curve was prepared using bovine serum albumin. Protein assay solution was purchased from Bio-Rad and used as described by the manufacture.

Plasmids

Unless otherwise noted all plasmid construction was completed in DH5α or XL1 Blue on appropriate antibiotics and was verified by both enzymatic digestion and sequencing in both directions.

Plasmid pJA3.131A

Plasmid pJA3.131A is a 8.2 kb plasmid derived from pJA2.042. Plasmid pJA2.042 was created by insertion of phlD behind the T7 promoter of pHIS-8, a pET28a(+) derivative (Novagen). Insertion of a 1.6 kb fragment encoding serA from SmaI digested pRC1.55B into the *Bgl*II site of pJA2.042 afforded pJA3.131A in which the phlD gene and serA gene are transcribed in opposite directions.

Plasmid pBC1.146

Plasmid pBC1.146 is a 7.0 kb plasmid. As a negative phlD control of pJA3.131A, pBC1.146 is derived from pHIS-8. SmaI digested pRC1.55B excising a 1.6kb serA gene fragment was cloned into the BgIII site after blunting with Klenow large fragment. The serA gene is transcribed in the opposite direction of the T7 promoter.

Plasmid pBC2.055

Plasmid pBC2.055 is a 3.9 kb plasmid. Pf-5 phlD was cloned into the pKD3 host vector. The T7 promoter region with the Pf-5 phlD gene was PCR amplified from pJA3.242 with engineered SphI and BmgBI cutting sites. JWF 1637 5'-GTACCTGCATGCTCTCGATCCCGCGAAATTA-3' was used as the forward primer and JWF 1610 was the reverse primer 5'-AATTTAACACGTCAGGCACAGGCAGTC ACATCA-3'. PKD3 and the column purified PCR product was digested with SphI and BmgBI, purified and ligated with the Fast-link Ligation kit. Along the lines with

experimental design the PF-5 phlD fragment is in the opposite orientation as the cm^R gene. Verification was observed by digestion with HindIII.

Plasmid pBC2.179

Plasmid pBC2.179 is a 6.4 kb plasmid. pJA3.131A has DNA followed by a stop codon between the T7 promoter and the transcribed phlD sequence. pBC2.179 chose the same pET-based expression system in attempts to give the phlD gene optimal positioning for unperturbed transcription. pET-27b(+) was purchased from Novagen. phlD was PCR amplified with primers installing NdeI and BamHI sites from pJA3.131A. The forward primer being JWF1668 5'-GGAATTCCATATGTCTACACTTTGCCTTCC-3' and the reverse primer used was JWF1669 5'-CGCGGATCCTCAGGCGGTCCACTCGC-3'. The gel purified PCR product and pET-27b(+) were independently digested sequentially with BamHI and NdeI. The digested vector was treated with CIAP prior to ligation with the Fast-link ligation kit. Verification was observed by digestion with SmaI.

Plasmid pBC2.187

Plasmid pBC2.187 is a 8.1 kb plasmid. Insertion of the serA gene locus involved in the production of serine into pBC2.179 was achieved to provide a nutritional marker for a host with a serA deletion offering an alternative to antibiotic pressure that is not practical in an industrial setting. The serA fragment origin is pRC1.55b which was cloned into pSU18. pRC1.55b is a plasmid produced by Rachel Christ of our lab. Digestion of pRC1.55b with SmaI afforded a 1.6 kb serA encoding fragment. pBC2.179 was digested with SphI, blunted with Klenow, dephosphorylated with CIAP and ligated with the serA

fragment. serA and phlD are transcribed in opposite directions. Orientation was verified by digestion with PstI.

Plasmid pBC2.212

Plasmid pBC2.212 is a 6.4 kb plasmid. The Pf-5 phlD sequence was visually optimized for transcription of the proper statistical alignment of *E. coli* compared to the *Pseudomonas* host (See "in-house optimized phlD sequence"). Attention was focused with preference of common codon usage towards the leading end of phlD. pJ201:13176 encoded the optimized phlD sequence and was synthesized by DNA2.0 with engineered with BamHI and NdeI cutting sites. pJ201:13176 and pET-27b(+) were independently digested sequentially with BamHI and NdeI. The digestion mixtures were independently gel purified using the Zymo kit. The digested vector was treated with CIAP prior to ligation with the Fast-link ligation kit. Verification was observed by digestion with EagI.

Plasmid pBC2.219

Plasmid pBC2.219 is a 8.1 kb plasmid. Insertion of the serA gene locus involved in the production of serine into pBC2.212 was achieved to provide a nutritional marker for a host with a serA deletion offering an alternative to antibiotic pressure that is not practical in an industrial setting. The serA fragment origin is pRC1.55b which was cloned into pSU18. pRC1.55b is a plasmid produced by Rachel Christ of our lab. Digestion of pRC1.55b with SmaI afforded a 1.6 kb serA encoding fragment. pBC2.212 was digested with SphI, blunted with Klenow, dephosphorylated with CIAP and ligated with the serA

fragment. serA and phlD are transcribed in opposite directions. Orientation was verified by with a PstI and XhoI double enzyme digestion.

Plasmid pBC2.252

Plasmid pBC2.252 is a 6.4 kb plasmid. The Pf-5 phlD sequence was visually optimized for transcription of the proper statistical alignment of *E. coli* compared to the *Pseudomonas* host (See "in-house optimized phlD sequence"). Attention was focused with preference of common codon usage towards the leading end of phlD. pJ201:13176 encoded the optimized phlD sequence and was synthesized by DNA2.0. The optimized phlD was PCR amplified from pBC2.219 using JWF1695 5'-AACGCGGATCCATGTC TACACTTTGCCTTCCA-3' and JWF1696 5'-AATCCCAAGCTTTTAAGCCGTCCA CTCTCCAA-3' inserting BamHI and HindIII sites respectively. The purified PCR product and pJF118EH were independently digested sequentially with BamHI and HindIII. The vector was dephophorylated with CIAP before ligation with the Fast-link kit. Verification was observed with digestion by NdeI.

Plasmid pBC2.257

Plasmid pBC2.257 is a 8.1 kb plasmid. Insertion of the serA gene locus involved in the production of serine into pBC2.252 was achieved to provide a nutritional marker for a host with a serA deletion offering an alternative to antibiotic pressure that is not practical in an industrial setting. The serA fragment origin is pRC1.55b which was cloned into pSU18. pRC1.55b is a plasmid produced by Rachel Christ of our lab. Digestion of

pRC1.55b with SmaI afforded a 1.6 kb serA encoding fragment. pBC2.252 was digested with NdeI, blunted with Klenow, dephosphorylated with CIAP and ligated with the serA fragment. serA and phlD are transcribed in the same direction. Orientation was verified by with a PstI and ScaI double enzyme digestion.

Plasmid pBC2.264

Plasmid pBC2.264 is a 8.1 kb plasmid. Insertion of the serA gene locus involved in the production of serine into pBC2.252 was achieved to provide a nutritional marker for a host with a serA deletion offering an alternative to antibiotic pressure that is not practical in an industrial setting. The serA fragment origin is pRC1.55b which was cloned into pSU18. pRC1.55b is a plasmid produced by Rachel Christ of our lab. Digestion of pRC1.55b with SmaI afforded a 1.6 kb serA encoding fragment. pBC2.252 was digested with ScaI, blunted with Klenow, dephosphorylated with CIAP and ligated with the serA fragment. pBC2.264 was a back-up strategy cloned concurrently with pBC2.257 and was not characterized by microbial synthesis.

Plasmid pBC2.271

Plasmid pBC2.271 is a 6.4 kb plasmid. The Pf-5 phlD sequence was optimized for transcription of the proper statistical alignment of *E. coli* compared to the *Pseudomonas* host (See "DNA2.0 optimized phlD sequence") using the gene designer software offered by DNA2.0. pJ201:15277 encoded the optimized phlD sequence and was synthesized by DNA2.0 with engineered with BamHI and NdeI cutting sites. pJ201:15277 and pET-

27b(+) were independently digested sequentially with BamHI and NdeI. The digestion mixtures were independently gel purified using the Zymo kit. The digested vector was treated with CIAP prior to ligation with the Fast-link ligation kit. Orientation was verified by with a PstI and EagI double enzyme digestion.

Plasmid pBC2.274

Plasmid pBC2.274 is a 8.1 kb plasmid. Insertion of the serA gene locus involved in the production of serine into pBC2.271 was achieved to provide a nutritional marker for a host with a serA deletion offering an alternative to antibiotic pressure that is not practical in an industrial setting. The serA fragment origin is pRC1.55b which was cloned into pSU18. pRC1.55b is a plasmid produced by Rachel Christ of our lab. Digestion of pRC1.55b with SmaI afforded a 1.6 kb serA encoding fragment. pBC2.271 was digested with SphI, blunted with Klenow, dephosphorylated with CIAP and ligated with the serA fragment. serA and phlD are transcribed in opposite directions. Orientation was verified by digestion with PstI.

Comprehensive reference list of strains and plasmids

strain	relavant characteristics	source
DH5α	*F' ϕ80lacZΔM15 Δ(lacZYA-argF)U169 deoR recA1 endA1 hsdR17(r_k^-, m_k^+) phoA λ⁻ supE44 thi-1 gyrA96 relA1*	Invitrogen
BL21(DE3)	*E. coli B F⁻ dcm ompT hsdS(r_B- m_B-) gal λ (DE3)*	Novagen
XL1-Blue	*recA1 endA1 gyrA96 thi-1 hsdR17 supE44 relA1 lac* [F′ *proAB lacI*qZΔ*M15* Tn*10* (Tet)].	Stratagene
BW25113	DE(araD-araB)567lacZ47879del)(::rrnB-3)LAM-rph-1DE(rhaD-rhaB)568hsdR514	CGSC
W3110	wild-type K12	ATCC
Pseudomonas Fluorescens Pf-5	wild-type	ATCC

plasmid	relavant characteristics	source
pUC18	Ap^R, P_{lac}	ref
pKD3	Ap^R, FRT-flanked Cm^R	ref
pKD4	Ap^R, FRT-flanked Km^R	ref
pKD46	Ap^R, *araC*, P_{araB}*γ*, *β*, *exo*, *ts*-pA101 replicon	CGSC
pCP20	Ap^R, Cm^R, Flp^+, λ $cI857^+$	ref
pRC1.55B	*serA* in pSU18	lab
pJF118EH	Ap^R, $lacI^Q$ in pKK223-3	lab[4]
pET27b(+)	Km^R, $lacI^Q$, P_{T7}	Novagen
pBC1.146	Km^R, $lacI^Q$, P_{T7}	This study
pBC2.055	Ap^R, *phlD* FRT-flanked Cm^R	This study
pBC2.179	Km^R, $lacI^Q$, P_{T7}, *phlD*	This study
pBC2.187	Km^R, $lacI^Q$, P_{T7}, *phlD*, *serA*	This study
pBC2.212	Km^R, $lacI^Q$, P_{T7}, in house opt *phlD*	This study
pBC2.219	Km^R, $lacI^Q$, P_{T7}, in house opt *phlD*, *serA*	This study
pBC2.252	Ap^R, $lacI^Q$ in pKK223-3, in house opt *phlD*	This study
pBC2.257	Ap^R, $lacI^Q$ in pKK223-3, in house opt *phlD*, *serA*	This study
pBC2.271	Km^R, $lacI^Q$, P_{T7}, 2.0 opt *phlD*	This study
pBC2.274	Km^R, $lacI^Q$, P_{T7}, 2.0 opt *phlD*, *serA*	This study

In house optimized phlD sequence

The Pf-5phlD sequence was visually optimized for transcription of the proper statistical alignment of *E. coli* compared to the *Pseudomonas* host (see text for comparison and statistical aligments). The optimized sequence is as follows with changes from PF-5 wild type phlD in light grey:

ATGTCTACACTTTGCCTTCCACATGTTATGTTTCCGCAACACAAAATTACCCAG
CAACAGATGGTTGATCACCTGGAAAACTTGCACGCGGATCATCCACGTATGGC
CCTGGCGAAACGCATGATCGCCAATACCGAAGTCAACGAACGTCATCTGGTGT
TGCCGATTGATGAATTGGCAGTGCACACCGGTTTTACGCATCGCAGCATCGTC
TATGAACGTGAAGCGCGTCAGATGAGTTCGGCCGCGGCGCGTCAAGCAATCG
AAAATGCCGGGTTACAGATTAGCGATATTCGCATGGTGATTGTCACTTCTTGC
ACCGGGTTTATGATGCCGTCGTTAACGGCGCACCTGATCAATGATTTAGCACT
GCCAACCTCCACCGTGCAGTTGCCGATTGCTCAGCTGGGCTGTGTGGCAGGTG
CCGCGGCCATCAATCGTGCCAACGACTTTGCACGTCTCGATGCTCGCAATCAT
GTATTAATTGTGTCTCTGGAATTCTCCAGTCTGTGCTATCAGCCGGACGATACG
AAGCTGCACGCTTTTATCTCCGCGGCGCTGTTCGGCGATGCGGTATCTGCCTGT
GTTCTGCGTGCTGATGATCAAGCCGGTGGCTTTAAAATCAAAAAGACGGAGA
GTTACTTCTTGCCGAAAAGCGAGCACTATATCAAATACGACGTGAAAGATACC
GGCTTTCATTTTACCCTTGATAAAGCGGTGATGAATTCCATTAAAGACGTTGC
ACCGGTCATGGAGCGGCTCAACTATGAGAGCTTTGAACAGAATTGTGCGCATA
ACGATTTCTTTATCTTCCACACAGGTGGTCGCAAGATTCTTGACGAGCTGGTG
ATGCATTTAGACCTGGCATCCAATCGGGTCTCACAAAGTCGCAGCAGCCTGTC
GGAAGCTGGCAACATTGCCTCAGTGGTTGTGTTCGACGTACTCAAACGGCAGT
TTGATTCCAACCTCAATCGCGGCGACATCGGACTGCTGGCAGCCTTCGGCCCT
GGGTTTACTGCGGAAATGGCGGTTGGAGAGTGGACGGCTTAA

DNA2.0 gene designer optimized phlD sequence

The PF-5 phlD sequence was optimized for transcription of the proper statistical alignment of *E. coli* compared to the *Pseudomonas* host (see text for detail). The optimized sequence is as follows:

ATGTCTACTCTGTGCCTGCCACACGTAATGTTCCCACAACACAAAATCACTCA
GCAGCAAATGGTTGACCACCTGGAAAACCTGCACGCCGATCACCCACGTATG
GCTCTGGCTAAACGTATGATCGCTAACACCGAGGTTAACGAGCGTCATCTGGT
ACTGCCGATTGACGAGCTGGCAGTTCATACCGGCTTTACCCACCGCTCTATCG
TGTACGAACGCGAAGCGCGCCAGATGTCTTCTGCAGCGGCTCGTCAGGCGATT
GAGAACGCAGGTCTGCAAATCAGCGACATCCGTATGGTGATCGTTACCAGCTG
TACTGGTTTTATGATGCCTTCTCTGACTGCCCATCTGATTAATGATCTGGCCCT
GCCAACTAGCACCGTACAACTGCCGATTGCGCAGCTGGGCTGTGTTGCTGGTG
CGGCAGCTATTAATCGCGCTAACGATTTTGCACGCCTGGATGCTCGTAATCAT
GTTCTGATTGTGTCTCTGGAATTCTCTAGCCTGTGCTACCAACCGGATGACACG
AAACTGCACGCGTTTATCTCCGCTGCTCTGTTCGGTGATGCGGTTTCCGCATGT
GTACTGCGCGCGGATGACCAAGCTGGCGGTTTCAAAATTAAAAAGACCGAAT
CTTACTTCCTGCCAAAAAGCGAACATTACATTAAATATGATGTTAAGGATACC
GGTTTCCATTTTACGCTGGATAAAGCTGTTATGAACTCTATCAAAGACGTTGCT
CCGGTCATGGAACGTCTGAACTATGAATCTTTTGAGCAGAACTGCGCTCATAA
CGACTTCTTTATCTTCCATACCGGCGGTCGTAAAATCCTGGATGAACTGGTTAT
GCACCTGGACCTGGCGTCTAACCGTGTAAGCCAGTCTCGCAGCTCTCTGTCCG
AAGCTGGCAACATCGCGTCTGTGGTGGTCTTTGATGTGCTGAAACGTCAGTTC
GATAGCAATCTGAACCGTGGCGATATCGGTCTGCTGGCCGCCTTCGGTCCTGG
CTTCACTGCTGAAATGGCGGTGGGTGAGTGGACCGCATAATGAGGATCCTAAT
GA

Culture mediums

All solutions were prepared in distilled, deionized water. LB medium (1 L) contained Bacto tryptone (10 g), Bacto yeast extract (5 g), and NaCl (10 g). YT medium (1 L) contained Bacto-tryptone (16 g), Bacto-yeast extracts (10 g) and NaCl (5 g) in distilled, deionized water. TB medium (1 L) contained tryptone (10 g) and NaCl (5 g). After autoclaving and directly before use, $MgSO_4$ (10 mL of 1 M stock) was added to the TB medium. M9 salts (1 L) contained Na_2HPO_4 (6 g), KH_2PO_4 (3 g), NH_4Cl (1 g) and NaCl (0.5 g). M9 medium contained D-glucose (10 g), $MgSO_4$ (0.12 g) and thiamine (0.001 g) in 1 L of M9 salts. CAYE medium (100 mL) contained casamino acids (2 g) and yeast extract (10 g). Minimum salts (1 L) contained $(NH_4)_2SO_4$ (0.2 g), KH_2PO_4 (0.6 g), K_2HPO_4 (1.4 g), sodium citrate (0.1 g) and magnesium sulphate (0.02 g). SOC medium (1 L) contained Bacto tryptone (20 g), Bacto yeast extract (5 g), NaCl (10 mL, 1 M), KCl (2.5 mL, 1 M), $MgCl_2$ (10 mL, 1 M), $MgSO_4$ (10 mL, 1 M) and glucose (10 mL, 2 M). 2×YT medium (1 L) contained Bacto tryptone (16 g), yeast extract (10 g) and NaCl (5 g). Solutions of inorganic salts, magnesium salts and X-Gal indicator plates[5] contained glucose (4 g), lactose (4 g), X-gal (5-bromo-4-chloro-3-indolyl-β-D-galactopyranoside) (1 mL, 3 mg/mL in EtOH:H_2O, 1:1, v/v) in medium E (1 L) with 1.5% (w/v) Difco agar.

Antibiotics were added where appropriate to the following final concentrations unless noted otherwise: ampicillin, 50 μg/mL; kanamycin, 50 μg/mL. Stock solutions of antibiotics were prepared in water with the exceptions of tetracycline, which was prepared

in 50% aqueous ethanol. Antibiotics, isopropyl β-D-thioglucopyranoside (IPTG), thiamine, and amino acid supplementations were sterilized through 0.22-μm membranes prior to addition to M9 medium. Solid medium was prepared by addition of 1.5% (w/v) Difco agar to the medium.

Microbial synthesis medium (1 L) contained K_2HPO_4 (7.5 g), ammonium iron (III) citrate (0.3 g), citric acid monohydrate (2.1 g and concentrated H_2SO_4 (1.2 mL). The culture medium was adjusted to pH 7.0 by addition of concentrated NH_4OH before autoclaving. The following supplements were added immediumtely prior to initiation of the microbial synthesis: glucose (19 to 22 g) $MgSO_4$ (0.24 g) and trace minerals $(NH_4)_6(Mo_7O_{24}).4\ H_2O$ (0.0037 g), $ZnSO_4.7\ H_2O$ (0.0029 g), H_3BO_3 (0.0247 g), $CuSO_4.5\ H_2O$ (0.0025 g), and $MnCl_2.4\ H_2O$ (0.0158 g). Solutions of D-glucose and $MgSO_4$ were autoclaved separately. Trace minerals were sterilized through 0.22-μm membranes prior to addition to the medium.

Fed-batch microbial synthesis

Microbial syntheses were conducted in a B. Braun M2 culture vessel with a 2 L working capacity. Environmental conditions were supplied by a B. Braun Biostat MD controlled by a DCU-1. Data was acquired on a Dell Optiplex Gs+ 5166M personal computer using B. Braun MFCS/Win software. PID control loops were used to control temperature, pH, and glucose addition. The temperature was maintained at 33 °C or 36 °C as indicated and the pH was maintained at 7.0 by addition of NH_4OH and 2 N H_2SO_4.

Glucose was added as a 60% (w/v) solution. Dissolved oxygen (D.O.) was monitored using a Mettler-Toledo 12 mm sterilizable O_2 sensor fitted with an Ingold A-type O_2 permeable membrane. D.O. was maintained at 20% air saturation throughout the course of the microbial synthesis unless otherwise specified. Antifoam (Sigma 204) was manually pumped into the vessel as needed.

Inoculants were prepared by introduction of a single colony from a freshly transformed plate onto M9 minimal medium with glucose into 20 mL of M9 minimal medium with glucose. The culture was grown at 37 °C with agitation at 250 rpm until an OD_{600} ~ 0.5-1.0 (~18 h) and subsequently 0.5 - 1.0 mL, depending on previous optical density, was transferred to another 20 mL of M9 glucose medium. Cultures were grown at 37 °C for an additional ~ 6-8 h. The inoculant (OD_{600} = 0.5 - 1.0) was then transferred into the fermenter vessel and the batch microbial synthesis was initiated.

Three staged methods were used to maintain D.O. concentrations at desired air saturation during the microbial synthesis. With the airflow at an initial setting of 0.06 L/L/min, the D.O. concentration was maintained by increasing the impeller speed from its initial set point of 50 rpm to its preset maximum rate. With the impeller speed constant, the mass flow controller then maintained the D.O. concentration by increasing the airflow rate from 0.06 L/L/min to a preset maximum of 1.0 L/L/min. At constant impeller speed and constant airflow rate, the D.O. concentration was finally maintained at the desired air saturation for the remainder of the microbial synthesis by oxygen sensor-controlled carbon source feeding. At the beginning of this stage, the D.O. concentration fell below the desired air saturation due to residual initial carbon source in the medium. This lasted for

approximately 10 min to 30 min before carbon source feeding commenced. The carbon source feed PID control parameters were set to 0.0 s (off) for the derivative control (τ_D) and 999.9 s (minimum control action) for the integral control (τ_I). X_P was set to 950% to achieve a K_c of 0.1.

Process description of the biosynthesis of phloroglucinol

Fed-batch single stage continuous extractive microbial synthesis protocol

Phloroglucinol is produced directly from glucose by a transformed strain of *E. coli* K-12. The host strain and plasmid contain the necessary genes to provide efficient metabolism of glucose to phloroglucinol. During the course of the microbial synthesis, phloroglucinol is continuously extracted from the microbial synthesis medium by passage through Dowex 1 strong anion exchange resin. Maintaining low glucose concentrations in the microbial synthesis medium (< 0.1mM) results in optimal synthesis of phloroglucinol. Host strain W3110serA(DE3) was constructed from *E. coli* K-12 strain W3110 (ATCC). W3110serA(DE3) was created by inactivating the serA gene of W3110 to create W3110serA followed by insertion of the T7 gene 1 onto the chromosome to obtain W3110serA(DE3). The T7 gene 1 encodes for T7 RNA polymerase, which is needed to overexpress genes cloned behind the T7 promoter. Phloroglucinol production occurs when W3110serA(DE3) is transformed with plasmid pBC2.274, an 8.1 kb plasmid that includes a 1.1 kb fragment expressing the *phlD* gene of *Pseudomonas fluorescens* Pf-5 optimized for *E. coli* cloned behind a T7 promoter. Plasmid pBC2.274 also contains the *E. coli* serA gene. In the absence of serine supplementation W3110serA(DE3) does not

grow in minimal salts medium. The functional serA gene of pBC2.274 allows the transformed host W3110serA(DE3)/pJA3.131A to grow in minimal salts medium without the addition of serine.

Phloroglucinol strain prior to microbial synthesis supplemental

Seedtrain for phloroglucinol biosynthesis

The complete microbial synthesis process consists of a fed-batch production phase inoculated from a two-stage seedtrain that has been grown from a single colony from a freshly transformed plate. A 1% inoculum is used to inoculate the microbial synthesis at bench-scale, but only for operational convenience. There has been no investigation of inoculum volume at this time. The first inoculum seedtrain from F1 to F2 is a volume of 5% with a cell density (OD_{600}) of approximately 1 (between 0.2 and 1.3 OD is sufficient). There are differences between the seedtrain medium and the production medium. Following 1% inoculation from F2 to the fermenter, the production phase runs for approximately 60 hours as a fed-batch (glucose feed) microbial synthesis.

Control of fermentation vessel for phloroglucinol biosynthesis

Active pH control is required and the pH set-point is 7.0 ± 0.1. Concentrated ammonium hydroxide and 2 N sulfuric acid are used. Typically, only the ammonium hydroxide is required. Antifoam 204 (Sigma-Aldrich) is also in place during the microbial synthesis but is used only on an as-needed basis under manual control. No automated antifoam control is used. The production vessel is batched with all the medium

components listed except the glucose feed solution. The medium pH is adjusted to 7 with concentrated NH_4OH prior to sterilization. The glucose for the initial batch is sterilized separately as a 50% w/v solution. Following sterilization the temperature is brought to 36 °C, the glucose solution is added to the production vessel to give a final concentration of 25 g/L, the pH is adjusted to 7.0 and the inoculum is added. DO levels are maintained at 20% during initial growth of the microbial synthesis using the following cascade control. With the airflow at an initial setting of 0.06 vvm, the dissolved oxygen is maintained by increasing the impeller speed from an initial set point of 50 rpm (0.14 m/sec) to a preset maximum of 1000 rpm (2.8 m/sec). Then with the impeller rate constant at 1000 rpm, the mass flow controller maintains the dissolved oxygen concentration by increasing the airflow rate from 0.06 vvm to a preset maximum of 1.0 vvm. During this part of the microbial synthesis, glucose feeding does not occur while the cells consume the glucose initially added to the medium. Typically, the cell density (OD_{600}) of the microbial synthesis will reach a value of 30-40 by the time agitation and airflow reach the maximum set-points.

After reaching maximum agitation and airflow, DO levels are controlled by glucose addition; glucose is added based on DO sensor readings to maintain a DO level of 20%. This event is referred to as the phase change and is defined by manual manipulation from DO control by agitation and airflow to DO control by nutrient addition of glucose. Airflow is set at 1.0 vvm and impeller speed is set at 1000 rpm (2.8 m/sec). After phase change the DO level typically drops to 1-5% as glucose is consumed rapidly. Usually 0.5 to 1.0 h after the phase change is executed, all the initial glucose is consumed and glucose addition begins when the DO level rises above 20%. The glucose feed PID control

parameters are set to 0.0 s (off) for the derivative control (τ_D) and 999.9 s (minimum control action) for the integral control (τ_I). X_p was set to 200%.

At the outset of the run and throughout the exponential phase of cell growth, the temperature is set at 36 °C. Once the maximum agitation and airflow set-points are reached the phase change is executed and the temperature is decreased linearly from 36 °C to 33 °C over a 30 min period.

Phloroglucinol production by the cells requires addition of isopropyl-β-D-thiogalactopyranoside (IPTG) to the culture medium. IPTG induces production of T7 RNA polymerase which in turn recognizes the T7 promoter situated upstream of the *phl*D gene. IPTG (0.075 g/L) delivered as 3 mL of a 0.025 g/mL sterile-filtered solution) is added to the medium as soon as the temperature ramp from 36 °C to 33 °C is complete. IPTG (3 mL of 0.025 g/mL stock solution) is added to the medium 24, 36, and 48 h after initiation of the run. It should not be metabolized, but experimental evidence shows increased production with further additions of IPTG. If the run extends beyond 60 h, an equal amount of IPTG is added to the medium 60 h after initiation of the run. The IPTG added sequentially is most likely not necessary.

A 65% w/v glucose solution is used as the feed-stock. Over the course of the production phase, the addition of glucose feed solution increases the microbial synthesis volume by approximately 25-35%.

Phloroglucinol Extraction for phloroglucinol biosynthesis

Dowex 1x8-100 resin in the phosphate form is rinsed with 1 bed volume of ethanol (70%) for sterilization followed by 3 bed volumes of sterilized, deionized, distilled water. The *in situ* resin based extraction is performed as an external fluidized bed extraction cycle. The circulation flow is driven by a Manostat peristaltic pump (Cole-Parmer cat no EW-78210-00) that is positioned downstream from the extraction column. Effluent from the extraction column is then pumped directly back into the fermenter. 4 Bio-Rad econo columns (2.5 x 20 cm) each packed with 80 mL of resin were individually used for a single 12 h increment. Circulation of culture through the resin column is started 3 h after induction with IPTG (typically at 15 h). The column is replaced at 24 h, 36 h, and 48 h. If the microbial synthesis is run beyond 60 h, a new column is put in place at 60 h. The typical flowrate is between 8-12 mL/min. Because most of the phloroglucinol is bound to the resin, it is difficult to determine in real time when phloroglucinol production has ceased. Historically, the amount of phloroglucinol produced after 60 h is minimal, and microbial syntheses are generally stopped at this time.

Step	Parameters	Time (h)	Volume (as V_i)
Seed train	• One transformed colony plated on minimal media inoculates F1 culture tube containing 20 mL M9 seedtrain medium. 5% inoculum into F2 shake flask containing 20 mL M9 seedtrain medium. • 1% inoculation into F3 at 0.3-1.3 OD	F1 – 16 h F2 – 6 h	F1 – fixed 20 mL F2 – fixed 20 mL F3 – fermentor
Production Phase Fermentation	• **Initial batch of Production medium** o Production medium without glucose o 65% w/v glucose batching solution o trace inorganic nutrients stock solution o magnesium stock solution o 10% inoculum • **Process feed tanks** o antifoam o pH control (acid AND base) o 65% w/v glucose feed stock solution • Process Control o Temperature: 36→33 °C o DO control: 20% ▪ Agitation: (max tip-speed 2.8 m/s) ▪ Air Flow: 0.06 - 1.0 vvm ▪ Backpressure 3 psi o pH control: 7.0 ▪ conc. NH_4OH (max rate 0.1% Vi/min) o glucose feed (max rate 0.2 mL/min) • Glucose-minimal feed strategy o Glucose permitted: < 0.1 mM o Sampling every 12 h (OD_{600} and titer) • In-process titer determination GC method; 4 h turnaround	48 h	**1.00** 0.85 0.05 0.001 0.002 0.1 **0.45** <0.01 0.10 0.35
	• **Final volume**		**1.45**
Continuous Extraction	• Dowex 1x8 100 mesh Phosphate form Fluidized bed Extraction rate 8-12 mL/min		0.08 x 4

Seedtrain Medium for phloroglucinol biosynthesis

The seed stage is grown using glucose in M9 salts supplemented with magnesium sulfate and thiamine hydrochloride. Trace minerals are not added to the seed medium. M9 salts medium is made up in de-ionized water and autoclaved separately. Magnesium sulfate is prepared as a 1M solution and autoclaved separately. Glucose is prepared as a 50% solution and autoclaved separately. Thiamine hydrochloride is prepared as a 1

mg/mL stock in water and sterilized by filtration through a .22 μm membrane. The separate solutions are combined immediumtely before inoculation to give a complete seed medium with the following final concentrations in the seedtrain medium.

Component	Concentration (g/L)
Na_2HPO_4	6
KH_2PO_4	3
NH_4Cl	1
NaCl	0.5
$MgSO_4 \cdot 7H_2O$	0.24
Glucose	10
Thiamine HCl	0.001

Production Medium for phloroglucinol biosynthesis

The production microbial synthesis medium contains K_2HPO_4 ammonium iron (III) citrate and citric acid monohydrate. Concentrated H_2SO_4 is added to the aqueous solution and after the salts have been dissolved, the microbial synthesis medium is adjusted to pH 7.0 by addition of concentrated NH_4OH before autoclaving. Magnesium sulfate is prepared as a 1M solution and autoclaved separately. Immediumtely prior to inoculation it is added to give a final concentration of 0.24 g/L.

Component	Concentration in Initial Batch (g/L)
K_2HPO_4	7.50
Citric Acid H_2O	2.10
Ammonium Iron (III) Citrate	0.30
Conc. H_2SO_4	1.20 mL
NH_4OH	qs. to pH 7.0
$MgSO_4 \cdot 7H_2O$	0.24
trace inorganic nutrients stock solution	1 mL

Trace Inorganic Nutrients Stock Solution for phloroglucinol biosynthesis

The trace inorganic nutrients are prepared as a 1000x stock solution and sterilized by filtration. This supplement is added to the production microbial synthesis medium immediumtely prior to inoculation of the microbial synthesis to give final concentrations of 0.1% of the stock concentrations.

Component	Concentration in Stock Solution (g/L)
H_3BO_3	24.7
$MnCl_2,4H_2O$	15.8
$(NH_4)_6(Mo_7O_{24}) \cdot 4H_2O$	3.7
$ZnSO_4 \cdot 7H_2O$	2.9
$CuSO_4 \cdot 5H_2O$	2.5
qs to 0.001 initial batch volume	

Glucose Solution for Initial Batching for phloroglucinol biosynthesis

Anhydrous glucose (25 g) is dissolved in water (50 mL), and the solution is sterilized separately. The entire solution is added to the production medium prior to initiation of the microbial synthesis to give an initial concentration of 25 g/L. The supplement was added immediumtely prior to inoculation of the production microbial synthesis.

Component	**Concentration in Stock Solution (g/L)**
Glucose (anhyd.)	500
qs. To 0.05 initial batch volume	

Glucose Feed Solution for phloroglucinol biosynthesis

A 65% w/v solution of glucose is prepared for feeding. To prepare a 65% solution of glucose, 300 g of anhydrous glucose is added to 280 mL of deionized water. The mixture is autoclaved separately and stirred continuously following sterilization.

Component	**Concentration in Feed Solution (g/L)**
Glucose (anhyd.)	650.0
qs to 0.25-0.35 initial batch volume	

Antifoam

A solution of antifoam 204 (Sigma-Aldrich) is present during the microbial synthesis although foaming generally does not occur. Antifoam is added by manual control if foaming is observed; a foam probe is not used. Excess antifoam has a deleterious effect on the microbial synthesis.

Nutrient Addition during phloroglucinol biosynthesis

Nutrients are also consumed during the course of the microbial synthesis and supplementation has shown to be beneficial. 1 mL of 1 M magnesium sulfate, 0.5 mL trace mineral stock solution (outlined above), 0.15 g ammonium iron(III)citrate, 2.5 g dibasic sodium phosphate and 2.0 g monobasic potassium phosphate are added to the microbial synthesis medium through an external port outside of a sterile hood at 24 h and 12 h intervals thereafter.

In a two-stage microbial synthesis scheme nutrients were added to the auto-claved glucose feed and were allowed to supplement the microbial synthesis medium continually as glucose consumption occurred. (A modest 10% PG titer increase was observed). The amounts of nutrients added externally at 24, 36, and 48 h were summed for 3 additions (running a 60 h microbial synthesis); giving additive totals of 3 mL of 1 M magnesium sulfate, 1.5 mL trace mineral stock solution, 0.45 g ammonium iron(III)citrate, 7.5 g dibasic sodium phosphate and 6 g monobasic potassium phosphate that were dissolved in the glucose feed.

Overall Phloroglucinol Process Schematic

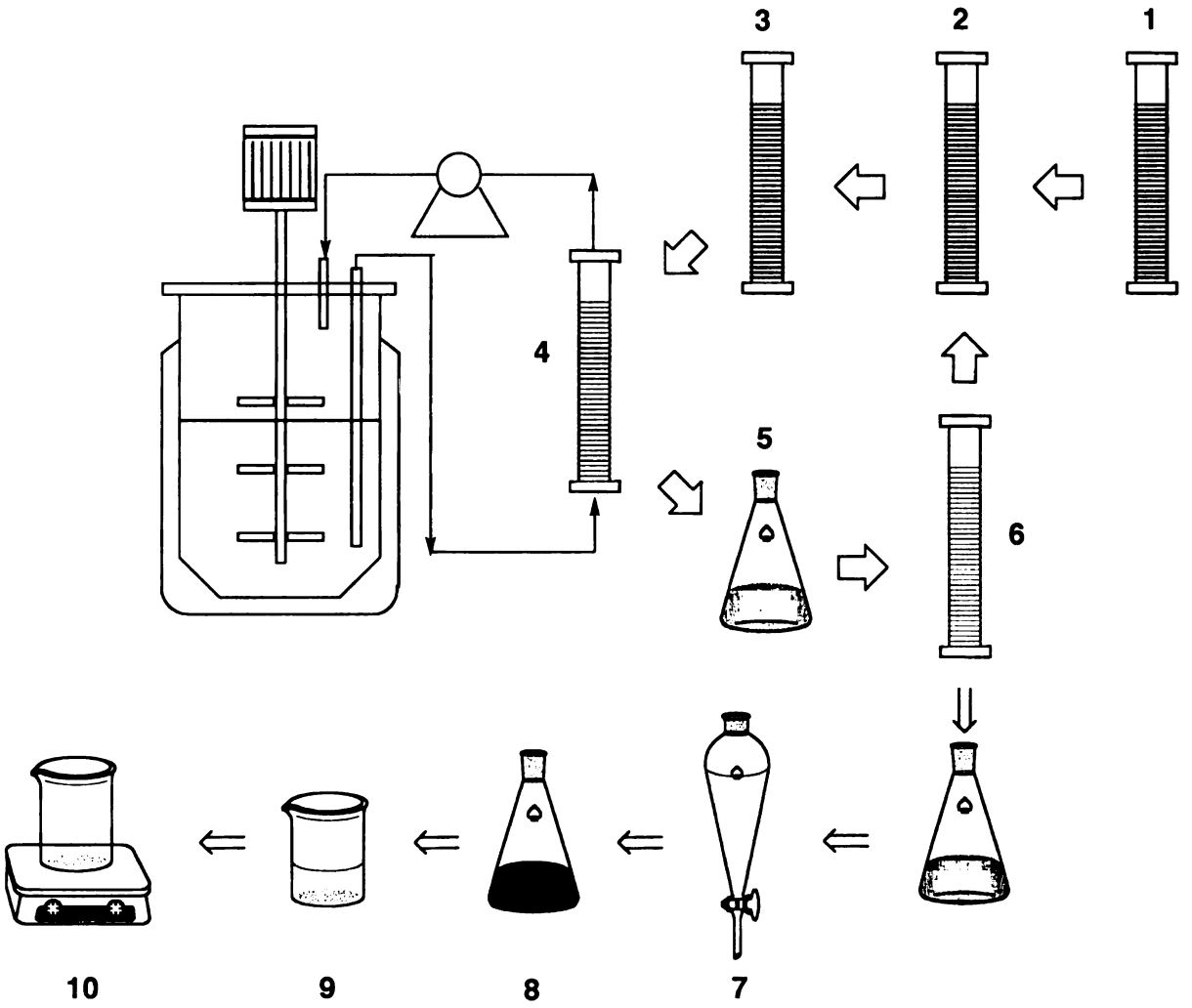

Resin Preparation for phloroglucinol biosynthesis

1) Dowex 1x8 100 mesh (chloride form) (Sigma Aldrich) was exchanged to the phosphate form. Following the manufacturers protocol, a total of 17 bed volumes (BV) of 1 M monobasic sodium phosphate passed through resin beds at 10-15 mL/min in a fixed bed mode.

2) The resin bed was sterilized by 1 BV of 70% ethanol at 10-15 mL/min in a fixed bed mode.

3) The resin bed was then washed with 3 BV of distilled, deionized, sterile water in a fixed bed mode at 10-15 mL/min to prepare the resin for extraction.

4) Beginning 3 h after induction with IPTG, microbial synthesis medium was passed through a single column of resin in a fluidized bed mode at a rate of 8-12 mL/min. Resin columns were exchanged for fresh resin columns 24 h, 36 h, 48 h, and 60 h after initiation of the microbial synthesis batch.

Downstream Processing Description for phloroglucinol biosynthesis

5) Phloroglucinol-containing resin was transferred from the columns and combined in an Erlenmeyer flask. After brief agitation in 1 BV of water (4 °C), the resin was allowed to settle and the cloudy liquid decanted. This process was repeated several times until the water was no longer cloudy (typically 3-5 BV water total). Approximately 2-3% of phloroglucinol is lost in this washing step. If water is at room temperature, phloroglucinol loss increases to 15%.

6) Phloroglucinol-containing resin was transferred to a column and eluted in a fixed bed mode with 5 BV of 0.1 M monobasic sodium phosphate initially at 95 °C. The elution rate was 10 mL/min and the temperature at the conclusion of the elution was typically 65

°C. In this step, phloroglucinol was eluted from the resin and the resin was simultaneously regenerated for the subsequent microbial synthesis.

7) The eluent was extracted with an equal volume of ethyl acetate. The extraction was repeated two additional times and the organic layers were combined. Most of the intense coloration remains in the aqueous layer while the phloroglucinol is in the organic layer.

8 i) Decolorization with 2 x 5% by weight Darco KB (100 mesh) wet powder activated charcoal commenced in an Erlenmeyer flask. The mixture was stirred vigorously for 1 h.

8 ii) Vacuum filtration of charcoal was conducted in a Buchner funnel through a small pad of celite. On average, 5-7% of the phloroglucinol is lost at this step.

9 i) Hexanes were added to the colorless ethyl acetate layer to precipitate the phloroglucinol. The amount of hexanes added varies with concentration of phloroglucinol in the ethyl acetate, up to an approximate ratio of 3:1 (hexanes:ethyl acetate) to precipitate the vast majority of phloroglucinol. To reduce the amount of hexanes added, the phloroglucinol-containing ethyl acetate solution can be concentrated prior to precipitation.

9 ii) Phloroglucinol was collected by vacuum filtration in a Buchner funnel through Whatman filter paper.

10) The white precipitate has been characterized by ^{1}H NMR, ^{13}C NMR, and GC. The isolated material was the dihydrate of phloroglucinol and no impurities were detected. Hydration was removed upon heating at 110 °C or at lower temperatures *in vacuo* to yield phloroglucinol in > 90% from Step 4.

Multiple-stage Fed-batch Extractive Microbial synthesis

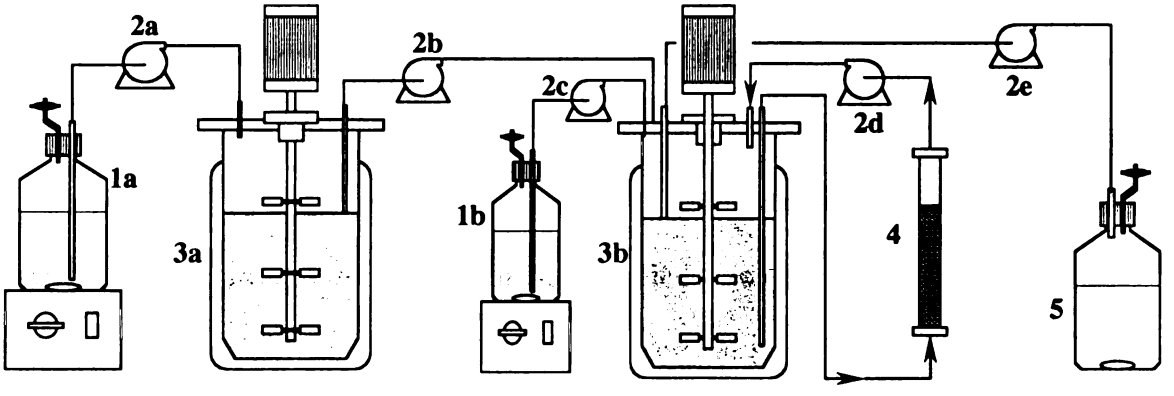

Figure 78. Schematic diagram of a two-stage continuous extractive microbial synthesis (1) feed tank; (2) peristaltic pump; (3) fermenters, [3a uninduced]; (4) resin column; (5) broth collector.

In a two-stage, fed batch extractive microbial synthesis, the production vessel (fermenter 3b) has the analogous characteristics as the single stage fed batch extractive microbial synthesis. The feed vessel (fermenter 3a) contains the identical construct as the production vessel without ever being induced with IPTG. The glucose addition feed (1a) for the feed vessel (3a) is diluted compared with the glucose addition feed (1b) for the production vessel (3b). Preparation of the glucose feed preparations are identical except that (1a) is at a 200 g/L concentration instead of 650 g/L as feed (1b). This dilution is

necessary for replenishing volume to the feed fermenter (3a) as it is drained into the production vessel (3b). Flow from the feed tank (3b) started 12 h after induction of the production tank (3a) at a rate of about 1-3 mL/min. Collection tank (5) is 5 L in volume and is used to capture the overflow of the production vessel as the contents of the feed vessel. The flow to the collector tank is orchestrated from the top of the vessel with a steel tube at a maximum level and may be run without a pump. The distance between each microbial synthesis vessel was kept at a minimum.

The five-stage, fed batch extractive microbial synthesis was analogous to the two-stage swapping in new feed vessels (3a) that's initial growth was staggered every 24 h. Only three vessels were used, a production vessel and two feed vessels. As the first vessel started feeding (12 h post-induction) the second feed vessel was inoculated and did not start feeding the production vessel until 36 h post-induction, etc.

Analysis of microbial synthesis broth

Samples (10-20 mL) of microbial synthesis supernatant were removed at the indicated timed intervals. Cell densities were determined by dilution of microbial synthesis broth with water (1:100) followed by measurement of absorption at 600 nm (OD_{600}). Dry cell weight of *E. coli* cells (g/L) was calculated using a conversion coefficient of 0.43 g/L/OD_{600}. 20 mL of microbial synthesis broth was centrifuged to obtain cell pellets for enzymatic assays and either used immediumtely whenever possible, but flash frozen in liquid N_2 when timing could not be accommodated.

Glucose concentrations in cell-free broth were measured using the Glucose Diagnostic Kit purchased from Sigma. For the biosynthesis of phloroglucinol the concentration was quantified by GC analysis. A portion of the microbial synthesis broth (0.5-1.0 mL) was concentrated to dryness under reduced pressure. Derivatization of the product mixture was initiated by dissolving the material in pyridine (1 mL) followed by the addition of dodecane (0.001 mL) and bis(trimethylsilyl)fluoroacetamide BSTFA (1 mL). A stock of the derivatization components is generally prepared and used promptly within 3 h. Derivatization reactions are stirred at room temperature in darkness for a minimum of 2 h. No change in yield was observed when reaction times were increased up to 12 h. Yield was determined using response factors obtained when authentic phloroglucinol (Fluka, catalog number 79330) derivitized using the same protocol. Reaction samples were analyzed on an Agilent 6890N gas chromatograph equipped with an HP-5 phenyl methyl siloxane column (30 m length, 0.25 mm ID). The temperature profile is as follows: hold at 120 °C for 3 minutes, ramp linearly to 210 °C over 6 minutes, hold at 210 °C for 5 minutes. Retention times: dodecane (3.74 min), phloroglucinol (8.68 min).

Genetic manipulations

Recombinant DNA manipulations generally followed methods described by Sambrook et al.[6] Restriction enzymes were purchased from Invitrogen or New England Biolabs. T4 DNA ligase was obtained from Invitrogen. Fast-Link™ DNA Ligation Kit was obtained from Epicentre. Zymoclean Gel DNA Recovery Kit and DNA Clean &

Concentrator Kit was obtained from Zymo Research Company. Maxi and Midi Plasmid Purification Kits were obtained from Qiagen. Calf intestinal alkaline phosphatase was obtained from Invitrogen. Agarose (electrophoresis grade) was obtained from Invitrogen. SEVAG was a mixture of chloroform and isoamyl alcohol (24:1, v/v). TE buffer contained 10 mM Tris-HCl (pH 8.0) and 1 mM Na_2EDTA (pH 8.0). TAE buffer contained 40 mM Tris-acetate (pH 8.0) and 2 mM Na_2EDTA. Endostop solution (10× concentration) contained 50% glycerol (v/v), 0.1 M Na_2EDTA pH 7.5, 1% sodium dodecyl sulfate (SDS) (w/v), 0.1% bromophenol blue (w/v), and 0.1% xylene cyanole FF (w/v) and was stored at 4 °C. Prior to use, 0.12 mL of DNase-free RNase was added to 1 mL of 10X Endostop solution. DNase-free RNase (10 mg mL^{-1}) was prepared by dissolving RNase in 10 mM Tris-HCl (pH 7.5) and 15 mM NaCl. DNase activity was inactivated by heating the solution at 100 °C for 15 min. Aliquots were stored at -20 °C. PCR amplifications were carried out as described by Sambrook et al.

Small scale purification of plasmid DNA

An overnight culture (10 mL) of the plasmid-containing strain was grown in LB containing the appropriate antibiotics. Cells from 10 mL of the culture were collected in a 14 mL falcon tube by centrifugation. The resulting cell pellet was liquefied by vortexing and then resuspended

Restriction enzyme digestion of DNA

Restriction enzyme digests were performed in buffers provided by Invitrogen or New England Biolabs. A typical restriction enzyme digest contained 0.8 μg of DNA, 2 μL of restriction enzyme buffer (10× concentration), 1 μL of bovine serum albumin (0.1 mg/mL), 1 μL of restriction enzyme and 8 μL TE. Reactions were incubated at 37 °C for 1 h, terminated by addition of 2.2 μL of 10X Endostop solution and analyzed by agarose gel electrophoresis. When DNA was required for cloning experiments, the digest was terminated by addition of 1 μL of 0.5 M Na_2EDTA (pH 8.0) or by heating at 70 °C for 15 min followed by extraction of the DNA using Zymoclean gel DNA recovery kit.

Determination of DNA concentration

The concentration of DNA in the sample was determined as follows. An aliquot (10 μL) of the DNA was diluted to 1 mL in TE and the absorbance at 260 nm was measured relative to the absorbance of TE. The DNA concentration was calculated based on the fact that the absorbance at 260 nm of 50 μg/mL of double stranded DNA is 1.0.

Small scale cell lysis

Lysis began with 10 ml of 10 OD_{600} culture. To calculate the volume of culture needed, divide the OD of the culture into 100. For example, for a culture of 25 OD, 4 ml of culture would be needed. The lysis buffer contains 50 mM Tris pH 8.0, 5 mM CHAPS and 10 mM $MgCl_2$. Collect the cell pellet by centrifugation at 3220*g* for 10 min at 4 °C.

Decant the supernatant and resuspend the pellet in 5 mL lysis buffer. Add 2.5 mg of lysozyme as a solution and 2 μL Benzonase (500,000 units; invitrogen) and vortex. The sample should be allowed to freeze at -80 °C for at least 1 h. Allow the sample to thaw and save 1 mL for analysis before centrifugating for 5 min at 20,817*g* and 4 °C. Save the lysate for analysis. Resuspend the lysate pellet in water and centrifugate for 5 min at 20,817*g* and 4 °C to wash. Remove water and resuspend in 1 mL 1% SDS and save for analysis by protein SDS-PAGE.

Protein SDS-PAGE analysis

Protein SDS-PAGE analysis followed the procedure described by Harris.[7] Preparation of a 10% separating gel started from mixing 3.33 mL of 30% (w/v) aqueous acrylamide stock solution containing N, N'-methylene-bisacrylamide (0.8% (w/v)), 2.5 mL of 1.5 M Tris-HCl (pH 8.8), and 4 mL of distilled deionized water. After degassing the solution using a water aspirator for 30 min, 0.1 mL of 10% (w/v) aqueous ammonium persulfate solution, 0.1 mL 10% (w/v) aqueous SDS solution, and 0.005 mL of N, N, N', N'-tetramethylethylenediamine (TEMED) were added. The solution was mixed thoroughly and poured into a 0.1 cm-width gel cassette to about 1.5 cm below the top of the gel cassette. *t*-Amyl alcohol was overlaid on top of the solution and the gel was allowed to polymerize for 1 h at rt. The stacking gel was prepared by mixing 1.7 mL 30% acrylamide stock solution containing N,N'-methylene-bisacrylamide (0.8% (w/v)), 2.5 mL Tris-HCl solution (0.5 M, pH 6.8), and 5.55 mL of distilled, deionized water. After degassing for 30 min, 0.1 mL of 10% ammonium persulfate, 0.1 mL 10% SDS, and 0.01 mL of TEMED was added, and the solution was mixed thoroughly. *t*-Amyl alcohol was

removed from the top of the gel cassette, which was subsequently rinsed with water and wiped dry. After insertion of the comb, the gel cassette was filled with stacking gel solution, and the stacking gel was allowed to polymerize for 1 h at rt. After removal of the comb, the gel cassette was installed into the electrophoresis apparatus. The electrode chamber was then filled with electrophoresis buffer containing glycine (192 mM), Tris base (25 mM), and 0.1% SDS (w/v). Following dilution with Laemmli sample buffer (10 μL, Sigma S-3401) consisting of 4% SDS, 20% glycerol, 10% 2-mercaptoethanol, 0.004% bromophenol blue, and Tris-HCl (125 mM, pH 6.8), each protein sample (10 μL) was heated at 100 °C for 10 min. Samples and markers (MW-SDS-200, Sigma) were then loaded into the sample wells and the gel was run under constant current at 30 mA until the blue tracking dye (bromophenol blue) reached the interface of stacking gel and separating gel. The protein gel was then run at a higher current (50 mA). When the blue tracking dye reached the bottom of the gel, electrophoresis was terminated. The protein gel was subsequently removed from the cassette and submerged in 10% (w/v) aqueous trichloroacetic acid solution with constant shaking for 30 min. The protein gel was then transferred into a solution containing 0.1% (w/v) Comassie Brilliant Blue R, 45% (v/v) MeOH, 10% (v/v) HOAc in H_2O and stained with constant shaking for 4 h. Destaining of the protein gel was carried out in a solution containing 45% (v/v) MeOH, 10% (v/v) HOAc in H_2O for 2-3 h. For long-term storage, SDS-PAGE gels were sealed in plastic bags containing 10% glycerol.

Alternatively acrylamide gels were purchased from Invitrogen with a 10-20% Tricene gradient (cat. no. EC6625 or EC66255). A 5x stock resolving diluent was made consisting of 5% SDS, 50% glycerol, 0.01% bromophenol blue, and Tris-HCl (250 mM,

pH 6.8). In the sample preparation of 100 μL, 20 μL of the 5x diluent was added to a culture sample normalized to an of OD_{600} = 1 (use equation 100 μL/OD_{600} of sample = amount culture added), then diluted up to 100 μL. Prior to separation each sample was heated at 90 °C for 10 min. The cathode buffer contained 0.1 M Trizma/0.1 M Tricine pH 8.25 with 0.1 % SDS while at the anode the buffer contained 0.2 M Tris(Cl-) pH 8.9.

Agarose gel electrophoresis

Agarose gel typically contained 0.7% agarose (w/v) in TAE buffer. Ethidium bromide (0.5 μg/ml) was added to the agarose to allow visualization of DNA fragments under a UV lamp. Agarose gel was run in the TAE buffer. The size of the DNA fragments were determined using two sets of DNA molecular weight standards: Lambda DNA digested with *Hin*dIII (23.1-kb, 9.4-kb, 6.6-kb, 4.4-kb, 2.3-kb, 2.0-kb and 0.6-kb) and Lambda DNA digested with *Eco*RI and *Hin*dIII (21.2-kb, 5.1-kb, 5.0-kb, 4.3-kb, 3.5-kb, 2.0-kb, 1.9-kb, 1.6-kb, 1.4-kb, 0.9-kb, 0.8-kb and 0.6-kb).

Isolation of DNA from agarose

The band of agarose containing DNA of interest was excised from the gel while visualized with long wavelength UV light. Two methods were used for isolating DNA from agarose gels. The first method used Zymoclean gel DNA recovery kit to isolate DNA from the agarose gel according to the procedure provided by Zymo Research.

Treatment of DNA with Klenow fragment

DNA fragments with recessed 3' termini were modified to DNA fragments with blunt ends by treatment with the Klenow fragment of *E. coli* DNA polymerase I. After restriction digestion (20 μL) of the DNA (0.8-2 μg) was complete, a solution (1 μL) containing each of the four dNTPs was added to a final concentration of 1 mM for each dNTP. Addition of 1-2 units of Klenow fragment was followed by incubation at room temperature for 20-30 min. Since the Klenow fragment works well in the common restriction enzyme buffers, there was generally no need to purify the DNA after restriction digestion and prior to filling recessed 3' termini. DNA was recovered using the Zymoclean gel DNA recovery kit or by precipitation as described previously and subsequently dissolved in TE.

Treatment of vector DNA with calf intestinal alkaline phosphatase

Following restriction enzyme digestion, plasmid vectors were dephosphorylated to prevent self-ligation. Digested vector DNA was dissolved in TE (88 μL). To this sample was added 10 μL of dephosphorylation buffer (10× concentration) and 2 μL of calf intestinal alkaline phosphatase (2 units). The reaction was incubated at 37 °C for 1-2 h. The phosphatase was inactivated by heat treatment (70 °C, 15 min) and the DNA was purified as previously described.

Ligation of DNA

Molar ratios of insert to vector were typically maintained at 2 to 1 for DNA ligations with compatible ends, while for blunt-end ligations a ratio of 4 to 1 was used. A typical reaction contained 0.1 μg of vector DNA and 0.05 to 2.0 μg of insert DNA in a total volume of 7 μL. To this was added 2 μL of T4 ligation buffer (5× concentrations) and 1 μL of T4 DNA ligase (2 units). The reaction was incubated at 16 °C for at least 4 h and then used to transform competent cells. Alternatively, Fast-Link™ DNA Ligation Kit (Epicentre, Madison, WI) was used for ligation of insert DNA with cohesive or blunt ends into predigested vectors with compatible ends according to the protocol provided by Epicentre.

Preparation and transformation of competent E. coli *cells*

Competent cells were prepared according to a procedure modified from Sambrook et al. LB medium (5 mL) containing antibiotics where appropriate, was inoculated with a single colony from a LB plate containing antibiotics where appropriate. The culture was grown at 37 °C with shaking at 250 rpm for 10-12 h. An aliquot (1 mL) from the culture (5 mL) was used to inoculate LB (100 mL) containing the appropriate antibiotics. The culture was grown at 37 °C with shaking at 250 rpm in a NBS series 25 incubator shaker until the optical density at 600 nm was between 0.4 and 0.6. The culture was transferred to a centrifuge bottle that had been sterilized with a 25% (v/v) bleach solution and rinsed four times with sterile, deionized water. The cells were harvested by centrifugation (4000g, 5 min, 4 °C) and the culture medium was decanted. All subsequent manipulations

were carried out on ice. The harvested cells were resuspended in ice-cold 0.9% NaCl (100 mL), and the cells were collected by centrifugation (4000 *g*, 5 min, 4 °C). The 0.9% NaCl solution was decanted, the cells were resuspended in ice-cold 100 mM $CaCl_2$ (50 mL) and stored on ice for 30 min. After centrifugation (4000 *g*, 5 min, 4 °C), the cells were resuspended in 4 mL of ice-cold 100 mM $CaCl_2$ containing 15% glycerol (v/v). Aliquots (0.25 mL) of competent cells were added to 1.5 mL microfuge tubes, immediumtely frozen in liquid nitrogen, and stored at -78 °C.

Frozen competent cells were thawed on ice for 5 min before transformation. A small aliquot (1 to 10 μL) of plasmid DNA or a ligation reaction was added to the thawed competent cells (0.1 mL). The solution was gently mixed by tapping and stored on ice for 30 min. The cells were then heat shocked at 42 °C for 30 seconds and returned to ice briefly (1 min). LB (0.5 mL, no antibiotics) was added to the cells, and the sample was incubated at 37 °C (no agitation) for 1 h. Cells were collected by centrifugation (30 s) in a microcentrifuge. If the transformation was to be plated onto LB plates, 0.5 mL of the culture supernatant was removed, and the cells were resuspended in the remaining 0.1 mL of LB and subsequently spread onto plates containing the appropriate antibiotics. If the transformation was to be plated onto minimal medium plates, the cells were washed twice with a solution of M9 inorganic salts (0.5 mL). After resuspension in a fresh aliquot of M9 salts (0.1 mL), the cells were spread onto a plate. An aliquot of competent cells with no DNA added was also carried through the transformation protocol as a control. These cells were used to check the viability of the competent cells and to verify the absence of growth on selective medium.

Transformations were also performed by electroporation using electrocompetent cells. An aliquot (1 mL) from an overnight culture (5 mL) was used to inoculate 500 mL of 2×YT containing the appropriate antibiotics. The cells were cultured at 37 °C with shaking at 250 rpm. Once an absorbance of 0.6-0.8 at 600 nm was observed, the cells were kept on ice for 10 min and harvested (3 000*g*, 5 min, 4 °C). The cells were gently washed three times with sterile, cold water (450 mL once and 250 mL twice) and then resuspended in 100 mL sterile, ice-cold aqueous 10% glycerol (v/v). After centrifugation (3000*g*, 5 min, 4 °C), the cells were resuspended in 1.5 mL sterile ice-cold aqueous 10% glycerol (v/v). Aliquots (0.1 mL) of electrocompetent cells were dispensed into 1.5 mL microfuge tubes, and immediumtely frozen in liquid nitrogen and stored at –78 °C.

The electroporation was performed in Bio-Rad Gene Pulser cuvettes with an electrode gap of 0.2 cm. The cuvettes were chilled on ice for 5 min prior to use. Electrocompetent cells were thawed in ice for 5 min, and 40 μL of thawed cells was added to the chilled cuvette. To this was added 1-10 μL of plasmid DNA (1 μg mL^{-1}), and the mixture was gently shaken. The Bio-Rad Gene Pulser was set at 2.5 kvolts, 25 μF and 200 Ohms. The outside surface of the cuvette was wiped clean and it was placed in the sample chamber. A single pulse was applied, the cuvette was removed, and 1 mL of freshly prepared SOC was added into it. The contents of the cuvette were transferred to a 15 mL sterile centrifugation tube. The cells were incubated at 37 °C for 1 h with shaking at 250 rpm. The transformed cells were plated in the same manner as in the transformation with chemically competent cells.

λDE3 Lysogeny

The λDE3 lysogeny was performed according to the protocol provided by Novagen. The λDE3 lysate (2.5 x 10^{10} pfu/mL), Helper phage lysate (3.6 x10^{10} pfu/mL), and Selection phage lysate (5.6 x 10^{10} pfu/mL) were stored at -78 °C and thawed on ice immediumtely before use. A colony of the strain to be lysogenized was inoculated into 5 mL of LB containing the appropriate antibiotics, 0.2% maltose and 10 mM $MgSO_4$. The maltose stock solution was sterilized by passage through 0.22-μm membranes and the $MgSO_4$ solution was separately autoclaved. The culture was grown at 37 °C with agitation until the OD_{600} reached 0.5. Various amounts (1, 3, 5, 7, 10 μL) of the culture were transferred to individual microfuge tubes. λDE3 lysate (4 μL), Helper phage lysate (2.78 μL), and Selection phage lysate (1.79 μL) were added to each tube and mixed gently. The host/phage mixture was incubated at 37 °C for 20 min. The mixture was plated onto LB plates with appropriate antibiotics and incubated overnight at 37 °C. Several of the resulting colonies were selected, transformed with a plasmid containing an assayable gene under a T7 promoter, and the specific activity of the enzyme expressed from the T7 promoter was measured. The host strain providing the highest specific activity was chosen and named as the (DE3) strain.

Wanner type gene inactivation technique

PCR step

Design primers for PCR amplification of an antibiotic (kanamycin PKD4 or chloraphenicol PKD3) gene flanked by two FRT (Flipase Recognition Target) sequences. Designed primer has 40 nt homologous sequence (H1) to the genetic region to be deleted and 20 nt homologous sequence (P1) to the priming site that is located just before FRT sequence (Figure 79). To reduce background colonies on rich selection plates the PCR product should be digested with DpnI and purified by gel electrophoresis. DpnI digests only methylated DNA which is not a modification in PCR amplified DNA therefore only template DNA will be digested and will minimize false positive clones from transformation of template pKD3 or 4.

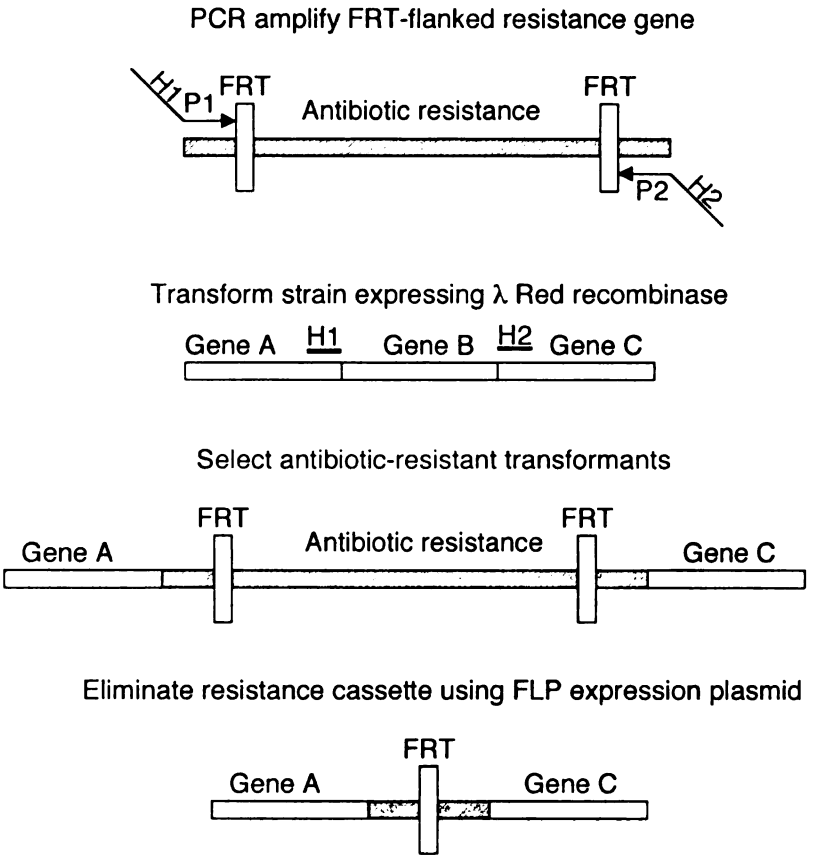

Figure 79. Gene knock-out strategy.

Host preparation step

Transform any *E. coli* host (K-12 derived strains are much easier to work with and although B-type *E. coli* have had minimal success, the deletion can be made in a K-12 strain and P1-phage transduced into a B-type strain) with pKD46 on LB/Ap plates. Incubate at 37 °C overnight. Plasmid pKD46 encodes λ Red (γ, β, *exo*) recombinase under the arabinose promoter. Inoculate a single colony of *E. coli*/pKD46 in 10 mL of 2xYT/Ap. Grow the culture at 30 °C (not 37 °C) for approximately 5-6 h (slightly turbid culture). Add 100 μL of 1 M arabinose solution (10 mM final concentration) and grow it for additional 1 h. The final OD_{600} of the culture should be approximately 0.6-0.7. The

arabinose solution can be introduced before turbidity is observed, but the growth curve is slowed by 2-3 h. Harvest the culture by centrifugation at 1,900*g* at 4 °C for 5 min. Re-suspend cell pellet in 1 mL of sterile ice-chilled water. Centrifuge at 1,500*g* at 4 °C for 2 min. Repeat this wash step three times. (Total 4 washes). Resuspend cell pellet in 80 μL of sterile, ice-chilled water or 10% glycerol.

Gene knock-out

Transform freshly prepared *E. coli*/pKD46 with the PCR amplified FRT flanked antibiotic resistance cassette product by electroporation. Mix 40 μL competent *E. coli*/pKD46 with 400-1000 ng of PCR product (no more than 10 μL volume), electroporate using standard *E. coli* protocol, add 1 mL of SOC and cure for 1 h in 37 °C. Plate 0.5 mL on LB/antibiotic (Cm or Kan) plate to incubate overnight at 37 °C while incubating the other half of the culture overnight at rt and plating if colonies are not observed.

Verification of the mutant

Verify gene knock out by replicating on selective plates. Colonies should be sensitive for Ap (indicates loss of pKD46 plasmid) but should grow on Cm or Kan plate (depending which marker was used) keeping in mind that the deleted gene may be needed for survival. Once the desired phenotype is observed verify the gene interruption by using PCR to amplify regions outside the targeted deletion site and look for shifts in the corresponding band sizes. Design primers, which are outside of knock-out region and run

PCR using genomic DNA from mutants alongside the host as a control. Mutant possessing the FTR-antibiotic-FRT insert in the desired gene will have different size PCR product than the control.

P1 phage mediumted transduction

P1 phage transduction was used to transfer a gene deletion from a donor *E. coli* strain to a recipient strain. P1 phage lysate was prepared by propagation of phage in the donor strain to generate the P1 phage library used to infect recipient strain. The recipient strain was plated on LB/kan plates after phage infection and incubated at 37 °C overnight. The recipient strain was verified by growth phenotype and PCR amplification of genomic DNA as described above. Use of P1 phage transduction was the preferred way to inactivate *E. coli* B strains.

Recombination and excision of antibiotic resistance

In some instances leaving in the resistance gene can have hindered effects on growth and subsequent molecular production and is usually common practice to relieve the targeted gene deficient host of the antibiotic marker. A properly verified mutant was transformed with pCP20, carrying the flipase gene. Electroporation was performed using standard *E. coli* protocol. The curing step was performed at 30 °C (not at 37 °C). Transformation of the mixture was plated on LB/Ap plates and incubated overnight at 30 °C (not 37 °C). Plasmid pCP20 has temperature sensitive replicon, therefore it cannot replicate at 37 or 43 °C. Several colonies from overnight plates were inoculated in liquid

LB or 2xYT culture medium and grown at 43 °C. Cells were streaked on LB plates and grown up at 37 °C to obtain single colonies. Single colonies from LB plate were used to verify deletion by selective plates and PCR amplification of flanking genomic DNA as described above.

Transcriptome analysis

RNA isolation

Total RNA was isolated through extraction with hot phenol to remove protein and used to prepare cDNA as described. *E. coli* cell pellets were resuspended in 1 mL of TE and rapidly transferred to a 17 × 100 mm sterilized test tube containing 4 mL of hot lysis buffer (1% sodium dodecyl sulfate, 30 mM sodium acetate, 3 mM EDTA, pH 5.0) in a boiling water bath. The tubes were held for 5 min with intermittent mixing. Cell lysates were extracted with 3 mL acidic phenol (warmed to 65 °C) with vigorous intermittent mixing for 3 min. The sample was centrifuged (12000*g*, 4 °C) for 10 min. The aqueous layer was extracted a second time with 3 mL acidic phenol (warmed to 65 °C) followed by extraction with equal volumes (1.5 mL) of phenol and SEVAG (chloroform:isoamyl alcohol, 24:1, v/v) at room temperature. After the final extraction with 3 mL of SEVAG at room temperature, the aqueous layer was transferred to a fresh tube. One-tenth volume of 3 M sodium acetate (pH 5.2, ice cold) was added to the aqueous phase followed by 2.5 volumes of 100% ethanol (-20 °C). The sample was kept at -20 °C for at least 2 h.

Total RNA was pelleted by centrifugation (12 000*g*, 4 °C) for 20 min, washed carefully by addition of 70% ethanol (ice cold), and then pelleted again by centrifugation (12 000*g*, 4 °C) for 20 min. The RNA pellet was washed again by addition of 70% ethanol (ice cold) followed by centrifugation (12 000*g*, 4 °C) for 20 min. The RNA pellet at the bottom of the tube was marked outside the tube with a pen and then dried at room temperature under air for 2-3 h. When the RNA pellet appeared clear or translucent, RNA was dissolved in 80 μL of sterile RNase-free water. Contaminating DNA was removed from RNA by hydrolysis with DNaseI. RNA solution (80 μL), 10 μL DNaseI reaction buffer (10×, Ambion), DNaseI (8 μL, Ambion, 200 U) and RNase inhibitor (2 μL, 80 U) were incubated at room temperature for 25 min. After the reaction, a Qiagen RNeasy Mini Kit was used to purify the RNA according to the procedure provided by the manufacturer. The purified RNA sample (approximately 30 μL) was quantified by measuring the absorbance at 260 nm (usually 5 μL of RNA in 795 μL water). The RNA concentration was calculated based on the fact that the absorbance at 260 nm of a 40 μg mL^{-1} of RNA is 1.0. The integrity of the RNA and the amount of genomic DNA contamination was checked with a RNAPico Labchip on an Agilent Bioanalyzer 2100.

cDNA synthesis

10 μg of total RNA was mixed with 10 μL of random primers (Invitrogen), 2 μL of diluted poly-A RNA controls and appropriate amount of water to 30 μL. The RNA/Primer mixture was incubated on a PCR apparatus at 70 °C for 10 min followed by 25 °C for 10 min. The reaction mixture was briefly centrifuged and added to the cDNA synthesis mix. The 30 μL cDNA synthesis mix contains 12 μL 5×1st strand buffer, 6 μL 100 mM DTT, 3

μL 10 mM dNTPs, 1.5 μL SUPERase•In and 7.5 μL SuperScript II. The mixture was incubated at 25 °C for 10 min, followed by 37 °C for 60 min, and finally 42 °C for 60 min, then the SuperScript II was inactivated by heating at 70 °C for 10 min. The RNA template was removed by adding 20 μL 1 N NaOH and incubated at 65 °C for 10 min. The solution was then neutralized with 20 μL 1 N HCl. The synthesized cDNA was purified using MiniElute PCR purification columns following the manufacturer's protocol. The cDNA was quantified by measuring the absorbance at 260 nm (usually 1-2 μL of cDNA in 795 μL water). The RNA concentration was calculated based on the fact that the absorbance at 260 nm of a 33 μg mL^{-1} of single-stranded DNA is 1.0.

cDNA fragmentation

The cDNA purified from the previous step (10 μL) was mixed with 2 μL 10 One-Phor-All buffer, about 3 μL DNase I (Ambion) and appropriate Nuclease-free water to 20 μL. The dosage (unit of DNase I per μg of cDNA) of DNase I to be used is critical for obtaining DNA fragments with suitable size. A titration assay is carried out prior to determine the suitable dosage. DNase I from Ambion was determined to be 0.35 U per μg cDNA. The reaction mixture was incubated at 37 °C for 10 min, the DNase I was inactivated by incubating at 98 °C for 10 min, and the fragmented cDNA was directly applied to the terminal labeling reagents.

Terminal labeling, hybridization and data analysis

The fragmented cDNA was labeled with Genechip labeling reagents (Affymetrix) in a 60 μL solution containing 10 μL cDNA fragmentation products, 10 μL 5× reaction buffer, and 2 μL terminal deoxynucleotidyl transferase. The solution was incubated at 37 °C for 60 min. The reaction was stopped by addition of 2 μL 0.5 M EDTA. A gel shift assay was performed to estimate the efficiency of labeling. Hybridization was performed in the Genomic Technology Support Facility at Michigan State University. Data analysis was performed with Arrayassist software (Stratagene). Gene annotations were retrieved from NetAffx analysis center (Affymetrix), Ecocyc and ERGO servers.

Genes upregulated in producing transcriptome analysis (4x) W3110serA(DE3)/pJA3.131A				
acpD	bioAD	moaBC	wecB	yegN
acrD	**cchB**	mopAB	xerC	yfaE
apaH	celF	nagABC	yabN	yfbN
argA**BCDFGHI**	clpB	nrdABCDE**FGHI**	**yacH**	yfiA
aroH	**cspI**	nth	yaeC	ygbE
artJMPQ	cysACD**HIJMNW**	plsB	yagDL	ygcK
asnC	dnaJK	ppx	ybbN	ygiAC
b0830, b0832,b0833	elaD	pykF	**ybcK**	**yhdV**
b1436	eno	rfaC	ybeFZ	yibG
b1498, **b1499, b1500, b1501, b1502, b1503, b1504**	evgS	rfaL	ybg**DH**	**yigB**
b1551	fimE	rffGH	ybhRS	yjcV
b1632	glnD	**rygAB**	ybiJM	**yjfN**
b2074	gltB	selB	**ycbB**	yjhB**C**
b2085	hisP	sgcQ	ycel	yjiD
b2385	Hpr	**sodA**	ycfS	**yjjM**
b2460	htp**GX**	**spy**	**yciW**	ykgH
b2758	**ibpAB**	sseB	ycjFX	ymfDE
b3400, b3401	manXYZ	trpA	**ydeH**	yqelJ
b3913,b3914	mcrC	udhA	ydgQ	**yqhD**
betA	metJK	uvrC	**yeaD**	yqjBI
bglA	micF	uxuB	yebE	yrfHI

Table 14. Phloroglucinol producing transcriptome analysis: Upregulated at least 4x.
(Bold indicates an 8x upregulation)

Genes up-regulated in fermentative analysis (2-4x) W3110serA(DE3)/pJA3.131A			
acrA	b3112	murF	ybhBL
adhE	b3553	nfnB	ybjC
alpA	b3706	nfo	ycdW
amn	b3835	nlpA	yceF
ampG	b3839,b3940	ogrK	ycfHQ
apaG	b4085	ompC	ycjD
argE	baeS	parE	ydbL
asmA	bcr	pbpG	ydcAEH
atpG	caiD	pdxA	ydiD
b0476	cchA	pfkAB	yecE
b0631	crcA	pflA	yecP
b0655	cutA	pgsA	yehA
b0829	cybBC	prlC	yeiG
b0831	degQ	prmA	yfbM
b0834	dsbD	ptsGN	yfcA
b0836	elaC	recR	yffB
b0851	eutG	rfaDFS	yfhJ
b0936	fabB	rho	yfjK
b1057	fdx	rhsB	ygcB
b1134	fimZ	rpe	ygeF
b1163	fpr	rpoN	yggVW
b1451	fumC	sapABDF	ygiB
b1459	galEKT	sbcC	yhaK
b1520	gapA	selA	yhbHW
b1541	garD	sgcAER	yhcDR
b1583	gidB	speG	yheTU
b1601	glk	spoT	yhgF
b1630,b1631	gloB	sufS	yhhH
b1679	gltFL	talB	yhiJS
b1683,b1684	glyS	tdcD	yibAJ
b1706	gor	tdh	yicM
b1730	gph	tdk	yidA
b1768	gyrB	thiL	yieEFO
b1843	hemL	tpx	yigAFG
b1936	hflK	trkA	yiiX
b2254	hscA	trpBRS	yjePS
b2324	imp	trxA	yjgDGL
b2351	intF	tus	yojN
b2363	iscR	wecCD	yqfB
b2438,b2439	kdpB	wzzE	yqjDG
b2461	kefB	yacFG	yrfE
b2504	ksgA	yadCT	ytfL
b2680	lipB	yaeB	
b2760	lnt	yagN	
b2858	lon	yaiW	
b2925	mcrB	ybaBNP	
b3012	metJL	ybcL	
b3050,b3051	moaE	ybeXY	

Table 15. Phloroglucinol producing transcriptome analysis: Upregulated 2-4x.

Genes down-regulated in fermentative analysis (2-4x) W3110serA(DE3)/pJA3.131A				
accD	b2740	hisL	ryfA	yeiHL
adk	b2832	hmpA	rygC	yfaL
afuC	b3322	hokC	secDF	yfcF
amiA	b3325	hrpB	serB	yfdL
amtB	b3335	hybE	smf	yfeN
aqpZ	b3419,b3420	ilvG	smpA	yfhHK
aroF	b3470	intD	speD	yfiF
ascB	b3475	kdgKT	sraB	yfjN
aslB	b3996	kgtP	sulA	ygaE
b0070	b4003	lexA	tehA	ygcS
b0123	bfr	malK	tesB	ygdDL
b0189	bglF	melA	tolABQR	yggH
b0263	bioH	mglC	tonB	ygiEP
b0441	blr	mlc	torDRT	ygjM
b0484	celA	mltE	tyrA	yhaJ
b0505,b0506	chpAB	mrr	ucpA	yhcO
b0539	cmk	msbA	uhpA	yhdAG
b0847	cobSU	mukF	wzzB	yhjGOR
b0964	crcB	nadA	xapR	yi91b
b1339	cutC	napBDF	xylE	yidI
b1447	cyoA	narQX	yaeJ	yigN
b1483	dbpA	nhaA	yafKNP	yihVW
b1485	dcuC	nlpC	yagF	yiiR
b1509	dgkA	nrfF	yaiU	yijP
b1522	dicC	nuoA	yajC	yjcE
b1533	dinB	oraA	ybaQZ	yjeAM
b1543	dnaAB	pcnB	ybcR	yjgAPQ
b1565	dsbB	pdxK	ybeBH	yjhDER
b1582	entD	perM	ybfE	yjiK
b1625,b1626,b1627	exbBD	pflC	ybhC	ykfA
b1627	fadR	phnA	ybiA	ymjA
b1663	fdhF	phrB	ybjFM	yneH
b1741	fdnI	pnuC	ycbBOWY	yohDLM
b1758,b1759,b1760	fdoHI	potAEI	yceGLP	yphAEF
b1810	fecB	priC	ycfFLP	yqgA
b1822	fepA	proY	ycgLR	zipA
b1998	fhuE	pssAR	ychEM	
b2070	fimC	rdlC	yciLS	
b2191	flgN	relE	ydaL	
b2340	frdAD	rfaH	ydbAC	
b2343	fruR	rhlE	ydcP	
b2354	ftsY	ribBF	ydgC	
b2538	glcG	rpiBSY	ydhU	
b2608	glpEG	rpmA	yecF	
b2638	gntT	rpoES	yedI	
b2639	gpmB	rpsI	yeeP	
b2640	gsk	rtT	yegD	
b2710	hemF	ruvAB	yehZ	

Table 16. Phloroglucinol producing transcriptome analysis: Downregulated 2-4x.

Genes down-regulated in fermentative analysis (4x) W3110serA(DE3)/pJA3.131A			
araE	fis	tyrP	yjaA
aroG	flgM	umuCD	yjcB
b0174	hokDE	yaeL	ymfJ
b0627	hupB	yagEU	yohI
b1016, b1017	hybAB	yahA	
b1146	IS102	yaiB	
b1445	motA	ybeM	
b1657	narP	ybgC	
b1722	ndk	ybiN	
b1728	ppsA	ybjO	
b1748	psiF	ycaD	
b1858, b1859	purR	ycbCGZ	
b2997	putP	yciA	
b3020, b3021, b3022	pyrL	yeaS	
b3776	rem	yebFGK	
cdsA	rph	yeeW	
cspBFGH	rpsT	yegQ	
dinG	sfa	yfhL	
fdnH	smtA	ygjN	
fhuB	tke1	yhbEZ	

Table 17. Phloroglucinol producing transcriptome analysis: Downregulated at least 4x.

Genes Up-regulated in producing transcriptome Analysis (4x) W3110serA(DE3)/pJA3.131A	
Genes encoding transport or membrane proteins	Description
artQ	arginine 3rd transport system permease protein
htpX	Zn metalloprotease participates in proteolytic quality control of membrane proteins
yjcV	putative transport system permease protein
ybgH	(glnT) Glutamine transporter
acrD	RND multidrug efflux pump (typical substrate: aminoglycosides)
yjhB	putative transport protein involved in sialic acid metabolism
hisP	ATP-binding component of histidine transport
yacH	putative membrane protein
yabN	putative transport protein activates SgrS leads to ptsG mRNA degradation which leads to decreased production of glucose transport machinery
YegN	(mdtB) RND multidrug transporter

Table 18. Membrane or transport transcriptome gene list: Upregulated at least 4x.

Genes Up-regulated in producing transcriptome Analysis (2-4x) W3110serA(DE3)/pJA3.131A	
Genes encoding transport or membrane proteins	Description
acrA	acridine efflux pump
atpG	membrane-bound ATP synthase, F1 sector, gamma-subunit
b0655	putative periplasmic binding transport protein
b0829	putative ATP-binding component of a transport system
b0831	putative transport system permease protein
b1451	putative outer membrane receptor for iron transport
b1601	putative transport protein
b1630	electron transport complex protein
b3051	putative membrane protein
bcr	bicyclomycin resistance protein; transmembrane protein
cydC	ATP-binding component of cytochrome-related transport
gltL	ATP-binding protein of glutamateaspartate transport system
kdpB	ATPase of high-affinity potassium transport system, B chain
kefB	K+ efflux; NEM-activable K+H+ antiporter
lnt	apolipoprotein N-acyltransferase, copper homeostasis protein, inner membrane
ompC	outer membrane protein 1b
sapA	homolog of Salmonella peptide transport periplasmic protein
sapB	homolog of Salmonella peptide transport permease protein
sapD	putative ATP-binding protein of peptide transport system
sapF	putative ATP-binding protein of peptide transport system
trkA	transport of potassium
wzzE	putative transport protein
ybeX	putative transport protein
yhcD	putative outer membrane protein
yicM	putative transport protein
yieO	putative transport protein (MFS family)
ytfL	putative transport protein

Table 19. Membrane or transport transcriptome gene list: Upregulated 2-4x.

Genes Down-regulated in producing transcriptome Analysis (4x) W3110serA(DE3)/pJA3.131A	
Genes encoding transport or membrane proteins	Description
fhuB	hydroxamate-dependent iron uptake, cytoplasmic membrane component
hokE	small toxic membrane polypeptide
ycaD	putative transport
hokD	polypeptide destructive to membrane potential
b1657	putative transport protein
b1858	putative ATP-binding component of a transport system
tyrP	tyrosine-specific transport system
araE	low-affinity L-arabinose transport system proton symport protein
b3020	putative transport periplasmic protein

Table 20. Membrane or transport transcriptome gene list: Downregulated at least 4x.

Genes Down-regulated in producing transcriptome Analysis (2-4x) W3110serA(DE3)/pJA3.131A	
Known genes encoding transport or membrane proteins	Description
afuC	putative ATP-binding component of a transport system
amtB	probable ammonium transporter
aqpZ	transmembrane water channel; aquaporin Z
b0070	putative transport protein
b0263	putative transport system permease protein
b0847	putative transport protein
b1483	putative ATP-binding component of a transport system
b1485	putative transport protein
b1509	putative ATP-binding component of a transport system and adhesin protein
b1533	amino acid metabolite efflux pump
b1543	putative transport protein
b1663	multidrug resistance protein norM (Na(+)drug antiporter) (Multidrug-efflux transporter)
b2740	putative transport protein
b2832	putative transport protein
dcuC	transport of dicarboxylates
fecB	citrate-dependent iron transport, periplasmic protein
fepA	outer membrane receptor for ferric enterobactin (enterochelin) and colicins B and D
fhuE	outer membrane receptor for ferric iron uptake
frdD	fumarate reductase, anaerobic, membrane anchor polypeptide
ftsY	cell division membrane protein
gntT	high-affinity transport of gluconate gluconate permease
hokC	small toxic membrane polypeptide
kdgT	2-keto-3-deoxy-D-gluconate transport system
malK	ATP-binding component of transport system for maltose
mglC	methyl-galactoside transport and galactose taxis
msbA	ATP-binding transport protein; multicopy suppressor of htrB
pnuC	required for NMN transport
potA	ATP-binding component of spermidineputrescine transport
potE	putrescine transport protein
potI	putrescine transport protein; permease
proY	proline permease transport protein
secD	protein secretion; membrane protein, part of the channel
secF	protein secretion, membrane protein
smpA	small membrane protein A
tolA	membrane spanning protein, required for outer membrane integrity
tolQ	inner membrane protein, membrane-spanning, maintains integrity of cell envelope; tolerance to group A colicins
tolR	putative inner membrane protein, involved in the tonB-independent uptake of group A colicins
ychM	putative sulfate transporter
yehZ	putative transport system permease protein
yfaL	putative ATP-binding component of a transport system
ygcS	putative transport protein
yjeM	putative transport protein
yphE	putative ATP-binding component of a transport system
yqgA	putative transport protein

Table 21. Membrane or transport transcriptome gene list: Downregulated 2-4x.

Genes Down-regulated In Fermentative Transcriptome Analysis (4x) W3110serA(DE3)/pJA3.131A	
	Description
araE	low-affinity L-arabinose transport system proton symport protein
aroG	3-deoxy-D-arabinoheptulosonate-7-phosphate synthase (DAHP synthetase, phenylalanine repressible)
b0174	hypothetical protein
b0627	hypothetical protein
b1016	hypothetical protein
b1017	high-affinity iron permease
b1146	hypothetical protein
b1445	hypothetical protein
b1657	putative transport protein
b1722	hypothetical protein
b1728	hypothetical protein
b1748	acetylornithine delta-aminotransferase
b1858	putative ATP-binding component of a transport system
b1859	hypothetical protein
b2997	putative hydrogenase subunit
b3020	putative transport periplasmic protein
b3021	hypothetical protein
b3022	hypothetical protein
b3776	hypothetical protein
cdsA	CDP-diglyceride synthetase
cspB	
cspF	
cspG	homolog of Salmonella cold shock protein
cspH	cold shock-like protein
dinG	ATP-dependent helicase
fdnH	formate dehydrogenase-N, nitrate-inducible, iron-sulfur beta subunit
fhuB	hydroxamate-dependent iron uptake, cytoplasmic membrane component
fis	site-specific DNA inversion stimulation factor; DNA-binding protein; a trans activator for transcription
flgM	anti-FliA (anti-sigma) factor; also known as RflB protein
hokD	polypeptide destructive to membrane potential
hokE	small toxic membrane polypeptide
hupB	DNA-binding protein HU-beta, NS1 (HU-1)
hybA	hydrogenase-2 small subunit
hybB	probable cytochrome NiFe component of hydrogenase-2
IS102	
motA	proton conductor component of motor; no effect on switching
narP	nitratenitrite response regulator (sensor NarQ)
ndk	nucleoside diphosphate kinase

Table 22. Total transcriptome gene list: Downregulated at least 4x.

Table 22. continued

ppsA	phosphoenolpyruvate synthase
psiF	induced by phosphate starvation
purR	transcriptional repressor for pur regulon, glyA, glnB, prsA, speA
putP	major sodiumproline symporter
pyrL	pyrBI operon leader peptide
rem	hypothetical protein
rph	RNase PH
rpsT	ribosomal subunit protein S20
sfa	suppresses fabA and ts growth mutation
smtA	S-adenosylmethionine-dependent methyltransferase
tke1	
tyrP	tyrosine-specific transport system
umuC	SOS mutagenesis and repair
umuD	SOS mutagenesis; error-prone repair; processed to UmuD; complex with UmuC
yaeL	hypothetical protein
yagE	putative lyasesynthase
yagU	hypothetical protein
yahA	hypothetical protein
yaiB	hypothetical protein
ybeM	putative amidase
ybgC	hypothetical protein
ybiN	hypothetical protein
ybjO	hypothetical protein
ycaD	putative transport
ycbC	hypothetical protein
ycbG	putative dehydrogenase
ycdZ	hypothetical protein
yciA	hypothetical protein
yeaS	hypothetical protein
yebF	hypothetical protein
yebG	hypothetical protein
yebK	hypothetical protein
yeeW	hypothetical protein
yegQ	hypothetical protein
yfhL	hypothetical protein
ygjN	hypothetical protein
yhbE	hypothetical protein
yhbZ	putative GTP-binding factor
yjaA	hypothetical protein
yjcB	hypothetical protein
ymfJ	hypothetical protein
yohI	putative regulator protein

Genes Down-regulated in fermentative transcriptome Analysis (2-4x) W3110serA(DE3)/pJA3.131A	
	Description
accD	acetylCoA carboxylase, carboxytransferase component, beta subunit
adk	adenylate kinase activity; pleiotropic effects on glycerol-3-phosphate acyltransferase activity
afuC	putative ATP-binding component of a transport system
amiA	N-acetylmuramoyl-l-alanine amidase I
amtB	probable ammonium transporter
aqpZ	transmembrane water channel; aquaporin Z
aroF	3-deoxy-D-arabinoheptulosonate-7-phosphate synthase (DAHP synthetase, tyrosine repressibl
ascB	6-phospho-beta-glucosidase; cryptic
aslB	putative arylsulfatase regulator
b0070	putative transport protein
b0123	hypothetical protein
b0189	hypothetical protein
b0263	putative transport system permease protein
b0441	putative protease maturation protein
b0484	putative ATPase
b0505	hypothetical protein
b0506	putative regulator
b0539	putative exonuclease
b0847	putative transport protein
b0964	hypothetical protein
b1339	putative transcriptional regulator LYSR-type
b1447	hypothetical protein
b1483	putative ATP-binding component of a transport system
b1485	putative transport protein
b1509	putative ATP-binding component of a transport system and adhesin protein
b1522	hypothetical protein
b1533	amino acid metabolite efflux pump
b1543	putative transport protein
b1565	hypothetical protein
b1582	hypothetical protein
b1625	hypothetical protein
b1626	hypothetical protein
b1627	hypothetical protein
b1663	multidrug resistance protein norM (Na(+)drug antiporter) (Multidrug-efflux transporter)
b1741	putative excinuclease subunit
b1758	putative cytochrome oxidase
b1759	hypothetical protein
b1760	hypothetical protein
b1810	hypothetical protein
b1822	hypothetical protein
b1998	hypothetical protein
b2070	putative chaperonin
b2191	hypothetical protein
b2340	hypothetical protein

Table 23. Total transcriptome gene list: Downregulated 2-4x.

Table 23. continued

b2343	hypothetical protein
b2354	hypothetical protein
b2538	large terminal subunit of phenylpropionate dioxygenase
b2608	hypothetical protein
b2638	hypothetical protein
b2639	putative pump protein
b2640	hypothetical protein
b2710	putative flavodoxin
b2740	putative transport protein
b2832	putative transport protein
b3322	calcium-binding protein required for initiation of chromosome replication
b3325	YheF
b3335	leader peptidase
b3419	RNA phosphage cyclase
b3420	RNA 3-terminal phosphate cyclase
b3470	hypothetical protein
b3475	hypothetical protein
b3996	NADH pyrophosphatase
b4003	HydH
bfr	bacterioferrin, an iron storage homoprotein
bglF	PTS system beta-glucosides, enzyme II, cryptic
bioH	biotin biosynthesis; reaction prior to pimeloyl CoA
blr	beta-lactam resistance protein
celA	PEP-dependent phosphotransferase enzyme IV for cellobiose, arbutin, and salicin
chpA	probable growth inhibitor, PemK-like, autoregulated
chpB	probable growth inhibitor, PemK-like, autoregulated
cmk	cytidylate kinase
cobS	cobalamin 5-phosphate synthase
cobU	cobinamide kinasecobinamide phosphate guanylyltransferase
crcB	hypothetical protein
cutC	copper homeostasis protein
cyoA	cytochrome o ubiquinol oxidase subunit II
dbpA	ATP-dependent RNA helicase
dcuC	transport of dicarboxylates
dgkA	diacylglycerol kinase
dicC	regulator of dicB
dinB	DNA polymerase IV -!- DNA polymerase IV, devoid of proofreading, damage-inducible protein P
dnaA	DNA biosynthesis; initiation of chromosome replication; can be transcription regulator
dnaB	replicative DNA helicase; part of primosome
dsbB	reoxidizes DsbA protein following formation of disulfide bond in P-ring of flagella.
entD	enterochelin synthetase, component D
exbB	uptake of enterochelin; tonB-dependent uptake of B colicins
exbD	uptake of enterochelin; tonB-dependent uptake of B colicins
fadR	negative regulator for fad regulon, and positive activator of fabA

Table 23. continued

fdhF	selenopolypeptide subunit of formate dehydrogenase H
fdnI	formate dehydrogenase-N, nitrate-inducible, cytochrome B556(Fdn) gamma subunit
fdoH	formate dehydrogenase-O, iron-sulfur subunit
fdoI	formate dehydrogenase, cytochrome B556 (FDO) subunit
fecB	citrate-dependent iron transport, periplasmic protein
fepA	outer membrane receptor for ferric enterobactin (enterochelin) and colicins B and D
fhuE	outer membrane receptor for ferric iron uptake
fimC	periplasmic chaperone, required for type 1 fimbriae
flgN	protein of flagellar biosynthesis
frdA	fumarate reductase, anaerobic, flavoprotein subunit
frdD	fumarate reductase, anaerobic, membrane anchor polypeptide
fruR	transcriptional repressor of fru operon and others
ftsY	cell division membrane protein
glcG	hypothetical protein
glpE	rhodanese (thiosulfate:cyanide sulfertransferase)
glpG	protein of glp regulon
gntT	high-affinity transport of gluconate gluconate permease
gpmB	phosphoglyceromutase 2
gsk	inosine-guanosine kinase
hemF	coproporphyrinogen III oxidase
hisL	his operon leader peptide
hmpA	dihydropteridine reductase, ferrisiderophore reductase activity
hokC	small toxic membrane polypeptide
hrpB	helicase, ATP-dependent
hybE	hypothetical protein
ilvG	acetolactate synthase II, large subunit, cryptic, interrupted
intD	prophage DLP12 integrase
kdgK	ketodeoxygluconokinase
kdgT	2-keto-3-deoxy-D-gluconate transport system
kgtP	alpha-ketoglutarate permease
lexA	regulator for SOS(lexA) regulon
malK	ATP-binding component of transport system for maltose
melA	alpha-galactosidase
mglC	methyl-galactoside transport and galactose taxis
mlc	putative NAGC-like transcriptional regulator
mltE	murein transglycosylase E
mrr	restriction of methylated adenine
msbA	ATP-binding transport protein; multicopy suppressor of htrB
mukF	mukF protein (killing factor KICB)
nadA	quinolinate synthetase, A protein
napB	cytochrome c-type protein
napD	hypothetical protein
napF	ferredoxin-type protein: electron transfer
narQ	sensor for nitrate reductase system, protein histidine kinase (acts on NarP and narL)

Table 23. continued

narX	nitratenitrate sensor, histidine protein kinase acts on NarL regulator
nhaA	Na+H antiporter, pH dependent
nlpC	lipoprotein
nrfF	part of formate-dependent nitrite reductase complex
nuoA	NADH dehydrogenase I chain A
oraA	regulator, OraA protein
pcnB	poly(A) polymerase I
pdxK	pyridoxalpyridoxinepyridoxamine kinase
perM	putative permease
pflC	probable pyruvate formate lyase activating enzyme 2
phnA	
phrB	deoxyribodipyrimidine photolyase (photoreactivation)
pnuC	required for NMN transport
potA	ATP-binding component of spermidineputrescine transport
potE	putrescine transport protein
potI	putrescine transport protein; permease
priC	primosomal replication protein N
proY	proline permease transport protein
pssA	phosphatidylserine synthase; phospholipid synthesis
pssR	regulator of pssA
rdlC	antisense RNA, trans-acting regulator of ldrC translation
relE	hypothetical protein
rfaH	transcriptional activator affecting biosynthesis of lipopolysaccharide core, F pilin, and haemolysin
rhlE	putative ATP-dependent RNA helicase
ribB	3,4 dihydroxy-2-butanone-4-phosphate synthase
ribF	putative regulator
rpiB	ribose 5-phosphate isomerase B
rplS	50S ribosomal subunit protein L19
rplY	50S ribosomal subunit protein L25
rpmA	50S ribosomal subunit protein L27
rpoE	RNA polymerase, sigma-E factor; heat shock and oxidative stress
rpoS	RNA polymerase, sigma S (sigma38) factor; synthesis of many growth phase related proteins
rpsI	30S ribosomal subunit protein S9
rtT	rtT RNA; may modulate the stringent response
ruvA	Holliday junction helicase subunit B; branch migration; repair
ruvB	Holliday junction helicase subunit A; branch migration; repair
ryfA	hypothetical protein
rygC	hypothetical protein
secD	protein secretion; membrane protein, part of the channel
secF	protein secretion, membrane protein
serB	3-phosphoserine phosphatase
smf	hypothetical protein
smp	
smpA	small membrane protein A
speD	S-adenosylmethionine decarboxylase
sraB	hypothetical protein
sulA	suppressor of lon; inhibits cell division and ftsZ ring formation
tehA	hypothetical protein
tesB	acyl-CoA thioesterase II

Table 23. continued

tolA	membrane spanning protein, required for outer membrane integrity
tolB	periplasmic protein involved in the tonb-independent uptake of group A colicins
tolQ	inner membrane protein, membrane-spanning, maintains integrity of cell envelope; tolerance to group A colicins
tolR	putative inner membrane protein, involved in the tonB-independent uptake of group A colicins
tonB	energy transducer; uptake of iron, cyanocobalimin; sensitivity to phages, colicins
torD	part of trimethylamine-N-oxide oxidoreductase
torR	response transcriptional regulator for torA (sensor TorS)
torT	part of regulation of tor operon, periplasmic
tyrA	chorismate mutase-T and prephenate dehydrogenase
ucpA	putative oxidoreductase
uhpA	response regulator, positive activator of uhpT transcription (sensor, uhpB)
wzzB	regulator of length of O-antigen component of lipopolysaccharide chains
xapR	regulator for xapA
xylE	xylose-proton symport
yaeJ	hypothetical protein
yafK	hypothetical protein
yafN	hypothetical protein
yafP	hypothetical protein
yagF	putative dehydratase
yaiU	putative flagellin structural protein
yajC	hypothetical protein
ybaQ	hypothetical protein
ybaZ	hypothetical protein
ybcR	hypothetical protein
ybeB	hypothetical protein
ybeH	hypothetical protein
ybfE	hypothetical protein
ybhC	putative pectinesterase
ybiA	hypothetical protein
ybjF	putative enzyme
ybjM	hypothetical protein
ycbW	hypothetical protein
ycbY	putative oxidoreductase
ycdB	hypothetical protein
ycdO	hypothetical protein
yceG	putative thymidylate kinase (EC 2.7.4.9)
yceL	hypothetical protein
yceP	hypothetical protein
ycfF	hypothetical protein
ycfL	hypothetical protein
ycfP	hypothetical protein
ycgL	hypothetical protein
ycgR	hypothetical protein
ychE	putative channel protein
ychM	putative sulfate transporter
yciL	hypothetical protein
yciS	hypothetical protein
ydaL	hypothetical protein
ydbA	hypothetical protein
ydbC	putative dehydrogenase
ydcP	putative protease

Table 23. continued

ydgC	hypothetical protein
ydhU	hypothetical protein
yecF	hypothetical protein
yedI	hypothetical protein
yeeP	putative histone
yegD	putative heat shock protein
yehZ	putative transport system permease protein
yeiH	hypothetical protein
yeiL	stationary phase nitrogen starvation regulator
yfaL	putative ATP-binding component of a transport system
yfcF	hypothetical protein
yfdL	putative RNA polymerase beta
yfeN	putative sugar hydrolase
yfhH	hypothetical protein
yfhK	putative 2-component sensor protein
yfiF	hypothetical protein
yfjN	putative cell division protein
ygaE	putative transcriptional regulator
ygcS	putative transport protein
ygdD	hypothetical protein
ygdL	hypothetical protein
yggH	hypothetical protein
ygiE	hypothetical protein
ygiP	putative transcriptional regulator LYSR-type
ygjM	hypothetical protein
yhaJ	putative transcriptional regulator LYSR-type
yhcO	hypothetical protein
yhdA	hypothetical protein
yhdG	putative dehydrogenase
yhjG	hypothetical protein
yhjO	putative cellulose synthase
yhjR	hypothetical protein
yi91b	IS911
yidI	hypothetical protein
yigN	putative alpha helix chain
yihV	putative kinase
yihW	putative DEOR-type transcriptional regulator
yiiR	hypothetical protein
yijP	hypothetical protein
yjcE	hypothetical protein
yjeA	putative lysyl-tRNA synthetase
yjeM	putative transport
yjgA	putative alpha helix protein
yjgP	hypothetical protein
yjgQ	hypothetical protein
yjhD	hypothetical protein

Table 23. continued

yjhE	hypothetical protein
yjhR	putative frameshift suppressor
yjiK	hypothetical protein
ykfA	putative GTP-binding protein
ymjA	hypothetical protein
yneH	putative glutaminase
yohD	hypothetical protein
yohL	hypothetical protein
yohM	hypothetical protein
yphA	hypothetical protein
yphE	putative ATP-binding component of a transport system
yphF	putative LACI-type transcriptional regulator
yqgA	putative transport protein
zipA	cell division protein involved in FtsZ ring

Genes Up-regulated in fermentative transcriptome Analysis (2-4x) W3110serA(DE3)/pJA3.131A	
	Definition
acrA	acridine efflux pump
adhE	CoA-linked acetaldehyde dehydrogenase and iron-dependent alcohol dehydrogenase; pyruvate-formate-lyase deactivase
alpA	prophage CP4-57 regulatory protein alpA
amn	AMP nucleosidase
ampG	regulates beta-lactamase synthesis
apaG	hypothetical protein
argE	acetylornithine deacetylase
asmA	suppressor of ompF assembly mutants
atpG	membrane-bound ATP synthase, F1 sector, gamma-subunit
b0476	putative lipase
b0631	hypothetical protein
b0655	putative periplasmic binding transport protein
b0829	putative ATP-binding component of a transport system
b0831	putative transport system permease protein
b0834	hypothetical protein
b0836	putative receptor
b0851	modulator of drug activity A
b0936	hypothetical protein
b1057	putative cytochrome
b1134	putative phosphohydrolase
b1163	hypothetical protein
b1451	putative outer membrane receptor for iron transport
b1459	hypothetical protein
b1520	hypothetical protein
b1541	hypothetical protein
b1583	hypothetical protein
b1601	putative transport protein
b1630	electron transport complex protein
b1631	hypothetical protein
b1679	hypothetical protein
b1683	hypothetical protein
b1684	hypothetical protein
b1706	hypothetical protein
b1730	hypothetical protein
b1768	hypothetical protein
b1843	hypothetical protein
b1936	hypothetical protein
b2254	putative sugar transferase
b2324	putative peptidase
b2351	putative glycan biosynthesis enzyme
b2363	hypothetical protein
b2438	hypothetical protein
b2439	hypothetical protein
b2461	hypothetical protein
b2504	hypothetical protein
b2680	hypothetical protein

Table 24. Total transcriptome gene list: Upregulated 2-4x.

Table 24. continued

b2760	hypothetical protein
b2858	hypothetical protein
b2925	fructose-bisphosphate aldolase, class II
b3012	hypothetical protein
b3050	putative oxidoreductase
b3051	putative membrane protein
b3112	putative L-serine dehydratase
b3553	putative dehydrogenase
b3706	GTP-binding protein in thiophene and furan oxidation
b3835	
b3839	
b3840	Mg-dependent DNase
b4085	putative epimerase
baeS	sensor protein (for BaeR)
bcr	bicyclomycin resistance protein; transmembrane protein
caiD	carnitine racemase
cchA	detox protein
crcA	hypothetical protein
cutA	divalent cation tolerance protein; cytochrome c biogenesis
cybB	cytochrome b(561)
cydC	ATP-binding component of cytochrome-related transport
degQ	serine endoprotease
dsbD	thiol:disulfide interchange protein; copper tolerance
elaC	hypothetical protein
eutG	ethanolamine utilization; homolog of Salmonella enzyme, similar to iron-containing alcohol dehydrogenase
fabB	3-oxoacyl-(acyl-carrier-protein) synthase I
fdx	(2FE-2S) ferredoxin, electron carrer protein
fimZ	fimbrial Z protein; probable signal transducer
fpr	ferredoxin-NADP reductase
fumC	fumarate hydratase Class II; isozyme
galE	UDP-galactose-4-epimerase
galK	galactokinase
galT	galactose-1-phosphate uridylyltransferase
gapA	glyceraldehyde-3-phosphate dehydrogenase A
garD	(D)-galactarate dehydrogenase
gidB	glucose-inhibited division; chromosome replication?
glk	glucokinase
gloB	probable hydroxyacylglutathione hydrolase
gltF	regulator of gltBDF operon, induction of Ntr enzymes
gltL	ATP-binding protein of glutamateaspartate transport system
glyS	glycine tRNA synthetase, beta subunit
gor	glutathione oxidoreductase
gph	phosphoglycolate phosphatase
gyrB	DNA gyrase subunit B, type II topoisomerase, ATPase activity
hemL	glutamate-1-semialdehyde aminotransferase (aminomutase)
hflK	protease specific for phage lambda cII repressor
hscA	DnaK-homologue chaperone Hsc66
imp	organic solvent tolerance

Table 24. continued

intF	putative phage integrase
iscR	Fe-S cluster-containing transcription factor -!- transcriptional repressor of iscRSUA operon
kdpB	ATPase of high-affinity potassium transport system, B chain
kefB	K+ efflux; NEM-activable K+H+ antiporter
ksgA	S-adenosylmethionine-6-N,N-adenosyl (rRNA) dimethyltransferase
lipB	protein of lipoate biosynthesis
lnt	apolipoprotein N-acyltransferase, copper homeostasis protein, inner membrane
lon	DNA-binding, ATP-dependent protease La; heat shock K-protein
mcrB	component of McrBC 5-methylcytosine restriction system
metJ	repressor of all met genes but metF
metL	aspartokinase II and homoserine dehydrogenase II
moaE	molybdopterin converting factor, subunit 2
murF	D-alanine:D-alanine-adding enzyme
nfnB	oxygen-insensitive NAD(P)H nitroreductase
nfo	endonuclease IV
nlpA	lipoprotein-28
ogrK	prophage P2 ogr protein
ompC	outer membrane protein 1b
parE	DNA topoisomerase IV subunit B
pbpG	penicillin-binding protein 7
pdxA	pyridoxine biosynthesis
pfkA	6-phosphofructokinase I
pfkB	6-phosphofructokinase II; suppressor of pfkA
pflA	pyruvate formate lyase activating enzyme 1
pgsA	phosphatidylglycerophosphate synthetase = CDP-1,2-diacyl-sn-glycero-3-phosphate phosphatidyl transferase
prlC	oligopeptidase A
prmA	methylase for 50S ribosomal subunit protein L11
ptsG	PTS system, glucose-specific IIBC component
ptsN	phosphotransferase system enzyme IIA, regulates N metabolism
recR	recombination and repair
rfaD	ADP-L-glycero-D-mannoheptose-6-epimerase
rfaF	ADP-heptose--lps heptosyltransferase II; lipopolysaccharide core biosynthesis
rfaS	lipopolysaccharide core biosynthesis
rho	transcription termination factor Rho; polarity suppressor
rhsB	rhsB protein in rhs element
rpe	D-ribulose-5-phosphate 3-epimerase
rpoN	RNA polymerase, sigma(54 or 60) factor; nitrogen and fermentation regulation
sapA	homolog of Salmonella peptide transport periplasmic protein
sapB	homolog of Salmonella peptide transport permease protein
sapD	putative ATP-binding protein of peptide transport system
sapF	putative ATP-binding protein of peptide transport system
sbcC	ATP-dependent dsDNA exonuclease
selA	selenocysteine synthase: L-seryl-tRNA (Ser) selenium transferase
sgcA	putative PTS system enzyme II A component
sgcE	putative epimerase
sgcR	putative DEOR-type transcriptional regulator
speG	spermidine N1-acetyltransferase
spoT	(p)ppGpp synthetase II; also guanosine-3,5-bis pyrophosphate 3-pyrophosphohydrolase
sufS	selenocysteine lyase, PLP-dependent

Table 24. continued

talB	transaldolase B
tdcD	putative kinase
tdh	threonine dehydrogenase
tdk	thymidine kinase
thiL	thiamin-monophosphate kinase
tpx	thiol peroxidase
trkA	transport of potassium
trpB	tryptophan synthase, beta protein
trpR	regulator for trp operon and aroH; trp aporepressor
trpS	tryptophan tRNA synthetase
trxA	thioredoxin 1
tus	DNA-binding protein; inhibition of replication at Ter sites
wecC	UDP-N-acetyl-D-mannosaminuronic acid dehydrogenase; synthesis of enterobacterial common antigen (ECA)
wecD	
wzzE	putative transport protein
yacF	hypothetical protein
yacG	hypothetical protein
yadC	putative fimbrial-like protein
yadT	hypothetical protein
yaeB	hypothetical protein
yagN	hypothetical protein
yaiW	hypothetical protein
ybaB	hypothetical protein
ybaN	putative gene 58
ybaP	putative ligase
ybcL	hypothetical protein
ybeX	putative transport protein
ybeY	hypothetical protein
ybhB	hypothetical protein
ybhL	hypothetical protein
ybjC	hypothetical protein
ycdW	putative dehydrogenase
yceF	hypothetical protein
ycfH	hypothetical protein
ycfQ	hypothetical protein
ycjD	hypothetical protein
ydbL	hypothetical protein
ydcA	hypothetical protein
ydcE	hypothetical protein
ydcH	hypothetical protein
ydiD	putative ligasesynthetase
yecE	hypothetical protein
yecP	putative enzyme
yehA	putative type-1 fimbrial protein
yeiG	putative esterase (EC 3.1.1.-).
yfbM	hypothetical protein
yfcA	putative structural protein
yffB	hypothetical protein
yfhJ	hypothetical protein
yfjK	hypothetical protein

Table 24. continued

ygcB	hypothetical protein
ygeF	hypothetical protein
yggV	putative ribosomal protein
yggW	putative oxidase
ygiB	hypothetical protein
yhaK	hypothetical protein
yhbH	probable sigma-54 modulation protein
yhbW	putative enzyme
yhcD	putative outer membrane protein
yhcR	hypothetical protein
yheT	hypothetical protein
yheU	
yhgF	
yhhH	
yhiJ	
yhiS	
yibA	
yibJ	
yicM	putative transport protein
yidA	
yieE	
yieF	
yieO	putative transport protein (MFS family)
yigA	
yigF	
yigG	
yiiX	
yjeP	putative periplasmic binding protein
yjeS	
yjgD	
yjgG	
yjgL	
yojN	putative 2-component sensor protein
yqfB	hypothetical protein
yqjD	hypothetical protein
yqjG	putative transferase
yrfE	
ytfL	putative transport protein

Genes Up-regulated in fermentative transcriptome analysis (4x) W3110serA(DE3)/pJA3.131A	
Transport	Definition
artQ	arginine 3rd transport system permease protein
htpX	integral membrane protein
yjcV	putative transport system permease protein
ybgH	Hypothetical transporter
acrD	possible efflux pump
yjhB	putative transport protein
hisP	ATP-binding component of histidine transport
yacH	putative membrane protein
yabN	putative transport protein
YegN	multidrug transporter
Cellular	Definition
acpD	acyl carrier protein phosphodiesterase
apaH	diadenosine tetraphosphatase
argA	N-acetylglutamate synthase; amino acid acetyltransferase
argB	acetylglutamate kinase
argC	N-acetyl-gamma-glutamylphosphate reductase
argD	acetylornithine delta-aminotransferase
argF	ornithine carbamoyltransferase 2
argG	argininosuccinate synthetase
argH	argininosuccinate lyase
argI	ornithine carbamoyltransferase 1
aroH	3-deoxy-D-arabinoheptulosonate-7-phosphate synthase (DAHP synthetase)
artJ	arginine 3rd transport system periplasmic binding protein
artM	arginine 3rd transport system permease protein
artP	ATP-binding component of 3rd arginine transport system
asnC	regulator for asnA
betA	choline dehydrogenase
bglA	6-phospho-beta-glucosidase A; cryptic
bioA	8-diaminopelargonic acid synthetase
bioD	dethiobiotin synthetase
cchB	detox protein
celF	phospho-beta-glucosidase; cryptic
clpB	heat shock protein
cspI	cold shock-like protein
cysA	ATP-binding component of sulfate permease A protein; chromate resistance
cysC	adenosine 5-phosphosulfate kinase
cysD	ATP:sulfurylase (ATP:sulfate adenylyltransferase)
cysH	3-phosphoadenosine 5-phosphosulfate reductase
cysI	sulfite reductase
cysJ	sulfite reductase (NADPH) flavoprotein beta subunit
cysM	cysteine synthase B
cysN	ATP-sulfurylase (ATP:sulfate adenylyltransferase)
cysW	sulfate transport system permease W protein
dnaJ	chaperone with DnaK; heat shock protein
dnaK	chaperone Hsp70; DNA biosynthesis; autoregulated heat shock proteins
elaD	putative sulfatase / phosphatase
eno	enolase
evgS	putative sensor for regulator EvgA
fimE	recombinase involved in phase variation; regulator for fimA
glnD	protein PII; uridylyltransferase acts on regulator of glnA
gltB	glutamate synthase
Hpr	phosphocarrier protein HPr-like NPr

Table 25. Total transcriptome gene list: Upregulated at least 4x.

Table 25. continued

htpG	chaperone Hsp90
htpX	integral membrane protein
ibpA	heat shock protein
ibpB	heat shock protein
manX	PTS enzyme IIAB
manY	PTS enzyme IIC mannose-specific
manZ	PTS enzyme IID mannose-specific
mcrC	component of McrBC 5-methylcytosine restriction system
metJ	Met repressor
metK	methionine adenosyltransferase 1 (AdoMet synthetase); methyl and propylamine donor
moaB	molybdopterin biosynthesis
moaC	molybdopterin biosynthesis
mopA	chaperone Hsp60
mopB	suppressing its ATPase activity
nagA	N-acetylglucosamine-6-phosphate deacetylase
nagB	glucosamine-6-phosphate deaminase
nagC	transcriptional repressor of nag (N-acetylglucosamine) operon
nrdA	alpha subunit ribonucleoside diphosphate reductase 1
nrdB	ribonucleoside-diphosphate reductase 1
nrdB	Ribonucleoside-diphosphate reductase 1 beta chain
nrdD	anaerobic ribonucleoside-triphosphate reductase
nrdE	ribonucleoside-diphosphate reductase 2
nrdF	ribonucleoside-diphosphate reductase 2
nrdG	anaerobic ribonucleotide reductase activating protein
nrdH	glutaredoxin-like protein; hydrogen donor
nrdI	
nth	endonuclease III; specific for apurinic and/or apyrimidinic sites
plsB	glycerol-3-phosphate acyltransferase
ppx	exopolyphosphatase
pykF	pyruvate kinase I (formerly F)
rfaC	heptosyl transferase I; lipopolysaccharide core biosynthesis
rfaL	O-antigen ligase; lipopolysaccharide core biosynthesis
rffG	dTDP-glucose 4
rffH	glucose-1-phosphate thymidylyltransferase
selB	selenocysteinyl-tRNA-specific translation factor
sgcQ	putative nucleoside triphosphatase
sodA	superoxide dismutase manganese
spy	
sseB	enhanced serine sensitivity
trpA	tryptophan synthase
udhA	putative oxidoreductase
uvrC	excinuclease ABC
uxuB	D-mannonate oxidoreductase
wecB	UDP-N-acetyl glucosamine -2-epimerase; synthesis of enterobacterial common antigen (ECA)
xerC	site-specific recombinase acts on cer sequence of ColE1

Table 25. continued

yabN	putative transport protein
yacH	putative membrane protein
yaeC	putative lipoprotein
yagD	
yagL	DNA-binding protein
ybbN	putative thioredoxin-like protein
ybcK	
ybeF	putative transcriptional regulator LYSR-type
ybeZ	putative ATP-binding protein in pho regulon
ybgD	putative fimbrial-like protein
ybgH	Hypothetical transporter
ybhR	
ybhS	
ybiJ	
ybiM	
ycbB	putative amidase
yceI	
ycfS	
yciW	putative oxidoreductase
ycjF	
ycjX	putative EC 2.1 enzymes
ydeH	
ydgQ	
yeaD	
yebE	
YegN	multidrug transporter
yegN	
yfaE	
yfbN	
yfiA	putative yhbH sigma 54 modulator
ygbE	putative cytochrome oxidase subunit
ygcK	
ygiA	
ygiC	putative synthetase/amidase
yhdV	
yibG	
yigB	putative phosphatase
yjcV	putative transport system permease protein
yjfN	
yjhB	putative transport protein
yjhC	putative dehydrogenase

Table 25. continued

yjiD	
yjjM	
ykgH	
ymfD	
ymfE	
yqeI	putative sensory transducer
yqeJ	
yqhD	putative oxidoreductase
yqjB	
yqjI	
yrfH	
yrfI	

When compared, the experiments adding authentic phloroglucinol in non-phloroglucinol producing strain W3110 and inducing a phloroglucinol producer W3110serA(DE3)/pJA3.131A there were 109 total and seven membrane or transport proteins encoded by its respective genes that were up-regulated at least twofold. An identification and brief description of the common genes are supplied.

Genes Up-regulated in both transcriptome Analysis W3110	
Known genes encoding transport or membrane proteins	Description
acrD	RND multidrug efflux pump (typical substrate: aminoglycosides)
b1451	putative outer membrane receptor for iron transport
b3051	putative membrane protein
bcr	bicyclomycin resistance protein; transmembrane protein
trkA	transport of potassium
yacH	putative membrane protein
YegN	(mdtB) RND multidrug transporter

Table 26. Comparitive transcriptome membrane or transport gene list: Upregulated

Genes Up-regulated in both transcriptome analyses W3110	
	Definition
acpD	acyl carrier protein phosphodiesterase
acrD	possible efflux pump
apaH	diadenosine tetraphosphatase
argA	N-acetylglutamate synthase; amino acid acetyltransferase
argB	acetylglutamate kinase
argC	N-acetyl-gamma-glutamylphosphate reductase
argD	acetylornithine delta-aminotransferase
argF	ornithine carbamoyltransferase 2
argG	argininosuccinate synthetase
aroH	3-deoxy-D-arabinoheptulosonate-7-phosphate synthase (DAHP synthetase
artJ	arginine 3rd transport system periplasmic binding protein
b0261	yagD
b0309	
b0476	putative lipase
b0833	
b0834	hypothetical protein
b0851	modulator of drug activity A
b1057	putative cytochrome
b1451	putative outer membrane receptor for iron transport
b1498	putative sulfatase
b1499	putative ARAC-type regulatory protein
b1500	
b1501	putative oxidoreductase, major subunit
b1502	putative adhesin; similar to FimH protein
b1504	putative fimbrial-like protein

Table 27. Comparitive transcriptome cellular gene list: Upregulated

Table 27. continued

b1679	hypothetical protein
b1683	hypothetical protein
b1684	hypothetical protein
b1730	hypothetical protein
b2074	putative membrane protein
b2085	
b2385	putative peptidase
b2680	hypothetical protein
b3050	putative oxidoreductase
b3051	putative membrane protein
b3840	Mg-dependent DNase
b3913	
b3914	
baeS	sensor protein (for BaeR)
bcr	bicyclomycin resistance protein; transmembrane protein
bioA	8-diaminopelargonic acid synthetase
bioD	dethiobiotin synthetase
celF	phospho-beta-glucosidase; cryptic
elaD	putative sulfatase / phosphatase
fimZ	fimbrial Z protein; probable signal transducer
fpr	ferredoxin-NADP reductase
garD	(D)-galactarate dehydrogenase
gidB	glucose-inhibited division; chromosome replication?
hscA	DnaK-homologue chaperone Hsc66
manX	PTS enzyme IIAB
manY	PTS enzyme IIC mannose-specific
manZ	PTS enzyme IID mannose-specific
metJ	repressor of all met genes but metF
metK	methionine adenosyltransferase 1 (AdoMet synthetase); methyl and propylamine donor
micF	regulatory antisense RNA affecting ompF expression
nagA	N-acetylglucosamine-6-phosphate deacetylase
nagB	glucosamine-6-phosphate deaminase
nrdE	ribonucleoside-diphosphate reductase 2
nrdF	ribonucleoside-diphosphate reductase 2
nrdH	glutaredoxin-like protein; hydrogen donor
nrdI	
pfkB	6-phosphofructokinase II; suppressor of pfkA
rffH	glucose-1-phosphate thymidylyltransferase
rhsB	rhsB protein in rhs element
rygA	
rygB	
spy	
sseB	enhanced serine sensitivity
sufS	selenocysteine lyase, PLP-dependent
tdcD	putative kinase
trkA	transport of potassium
uxuB	D-mannonate oxidoreductase
wecB	UDP-N-acetyl glucosamine -2-epimerase; synthesis of enterobacterial common antigen (ECA)
wecD	

Table 27. continued

yacH	putative membrane protein
yagL	DNA-binding protein
ybcK	
ybgD	putative fimbrial-like protein
ybhB	hypothetical protein
ybiJ	
ycbB	putative amidase
ydeH	
yebE	
yecP	putative enzyme
YegN	multidrug transporter
yfbN	
yfiA	putative yhbH sigma 54 modulator
ygcB	hypothetical protein
ygiB	hypothetical protein
ygiC	putative synthetase/amidase
yhaK	hypothetical protein
yhbW	putative enzyme
yhdV	
yibG	
yibJ	
yieF	
yigB	putative phosphatase
yigF	
yigG	
yiiX	
yjfN	
yjgL	
yjiD	
yjjM	
ykgH	
ymfD	
ymfE	
yqhD	putative oxidoreductase
yqjI	

When compared, the experiments adding authentic phloroglucinol in non-phloroglucinol producing strain W3110 and inducing a phloroglucinol producer W3110serA(DE3)/pJA3.131A there were 58 proteins encoded by its respective genes that were down-regulated. An identification and brief description of the common genes are supplied. Down regulated genes were not discounted in transcriptome interpretation and are presented below.

Genes Down-regulated in both transcriptome analyses W3110	
	Definition
speD	S-adenosylmethionine decarboxylase
b0123	hypothetical protein
dinB	DNA polymerase IV
yagU	hypothetical protein
psiF	induced by phosphate starvation
proY	proline permease transport protein
hupB	DNA-binding protein HU-beta
b0484	putative ATPase
b0627	hypothetical protein
phrB	deoxyribodipyrimidine photolyase (photoreactivation)
aroG	DAHP synthetase, phenylalanine repressible
rhlE	putative ATP-dependent RNA helicase
ybiA	hypothetical protein

Table 28. Comparitive transcriptome total gene list: Downregulated

Table 28. continued

dinG	probably ATP-dependent helicase
ybiN	hypothetical protein
sulA	suppressor of lon, inhibits cell division and ftsZ ring formation
putP	major sodium proline symporter
b1016	hypothetical protein
b1017	high-affinity iron permease
ycdO	hypothetical protein
ycdB	hypothetical protein
flgN	protein of flagellar biosynthesis
potA	ATP-binding component of spermidineputrescine transport
ymfJ	hypothetical protein
umuD	SOS mutagenesis; error-prone repair
yciL	hypothetical protein
b1339	putative transcriptional regulator LysR-type
b1445	hypothetical protein
b1533	amino acid metabolite efflux pump
cspB	cold shock protein
b1625	hypothetical protein
ppsA	phosphoenolpyruvate synthase
b1741	putative excinuclease subunit
b1748	acetylornithine delta-aminotransferase
yebG	hypothetical protein
yebK	hypothetical protein
b1858	putative ATP-binding component of a transport system
b1859	hypothetical protein
cutC	copper homeostasis protein
tyrP	tyrosine-specific transport system
yegD	putative heat shock protein
yegQ	hypothetical protein
yehZ	putative transport system permease protein
narP	nitratenitrite response regulator (sensor NarQ)
b2340	hypothetical protein
yfhL	hypothetical protein
tyrA	chorismate mutase-T and prephenate dehydrogenase
aroF	DAHP synthetase, tyrosine repressible
yfjN	putative cell division protein
b2997	putative hydrogenase subunit
b3020	putative transport periplasmic protein
yhcO	hypothetical protein
pssR	regulator of pssA
lexA	regulator for SOS(lexA) regulon
yjcB	hypothetical protein
yjcE	hypothetical protein
rpiB	ribose 5-phosphate isomerase B
phnA	hypothetical protein

Phloroglucinol reduction methodology

Resorcinol Phloroglucinol (1.0 g, 8.0 mmol) was dissolved in degassed 1.0 N aqueous NaOH (8 mL). To the solution was 1.2 mol% of 5% Rh on alumina catalyst. The suspension was shaken 12 h under 50 psi. H_2. After filtering the catalyst through Celite, pH was adjusted to 6.0 with 10% HCl. The solution was concentrated *in vacuo* to a yellow oil which was subsequently dissolved in 0.5 M H_2SO_4 (20 mL) then refluxed under argon for 9 hours. The cooled solution was extracted with 5 x 20 mL ether, then dried over $MgSO_4$, filtered, then concentrated *in vacuo*. The resulting brown oil was purified by Kugel-Rohr distillation *in vacuo* at 120 °C affording resorcinol as white crystals. ^{1}HNMR (*d*-6-acetone): δ 6.97 (dd, J = 8.0, 8.0 Hz, 1H), 6.35 – 6.30 (m, 3H) ; ^{13}C NMR (*d*-6-acetone): δ 159.4, 130.7, 107.4, 103.4.

CHAPTER FIVE REFERENCE

[1] Yang, J.; Frost, J. W. unpublished results.

[2] (a)Katrizky, A. R.; Zhang, S.; Hussein, A. H. M.; Fang, Y. *J. Org. Chem.* **2001**, *66*, 5606; (b) Hudlicky, M. *J. Org. Chem.* **1980**, *45*, 5377; (c) Marti, R. E.; Bleicher, K. H.; Bair, K. W. *Tetrahedron Lett.* **1997**, *38*, 6145.

[3] Bradford, M. M. A rapid and sensitive method for the quantitation of microgram quantities of protein utilizing the principle of protein-dye binding. *Anal. Biochem.* **1976**, *72*, 248-254.

[4] Tabor, S.; Richardson, C. C. *Proc. Natl. Acad. Sci. USA*, **1987**, *84*, 4767.

[5] Donnelly, M. I.; Sanville-Millard, C.; Chatterjee; R. Method for construction of bacterial strains with increased succinic acid production. U.S. Patent 6,159,738, 2000.

[6] Sambrook, J.; Russell, D. W. *Molecular Cloning: A Laboratory Manual*; Cold Spring Harbor Laboratory Press: Cold Spring Harbor, NY, 2001.

[7] Harris, E. L. V.; Angal, S. In *Protein Purification Methods: A Practical Approach*; Oxford University Express: Oxford, New York, Tokyo, 1989.